ANNUAL REVIEW

INSTITUTE FOR MOLECULAR SCIENCE

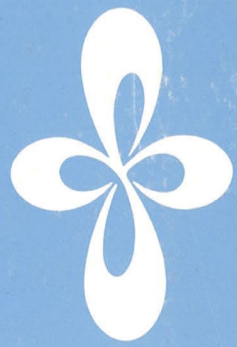

1982

Errata & Addenda (Annual Review 1982)

1. **Page v, 18th line from the bottom, F. .....**
   Transitionsin should read **Transitions in.**

2. **Page vi, D. .....**
   Cndensed should read **Condensed.**

3. **Page 2, in *Theoretical Studies I***
   After the line for Keiji MOROKUMA, add the following:
   Iwao OHMINE Associate Professor (December '82—)

4. **Page 2, in *Theoretical Studies II***
   After the line for Hiroki NAKAMURA, add the following:
   Keiichiro NASU Associate Professor (November '82—)

5. **Page 3, in *Solid State Chemistry***
   After the last line of the page, add the following:
   Yoshiki WADA Graduate Student from Univ. of Tokyo* (April '82—)

6. **Page 4, in *Photochemistry,* line 7**
   Yatsuhisa NAGANAO should read Yatsuhisa NAGANO.

7. **Page 4, in *Computer Center***
   After the last line of the page, add
   Minoru SAITO Graduate Student from Nagoya Univ.* (April '82—)

8. **Page 6, in Foreign Visiting Staff, line 10**
   Lawrence L. Rohr should read Lawrence L.Lohr.

9. **Page 80, in IV-K-3**
   One of the authors, **Yatsuhisa NAGONO** should read **Yatsuhisa NAGANO.**

ANNUAL REVIEW

INSTITUTE FOR MOLECULAR SCIENCE

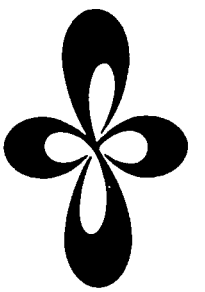

1982

Published by
Okazaki National Research Institutes
The Institute for Molecular Science
Myodaiji, Okazaki 444, Japan
Phone 0564—54—1111
Telex 4537-475 KOKKEN J
December 27, 1982

IMS 1982

It has been seven years since the Institute for Molecular Science was established in 1975. The Institute is now recognized internationally. We would like to make further efforts to promote the Institute as a major international center in molecular science through promotion of research activities in the Institute itself and also through development of joint and exchange programs with outside molecular scientists.

During 1982, several scientists in the Institute accepted new positions outside and we had new researchers joined us. Such an exchange of scientists is desirable from the position of the Institute as an inter-university national institute and also for maintaining the vitality of the Institute. Among the research staff to leave was Dr. M. Tsukada, Associate Professor of Theoretical Studies I, who moved to the Department of physics, Faculty of Science, the University of Tokyo. Joining the senior research staff were Dr. I. Ohmine, as Associate Professor of Theoretical Studies I, and Dr. K. Nasu, as Associate Professor of Thoretical Studies II. Besides these, there were several personnel changes in the positions of research associates and others.

A serious loss to the Institute was the death by heart attack in November 1981 of Professor T. Fujiyama of Molecular Dynamics. Since coming to the Institute as a professor in January 1980, he had worked hard and enthusiastically to establish the new research laboratory. Had he been able to have more years to live, he would undoubtedly have been rewarded with excellent fruits and made great contributions for development of his research field. We particularly regret his sudden death.

The Ultraviolet Synchrotron Orbital Radiation (UVSOR) project has steadily progressed. In the 1982 fiscal year, the sum of ¥659,800,000 was granted for the cost of equipment and official sanction was given to establish the UVSOR Facility as the parent organization to promote this project.

The two special research projects, "The Development and Control of Molecular Functions" and "Energy Transfer and Energy Conversion through Molecular Processes" continued, while a third special research project, "Molecular Science of Primordial Chemical Evolution", is to start in the 1982 fiscal year. We hope this research, which concerns the origin of material in space, will be greatly developed hereafter in the Institute.

We are very pleased that Professor Hideo Akamatu, *ex*-Director General of IMS, was named the first Professor Emeritus of this Institute in September, 1982.

A system of Distinguished Research Consultants was newly set up. We are grateful that Professor Masao Kotani and Professor Kenichi Fukui have accepted appointments as the first Consultants.

December 1982

S Nagakura

Saburo Nagakura
Director-General

CONTENTS

ORGANIZATION AND STAFF

Organization

The Institute for Molecular Science, upon completion, will comprise 15 research laboratories —each staffed by a professor, an associate professor, two research associates and a few technical associates— and six research facilities. The laboratories are grouped into five departments as follows:

Department of Theoretical Studies	Theoretical Studies I
	Theoretical Studies II
	Theoretical Studies III
Department of Molecular Structure	Molecular Structure I
	Molecular Structure II[2]
	Molecular Dynamics
Department of Electronic Sturcture	Excited State Chemistry
	Excited State Dynamics
	Electronic Structure[2]
Department of Molecular Assemblies	Solid State Chemistry
	Photochemistry
	Molecular Assemblies Dynamics[1]
	Molecular Assemblies[2]
Department of Applied Molecular Science	Applied Molecular Science I
	Applied Molecular Science II[2]
Research Facilities	Computer Center
	Instrument Center
	Low-Temperature Center
	Chemical Materials Center
	Equipment Development Center
	Ultraviolet Synchrotron Orbital Radiation (UVSOR) Facility[3]

1) To be established.

2) Professors and associate professors are adjunct professors from universities.

3) Established in April, 1982.

Scientific Staff

Saburo NAGAKURA **Professor, Director-General**

Department of Theoretical Studies

Theoretical Studies I

Keiji MOROKUMA	Professor
Masaru TSUKADA	Associate Professor (—January '82)[1]
Shigeki KATO	Research Associate
Chikatoshi SATOKO	Research Associate
Shigeru OBARA	Technical Associate
Nobuyuki SHIMA	Technical Associate
Yoshihiro OSAMURA	Research Fellow (April '81—)
Toshiharu HOSHINO	Research Fellow (April '80—March '82)
Mitsuyasu HANAMURA	Graduate Student from Tohoku Univ.* (April '79—March '82)
Yoshitaka WATANABE	Graduate Student from Osaka City Univ.* (April '81—March '82)

Theoretical Studies II

Hiroki NAKAMURA	Professor
Kazuo TAKATSUKA	Research Associate
Reiko HIROKAWA	Graduate Student from Ochanomizu Univ.* (October '81—March '82)

Theoretical Studies III

Takayuki FUENO	Adjunct Professor from Osaka Univ. (April '81—)
Masaru TSUKADA	Adjunct Associate Professor from the Univ. of Tokyo (April '82—)
Katsuhisa OHTA	Research Associate
Kiyoyuki TERAKURA	Adjunct Associate Professor from the Univ. of Tokyo (April '81—March '82)

Department of Molecular Structure

Molecular Structure I

Eizi HIROTA	Professor
Shuji SAITO	Associate Professor
Chikashi YAMADA	Research Associate
Yasuki ENDO	Research Associate
Kentarou KAWAGUCHI	Technical Associate
Tetsuo SUZUKI	Technical Associate
Shi-aki HYODO	Graduate Student from Tokyo Metropolitan Univ.* (October '79—)
Koichi TSUKIYAMA	Graduate Student from Tokyo Inst. of Tech.* (October '81—)

Molecular Structure II

Ikuzo TANAKA	Adjunct Professor from Tokyo Inst. of Tech. (April '81—)
Tamotsu KONDO	Adjunct Associate Professor from the Univ. of Tokyo (April '80—March '82)
Hiroyasu NOMURA	Adjunct Associate Professor from Nagoya Univ. (April '82—)
Kenji MURASAWA	Graduate Student from Nagoya Univ.* (April '82—)

Molecular Dynamics

Tsunetake FUJIYAMA	Professor (—November '81)[2]
Yasuo UDAGAWA	Associate Professor
Tadashi KATO	Research Associate
Keiji KAMOGAWA	Research Associate
Kazuyuki TOHJI	Technical Associate
Ryosaku IGARASHI	Research Fellow (April '81—)

Nobuyuki ITO	Graduate Student from Tokyo Metropolitan Univ.* (October '79—)
Hideji TANABE	Graduate Student from Toyohashi Univ. of Technology* (October '79—)
Hideki TANAKA	Graduate Student from Kyoto Univ.* (October '81—September '82)

Department of Electronic Structure

Excited State Chemistry

Keitaro YOSHIHARA	Professor
Takayoshi SAKATA	Associate Professor
Nobuaki NAKASHIMA	Research Associate
Tomoji KAWAI	Research Associate
Minoru SUMITANI	Technical Associate
Kazuhito HASHIMOTO	Technical Associate
Nobuo SHIMO	Visiting Research Fellow from Idemitsu Kosan Co., Ltd. (June '81—)
Shigemasa NAKAMURA	Graduate Student from Nagoya Univ.* (April '81—)
Noriaki IKEDA	Researc Fellow (April '82—)

Excited State Dynamics

Ichiro HANAZAKI	Professor
Nobuyuki NISHI	Associate Professor
Iwao NISHIYAMA	Research Associate
Hisanori SHINOHARA	Research Associate
Masaaki BABA	Technical Associate
Tohru OKUYAMA	Technical Associate
Ryoichi NAKAGAKI	IMS Fellow (May '80—October 30)
Susumu KUWABARA	Graduate Student from Osaka Univ.* (April '79—)
Masayuki UMEMOTO	Graduate Student from Kyushu Univ.* (April '80—March '82)

Electronic Structure

Noboru HITORA	Adjunct Professor from Kyoto Univ. (April '82—)
Hiroshi TSUBOMURA	Adjunct Professor from Osaka Univ. (April '80—March'82)
Hajime KATO	Adjunct Associate Professor from Kobe Univ. (April '81—)
Ryoichi NAKAGAKI	(November '82—) Research Associate

Department of Molecular Assemblies

Solid State Chemistry

Hiroo INOKUCHI	Professor
Inosuke KOYANO	Associate Professor
Kenichiro TANAKA	Research Associate
Kazuhiko SEKI	Research Associate
Naoki SATO	Technical Associate
Tatsuhisa KATO	Technical Associate
Kenji ICHIMURA	IMS Fellow (May 1, '80—November '81)[3]
Masaie FUJINO	Graduate Student from Osaka Univ.* (October '81—)
Shoji HIOKI	Graduate Student from Nagoya Univ.* (October '81—)
Eisuke NISHITANI	Graduate Student from Tokyo Inst. of Tech.* (October '81—)
Hiromichi YAMAMOTO	Graduate Student from Fukui Univ.* (October '81—)
Hiroaki KUMAGAI	Graduate Student from Nagoya Univ.* (April '82—)
Akira ISHIKAWA	Visiting Research Fellow from Kao Soap Co., Ltd. (May '82—)

Satoru YAMAZAKI	Visiting Research Fellow from Asahi Chemical Industry Co., Ltd. (May '82—)

Photochemistry

Katsumi KIMURA	Professor
Kosuke SHOBATAKE	Associate Professor
Yohji ACHIBA	Research Associate
Kiyohiko TABAYASHI	Research Associate
Kenii SATO	Technical Associate
Shinji TOMODA	Research Fellow (April '80—)
Yatsuhisa NAGANAO	Graduate Student from Osaka Univ.* (April '82—)

Molecular Assemblies

Motohiro KIHARA	Adjunct Professor from Nat. Lab. for High Energy Phys. (April '81—)
Yasuhiko SHIROTA	Adjunct Associate Professor from Osaka Univ. (April '81—)
Gunzi SAITO	Research Associate

Department of Applied Molecular Science

Applied Molecular Science I

Hiizu IWAMURA	Professor
Tasuku ITO	Associate Professor
Tadashi SUGAWARA	Research Associate
Koshiro TORIUMI	Research Associate
Yuzo KAWADA	Technical Associate (—March '82)[4]
Masako SUGIMOTO	Technical Associate
Shigeru MURATA	Technical Associate (May '82—)
Hideyuki TUKADA	IMS Fellow (March '82—)
Masahiro YAMASHITA	JSPS Fellow (April '82—)
Masamichi ATO	Graduate Student from Nagoya Univ.* (October '81—)
Fumio UENO	Graduate Student from Tohoku Univ.* (April '80—March '82)
Yukihiro YOKOYAMA	Graduate Student from Nagoya Inst. of Tech.* (April '80—March '82)
Makoto INADA	Graduate Student from Ehime Univ. (April '82—)

Applied Molecular Science II

Hideo YAMATERA	Adjunct Professor from Nagoya Univ. (April '81—)
Nobuyuki HARADA	Adjunct Associate Professor from Tohoku Univ. (April '80—March '82)
Kiyoshi MUTAI	Adjunct Associate Professor from the Univ. of Tokyo (April '82—)
Noboru KOGA	Research Associate (November '82—)

Research Facilities

Computer Center

Keiji MOROKUMA	Director
Hiroshi KASHIWAGI	Associate Professor
Shigeyoshi YAMAMOTO	Technical Associate
Unpei NAGASHIMA	Graduate Student from Hokkaido Univ.* (April '81—)

Instrument Center

Keitaro YOSHIHARA	Director
Iwao YAMAZAKI	Associate Professor
Keisaku KIMURA	Research Associate
Toshiro MURAO	Technical Associate

Low-Temperature Center

Hiroo INOKUCHI	Director
Toshiaki ENOKI	Research Associate
Keiichi HAYASAKA	Technical Section Chief

Chemical Materials Center

Hiizu IWAMURA	Director
Hidemasa TAKAYA	Associate Professor
Akira MIYASHITA	Research Associate (—June '82)[5]
Masashi YAMAKAWA	Technical Associate

Equipment Development Center

Eizi HIROTA	Director
Tadaoki MITANI	Associate Professor
Yoshihiro TAKAGI	Research Associate

Ultraviolet Synchrotron Orbital Radiation Facility

Hiroo INOKUCHI	Director
Makoto WATANABE	Associate Professor
Toshio KASUGA	Associate Professor
Takatoshi MURATA	Adjunct Associate Professor from Kyoto Univ. of Education (May '82—)

* Conduct graduate studies at IMS on the Cooperative Education Programs of IMS with graduate schools.
1) Present address: Dept. of Physics, Univ. of Tokyo, Hongo, Bunkyoku, Tokyo 153, Japan.
2) Deceased; passed away of heart failure on November 18, 1981.
3) Present address: Tritium Research Center, Toyama Univ., Gofuku, Toyama 930, Japan.
4) Present address: Dept. of Chem., Faculty of Science. Ibaraki Univ., Mito, Ibaraki 310, Japan.
5) Present address: Dept. of Appl. Chem., Faculty of Engineering, Saitama Univ., Urawa, Saitama 388, Japan.

Technical Staff

Akira UCHIDA	Technical Division Head
Kusuo SAKAI	Technical Section Chief
Satoshi INA	Computer Center (Unit Chief)
Fumio NISHIMOTO	Computer Center
Takaya YAMANAKA	Instrument Center
Shunji BANDO	Instrument Center
Kenichi IMAEDA	Low-Temperature Center
Kazuo HAYAKAWA	Equipment Development Center
Hisashi YOSHIDA	Equipment Development Center
Masaaki NAGATA	Equipment Development Center
Toshio HORIGOME	Equipment Development Center
Nobuo MIZUTANI	Equipment Development Center

Norio OKADA	Equipment Development Center
Mitsukazu SUZUI	Equipment Development Center
Shinji KATO	Equipment Development Center
Osamu MATSUDO	UVSOR Facility (Unit Chief)
Masami HASUMOTO	UVSOR Facility

Foreign Visiting Staff

Ewa Lipczyńska-Kochany	Tech. Univ. of Warsaw, Warsaw, Poland	Apr. 1, 1981—Sept. 30, 1982
Paul M. Guyon	Univ. Paris-Sud, France	Sept. 8—Dec. 28, 1981
Norbert A. Karl	Univ. Stuttgart, West Germany	Sept. 10—Oct. 7, 1981
Weston T. Borden	Univ. of Washington, USA	Sept. 23, 1981—Jan. 4, 1982
Wilhelm Brening	Tech. Univ. München, West Germany	Sept. 28, 1981—Jan. 5, 1982
Lawrence L. Rohr	Univ. of Michigan, Ann Arbor, USA	Sept. 14—Nov. 12, 1981
John R. Shapley	Univ. of Illinois, Urbana, USA	Dec. 18, 1981—Mar. 11, 1982
Masataka Mizushima	Univ. of Colorado, Boulder, USA	Jan. 4—June, 30, 1982
Desmond V. O'Connor	The Royal Institution, London, U.K.	Jan. 12, 1982—
Klaus Kemnitz	Univ. Erlangen-Nuernberg, West Germany	Mar. 24, 1982—
Kwang Yul Choo	Seoul National Univ., South Korea	Jan. 25—Apr. 10, 1982
Jon T. Hougen	NBS, Washington D.C., USA	Apr. 12—May 7, 1982
Chen Shang Xian	Institute of Chemistry, Academia Sinica, China	Apr. 16, 1982—
Imre G. Csizmadia	Univ. of Toronto, Canada	May 4—June 30, 1982
Robert D. Wyatt	Univ. of Texas, Austin, USA	May 17—Aug. 16, 1982
Peter G. Wolynes	Univ. of Illinois, Urbana, USA	May 17—Aug. 14, 1982
Thomas Ziegler	Univ. of Calgary, Canada	July 13—Aug. 29, 1982
Donald Bethell	Univ. of Liverpool, U.K.	July 19, 1982—Oct. 30, 1982
A. Robert W.-McKellar	NRC, Canada	Aug. 1, 1982—

COUNCIL

Saburo NAGAKURA, Director-General

Councillors

Chairperson	Yasutada UEMURA	Professor, The Science University of Tokyo
Vice-Chairperson	Kenichi FUKUI	President, Kyoto University of Industrial Arts and Textile Fibers
	Hideo AKAMATU	Professor Emeritus, The University of Tokyo and IMS
	Hiroaki BABA	Professor, The Research Institute of Applied Electricity, Hokkaido University
	Masao FUJIMAKI	President, Ochanomizu University
	Soichi IIJIMA	President, Nagoya University
	Tadao ISHIKAWA	President, Keio University
	Yoshiya KANDA	Professor Emeritus, Kyushu University
	Michael KASHA	Professor, Florida State University, U.S.A.
	Noboru KOMATSU	President, Toyota Central Research & Development Laboratories, INC.
	Masao KOTANI	Professor Emeritus, The University of Tokyo
	Daikichiro MORI	Director-General, The Institute of Space and Astronautical Science
	Takashi MUKAIBO	Professor Emeritus, The University of Tokyo
	Sir George PORTER	Director, The Royal Institution, U.K.
	Kazuo SAITO	Professor, Tohoku University
	Yoneichiro SAKAKI	President, Toyohashi University of Technology
	Osamu SHIMAMURA	Director, Sagami Chemical Research Center
	Yataro TAJIMA	Director-General, National Institute of Genetics

The Council is the advisory board for the Director-General. Two of the counsillors are selected among distinguished foreign scientists.

Professor Emeritus

Professor Hideo AKAMATU, *ex*-Director-General of IMS, was named the first Professor Emeritus of this Institute in September, 1982.

Distinguished Research Consultants

Kenichi FUKUI	President, Kyoto University of Industrial Arts and Textile Fibers
Masao KOTANI	Professor Emeritus, The University fo Tokyo

Administration Bureau

Akira MUROYA	Director-General, Administration Bureau
Katsuhiko HISAO	Director, General Affairs Department
Hiroshi HIGURASHI	Director, Finance and Facilities Department

BUILDINGS AND CAMPUS

The IMS campus covering 62,561 m^2 is located on a low hill in the middle of Okazaki City. The inequality in the surface of the hill and growing trees are preserved as much as possible, and low-storied buildings are adopted for conservation of the environment. The buildings of IMS are separated according to their functions as shown in the map. The Research Office Building and all Research Facilities except for the Computer Center are linked organically to the Main Laboratory Building by corridors. Computer Center, Library, and Administration Buildings are situated between IMS and the neighboring National Institute for Basic Biology and National Institute for Physiological Sciences, because the latter two facilities are common to these three institutes.

The lodging facility of IMS called Yamate Lodge, located within 10 min. walk, has sleeping accommodations for 20 guests. Since June 1, 1981 a new lodging facility called Mishima Lodge has been opened. Mishima Lodge, located within four minutes' walk east of IMS can accommodate 30 guests and six families. Scientists who visit IMS as well as the two other institutes can make use of these facilities. Foreign visiting scientists can also live at these lodgings with their families during their stay.

The Institute for Molecular Science

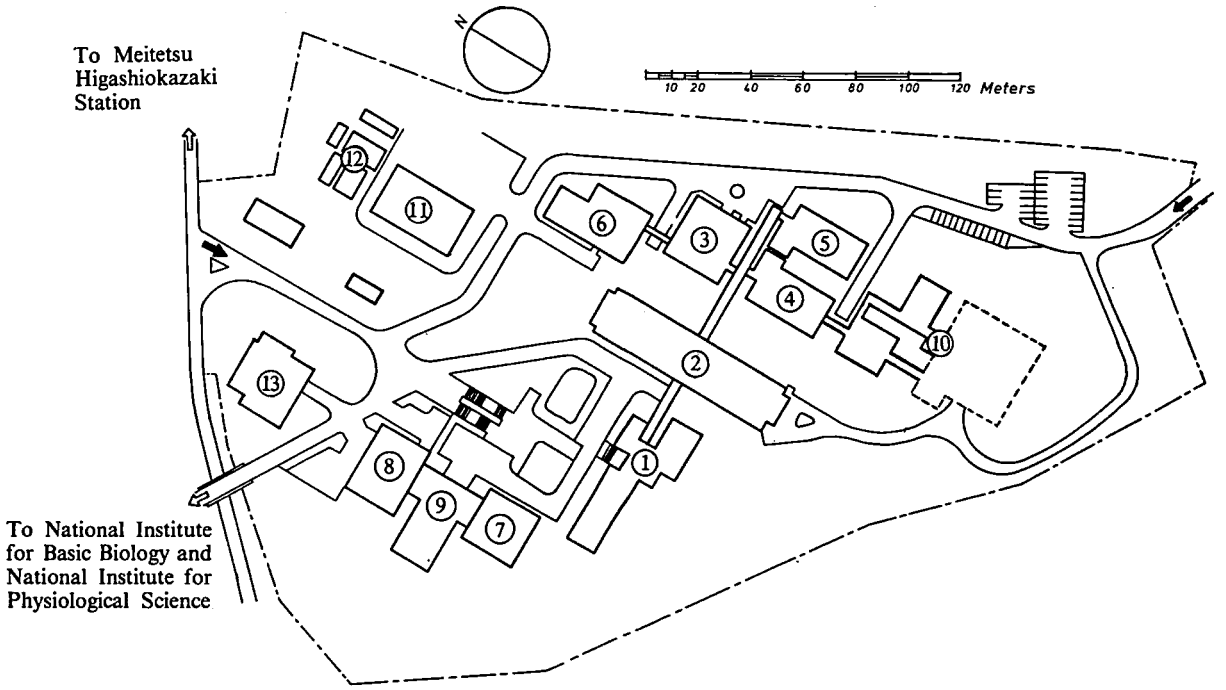

1. Research Office Building
2. Main Laboratory Building
3. Equipment Development Center
4. Instrument Center
5. Chemical Materials Center
6. Low-Temperature Center
7. Computer Center
8. Library
9. Central Administration
10. UVSOR Facility
11. Power Station
12. Waste-Water Disposition Facilities
13. Faculty Club

† Partially completed

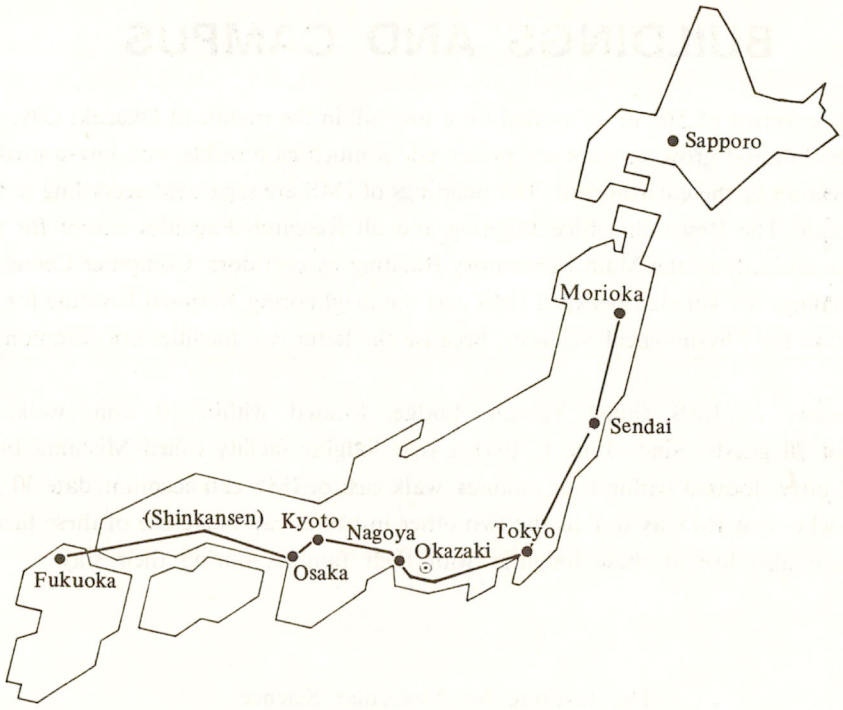

Okazaki (population 272,000) is 260 km southwest of Tokyo, and can be reached by train in about 3 hours from Tokyo via New Tokaido Line (Shinkansen) and Meitetsu Line.
The nearest large city is Nagoya, about 40 km west of Okazaki.

IMS, 1982

RESEARCH ACTIVITIES I
Department of Theoretical Studies

I—A Potential Energy Surfaces for Chemical Reactions

Molecular orbital studies of potential energy surfaces for chemical reactions remained to be one of the most important areas of study for our molecular quantum chemistry group. The energy gradient technique, both at the GVB and the SCF level, has been used to determine and characterize potential energy surfaces of simple organic reactions.

I-A-1 Potential Energy Surface of the Reaction $C^+ + H_2 \rightarrow CH^+ + H$

Shogo SAKAI, Sigeki KATO, and Keiji MOROKUMA, Isao KUSUNOKI *(Tohoku Univ.)*

[*J. Chem. Phys.*, **75**, 5398 (1981)]

Potential energy surfaces of six low lying states for the reaction $C^+ + H_2$ have been calculated with an *ab initio* MCSCF-POLCI method. An emphasis has been placed on the reaction channel leading to the chemiluminescent product $CH^+(A^1\Pi) + H(^2S)$. Based on the characteristics of the surfaces, a mechanism for this reaction has been proposed which involves a nonadiabatic transition from $2^2A'$ to $3^2A'$ in the vicinity of the C_{2v} symmetry. An alternative path involving a $1^2A'' \rightarrow 2^2A''$ transition cannot be denied.

I-A-2 Potential Energy Surface of the S_N2 Reaction in Hydrated Cluster

Keiji MOROKUMA

[*J. Am. Chem. Soc.*, **104**, 3732 (1982)]

We have presented the results of *ab initio* SCF calculations of potential energy surfaces for an S_N2 reaction:

$$Cl^-(H_2O)_n + CH_3Cl \rightarrow ClCH_3 + Cl^-(H_2O)_n$$

for n = 0 (unhydrated), 1, and 2. Relevant equilibrium and transition-state geometries and energies have been determined with the energy gradient method with the 3-21G basis set. The potential energy profiles are shown in Figure 1. We find that for n = 1 the H_2O migration and CH_3 transfer-inversion occurs either sequentially or simultaneously. For n = 2, the initial sequential or simultaneous H_2O migration and CH_3 transfer-inversion followed by the migration of the other H_2O is the most favorable path of reaction.

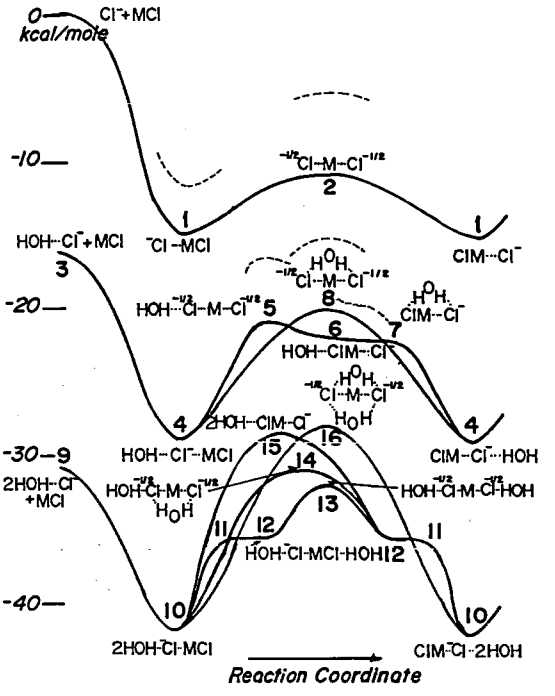

Figure 1. Profiles of the potential energy surfaces. The energy is relative to isolated molecules and ions. Broken lines are with Cl.

In the reaction of the complex **10** with a dihydrated chloride **9**, two H_2O migrations and a CH_3 transfer-inversion can take place one by one, two by one, or all three simultaneously. We find that the most favorable path is the initial migration of one H_2O with little or no barrier (**11**) to form the

intermediate complex **12**, followed by the CH_3 inversion through the transition state **13** and the final migration **12→11→10** of the other H_2O molecule. The first H_2O migration ensures that Cl^- is hydrated throughout the reaction and keeps the potential energy low. The initial simultaneous H_2O migration-CH_3 inversion, **10→14→12**, has a slightly larger barrier but cannot be excluded. The overall barriers **13** and **14** for n = 2 are higher in energy than the corresponding barriers for n = 1, which in turn is higher than the barrier for n = 0.

One notes that H_2O migrations, **6→7→4** and **12→11→10**, proceed with little or no barrier. The geometry of **11′** which is on the path connecting **12** and **10**, reveals an important role of Cl^- in the H_2O migration; Cl^- moves away from the C_{3v} axis to accompany the migration H_2O until H_2O is delivered to the opposite Cl atom, and then it flips back onto the C_{3v} axis. This close association of Cl^- keeps the potential energy low for the process.

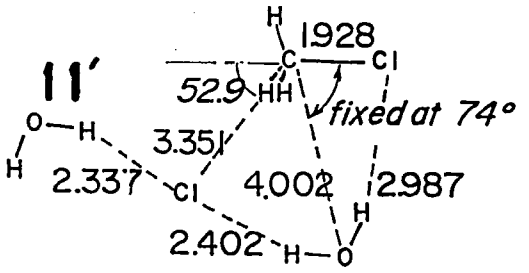

I-A-3 A Theoretical Study on the Mechanism of Electronic to Vibrational Energy Transfer in $Hg(^3P)$ + CO Collision

Shigeki KATO, Richard L. JAFFE (*NASA Ames Research Center*), **Andrew KOMORNICKI** (*Polyatomic Research Institute*), **and Keiji MOROKUMA**

[*J. Chem. Phys.*, in press]

The mechanism of electronic-to-vibrational (E-V) energy transfer in the $Hg(^3P)$ + CO collision has been studied theoretically. The configuration interaction (CI) method was employed to calculate potential energy surfaces of the collision system. A simplified theoretical model, based on the reaction coordinate concept and the calculated potential energy characteristics, was used to discuss the mechanims of the singlet-triplet transition and the energy disposal. The results obtained were that (a) the quenching process proceeds via a collision complex mechanism and that (2) the triplet-singlet transition occurs near the collinear geometry. A model classical trajectory calculation gives a product CO vibrational distribution in good agreement with the experimental result.

I-A-4 The 1,2 Hydrogen Shift as an Accompaniment to Ring Closure and Opening: *Ab Initio* MO Study of Thermal Rearrangements on the C_2H_3N Potential Energy Hypersurface

L. L. LOHR (*Univ. of Michigan*), **M. HANAMURA** (*Tohoku Univ.*), **and K. MOROKUMA**

Ab initio electronic structure calculations employing both 4-31G and DZP (double-zeta plus polarization) basis sets have been made for equilibrium geometries and transition states involved in thermal rearrangements on the C_2H_3N potential energy hypersurface. The principal rearrangements studied are those involving the species vinyl nitrene (singlet), 2*H*-azirine, and acetonitrile. From the computed energies of stationary points and from the pathways connecting these points, several conclusions are drawn. First, singlet vinyl nitrene can undergo a ring closure without any appreciable activation energy to form 2*H*-azirine. Second, the combined 1,2 hydrogen shift and ring opening required to form acetonitrile from 2*H*-azirine proceeds optimally but indirectly via methyl isocyanide as an intermediate. Thus hydrogen transfer precedes C-N bond breakage, necessitating a subsequent ring closure and re-opening. Third, there does exist a more direct but somewhat higher energy pathway to acetonitrile. The latter pathway involves a transition state totally lacking in symmetry so that an asymmetrically substituted azirine $R_1R_2\overline{C}\text{-}CR_3\text{-}\overline{N}$ would produce a mixtue of optical isomers of $R_1R_2R_3CCN$, while the former indicrect but lower energy pathway, preserving a mirror plane of symmetry throughout, would produce only one isomer.

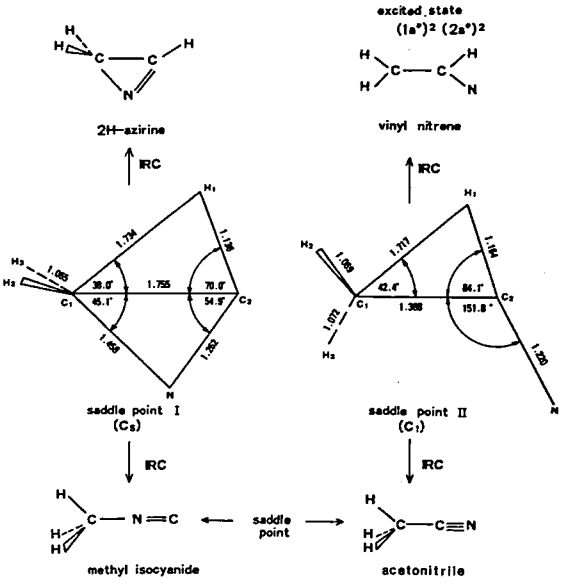

Figure 1. Some stationary points on the rearrangement potential surface of C_2H_3N. Distances are in Å and angles are in degrees.

I—B Problems of Molecular Structure and Molecular Interaction

The energy gradient technique in the *ab initio* method has found a wide range of application to problems of molecular structure and molecular interaction.

I-B-1 Theoretical Studies on Low-Lying Electronic States of the CCl^+, $SiCl^+$, and $GeCl^+$ Ions

Yukio NISHIMURA,* Toshinori MIZUGUCHI,* Masaharu TSUJI* (*Kyushu Univ.), Shigeru OBARA, AND keiji MOROKUMA

Potential energy curves for the ground state and low-lying Π states of the CCl^+, $SiCl^+$, and $GeCl^+$ ions have been determined by *ab initio* configuration interaction (CI) calculation. Molecular constants are given for the bound states and are compared with available experimental data.

I-B-2 *Ab Initio* Study on Cyanamide and Isocyanamide

Kazuo ICHIKAWA,* Yoshiaki HAMADA,* Yoko SUGAWARA,* Masamichi TSUBOI,* (*Univ. of Tokyo) Shigeki KATO, and Keiji MOROKUMA

[*Chem. Phys.*, in press]

Spectroscopic parameters, namely force constants and dipole moment derivatives at the equilibrium geometry, were studied by *ab initio* MO method. It turned out that the former configuration of the two structural isomers has characters of amides, and the latter amines. The assignments of skeletal deformation vibrations were reinvestigated experimentally as well. This study supports Ogilvie's attribution of what he observed to the vibrational spectrum of isocyanamide and explains the anormalous infrared intensity in the spectrum. A special theoretical treatment of wagging motion was presented, which includes the inversion effect enables to predict the inversion splitting of isocyanamide.

I-B-3 Force Field in the Methylamine Molecule from *Ab Initio* MO Calculation

Yoshiaki HAMADA,* Naoki TANAKA,* Yoko SUGAWARA,* Akiko Y. HIRAKAWA,* and Masamichi TSUBOI* *(*Univ. of Tokyo)*, **Shigeki KATO and Keiji MOROKUMA**

[*J. Mol. Spectr.*, in press]

Ab initio SCF MO calculations on the equilibrium geometry, force constants, vibrational frequencies, and dipole moment derivatives of methylamine have been carried out using the STO-3G, 4-31G, 4-31G(N*), and 4-31G* basis sets and an energy gradient method. The results were compared with the re-examined infrared absorption spectra for CH_3NH_2, CH_3ND_2, CH_3NH_2, CD_3ND_2, and CD_3NHD. A detailed discussion has been made for the off-diagonal elements of the potential energy matrix (F-matrix), including the NH_2 twisting/CH_3 rocking (A″) element. Starting from the 4-31G* F-matrix, a corrected F matrix has been reached, by adjusting the diagonal elements to fit the observed frequencies and by keeping the off-diagonal elements at their *ab initio* values. The amino-twisting vibration was assigned to a weak absorption band at 1335 cm^{-1} of CH_3NH_2 and that at 1326 cm^{-1} of CD_3NH_2.

I-B-4 Emission Spectra of CF_3 Radicals. Excitation Spectra, Quantum Yields, and Potential Energy Surfaces of the CF_4 Fluorescences

Nobuaki WASHIDA,* Masako SUTO,* *(*National Institute for Environmental Studies)*, **Shigeru NAGASE** *(Yokohama National Univ.)*, **Umpei NAGASHIMA** *(Hokkaido Univ.)*, **and Keiji MOROKUMA**

[*J. Chem. Phys.*, in press]

Cross sections, quantum yields, and threshold energies for the production of UV and visible emission bands of CF_3 from photodissociation of CF_3Br and CF_3Cl were measured in the 115-130 nm region. The quantum yields for the production of UV and visible emission bands are 0.2-1.0 and 1-5%, respectively, both for the photolysis of CF_3Br and CF_3Cl. Appearance energies of the UV and visible emissions are (9.41 ± 0.05) and (9.39 ± 0.02) eV, respectively, in the photolysis of CF_3Br, and (10.10 ± 0.08) and (10.08 ± 0.07) eV, respectively, in the case of CF_3Cl. These results show that the upper states energies of the UV and visible emissions are very close to 6.4 eV above the CF_3 ground state. Potential energy surfaces of CF_3 radicals were calculated by the *ab initio* CI method. Possible transitions suggested for the UV and visible emission bands are $2A_1'$(Rydberg state) → $1A_2''$(ground state) and 1E′ and/or $2A_2''$(both are Rydberg states) → $1A_1'$(Rydberg state), respectively. These upper states, $2A_1'$, 1E′ and $2A_2''$, are most stable in the D_{3h} structure.

I—C Structure, Bonding and Reactivity of Transition Metal Complexes

The structure, bonding and reactivity of transition metal complexes became one of the most important areas of activity of our molecular quantum chemistry group. The development of the energy gradient technique with the effective core potential approximation, which was reported last year, provided an efficient means of probing potential energy surfaces of transition metal complexes. The method has been applied to several important systems of transition metal complexes.

I-C-1 Cobalt Metallocycles. On the Transformation of Bis(acetylene)cobalt to Cobaltacyclopentadiene

Yasuo WAKATSUKI,* Okio NOMURA,* Kazuo KITAURA *(Osaka City Univ.)*, **Keiji MOROKUMA, and Hiroshi YAMAZAKI*** *(*Institute of Physical and Chemical Research)*

[*J. Am. Chem. Soc.*, in press]

Formation of η^5-cyclopentadienyl(triphenylphos-

phine)cobaltacyclopentadienes (4) by the reaction of acetylenes with η^5-cyclopentadienyl (triphenyl-phosphine) (acetylene)cobalt (1) has been investigated in detail. Kinetic studies indicate the intermediacy of η^5-cyclopentadienylbis(acetylene)cobalt (2) which cyclizes to coordinatively unsaturated η^5-cyclopentadienylcobaltacyclopentadiene (3) by spontaneous oxidative coupling reaction. Regioselectivity of the cyclization process is controlled by steric factor of substituents rather than their electronic factor. The structures and bonding of intermediates 2 and 3 are studied with *ab initio* molecular orbital calculations. The transition state of the cyclization reaction is postulated to be low symmetric C_s conformation derived from an "upright" bis-(acetylene)cobalt. This accounts for the observed regioselectivity that the acetylenic carbon bearing a bulky substituent becomes the α-carbon of the metallocycle.

I-C-2 An *Ab-initio* MO Study of Ni(0) Complexes: Stereochemistry of $Ni(PH_3)_2L$ (L = H_2CO or $(CO)_2$) and Comparison of Coordinate Bonds of Various Ligands

Shigeyoshi SAKAKI,* Kazuo KITAURA *(Osaka City Univ.)*, **Keiji MOROKUMA, and Katsutoshi OHKUBO*** *(*Kumamoto Univ.)*

[*Inorg. Chem.*, in press]

Stereochemistry of $Ni(PH_3)_2(H_2CO)$ and $Ni(PH_3)_2(CO)_2$ was studied with the *ab initio* MO method. In $Ni(PH_3)_2(H_2CO)$ the energy decomposition analysis shows that, due to stronger back donation, the planar side-on coordinated complex is more stable than both the pseudo-tetrahedral side-on and the end-on complex. The H_2CO ligand is much distorted in the side-on complex, for the distortion relieves the exchange repulsion and enhances the back-donation. In $Ni(PH_3)_2(CO)_2$, the pseudotetrahedral structure is more stable than the planar one, owing to smaller exchange repulsion. Coordinate bonds of C_2H_4, C_2H_2, CO_2, H_2CO and CO with $Ni(PH_3)_2$ are compared with each other. In the side-on coordination mode, the back-donation increases in the order $CO<C_2H_4<C_2H_2<H_2CO<CO_2$, which agrees with the lowering order of their π^* orbital energies. The electrostatic interaction becomes larger in the order $CO_2<<H_2CO<<CO<C_2H_4\sim C_2H_2$, roughly the increasing order of the negative charge on the coordinating atoms. A weaker back-donation makes the end-on coordination mode less stable than the side-on mode. Exceptional characters of the CO ligand are also discussed and explained.

I-C-3 Reaction Paths of CO Inserion into Pt(II)-CH_3 Bond. An MO Study

Shigeyoshi SAKAKI,* Kazuo KITAURA *(Osaka City Univ.)*, **Keiji MOROKUMA, and Katsutoshi OHKUBO*** *(*Kumamoto Univ.)*

[*J. An. Chem. Soc.*, in press]

The bonding nature and relative stability of $Pt(CH_3)F(CO)(PH_3)$ and $Pt(COCH_3)F(PH_3)$, the reactant and the product of CO insertion, were theoretically studied. The Pt-CH_3 bond in $Pt(CH_3)F(CO)(PH_3)$ is stronger in the structure where CH_3 is trans to PH_3, 1 than in the structure where CH_3 is trans to F, 2. For $Pt(COCH_3)F(PH_3)$ the Y-shaped form is the least stable and is not a local minimum. In the most stable T-shaped structure, F and PH_3 are trans to each other, the fact explainable in terms of the trans-influence effect. Furthermore, all of the probable reaction paths of the CO insertion were examined. The CH_3-migration is an easy path in both the reaction systems 1 and 2, and the concerted move of CO and CH_3 concurrent with the <FPtP opening is easy in 1 but difficult in 2, whereas the CO-migration is difficult in both 1 and 2. The factors determining the choice of reaction paths were presented.

I—D Electronic Structure of Low Dimensional Materials

Recently a great deal of attention is concentrated on the development of new low-dimensional compounds of practical importance. Typical example may be the search of one-dimensional metals or superconductors. Intercalated compounds of graphite or other layer crystals have attracted much interest from the view point of

superconductivity, catalyses, batteries and photovoltaic cells.

Reliable first principle calculations of the elctronic structure is essential for the study of the properties of these materials. During the past year we performed the energy band calculation of the $NbSe_3$, which is the one-dimensional metal with a peculiar transport property.

I-D-1 Electronic Structure and CDW Transitions of $NbSe_3$

Nobuyuki SHIMA

The elctronic band structure of $NbSe_3$ is calculated by the relativistic LCAO-Xα-SCF method.[1] There are five conduction bands whose main orbital component are dz^2 orbitals of Nb atoms. The charge distribution in a unit cell is investigated. About 0.6~0.7 electrons transfer from each Nb atoms to Se atoms. The energy density of states is calculated and compared with the XPS experiment. The partial densities of state of orbital components are also calculated to understand the character of each bands.

The two independent CDW transitions and the behaviors of the hall constant and the resistivity of $NbSe_3$ are explained by the independent nestigns of the Fermi surfaces obtained by the band calculation.[2]

References

1) N. Shima (to be published in *J. Phys. Soc.* Jpn)
2) N. Shima *J. Phys. Soc. Jpn.* **51**, (1982) 11

I—E Development and Application of the LCAO-Xα Direct Force Calculation Method

An energy gradient method is developed for the LCAO-Xα scheme, which is quite convenient for the numerical calculations of forces acting on each ions in the cluster. This method is applied for various problems including chemisorption systems.

I-E-1 Electronic Structure and Equilibirum Geometry of Metal Clusters

Chikatoshi SATOKO

It is experimentally known that surface bond distances between the first and second layers on the surface are contract as compared with bulk bond distances. It may be explained as follows. Surface atoms do not make bonds with the outside region on the surface so that lifting forces acting on the surface atom are missing. The equilibrium position of the surface atom moves into the inside direction for the unbalance between the bonding forces acting on the surface atoms. This explanation may put in the another words such as a surface tension. The larger the surface area of the metal cluster, the stronger the inwardly directing force. It can be expected that the bond length of the large metal cluster become larger with the increasing cluster size. These phenomena are observed experimentally and calculated theoretically in the case of copper and nickel clusters.[1,3]

However, the above discussion ignores the change of the surface electronic structure. If the electron of the surface atom polarizes into the outer direction, the lifting force acting on the surface atom occurs. The bond distance of the almost idatomic molecule except the alkali-earth metal is shorter than that of the bulk substance. On the contrary the bond distance of the alkali-earth metal diatomic molecule (7.35 for Mg and 8.08 a.u. for Ca) is longer than the bulk distance (6.04 a.u. for Mg and 7.46 a.u. for Ca). The calculating results show that the bond distance of the larger metal cluster gradually approaches the bond distance of the bulk.[2] We are now in progress on the study of the relation between the metal cluster and surface relaxations.

References

1) B. Delly, T. Jarborg, A. J. Freeman, and D. E. Ellis, (to be published).
2) C. Satoko, B. Delly, and D. E. Ellis, (to be published)

3) G. Apai, J. F. Hamiltons, T. Stohr, and A. Thompson, *Phys. Rev. letters* **43**, 165 (1979)

I-E-2 Oxidation Process on Metal Surfaces

Chikatoshi SATOKO

Oxidation processes on metal surfaces have been studied by many experimental methods such as LEED, XPS, AES, ELS, SEXAFS and so on. Oxygen molecules are chemisorbed as the molecules or dissociative atoms according to the order of the pressure and the temperature. The dissociative atoms remain on the surface or incoporate into the bulk. The distortion of the surface atom also occurs with a chemisobed atom approaching the surface. It is important to consider the order of surface relaxation on the chemisorption process. The activation energy of the chemisorbed atom is highly depend on the order of the relaxation. The analysis of force calculation is very powerful to decide whether the surface atoms are lifted up or depressed down by the chemisorbed atoms. A method of total energy calculation can not estimate easily the order of the surface relaxation.

In this review we report the result of oxygen chemisorption on the Al(111) and Mg(0001) surfaces.[1,2] An activation energy for the oxygen penetration into the surface is about 1 eV on the Al surface, while not on the Mg surface. This is due to the difference of the surface bonding properties between them. The 3p electrons contribute to the bonding between the Al atoms. The bonding between the Mg atoms is mainly composed of the 3s electrons. The bonding property of the Al atoms is directional as compared with that of the Mg atoms. The oxygen approach must induce the break of the bonding between the surface atoms. The bonding on the Mg surface is more insensitive to the oxygen approach to the surface than that on the Al surface.

References

1) C. Satoko, *Chem. Phys. Lett.*, **83**, 111 (1981)
2) C. Satoko, (to be published.)

I—F Semiclassical Theoretical Studies of Nonadiabatic Transitions in Atomic Processes

Electronically non-adiabatic transitions among low-lying excited adiabatic states have been investigated using the semi-classical collision theory. We have proposed a general analytical procedure to treat a many-state atomic collision problem involving both radial and rotational couplings.

I-F-1 Semiclassical Theory of Rotationally Induced Nonadiabatic Transitions

Hiroki NAKAMURA and Masatoshi NAMIKI
(Takachiho College)

[*Phys. Rev.*, **A24**, 2963 (1981)]

A general procedure is proposed to treat a many-state atomic-collision problem involving both nonadiabatic radial and rotational couplings. The procedure is based on the classical S-matrix theory in a new "dynamical-state" representation. The dynamical states are defined as the eigenstates of a new Hamiltonian operator which is composed of an ordinary electronic Hamiltonian and a Coriolis coupling term. The dynamical potential energies thus obtained avoid crossings even for the rotationally coupled states. At these avoided crossing points the rotationally induced transitions predominantly occur, which are delocalized in the ordinary adiabatic-state representation. The theory is applied to certain two-state- and three-state-model problems, and is shown to work well. An interesting catalytic phenomenon is found in a three-state problem. A certain transition is enhanced by a rotational coupling not directly associated with that transition; besides, a transition directly induced by that rotational coupling is not affected by the coupling responsible for the first transition. This phenomenon can be successfully explained and reproduced by the theory. A condition is discussed for this kind of phenomenon

to occur in a general many-state collision problem involving rotational couplings.

I-F-2 Dynamical-state Representation and Nonadiabatic Electronic Transitions in Atomic Collisions

Hiroki NAKAMURA

[*Phys. Rev.*, in press]

Quantum mechanical elucidation is made to the semiclassical theory in the dynamical state representation previously proposed to deal with analytically the nonadiabatic rotationally induced transitions.[1] This representation transforms the analytical structure of rotational coupling problems into the one equal to that of the ordinary radial coupling problems; thus enables us to apply the conventional analytical formulae such as the Landau-Zener-Stueckelberg or Rosen-Zener formulae. A big advantage of this representation lies in the fact that both radial and rotational nonadiabatic transitions are made to occur locally at the avoided crossing points of the dynamical state potential energies. A general path-integral formulation of scattering matrix is given in terms of a product of two kinds of matrices. A qualitative difference is made clear for the collision energy dependences of the ordinary Landau-Zener type radial transitions and rotationally induced transitions.

Reference

1) H. Nakamura and M. Namiki, *J. Phys. Soc. Japan* **49**, 843 (1980), *Phys. Rev.* **A24**, 2963 (1981).

I—G Theoretical Studies of Dynamic Processes for the e + H_2^+ System

An ultimate purpose of these studies is to understand the mechanism of various dynamic processes of higher- (super-) excited states of molecules.

I-G-1 Two-Electron Excited States and Adiabatic Quantum Defects of H_2: Analysis of Elastic Scattering of Electrons from H_2^+

Hidekazu TAKAGI *(Kitasato Univ.)* **and Hiroki NAKAMURA**

[*Phys. Rev.* in press]

Elastic scattering of electrons from molecular ions presents a basic problem for understanding the various dynamic processes of higher excited states of neutral molecules such as photoionization, preionization and dissociative recombination. Elastic scattering phaseshifts for the spheroidal sσ-, pσ-, pπ-, and dσ-wave are calculated at various internuclear distances and collision energies by using the Kohn-type variational method formulated in the prolate spheroidal coordinate system.[1] The positions and widths of the 1st and 2nd lowest two-electron excited resonance states are obtained for the symmetries $^1\Sigma_g$, $^{1,3}\Sigma_u$, and $^{1,3}\Pi_u$. Some of them are compared with the available data. Adiabatic quantum defects are also obtained by extrapolating the phaseshifts to low energy limit.

Reference

1) H. Takagi and H. Nakamura, *J. Phys.* **B11**, L675 (1978), *ibid* **B13**, 2619 (1980).

I-G-2 Theoretical Studies of Photoionization of Hydrogen Molecules

Yukikazu ITIKAWA *(Inst. of Space and Astron. Science)*, **Hidekazu TAKAGI** *(Kitasato Univ.)*, **Hiroki NAKAMURA, and Hiroshi SATO** *(Ochanomizu Univ.)*

[*Phys. Rev.*, in press]

Quite an accurate estimate of the cross section for the direct photoionization of H_2 is made at three photon energies (λ=736, 650, 584Å). the Hagstrom-Shull type wavefunction is employed to represent the initial ground state of H_2.[1] The final continuum wave function is calculated by the variational method mentioned above. Both cross section (σ) and asymmetric parameter (β) are found to be

sensitive to the accuracy of the inital and final state wavefunctions. Some of the results are shown in Table I. Agreement of the present results with experiments is satisfactory.

Table I. Final vibrational state (v') dependence

$\sigma(v')$ ($10^{-18}cm^2$)	v'=0	1	2	3
present	0.505	0.945	1.082	0.992
Itikawa[2]	0.391	0.746	0.875	0.822
experiment[3]	0.477	0.907	1.048	0.975
$\beta(v')$	v'=0	1	2	3
present	1.797	1.843	1.873	1.895
Itikawa[2]	1.758	1.793	1.820	1.842
experiment[4]	1.76	1.82	1.87	1.88

References

1) S. Hagstrom and H. Shull, *Rev. Mod. Phsy.*, **35**, 624 (1963).
2) Y. Itikawa, *Chem. Phys.*, **37**, 401 (1979).
3) J. E. Pollard, D. J. Trevor, J. E. Reutt, Y. T. Lee, and D, A, Shirley, *J. Chem. Phys.*, **77**, 34 (1982).
4) J. Kreile and A. Schweig, *J. Electron Spect. Relat. Phenom.*, **20**, 191 (1980).

I—H Mode-Selective Multiphoton Excitation in a Model Anharmonic System

Robert E. WYATT *(Univ. of Texas and IMS)*

A computational study was made of the efficienty of mode-selective multiphoton excitation in a model nonseparable anharmonic oscillator system. The well studied Heńon-Heiles potential (two degrees of freedom; cubic coupling term) was used. The time evolution of quantal wavepackets was treated *via* Floquet theory; periodicity of the classical laser field, $E_0\cos\omega t$, was utilized to formulate the propagator. In a previous study by Hose and Taylor,[1] a criterion was developed in order to identify those quantum eigenstates corresponding to classical quasiperiodic motion (precessing or librating trajectories). In the present dynamical study, it was found that high level multiphoton excitation into a subset of the quantum quasiperiodic states (precessing, high angular momentum trajectories) can occur with high efficiency. The requirements on the laser are: (a) $\hbar\omega$ must be close to the ladder spacing, or a multiple of it; (b) the field strength E_0 must be large enough to compensate for detunings in the ladder; (c) the field strength must not be so large that many "background" states are included within the power-broadened width of each ladder state. In addition, the dipole coupling elements between successive ladder states must be greater than the coupling between ladder states and background states (pseudoselection rule).

Reference

1) G. Hose and H. S. Taylor, *J. Chem. Phys.*, **76**, 5356 (1982).

RESEARCH ACTIVITIES II
Department of Molecular Structure

II—A High Resolution Spectroscopy of Transient Molecules

During the course of chemical reactions many transient molecules appear as intermediates. However, because of their high reactivities (*i.e.* short lifetimes), the knowledge on these transients is still very much limited. Many of them have open-shell electronic structures, which characterize such species as free radicals and cause splittings in their high-resolution spectra because of fine structure and/or hyperfine structure interactions of unpaired electrons. Analyses of these structures provide us with information on the electronic properties of molecules which is not obtainable for molecules without unpaired electrons. High resolution spectroscopy not only provides molecular constants of transient molecules at very high precision, but also allows us to unambiguously identify such species in chemical reaction systems and to unravel the details of reaction mechanisms. The present project will also be of some significance in related fields such as astrophysics and environmental researches.

II-A-1 Infrared-Optical Double Resonance Spectroscopy of the NH_2 Radical

Kentarou KAWAGUCHI, Tetsuo SUZUKI, Shuji SAITO, Takayoshi AMANO *(Univ. of Tokyo),* **and Eizi HIROTA**

Inrared (CO_2/N_2O laser) — optical (dye laser) double resonance has been proved to be useful in unraveling the details of the energy level structures in excited electronic states.[1] Particular attention has been paid to perturbations in the $\tilde{A}$ state of NH_2, and to detection of highly excited vibrational states associated with the ground electronic state through analyses of such perturbations. This sort of measurements has been extended to the following levels (the infrared transitions in the $\tilde{A}$ state are listed:)

(1) (0,9,0) $2_{20} \rightarrow$ (0,8,0) 3_{31}, (2) (0,10,0) $2_{12} \leftarrow$ (0,9,0) 2_{21} and (0,10,0) $3_{13} \leftarrow$ (0,9,0) 3_{22}, (3) (0,12,0) $N_{1,N-1} \leftarrow$ (0,11,0) $N_{0,N}$ with $N = 1 \sim 7$, and (4) (0,11,0) $3_{03} \leftarrow$ (0,10,0) 2_{12}, of which (3), as was already discussed briefly,[2] showed the presence of "u" levels for $N = 3$ and 5. Although the detailed analysis allowed us to determine the rotational quantum number N and which spin component, F_1 or F_2, they belong to, it is still difficult to assign their vibrational quantum numbers.

References

1) T. Amano, K. Kawaguchi, M. Kakimoto, S. Saito, and E. Hirota, *J. Chem. Phys.*, **77**, 159 (1982).
2) K. Kawaguchi, T. Suzuki, S. Saito, T. Amano, and E. Hirota, *IMS Ann. Rev.*, 31 (1981).

II-A-2 The Microwave Spectrum of the PH_2 Radical

Yasuki ENDO, Shuji SAITO, and Eizi HIROTA

In order to determine molecular parameters, including hyperfine coupling constants, three rotational transitions, $1_{10} \leftarrow 1_{01}$, $2_{20} \leftarrow 2_{11}$, and $3_{30} \leftarrow 3_{21}$, were observed by using a source-frequency modulation spectrometer with a 1 m long free space cell. The PH_2 radical was generated directly in the cell by glow discharge in a mixture of PH_3 and O_2. An analysis of the observed spectra, combined with far-infrared[1] and mid-infrared LMR spectra[2] and with laser induced fluorescence spectra described in **II-A-16**, improved the rotational and the spin-rotation interaction constants, as shown in Table I, where the data already reported[2,3] are also listed for comparison. The observed hyperfine structure gave the magnetic hyperfine coupling constants for both P and H nuclei and also the P nuclear spin-rotation interaction constatns, which are compared with the earlier LMR results in Table I.

Table I. Molecular Constans of PH_2 in the $\tilde{X}^2B_1$ State (MHz)[a]

Constant	Present	Ref. 2)	Ref. 3)
A	273 782.0(26)	273 784.0(60)	273 766.0(150)
B	242 346.6(26)	242 363.3(82)	242 342.3(115)
C	126 342.5(26)	126 344.5(60)	126 351.7(70)
Δ_N	16.554(112)	16.42(19)	16.15(30)
Δ_{NK}	−54.41(43)	−52.70(55)	−54.63(95)
Δ_K	87.27(48)	84.57(40)	84.85(163)
δ_N	7.470(25)	7.57(14)	7.180(150)
δ_K	−2.984(190)	−3.14(20)	−2.41(35)
ϵ_{aa}	−8 427.48(158)	−8 436.(28)	−8 438.(79)
ϵ_{bb}	−2 458.62(45)	−2 434.(18)	−2 454.(69)
ϵ_{aa}	−7.12(105)	−22.(13)	−2.(63)

Constant	Present	Ref. 1)
a_F(P)	207.25(13)	217.(8)
T_{aa}(P)	−300.24(13)	−303.(13)
T_{bb}(P)	−321.86(29)	−318.(10)
T_{cc}(P)	622.10(29)	621.(10)
a_F(H)	−48.84(13)	−49.(2)
T_{aa}(H)	−1.00(10)	−3.(6)
T_{bb}(H)	−4.46(24)	−3.(6)
T_{cc}(H)	5.46(26)	5.(6)
C_{aa}(P)	0.960(53)	—
C_{bb}(P)	0.523(75)	—
C_{cc}(P)	0.13(15)	—

a. Values in parentheses denote 2.5 times standard deviations and apply to the last digits of the constats. Higher-order (centrifugal distortion) terms are not listed.

References

1) P. B. Davies, D. K. Russell, and B. A. Thrush, *Chem. Phys. Lett.*, **37**, 43 (1976); P. B. Davies, D. K. Russell, B. A. Thrush, and H. E. Radford, *Chem. Phys.*, **44**, 421 (1979).
2) G. W. Hills and A. R. W. McKellar, *J. Chem. Phys.*, **71**, 1141 (1979); A. R. W. McKellar, *Faraday Discuss.*, **71**, 63 (1981).
3) F. W. Birss, G. Lessard, B. A. Thrush, and D. A. Ramsay, *J. Mol. Spectrosc.*, **92**, 269 (1982).

II-A-3 Perturbations in the $\tilde{A}^1A''(010)$ State of the HCF Molecule: the Zeeman Effect

Tetsuo SUZUKI, Shuji SAITO, and Eizi HIROTA

As was described previously,[1] the $A^1A''(010)$ state of HCF, one of the simplest carbenes, is subjected to large perturbations. Those found for $K_a' = 1$ levels were explained mainly in terms of an electronic Coriolis interaction with highly excited vibration-rotation levels associated with the ground electronic state. However, other perturbations that are more local in nature do not appear to conform to the same explanation. For example, the $J_{0,J}$ levels at $J = 13\sim18$ show Zeeman effects that are as large as the Bohr magneton, *i.e.* nearly one or two orders of magnitude larger than those expected from the electronic Coriolis interaction model. Figure 1 shows an example of such a perturbed line, $^PQ_1(17)$. These large Zeeman effects are rather ascribed to mixing of the $\tilde{A}$ state with the $\tilde{a}^3A''$ state. Triplet levels that interact with the $\tilde{A}^1A''(010)$ $J_{0,J}$ level through spin-orbit coupling are either $N_{1,N}$, $J = N$ (F_2) or $N_{1,N-1}$, $J = N \pm 1$ (F_1, F_3). It is, however, still difficult to quantitatively explain all the observed Zeeman effects in terms of a simple singlet-triplet pair-wise interaction model.

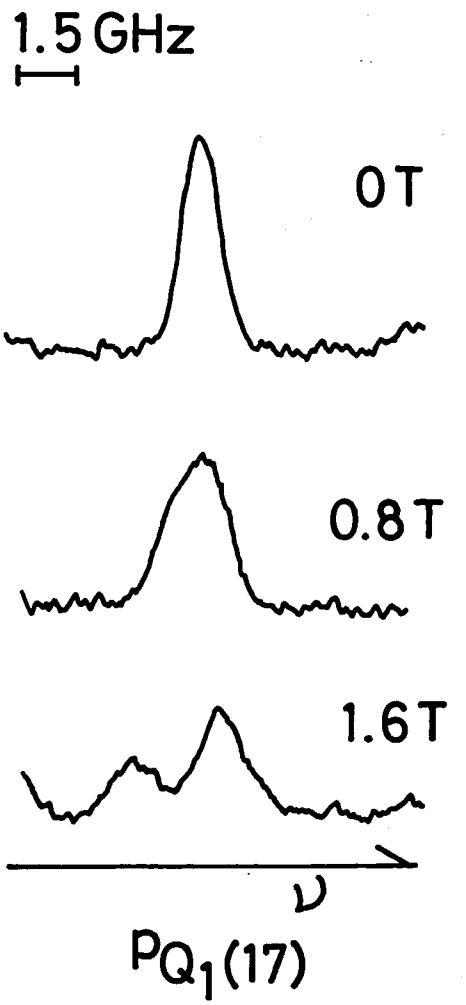

Figure 1. Zeeman effect observed for $^PQ_1(17)$ of the HCF $\tilde{A}^1A''(010) \leftarrow \tilde{X}^1A'(000)$ transition.

Reference

1) T. Suzuki, S. Saito, and E. Hirota, *IMS Ann. Rev.*, 38 (1981).

II-A-4 Microwave Spectroscopy of the Methoxy Radical

Yasuki ENDO, Shuji SAITO, and Eizi HIROTA

The methoxy radical has been known as one of the most important intermediates in hydrocarbon combustion reactions and other similar reactions, but it is only quite recently that high-resolution spectroscopic studies were carried out. Russell and Radford[1] have observed and analyzed the far-infrared LMR spectra of CH_3O. In the present work we observed the microwave spectra of both CH_3O and CD_3O, using a source-frequency modulation spectrometer with a 1 m long free space cell. The radical was produced by the reaction of methanol with microwave discharge products of CF_4. Figure 1 shows an example of the observed spectra; each rotational transition is split into K and proton hyperfine components, and also Λ-type doublet for $K = 1$. It is interesting to note that $K = 0$ and $^2E_{1/2}$ $K = -1$ transitions are split into two components of equal intensities, because the three protons are nonequivalent with respect to the unpaired electron orbital of E symmetry. A Hamiltonian mainly worked out by Hougen[2] was employed to analyze the observed spectra; the effects of the (2,2) (*i.e.* the Λ-doubling) and (2,−1) interactions were clearly observed and were well explained by Hougen's theory. The observed rotational constants lead to r(C−O) of about 1.363 Å, which is considerably smaller than those (1.44 Å, 1.405 Å) predicted by *ab initio* calculations.

References

1) H. E. Radford and D. K. Russell, *J. Chem. Phys.*, **66**, 2222 (1977); D. K. Russell and H. E. Radford, *J. Chem. Phys.*, **72**, 2750 (1980).
2) J. T. Hougen, *J. Mol. Spectrosc.*, **81**, 73 (1980).

II-A-5 A Rovibronic Interaction in the Π Linear Triatomic Molecule: Microwave Spectroscopic Investigation of the NCO Radical in the $\tilde{X}(010)$ $^2\Sigma$ State

Kentarou KAWAGUCHI, Shuji SAITO, and Eizi HIROTA

As was pointed out in a previous paper,[1] the Renner effect must be taken into account in discussing the rotational spectrum of the linear triatomic molecule in a Π state. In the present work the NCO radical was investigated by microwave spectroscopy, placing a special emphasis on the $v_2 = 1$ $\mu^2\Sigma$ and $\kappa^2\Sigma$ states. The observation extends from the $J = 1.5 \leftarrow 0.5$ transition at 45 GHz up to the $J =$

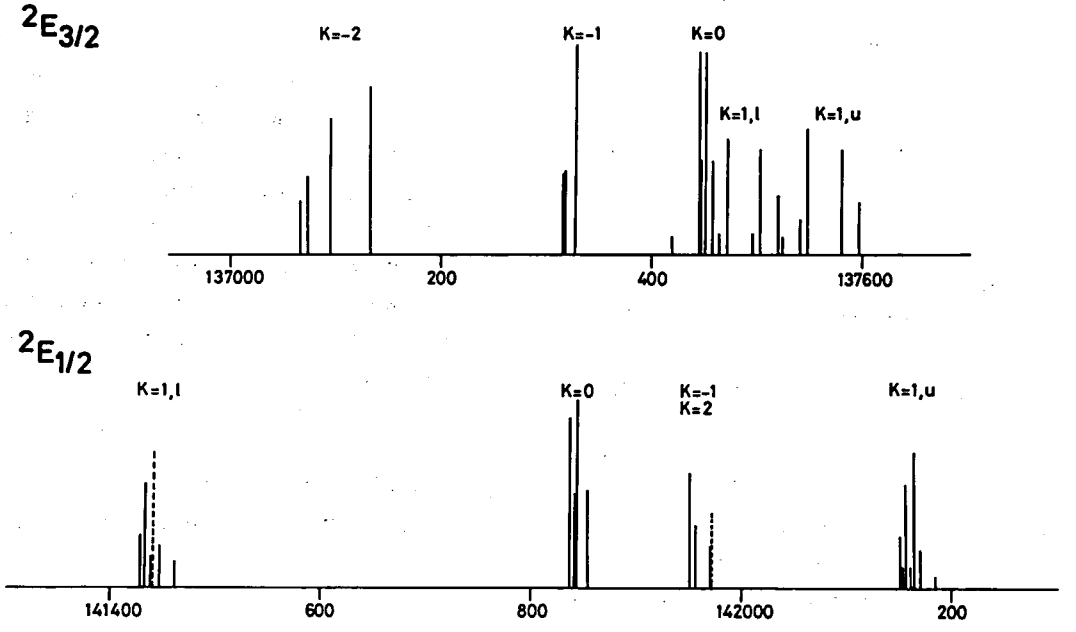

Figure 1. The $J = 2.5 \leftarrow 1.5$ transitions of CH_3O. The broken lines denote the transitions that could not be observed because of overlapping by other lines.

8.5 ← 7.5 transition at 166 GHz. The rotational Hamiltonian used for the (010) $^2\Sigma$ state has been obtained by taking into account the interactions with the (110), (011), and (030) states to the second and third order. The molecular constants thus obtained are listed in Table I; the parameters s and t make the rotational constants of the $\mu^2\Sigma$ and $\kappa^2\Sigma$ states different and γ_{vib} denotes the difference between the spin-rotation interaction constants of the two states. The rotational constant obtained differs from that in the (010) $^2\Delta$ state, and the discrepancy was explained by the third-order and fourth-order perturbation treatments of the interactions with the (030) and (110) states and with the (050), (130), and (210) states, respectively. This treatment has also been applied to other Π state molecules as shown in the Table II. The discrepancies for CO_2^+ and CCC remain to be explained.

Table I. Molecular Constants of NCO in v_2= 1$^2\Sigma$ (MHz)[a]

B	11 706.3014(69)	hyperfine	constant
γ	−54.77(11)	a	63.54(42)
s	−10.4818(66)	b	29.31(36)
γ_{vib}	11.591(24)	c	−46.22(48)
t	6.21(27)	eQq_1	−2.08(36)

a. Values in parentheses denote three standard errors and apply to the last digits of the constants.

Table II. Difference in the Rotational Constants, B[(010) $^2\Delta$] − B[(010) $^2\Sigma$] (MHz)

Molecule	State	ϵ[a]	obs.	calc.
NCO	$\tilde{X}\,^2\Pi$	−0.14	1.99	1.77
BO_2	$\tilde{X}\,^2\Pi$	−0.19	3.8	3.0
CNC	$\tilde{X}\,^2\Pi$	0.55	44.	40.
CO_2^+	$\tilde{X}\,^2\Pi$	−0.19	−30.	4.
CCC	$\tilde{A}\,^1\Pi$	0.54	99.	33.

a. Renner parameter.

Reference

1) K. Kawaguchi, E. Hirota, and C. Yamada *Mol. Phys.*, **44**, 509 (1981).

II-A-6 The Microwave Spectrum of the HCCN Radical

Shuji SAITO, Yasuki ENDO, and Eizi HIROTA

The HCCN radical is one of the simplest carbenes. An electron spin resonance (ESR) study[1] and an infrared and ultraviolet observation[2] of this radical in low temperature matrices have indicated that the molecule is linear and has the triplet ground state like the parent carbene CH_2. We have observed pure rotational transitions of HCCN in mm-wave region, using a source-frequency modulation spectrometer with a 1 m long free space cell. This is the first spectroscopic observation of the HCCN molecule in the gas phase. The radical was generated by the reaction of CF_4 discharge products with CH_3CN in the cell. Four successive rotational transitions, from N = 6←5 up to N = 9←8, each consisting of three fine structure components, were observed, and were analyzed using a Hamiltonian which consisted of the rotational, the centrifugal distortion, the spin-spin interaction, and spin-rotation interaction terms. No hyperfine structure has been resolved. The spin-spin interaction constant thus obtained agrees well with that obtained from the ESR spectra, 12935(5) MHz.[1] The observed spectra are completely consistent with the linear structure, although careful observation of excited state spectra would be necessary to eliminate the possibility of a bent structure.

References

1) R. A. Bernheim, R. J. Kempf, J. V. Gramas, and P. S. Skell, *J. Chem. Phys.*, **43**, 196 (1965).
2) A. Dendramis and G. Leroi, *J. Chem. Phys.*, **66**, 4334 (1977).

II-A-7 Infrared Diode Laser Spectroscopy of the CF_3 Radical: Molecular Structure and Force Field

Chikashi YAMADA and Eizi HIROTA

The observation of the ν_3 Q-branch transitions of CF_3 has previously been reported,[1] but P- and R-branch transitions could not have been assigned. Recently Endo *et al.*[2] succeeded in observing pure rotational transitions of CF_3 by microwave spectroscopy. This result has aided us to assign 465 lines observed for the ν_3 band. Because the ν_3 state is subjected to (2,−1) as well as (2,2) interactions, the present analysis permits us to estimate the C_0 rotational constant which is otherwise impossible to determine from infrared spectra. The molecular constants thus obtained are summarized in Table I.

The two ground-state rotational constants, B_0 and C_0, lead to the r_0 structure: r_0(C–F) = 1.318(2) Å and θ_0(FCF) = 110.7(4)° with the standard errors in parentheses. The general harmonic force field was calculated using the normal mode frequencies of both $^{12}CF_3$ and $^{13}CF_3$ in low temperature matrices[3] and also the Coriolis coupling constant ζ_3 obtained by present work. The results are shown in Table II.

Table I. Molecular Constant of CF_3 (MHz)[a]

Constant	Ground state[b]	ν_3 = 1
B	[10 900.9118]	10 880.64415(755)
C	5 653.9(102)	5 639.1(102)
D_N	[0.013882]	0.013 971 09(498)
D_{NK}	[–0.02343]	–0.023 876 3(220)
D_K	[0.0102]	0.009 551 2(468)
$C\zeta_3$		4 130.9(102)
q		–18.959 5(221)
η_N		0.289 073(685)
η_K		–0.202 764(697)
r		8.687(194)
E_v(cm^{-1})		1 260.16193(34)

a. Values in parentheses denote standard errors and apply to the last digits of the constants.
b. Values in square brackets were taken from Ref. 2) and were constrained in the fitting.

Table II. Harmonic Force Field of CF_3

F_{11}	8.2211 md/Å	F_{33}	6.0669	md/Å
F_{22}	3.0583 md/Å	F_{44}	1.2954	md/Å
F_{12}	0.8224 md	F_{34}	–0.7589	md

	$^{12}CF_3$		$^{13}CF_3$	
	obs.	calc.	obs.	calc.
ν_1 (cm^{-1})	1087.[a]	1086.9	1063.[a]	1063.1
ν_2 (cm^{-1})	703.[a]	702.8	695.[a]	695.2
ν_3 (cm^{-1})	1260.16[b]	1261.4	1228.[a]	1226.8
ν_4 (cm^{-1})	512.[a]	513.0	512.[a]	511.0
ζ_3	0.7326[b]	0.7326		

a. Ref. 3), b. Present work.

References

1) C. Yamada and E. Hirota, *IMS Ann. Rev.*, 42 (1980).
2) Y. Endo, C. Yamada, S. Saito, and E. Hirota, *J. Chem. Phys.*, **77**, 3376 (1982).
3) D. E. Milligan and M. E. Jacox, *J. Chem. Phys.*, **48**, 2265 (1968).

II-A-8 Difference Frequency Laser Spectroscopy of the ν_3 Band of the CH_3 Radical

Takayoshi AMANO *(NRC, Canada)*, **P. F. BERNATH** *(NRC, Canada)*, **Chikashi YAMADA, Yasuki ENDO, and Eizi HIROTA**

As an extension of the earlier work on the CH_3 ν_2 band,[1] the ν_3 fundamental band at 3 μm has been detected in absorption with a tunable difference frequency laser. The radical was generated directly in a multiple-reflection cell by a 60 Hz discharge in di-*tert*-butylperoxide, or by a DC discharge in one of CH_4, CH_3CN, and CH_3OH. Zeeman modulation was found to be rather inefficient because of small spin-rotation splitting, but has permitted us to observe 47 transitions. An analysis of the observed spectra gave molecular constants listed in Table I; the ground-state parameters were fixed to those reported in Ref. 1). The ν_3 band was found to be an order of magnitude weaker than the ν_2 band, in qualitative agreement with the observation made by Snelson[2] for the CH_3 radical trapped in a neon matrix.

TableI. Molecular Constants of CH_3 in the ν_3 State (cm^{-1})[a]

ν_0	3160.8212(12)	$C\zeta$	0.34588(22)
B	9.47110(14)	$\eta_N\times10^3$	–0.121(21)
C	4.70167(15)	$\eta_K\times10^3$	0.151(29)
$D_N\times10^3$	0.7590(37)	q	0.00642(25)
$D_{NK}\times10^3$	–1.366(11)	$q_N\times10^3$	0.0296(71)
$D_K\times10^3$	0.6371(95)		

a. Values in parentheses denote one standard error and apply to the last digits of the constants.

References

1) C. Yamada, E. Hirota, and K. Kawaguchi, *J. Chem. Phys.*, **75**, 5256 (1981).
2) A. Snelson, *J. Phys. Chem.*, **74**, 537 (1970).

II-A-9 The Microwave Spectrum of the CH_2F Radical

Yasuki ENDO, Shuji SAITO, and Eizi HIROTA

The fluorinated methyl radicals have been investigated by electron spin resonance (ESR)[1] and infrared spectroscopy[2] in low temperature matrices. Because CH_2F and CHF_2 are located between the

planar CH_3 and the pyramidal CF_3 radicals, either one of them may exhibit the effect of the inversion in their spectra. In the present work we observed microwave spectra of CH_2F. The radical was generated directly in a 1 m long free space cell by the reaction of CF_4 discharge products with CH_3F. Only gas-phase high-resolution spectra published heretofore are far-infrared LMR spectra by Mucha *et al.*,[3] who estimated $B + C$ to be 1.953 cm^{-1}. This result allowed us to readily observe the $N = 2 \leftarrow 1$ transitions at 117.1 GHz. The measurement was also performed for $N = 3 \leftarrow 2$, and 90 paramagnetic lines were observed, of which 57 were assigned to the ground-state transitions. The molecular constants obtained are listed in Table I. The assigned lines show proton spin statistical weights, indicating that the effective symmetry is C_{2v}, but the presence of satellite lines that are about 1/4 as strong as the ground-state lines suggests that the antisymmetric inversion state is located at about 300 cm^{-1} above the ground state.

Table I. Molecular Constants of the CH_2F Radical in the Ground State (MHz)

A	265 822.	ϵ_{aa}	−1 075.73
B	30 946.229	ϵ_{bb}	−185.81
C	27 729.873	ϵ_{cc}	−1.35
Δ_N	0.078 31		
Δ_{NK}	1.129 8		
δ_N	0.006 9		
a_F(F)	184.00	a_F(H)	−60.50
T_{aa}(F)	−255.20	T_{aa}(H)	−25.70
T_{bb}(F)	−212.49	T_{bb}(H)	31.0
T_{cc}(F)	467.69	T_{cc}(H)	−5.3

References

1) R. W. Fessenden and R. H. Schuler, *J. Chem. Phys.*, **43**, 2704 (1965).
2) M. E. Jacox and D. E. Milligan, *J. Chem. Phys.*, **50**, 3252 (1969)
3) J. A. Mucha, D. A. Jennings, K. M. Evenson, and J. T. Hougen, *J. Mol. Spectrosc.* **68**, 122 (1977).

II-A-10 Laser-excited Fluorescence Spectroscopy of the CH_2S $\tilde{a}^3A_2(v_3=1) \leftarrow \tilde{X}^1A_1$ Band

Tetsuo SUZUKI, Shuji SAITO, and Eizi HIROTA

Because of interest in metastable states with spin multiplicity different from that of the ground state, we have observed and analyzed laser excitation spectra of the H_2CS $\tilde{a}^3A_2(v_3=1) \leftarrow \tilde{X}^1A_1$ band. As is well known,[1] this forbidden band is made allowed mainly by spin-orbit mixing of $\tilde{a}^3A_2$ with $\tilde{B}^1A_1$. The molecule was generated by pyrolyzing trimethylene sulfide at 850°C. A dye laser, CR 599-21, with DCM dye was employed; the output was 20 ~ 50 mW. Nine hundred observed lines were combined with the data obtained from a MODR experiment **(II-A-11)** to determine upper-state constants, as shown in Table I. Ground-state parameters were constrained to the microwave result.[2] The analysis was straightforward up to $K_a' = 4$, but $K_a' = 5$ levels were found to be perturbed. A careful examination of the observed spectra, aided by ground-state combination differences, revealed that the perturbation was due to a Coriolis interaction between $v_3' = 1$ and $v_6' = 1$. Through the analysis of this perturbation some preliminary constants were obtained for $v_6' = 1$, as shown in Table I.

Table I. Molecular Constants of CH_2S in the $\tilde{a}^3A_2$ v_3=1 State (MHz)[a]

A	280 455.(10)	Spin-spin interaction constant	
B	16 399.60(27)	α	−43 493.(40)
C	15 495.49(25)	β	2 556.0(78)
Δ_N	0.024 68(18)	Spin-rotation interaction constant	
Δ_{NK}	1.038(29)	a_0	4 876.9(50)
Δ_N	23.16(46)	a	4 682.4(53)
δ_N	0.001 134(84)	b	−82.82(26)
δ_K	0.646(66)		
ν [$\tilde{a}$ v_3'=1 ← $\tilde{X}$] (cm^{-1})		15 369.0314(36)	
$\lvert G_c \rvert$ (Coriolis parameter)		5 470.(130)	
v_6'=1	$B + C$	32 184.6(28)	
ν [$\tilde{a}$ v_6'=1 − $\tilde{X}$] (cm^{-1})		15 269.607(70)	

a. Values in parentheses denote 3σ and apply to the last digits of the constants.

References

1) R. H. Judge, D. C. Moule, and G. W. King, *J. Mol. Spectrosc.*, **81**, 37 (1980).
2) Y. Beers, G. P. Klein, W. H. Kirchhoff, and D. R. Johnson, *J. Mol. Spectrosc.*, **44**, 553 (1972).

II-A-11 Microwave-Optical Double Resonance Spectroscopy of H_2CS: Hyperfine Structure in the $\tilde{a}^3A_2$ $v_3 = 1$ State

Tetsuo SUZUKI, Shuji SAITO, and Eizi HIROTA

As shown previously,[1] MODR is one of the most useful methods for exploring the level structures in excited electronic states. In the present work we applied it to the $\tilde{a}$ state of H_2CS. A ring dye laser SP 380 A was employed to excite the electronic transition $\tilde{a} \leftarrow \tilde{X}$; its output power 100 ~ 150 mW was large enough to saturate the transition. Microwave and rf sources were the same as those employed in Ref. 1). Signal averaging was often needed to observe weak signals. The observed rotational transitions were those between K-type doublets; $N = 4$, 5, and 9 and $N = 5 \sim 9$ (F_1 and/or F_3) were detected for $K = 1$ and $K = 2$, respectively. An analysis of the observed spectra yielded one dipole-dipole interaction hyperfine parameter $|T_{bb} - T_{cc}|$ to be 10.3 (27) MHz with 3σ in parentheses. Transition frequencies corrected for hyperfine contributions were combined with laser excitation spectra to obtain the rotational and fine structure constants, as described in **II-A-10**.

Reference

1) K. Takagi, S. Saito , M. Kakimoto, and E. Hirota, *J. Chem. Phys.*, **73**, 2570 (1980).

II-A-12 Dye Laser Excitation Spectroscopy of the CCN Radical

Kentarou KAWAGUCHI, Tetsuo SUZUKI, Takahiro KASUYA *(IPCR)*, Shuji SAITO, and Eizi HIROTA

Because of our interest in rovibronic interactions including Renner effect in linear molecules with unquenched electronic angular momentum along the molecular axis, we have observed and anlyzed the $\tilde{A}^2\Delta_i(010)$ (Φ and Π) $\leftarrow$ $\tilde{X}^2\Pi_r(010)$ (Δ and $\mu\Sigma$) bands of CCN. Merer and Travis[1] were the first to observe high-resolution spectra of CCN in the gas phase, and one of the three transitions they observed, $\tilde{A}(000)\ ^2\Delta \leftarrow \tilde{X}(000)\ ^2\Pi$, has recently been reinvestigated by Kakimoto and Kasuya[2] with Doppler-limited resolution. The radical was generated by the reaction of CH_3CN with CF_4 microwave discharge products. Using the same spectroscopic system as in Ref. 2) [a Kr^+ laser (CR 3000 K) – pumped dye laser (CR 599-21) with coumarine 460 dye as a source, with the output power of 10 ~ 20 mW] 325 lines were observed and 98% of them were assigned. A least-squares analysis yielded molecular constants shown in Table I. The difference in the B rotational constants, $B(^2\Delta) - B(^2\Sigma)$, when analyzed as in the case of NCO (**II-A-5**), yielded two anharmonic potential parameters, $W_1 = 48.1\ cm^{-1}$ and $W_2 = -3.8\ cm^{-1}$.

Table I. Molecular Constants of CCN in the $\tilde{X}(010)$ and $\tilde{A}(010)$ States (cm^{-1})[a]

	$\tilde{X}^2\Pi_r$ (010) $^2\Delta$	$\tilde{X}^2\Pi_r$ (010) $\mu^2\Sigma$
A	35.9977(18)	
B	0.401 249(33)	0.401 807(63)
γ	-0.009 00(13)	0.007 58(18)
$\gamma_D \times 10^7$		-0.85(39)
$D \times 10^6$	0.279(17)	0.135(39)
	$\tilde{A}^2\Delta_i$ (010) $^2\Phi$	$\tilde{A}^2\Delta_i$ (010) $^2\Pi$
A	-0.7864(18)	-0.7968(36)
B	0.414 984(33)	0.414 965(63)
γ	0.000 351(63)	[0.000 351][b]
$D \times 10^6$	0.188(18)	0.084(69)
ν_0 ($\tilde{A} \leftarrow \tilde{X}$)	21 427.5084(11)	21 527.6711(15)

a. Values in parentheses denote 3σ and apply to the last digits of constants.
b. Fixed.

References

1) A. J. Merer and D. N. Travis, *Can. J. Phys.*, **43**, 1795 (1965).
2) M. Kakimoto and T. Kasuya, *J. Mol. Spectrosc.*, **94**, 380 (1982).

II-A-13 The Microwave Spectrum of the SiN Radical

Shuji SAITO, Yasuki ENDO, and Eizi HIROTA

The SiN radical is attracting attention of spectroscopists and radioastronomers, because it is one of candidate molecules to be detected in interstellar space. A high-resolution spectroscopic study has recently been carried out by Bredohl *et al.*,[1] who determined the $^2\Sigma^+$ ground-state parameters by analyzing the $B^2\Sigma^+ \rightarrow X^2\Sigma^+$ band, but no microwave spectra have been observed, making

radioastronomical observation of this radical difficult. We succeeded in observing its microwave spectra, using a source-frequency modulation spectrometer with a 3.5 m long free space cell. The radical was generated directly in the cell by a DC discharge in a mixture of $SiCl_4$ and N_2. The reaction of active nitrogen with $SiCl_4$, as employed in Ref. 1), did not produce enough amount of SiN. Sixteen observed transitions with $N = 2 \leftarrow 1$, $3 \leftarrow 2$, and $4 \leftarrow 3$ yield molecular constants of SiN in the ground state, B_0, D_0, γ_0, b and c. The $eQq(^{14}N)$ constant was found to correlate with c, and was thus fixed to the value of CN. When the α_e constant of Ref. 1) was used, B_e and r_e were calculated to be 21 912.50 (46) MHz and 1.572 066 (35) Å, respectively. The observed Fermi contact term $b + c/3$ corresponds to the unpaired electron orbital s character of 3.4% at the N nucleus.

Reference

1) H. Bredohl, I. Dubois, Y. Houbrechts, and M. Singh, *Can. J. Phys.*, **54**, 680 (1976).

II-A-14 Infrared Diode Laser Spectroscopy of the CH_2F Radical

Chikashi YAMADA and Eizi HIROTA

As described in **II-A-9**, the CH_2F radical may exhibit the effect of the inversion in its high-resolution spectra. In the present work we have applied infrared diode laser spectroscopy to the C-F stretching band of CH_2F. According to Jacox and Milligan[1] this band appears at 1163 cm^{-1} in low temperature matrices. We have searched for vibration-rotation spectra in the region 1130 ~ 1190 cm^{-1}, and have detected more than 100 lines, using either Zeeman modulation or discharge current modulation. Two reactions, $CH_3F + F \rightarrow CH_2F + HF$ and glow discharge in $CH_2FCOOCH_3$, were found to generate CH_2F, the latter being more efficient. About 50 lines were assigned to a parallel band. Figure 1 shows four Q branch series; it is easily seen that lines with even K are stronger than those with odd K. Therefore, this band was assigned to the one originating from the ground vibrational state. As in the case of microwave spectroscopy (**II-A-9**), a hot band appears to accompany the main band, indicating that the potential for the out-of-plane mode is a symmetric double minimum type with a low potential hump at the center, *i.e.* at the planar configuration. The band origin of the main band was determined to be 1170.41515(39) cm^{-1} with σ in parentheses, which is about 7 cm^{-1} larger than the matrix frequency.[1]

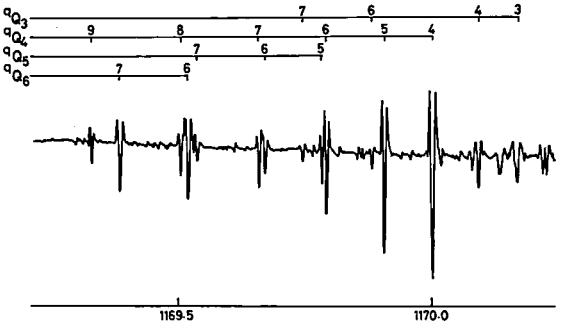

Figure 1. A part of the C-F stretching band of the CH_2F radical. Four Q branch series were recorded by Zeeman modulation.

Reference

1) M. E. Jacox and D. E. Milligan, *J. Chem. Phys.*, **50**, 3252. (1969); M. E. Jacox *Chem. Phys.*, **59**, 199 (1981).

II-A-15 The Microwave Spectrum of the CF Radical

Shuji SAITO, Yasuki ENDO, Michio TAKAMI *(IPCR)*, and Eizi HIROTA

The CF molecule is a typical $^2\Pi$ diatomic radical, and has attracted attention of molecular spectroscopists. After we reported the observation of the $^2\Pi_{1/2}$ $J = 3/2 \leftarrow 1/2$ transition,[1] Saykally *et al.*[2] analyzed the $^2\Pi_{3/2}$ $J = 11/2 \leftarrow 9/2$ transition observed by far-infrared LMR, by combining it with an earlier EPR data.[3] More recently Van den Heuvel *et al.*[4] observed a few rotational transitions around 1000 GHz by generating side bands of far-infrared laser lines, and have analyzed their data augmented by infrared diode laser spectra.[5] However, all of these previous works failed to determine the four hyperfine parameters, *a, b, c,* and *d,* precisely. The present work is an extension of Ref. 1), and now covers the $J = 3/2 \leftarrow 1/2$ and $5/2 \leftarrow 3/2$ transitions of both $^2\Pi_{1/2}$ and $^2\Pi_{3/2}$. A harmonic generator described in **II-B-1** was em-

ployed. Molecular constants obtained from the observed spectra are listed in Table I, along with those of previous works for comparison. The observed hyperfine coupling constants indicate that the unpaired electron spin distribution around the fluorine atom is very close to that of a p_π orbital.

References

1) S. Saito, Y. Endo, and E. Hirota, *IMS Ann. Rev.*, 42 (1980).
2) R. J. Saykally, K. G. Lubic, A. Scalabrin, and K. M. Evenson, *J. Chem. Phys.*, **77**, 58 (1982).
3) A. Carrington and B. J. Howard, *Mol. Phys.*, **18**, 225 (1970).
4) F. C. Van den Heuvel, W. L. Meerts, and A. Dymanus, *Chem. Phys. Lett.*, **88**, 59 (1982).
5) K. Kawaguchi, C. Yamada, Y. Hamada, and E. Hirota, *J. Mol. Spectrosc.*, **86**, 136 (1981).

Table I. Molecular Constants of the CF Radical in the $X^2\Pi_r$ State (MHz)

	Present[a,b]	Ref. 4)	Ref. 2)[a]	Ref. 5)[a]	Ref. 3)
Spectral data used	MW	FIR(IR)	FIR-LMR(EPR)	IR(MW)	EPR
B_0	42 196.663(21)	42 196.634(59)	42 196.35(7)	42 196.45(53)	
D_0	0.1993(11)	0.19870(23)		0.1991(38)	
A_J^{eff}	−3.7203(78)	−3.97(11)		−3.92(50)	
p_0	255.953(19)	255.60(35)		257.22(53)	
q_0	0.691(12)	0.760(14)	0.83(48)		
$a+(b+c)/2$	664.07(58)		666(21)		662.9(30)
$a-(b+c)/2$	747.58(23)				
b	269.2(34)	261(6)	253(55)		190(50)
d	792.17(21)	772(27)	782(773)		
a	705.82(41)	633(29)			
c	−352.7(42)				
μ(D)	0.645(14)				0.65(5)

a. Values in parentheses denote 2.5 times standard deviation and apply to the last digits of the constant.
b. A_0 is fixed to 77.11 cm^{-1} and γ is assumed to be zero.

II-A-16 Doppler-Limited Dye Laser Excitation Spectroscopy of the PH_2 Radical: the $\tilde{A}^2A_1(000) \leftarrow \tilde{X}^2B_1(000)$ Band

Masao KAKIMOTO and Eizi HIROTA

Because of its fundamental importance in various fields, the PH_2 radical has been the subject of many high-resolution spectroscopic studies. We have observed laser excitation spectra, with higher resolution than in previous studies, in the region 18158 to 18443 cm^{-1} for two purposes: (1) to obtain an extensive set of precise ground-state combination differences (GSCD), (2) to unravel the origin of perturbations in the $\tilde{A}$ state. We have detected 1076 lines, most of which we assigned by taking GSCD and by referring to the calculated relative intensities. In this way 272 GSCD were obtained for $K \lesssim 7$ and $N \lesssim 10$, and were employed to obtain precise ground-state parameters as described in **II-A-2**. Then, these parameters were used to calculate the ground-state term values, which in turn were added to the observed transition frequencies to obtain the term values for 135 upper-state levels with $K' \lesssim 5$ and $N' \lesssim 9$. It is rather difficult to analyze these term values because of perturbations. The following procedure was thus

Table I. Molecular Constants of PH_2 in the $\tilde{A}^2A_1$ State (MHz)[a]

A	612 004.(153)
B	168 084.(29)
C	128 693.(29)
Δ_N	4.91(21)
Δ_{NK}	−41.3(12)
Δ_K	1 109.(36)
δ_N	1.68(19)
δ_K	23.0(63)
H_K	5.8(26)
L_K	−0.021 (56)
ϵ_{aa}	36 670.(300)
ϵ_{bb}	370.(89)
ϵ_{cc}	−1 214.(94)
Δ_K^S	−212.(20)

a. Values in parentheses denote 2.5σ and apply to the last digits of the constatns.

taken: term values for which $|o-c|$ exceeded a certain value were omitted from the data set used for the least-squares analysis. When the limit was set to 0.1 cm^{-1}, only 14 levels were omitted and the standard deviation of the fit σ_{fit} was 0.060 cm^{-1}. Even when the limit was reduced to 0.03 cm^{-1}, still 95 levels remained to determine upper-state "unperturbed" parameters, as shown in Table I. The last set showed σ_{fit} = 0.017 cm^{-1}, which was nearly equal to the measurement error. The perturbations are more conspicuous for larger K, and many F_1/F_2 pairs show similar deviations, but some do not.

II-A-17 Third-Order Anharmonic Potential Constants and Equilibrium Structure of HNO

Eizi HIROTA

The HNO molecule has attracted much attention in various fields. Although its isoelectronic molecule O_2 has the $^3\Sigma_g^-$ ground state, the ground state of HNO is now established to be singlet $^1A'$. The present work will primarily concern the determination of the anharmonic potential function and the equilibrium structure in the ground electronic state, both of which are important in discussing dynamical behavior of the molecule such as predissociation. The calculation was started by refining the 5-parameter (*i.e.* F_{13} neglected) harmonic force field of Jacox and Milligan[1] [their 4-parameter (*i.e.* $F_{12} = F_{13} = 0$) force field was found to yield essentially identical results]. The input data for determing the third-order anharmonic potential constants were taken from a paper by Johns and McKellar[2] on laser Stark spectroscopy of the NHO ν_2 and ν_3 and the DNO ν_1 and ν_2 bands. As in other cases[3], not all ten F_{ijk} constants could be determined. As an example, Table I shows a set consisting of four F_{ijk}'s, three "diagonal F_{iii}" with $i = 1 - 3$ and one "off-diagonal F_{233}". The obs.-calc. values for the α_s constants show some systematic trends, suggesting that the experimental data might have to be revised. Table I also compares the r_e structure obtained by the present work with the r_0 structures already published.

Table I. Third-Order Anharmonic Potential Constants and Equilibrium Structure of HNO

A 4-parameter set:	F_{111} (md/Å^2)	−18.31(12)	(σ)
	F_{222} (md/Å^2)	−73.8(21)	
	F_{333} (mdÅ)	−1.343(38)	
	F_{233} (md)	−3.285(63)	

Vibr.-rot.	const. (MHz)	obs.	calc.
HNO	α_2^A	−2 986.7	−2 985.6
	α_2^B	320.2	276.7
	α_2^C	−98.0	33.7
	α_3^A	−10 388.3	−10 388.0
	α_3^B	86.9	180.0
	α_3^C	742.9	694.8
DNO	α_2^A	2 083.8	2 075.3
	α_2^B	353.0	303.9
	α_2^C	272.9	268.2
	$\alpha_1^A - \alpha_1^B$	3 597.5	3 597.5

	Present (r_e)	Dalby (r_0)[a]	Ogilvie (r_0)[b]
r(H-N) (Å)	1.0887(60)	1.0628	1.09026(H-N)
			1.0795(D-N)
r(N-O) (Å)	1.1976(50)	1.2116	1.2090
θ(NCO) (°)	110.76(50)	108.58	108.047

a. F. W. Dalby, *Can. J. Phys.*, **36**, 1336 (1958).
b. J. F. Ogilvie, *J. Mol. Structure*, **31**, 407 (1976).

References

1) M. E. Jacox and D. E. Milligan, *J. Mol. Spectrosc.*, **48**, 536 (1973).
2) J. W. C. Johns and A. R. W. McKellar, *J. Chem. Phys.*, **66**, 1217 (1977).
3) E. Hirota and Y. Endo, *IMS Ann. Rev.*, 41 (1981)

II-A-18 Infrared Diode Laser Spectroscopy of the NO_3 ν_3 Band

Takashi ISHIWATA *(Tokyo Inst. Tech.)*, **Kentarou KAWAGUCHI, Eizi HIROTA, and Ikuzo TANAKA** *(Tokyo Inst. Tech. and IMS)*

In view of their importance in atmospheric chemistry and many other fields, the so-called NO_x molecules have been thoroughly investigated, and now most of them are fairly well understood. There are, however, a few exceptions; NO_3 is such an example. Ramsay[1] attempted to observe visible spectra of NO_3 under high resolution, but he could not resolve rotational structures. We confirmed this result, but could have dispersed the fluorescence induced by exciting the 0-0 band to obtain four vibrational frequencies in the ground electronic state.[2] In the present work we applied infrared

diode laser spectroscopy to NO_3 to observe the ν_3 (degenerate N-O stretching) vibration-rotation band with high resolution. As in Ref. 2) we generated NO_3 by the reaction of NO_2 with excess O_3. When we increased the amount of O_3, a line of the NO_2 ν_1 band disappeared completely. Zeeman modulation was employed to detect NO_3 lines, and the region 1460 to 1505 cm^{-1} was scanned. Figure 1 shows an example of the spectra, ${}^rQ_0(N)$ with $N = 1 \sim 15$. If the molecule is planar with A_2' symmetry in the ground electronic state, only N = odd rotational levels are present for $K = 0$. In fact, the series shown in Figure 1 were fitted to a linear function of $N(N+1)$ better with only N = odd terms than with only N = even or all N terms.

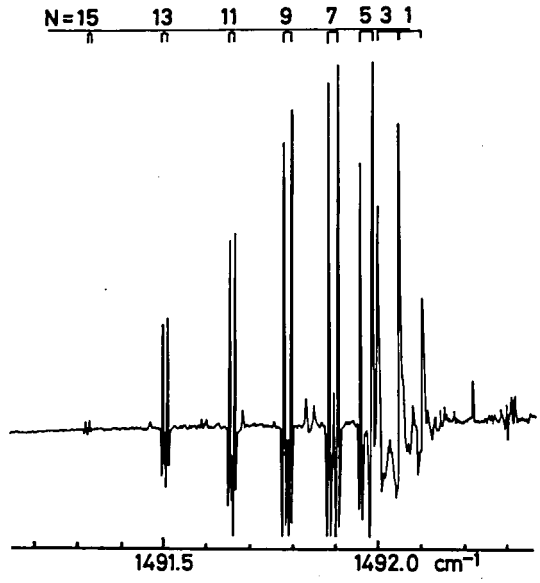

Figure 1. The ${}^rQ_0(N)$ branch series of the NO_3 ν_3 band recorded by Zeeman modulation. Each rotational line is split by spin-rotation interaction.

References

1) D. A. Ramsay, quoted in G. Herzberg, "Molecular Spectra and Molecular Structure" Vol. III, Van Nostrand, New York, 1966, p.525
2) T. Ishiwata, I. Fujiwara, Y. Naruge, K. Obi, and T. Tanaka, *Symp. Struct. Chem.*, Kyoto, 1981.

II-A-19 The Microwave Spectrum of the SiF Radical

Mitsutoshi TANIMOTO *(Sagami Chem. Res. Center)*, **Shuji SAITO, Yasuki ENDO, and Eizi HIROTA**

Because silane vigorously reacts with halogens while evolving a large amount of excess energy, slicon monohalides, resultants of these reactions, may be highly excited, and may even cause laser oscillation. Because of these characteristic behaviors of SiX molecules, high resolution spectroscopic studies have already been carried out; *e.g.* Martin and Merer[1] rotationally analyzed the $a^4\Sigma^- \rightarrow X^2\Pi_r$ transition around 3360 Å emitted from a microwave discharge in a mixture of SiF_4 and He. In the present work we have observed microwave spectra of SiF to improve the precisions of the rotational and Λ-doubling constants and also to determine hyperfine coupling constants. The radical was generated directly in an absorption cell by a DC discharge in SiF_4, with a small amout of SiH_4 added. In observing weak low-J lines, SiF_2 was first synthesized by the reaction of Si metal with SiF_4 at about 1050°C and then a glow discharge was induced in SiF_2. The $J = 5/2 \leftarrow 3/2$ to $J = 11/2 \leftarrow 9/2$ transitions were observed for both ${}^2\Pi_{3/2}$ and ${}^2\Pi_{1/2}$, and were analyzed to determine molecular constants, B_0, D_0, p_0, q_0, A_J^{eff}, a, b, c, and d.

Reference

1) R. W. Martin and A. J. Merer, *Can. J. Phys.*, **51**, 634 (1973).

II-A-20 The Microwave Spectrum of the SiCl Radical

Mitsutoshi TANIMOTO *(Sagami Chem. Res. Center)*, **Shuji SAITO, Yasuki ENDO, and Eizi HIROTA**

As in the case of SiF, the SiCl radical also has attracted attention of molecular spectroscopists. Its $B^2\Sigma^+ \rightarrow X^2\Pi_r$ band has been rotationally analyzed by Bredohl *et al.*[1] We have employed microwave spectroscopy to obtain more detailed and precise information on SiCl. The radical was generated by a DC discharge in $SiCl_4$ inside a 3.5 m long free space cell. The rotational transitions have been observed for the $J = 7/2 \leftarrow 5/2$ transitions at 53 GHz up to the $J = 21/2 \leftarrow 19/2$ transitions at 161 GHz for both ${}^2\Pi_{1/2}$ and ${}^2\Pi_{3/2}$ states. So far the observed spectra were analyzed for the $Si^{35}Cl$ species, and the B_0, D_0, A_J, Λ-type doubling (p and q), and hyperfine coupling (a, b, c, and d) constants were determined. The present values of B_0, D_0, and

p were found to agree with those of Ref. 1) within 3σ of the two measurements.

Reference

1) H. Bredohl, Ph. Demoulin, Y. Houbrechts, and F. Mélen, *J. Phys. B: At. Mol. Phys.*, **14** 1771 (1981).

II-A-21 Doppler-Limited Dye Laser Excitation Spectroscopy of the HSO Radical: the $\tilde{A}^2A'(002) \leftarrow \tilde{X}^2A''(000)$ Band

Koichi TSUKIYAMA[1], Shuji SAITO, Tetsuo SUZUKI, Ikuzo TANAKA *(Tokyo Inst. Tech. and IMS)*, **Eizi HIROTA**

As an extension of our earlier work[2] on the $\tilde{A}^2A'(003) \leftarrow \tilde{X}^2A''(000)$ of HSO, we have observed and analyzed the (002) ← (000) band in a similar way. The radical was generated by the reaction of O_2 discharge products with H_2S. The spectral region 15733 to 15835 cm^{-1} was scanned with the scan rate of about 100 MHz/sec, and 817 lines were observed, of which 585 lines were assigned to 685 transitions. Now precise microwave data are available for the ground state,[3] so that only upper-state parameters were adjusted in the least-squares analysis. The upper-state K_a' value ranged from 0 to 4, and the standard deviation of the fit was 0.0035 cm^{-1}. No evidence of perturbations has been observed. Molecular constants thus obtained are summarized in Table I. The (003) − (002) difference was calculated from the band origins to be 692.4819 cm^{-1}. The inertia defect in (002) is 0.308 u$Å^2$, which is to be compared with 0.407 u$Å^2$ in (003). Therefore, the inertia defect in the ground vibrational state of $\tilde{A}$ is probably close to 0.1 u$Å^2$.

Table I. Molecular Constants of HSO Radical in the $\tilde{A}^2A'(002)$ State (MHz)[a]

A	290 166.(18)
B	17 033.61(96)
C	15 933.12(94)
Δ_N	0.044 11(71)
Δ_{NK}	2.368(82)
Δ_K	19.2(29)
δ_N	0.003 89(52)
δ_K	2.88(39)
Φ_{NK}	0.000 25(11)
Φ_{KN}	−0.033 1(43)
Φ_K	−0.20(12)
ϵ_{aa}	16 656.(64)
ϵ_{bb}	82.9(56)
ϵ_{cc}	−353.1(58)
ν_0 [$\tilde{A}(002) \leftarrow \tilde{X}(000)$]	15 790.5377(32) cm^{-1}

a. Values in parentheses denote 2.5σ and apply to the last digits of the constants.

References

1) IMS Graduate Student 1981 — from Tokyo Inst. Tech.
2) M. Kakimoto, S. Saito, and E. Hirota, *J. Mol. Spectrosc.*, **80**, 334 (1980).
3) Y. Endo, S. Saito , and E. Hirota, *J. Chem. Phys.*, **75**, 4379 (1981).

II-A-22 Fra-Infrared Laser Magnetic Resonance Spectroscopy of the PD Radical in the $X^3\Sigma^-$ State

Nobukimi OHASHI *(Kanazawa Univ.)*, **Kentarou KAWAGUCHI, and Eizi HIROTA**

The PH radical has been known as a typical diatomic free radical with the $^3\Sigma^-$ ground state, and

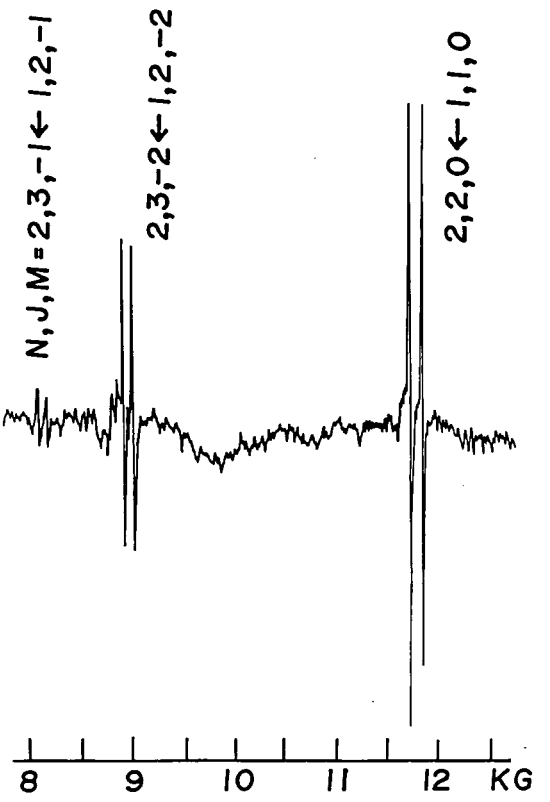

Figure 1. Far-infrared LMR spectra of PD in $^3\Sigma^-$ using the CH_3OH 570.5687 μm laser line as a source. The polarization of the laser light was chosen to be parallel to that of the magnetic field, so that the $\Delta M = 0$ selection rule was satisfied. Each M component is split by the ^{31}P hyperfine interaction.

has been well characterized by ultraviolet spectroscopy. Recently two types of LMR spectroscopy have been applied to this molecule. Davies *et al.*[1] have observed pure rotational transitions of PH in both $X^3\Sigma^-$ and $a^1\Delta$ by far-infrared LMR. On the other hand, Uehara and Hakuta[2] have reported the $v = 1 \leftarrow 0$ transition of PD in $^3\Sigma^-$ observed by CO LMR. We have recently completed a far-infrared LMR spectrometer.[3] As a test of its performance we have observed far-infrared LMR spectra of PD. The radical was generated by the reaction of red phosphorus with microwave discharge products of D_2O. We have observed absorption signals for five methanol far-infrared laser lines as sources, for two of which the observed signals were assigned to the $N = 2 \leftarrow 1$ and $N = 7 \leftarrow 6$ transitions. Figure 1 shows the $N = 2 \leftarrow 1$ transition recorded with $\Delta M = 0$ selection rule.

References

1) P. B. Davies, D. K. Russell, and B. A. Thrush, *Chem. Phys. Lett.*, **36**, 280 (1975); P. B. Davies, D. K. Russell, D. R. Smith, and B. A. Thrush, *Can. J. Phys.*, **57**, 522 (1979).
2) H. Uehara and K. Hakuta, *J. Chem. Phys.*, **74**, 4326 (1981).
3) K. Kawaguchi, C. Yamada, and E. Hirota, *IMS Ann. Rev.*, **44** (1981).

II—B Development of New Instruments and New Experimental Methods for High Resolution Spectroscopy

The scope of researches is limited by capabilities of instruments that are available. This is particularly true for spectroscopic investigations of simple molecules, one of the most fundamental problems the Department is interested in. When we repeat experiments using spectrometers of similar performance, we will obtain almost identical results. It is therefore very urgent for us to always maintain our research facilities at levels of performance as high as possible. High precision with which we determine molecular parameters often unravels new aspects of molecular properties that have escaped experimental observations. Needless to say, high sensitivity will supply us with fundamentally new information on molecular systems we are investigating. Along with these efforts to improve our facilities and with their applications to more interesting problems, we should also try to develop methods that are based upon something new. This project obviously premises not only detailed knowledge on molecules under investigations, but also that in related fields. Various kinds of technical problems are to be solved. In this sense joint researches including collaboration with the Equipment Development Center are indispensable. Developments of new instruments that are thus brought about will open new research areas in the field of molecular science.

II-B-1 A Micorwave Harmonic Generator for mm-Wave and submm-Wave Spectroscopy

Shuji SAITO, Yasuki ENDO, Michio TAKAMI *(IPCR)*, **and Eizi HIROTA**

Because the microwave absorption by molecules is roughly proportional to the square of the transition frequency, the effective sensitivity of a spectrometer can be increased by extending the working region to higher frequencies. There are, however, three major problems to be solved for submm-wave spectroscopy, namely generation, propagation, and detection of high-frequency microwave. We could have solved the second and the third problems, respectively, by introducing a

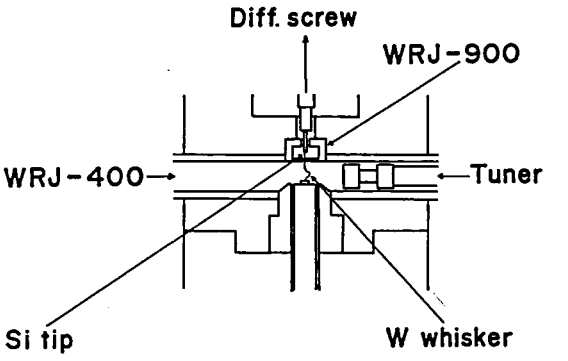

Figure 1. A harmonic generator which delivers microwave radiation in the region 200 to 400 GHz. The input microwave frequency is 40 GHz.

free space cell (combined with source modulation) and by installing an InSb detector for far-infrared radiation, operated at liquid He temperature. As to the first point, the klystrons which have been installed cover the region up to 221 GHz (with a gap between 203 and 218 GHz), but beyond that it would be almost impossible to make reliable klystrons. We have thus tried to set up a harmonic generator which accepts 40 GHz microwave as a primary input and generates mm- and submm-waves up to 400 GHz with enough power for absorption spectroscopy. As shown in Figure 1, the generator is made of a Si-W point contact mounted on a crossed waveguide; the primary is a WRJ-400 (5.690 × 2.845 mm) and the secondary a WRJ-900 (2.540 × 1.270 mm) waveguide. The harmonic generator was driven by an OKI 40V12 klystron with the output power of about 1.5W, and has been successfully employed in observing spectra of CF **(II-A-15)** and PH_2 **(II-A-2)**.

II—C High Resolution Spectroscopy of Molecules of Fundamental Importance

Needs for high quality spectroscopic data have recently been increasing, especially for fundamental molecules. Such spectroscopic data have been accumulated in the past perhaps because of interest in precise molecular structure determination. However, research activities in other related fields such as reaction kinetics, environmental sciences, and astronomy have recently been so advanced that precise spectroscopic data are indispensable as means of monitorning molecules. Spectroscopic data which are available are not necessarily good enough and must often be replaced by new spectra that meet necessary requirements. Such spectroscopic data on chemically stable molecules of fundamental importance will be presented in this section.

II-C-1 The Micorwave Spectrum of the Oxygen Molecule in the Ground Electronic State

Yasuki ENDO and Masataka MIZUSHIMA
(Univ. of Colorado and IMS)

[*Jap. J. Appl. Phys.*, **21**, L379 (1982)]

Many papers have already been published on the microwave spectrum of oxygen, which is due to the flipping of the electronic spin $\underset{\sim}{S}$ with respect to the rotational angular momentum $\underset{\sim}{N}$. However, the data are rather limited in number; 20 and 9 lines have been measured for $^{16}O_2$ in the ground vibrational state and in the $v = 1$ state, respectively. In the present work the observation was extended so that 8 and 19 lines were added for the two states. Inclusion of new data has allowed us to improve molecular constatns of $^{16}O_2$ in precision. The results are summarized in Table I. Additional measurements have also been made for two isotopic species, $^{16}O^{18}O$ in $v = 0$ and $^{18}O_2$ in $v = 0$ and 1.

Table I. Molecular Constants of the Oxygen Molecule ($^{16}O_2$) in the Ground Eelctronic State (MHz)

$B_v = 43\ 337.446 - 474.032\ (v + 1/2)$
$D_v = 0.1410 + 0.0052\ (v + 1/2)$
$\lambda_v = 59\ 429.841 + 144.7296\ (v + 1/2)$
$\lambda_{Dv} = 0.055\ 830 + 0.004\ 95\ (v + 1/2)$
$\lambda_{DDv} = 34. \times 10^{-6}$
$\gamma_v = -252.2850 - 0.605\ (v + 1/2)$
$\gamma_{Dv} = -0.241\ 46 \times 10^{-3} - 0.007\ 96 \times 10^{-3}\ (v + 1/2)$

II—D Study of Molecular Association in Condensed Phase

The space-time correlations between the positions and between the orientations of different molecules are useful informations for the mixing state from a molecuar standpoint. Coherent visible light scattering

experiments afford information about these correlations in the form of fluctuations in the semi-micro regions and has been pursued for a few years. The work on this line is still in progress. At the same time, it has been recognized that a complementary use of a variety of experimental as well as theoretical methods are necessary for the complete understanding of the molecular association in liquid. From this respect several spectroscopic studies and theoretical studies has been developed. Recently the study of molecular association has been extended to gas phase. Dimers or complexes in the gas phase serve as well-defined models to more complicated aggregates.

II-D-1 The Effects of Intermolecular Potentials on the Vibrational Sepctra of Condensed Systems

Tsunetake FUJIYAMA

[*J. Raman. Spectrosc.*, **12**, 199 (1982)]

The effects of the intermolecular interaction potential on the vibrational spectra of liquids or solutions are discussed for the cases where the molecualr field can be treated as a time or space-averaged quantity. It is shown that the introduction of an appropriate molecular field can yield information about molecular properties or about molecular arrangements of component molecules in the liquid and solution phases. Certain spectral characteristics, for instance absorption intensity in infrared spectra and scattering cross-section and depolarization ratio in Raman spectra, are discussed.

II-D-2 A Study of Local Structure Formation in Binary Solutions of 2-Butoxyethanol and Water by Rayleigh Scattering and Raman Sepctra

Nobuyuki ITO *(Tokyo Metropolitan Univ.)*, **Tsunetake FUJIYAMA and Yasuo UDAGAWA**

[*Bull. Chem. Soc. Jpn.*, in press]

The concentration dependence of concentration fluctuations at 21, 32 and 42°C and of Raman spectra at 21°C were measured for binary solutions of 2-butoxyethanol (BE) and water. The existence of the two kinds of local structures is inferred; clathrate hydrate-like structure $g[(H_2O)_{50}BE]$ and aggregate $h[(H_2O)_4BE]$. The compositions of these two structures are the same as those of the two phases into which the solution separates above the critical solution temperature. The phase separation is understood to be the end of the growth of the local structures, which already exist well below the critical solution temperature. Mixing state of BE-water mixtures is shown schematically in Figure 1.

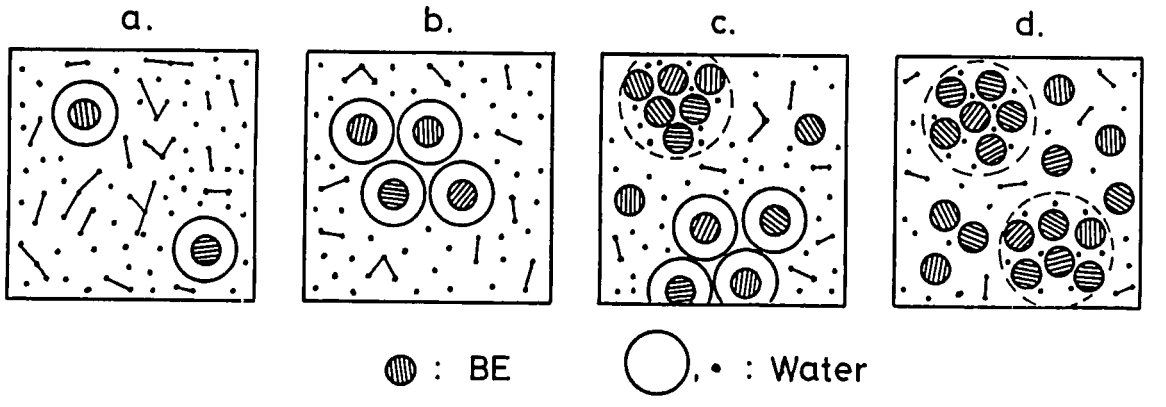

Figure 1. Mixing state of BE-water mixtures drawn schematically. (a) $x_{BE} < 0.02$, (b) $0.02 < x_{BE} < 0.05$, (c) $0.05 < x_{BE} < 0.2$ and (d) $x_{BE} > 0.2$. (• , ○) and ◍ correspond to the water molecule and the BE molecule, respectively. ⊛ and ⊛ mean clathrate hydrate-like structure $g[(H_2O)_{50}BE]$ and aggregate $h[(H_2O)_4BE]$, respectively.

II-D-3 The Application of Polarization Coherent Anti-Stokes Raman Spectroscopy to the Line-shape Analysis of Liquid Sample.

Ryosaku IGARASHI, Fumisato IIDA *(Tokyo Metropolitan Univ.)*, **Chiaki HIROSE** *(Tokyo Institute of Technology)*, **and Tsunetake FUJIYAMA**

[*Bull. Chem. Soc. Jpn.*, **54**, 3691 (1981)]

The polarization CARS spectra were observed for a few typical Raman lines at various experimental settings. Based upon the observed and calculated spectra, the usefulness and the validity of the polarization CARS method for the study of the overlapped Raman lines observed for a condensed system have been emphasized. Figure 1 shows the observed and calculated spectra for the case where two Raman lines are located very close to each other.

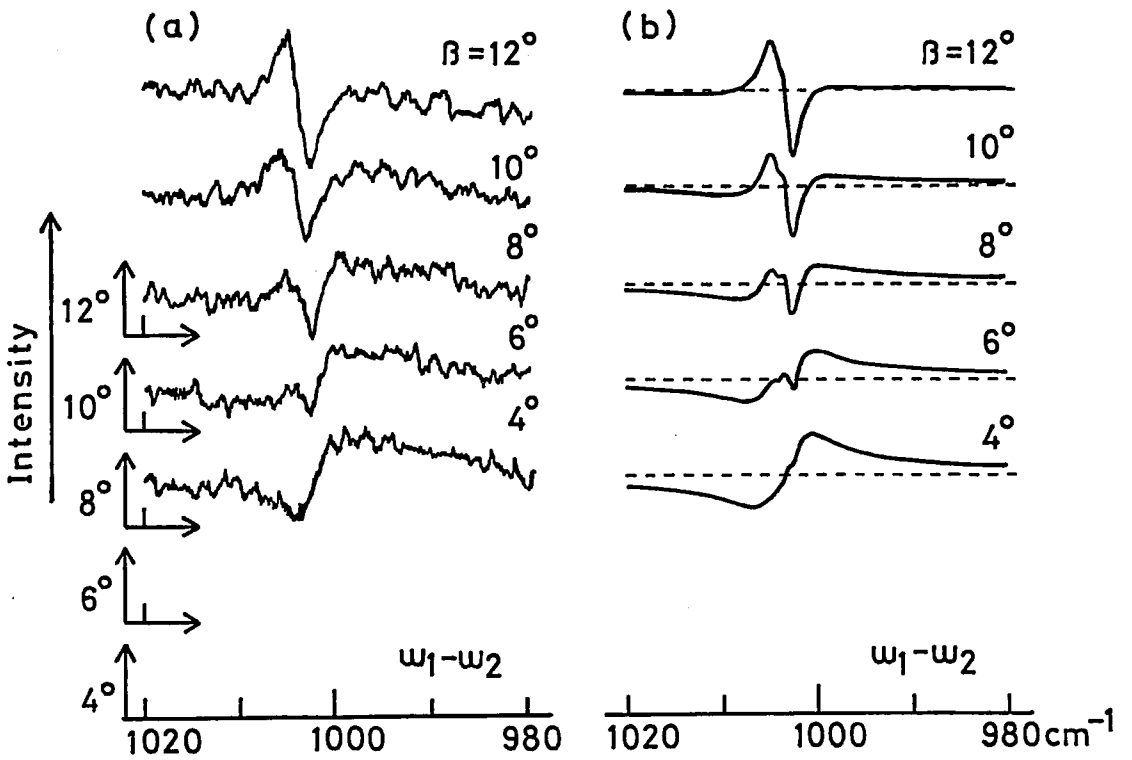

Figure 1. Polarization CARS spectra for the binary mixture of toluene and chlorobenzene, (1:1 mixture in volume). (a): Observed β-dependence, (b): Calculated β-dependence. The dotted lines indicate the background height.

II-D-4 Effects of Mechanical and Electrical Anharmonicities on Local Mode Spectrum

Keietsu TAMAGAKE *(Okayama Univ.)*, **Shi-aki HYODO** *(Tokyo Metropolitan Univ.)*, **and Tsunetake FUJIYAMA**

[*Bull. Chem. Soc. Jpn.*, **55**, 1267 (1982)]

The first and second order dipole moment parameters along the CH bond in benzene, chloroform and cyclohexane were obtained by deducing the local mode intensities on the basis of the one-dimensional Morse oscillator model. The validity of the one-dimensional model is discussed according to a newly introduced formula which helps us to understand the nature of local mode absorption. The relative intensities of the first overtones to the other bands were found to be crucially important in determining M_2/M_1 together with its sign, because the contributions of the

mechanical and electrical anharmonicities to M_2/M_1 are often cancelled out each other accidentally. The M_2/M_1 values for benzene, cyclohezane and chloroform were 2.3, 1.45 and -0.93 A^{-1}, respectively. These values for benzene and cyclohexane were excellently reproduced by the *ab initio* calculations for benzene and methane respectively.

II-D-5 High-overtone Spectra and Dipole Moment Functions for the C-H Stretching Vibration of Chloroform

Shi-aki HYODO *(Tokyo Metropolitan Univ.)*, **Keietsu TAMAGAKE** *(Okayama Univ.)*, **and Tsunetake FUJIYAMA**

[*Bull. Chem. Soc. Jpn.*, **55**, 1272 (1982)]

The absorption spectra of liquid chloroform were observed for the C-H stretching fundamental vibration and its overtones up to v=5. The spectral parameters were analyzed on the basis of the one-dimentional local mode representation, which led to the determination of the mechanical and electrical anharmonicities. The solvent effects on the absorption intensities are discussed from the viewpoint of the solvent effect on the dipole moment function. The finally obtained dipole moment funciton was compared with that obtained by the *ab inito* calculations.

II-D-6 Symmetrized Local Mode Analysis of CH_2 Stretching Mode in 1,1-dichloroethylene

Keietsu TAMAGAKE *(Okayama Univ.)*, **Shi-aki HYODO, and Tsunetake FUJIYAMA**

[*Bull. Chem. Soc. Jpn.*, **55**, 1277 (1982)]

A symmetrized local mode (SLM) based on the two dimensional Morse oscillator was developed and applied to the analysis of the spectrum of the CH stretching modes in 1,1-dichloroethylene in the range of 3000 − 17000 cm^{-1}. The calculated frequencies with finally determined parameters: ω_e = 3191.6, $\omega_e\chi_e$ = 57.63 and f_{12} = 2170 cm^{-1} agreed well with the observed ones. The kinetic coupling was found to be more responsible for the mixing between SLM states than the potential coupling. The observed intensity data were analyzed by the use of the obtained mixing coefficients and the two dimensional dipole moment function parameters, M_1, M_2, M_{12}, and θ. The finally determined dipole moment function parameters were: $M_1 = -0.290$ DA^{-1}, $M_2 = -0.875$ DA^{-2}, $M_{12} = -0.386$ DA^{-2}, and $\theta = 38.4°$. Careful examination of the influence of M_{12} upon the integrated intensities clarified the validity of the one dimensional intensity analysis of our preceding work. An SLM representation was ocnfirmed to be useful for the systematic analysis of the CH stretching spectrum through the fundamental and the high v local mode bands which include highly structured low v summation bands. An SLM representation was also found to be convenient for making a simple correlation between local mode and normal mode picture.

II-D-7 Salting-out Phenomenon and Clathrate Hydrate Formation in Aqueous Solution of Polar Nonelectrolyte

Tadashi KATO, Masako YUDASAKA *(Tokyo Metropolitan Univ.)*, **and Tsunetake FUJIYAMA**

[*Bull. Chem. Soc. Jpn.*, **55**, 1284 (1982)]

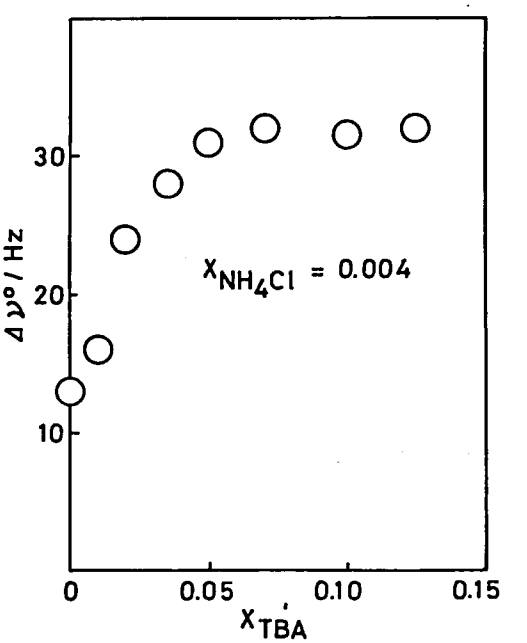

Figure 1. Dependence of the $\Delta\nu°$ values for t-butyl alcohol-water-ammonium chloride solution on the mole fraction of t-butyl alcohol (mole fraction of ammonium chloride is 0.004).

The salting-out phenomenon has been carefully observed by adding ammonium chloride into aqueous solutions of t-butyl alcohol, acetone, dioxane, and 2-butoxyethanol. The experimental results have been well explained by considering the formation of a clathrate hydrate-like local structure in the aqueous solution of each nonelectrolyte. In addition, the role of the chloride ion has been found to be the promotion of the aggregation of the clathrate hydrate-like local sturctures. The line-width measurement of ^{35}Cl-NMR spectra has been shown to be an extremely powerful method for studying the state of mixing of ions in solutions. Figure 1 shows the observed $\Delta\nu^\circ$ values ($\Delta\nu^\circ \equiv \Delta\nu/(\eta/\eta_0)$, where η is the viscosity of the solution, η_0 is that of the standard sample, and $\Delta\nu$ is the observed line-width) for t-butyl alcohol-water-ammonium chloride solutions.

II-D-8 Estimation of Parameters, G_{11}, G_{22}, and G_{12} in the Kirkwood-Buff Solution Theory on the Basis of the Concentration Fluctuation Data Obtained from Rayleigh Scattering

Tadashi KATO, Tsunetake FUJIYAMA, and Hiroyasu NOMURA *(Nagoya Univ. and IMS)*

[*Bull. Chem. Soc. Jpn.*, **55**, 3368 (1982).]

A concnetration fluctuation value obtained from Rayleigh scattering intensity was confirmed to give a thermodynamic quantity of an equilibrium system. An observation of concentraion fluctuation by a light scattering method was found the most direct and useful way of determining a concentration derivative of a chemical potential. For methanol, ethanol, and 1-propanol-carbon tetrachloride systems, the Kirkwood-Buff parameters, G_{11}, G_{22}, and G_{12},[1,2] were determined by the use of concentration fluctuation data. The structure of these systems was discussed on the basis of the calculated Kirkwood-Buff parameters. Figure 1 shows the concentration dependence of G_{ij} for a methanol-carbon tetrachloride solution ($G_{ij} = \int_0^\infty [g_{ij}(r) - 1]4\pi r^2 dr$, where $g_{ij}(r)$ is the radial distribution function between species i and j).

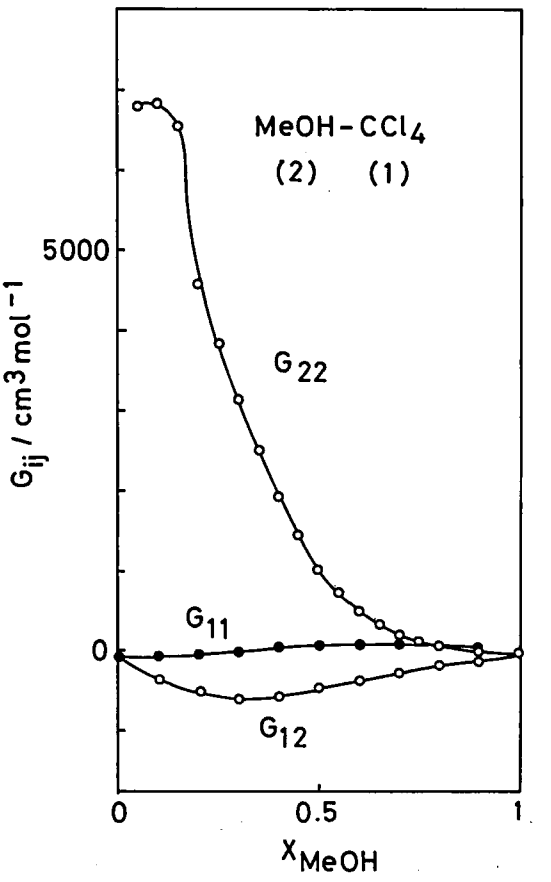

Figure 1. Concentration dependences of G_{11}, G_{22}, and G_{12} for carbon tetrachloride (1)-methanol (2) solution.

References

1) J. G. Kirkwood and F. P. Buff, *J. Chem. Phys.*, **19**, 774 (1951).
2) A. Ben-Naim, *J. Chem. Phys.*, **67**, 4884 (1977).

II-D-9 Relation between Kirkwood-Buff Parameters G_{ij} and Sizes of Clusters Formed in Binary Solution

Tadashi KATO

The radial distribution function $g_{ij}(r)$ of a binary solution in which large clusters are formed is discussed using a very simple model. The integral of $g_{ij}(r)$, that is, the Kirkwood-Buff parameters G_{ij} are expressed in terms of the volume, the volume fraction, and the composition of each cluster. Theoretical results are applied to a binary solution of methanol and carbon tetrachloride. The observed and calculated relations among G_{11}, G_{22}, and G_{12} agree quite well. The size of the cluster formed by

methanol moleucles is estimated from the observed G_{ij} values. Figure 1 shows an r dependence of the radial distribution function $[g_{22}(r) - 1]4\pi r^2$ calculated for a binary solution where species 2 forms a spherical cluster whose diameter is much larger than the nearest neighbor distance.

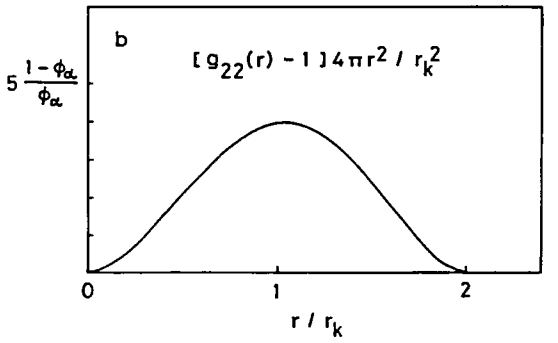

Figure 1. Calculated radial distribution function $[g_{22}(r) - 1]4\pi r^2$ for a binary solution where species 2 form a spherical cluster whose diameter, r_k, is much larger than the nearest neighbor distance. ϕ_α is the volume fraction of the cluster.

II-D-10 Kirkwood-Buff Parameters G_{ij} and Local Structure Formation in Aqueous Solution of 2-Butoxyethanol

Tadashi KATO

The concentration dependence of Kirkwood-Buff parameters G_{11}, G_{22}, and G_{12}, was determined for a binary solution of 2-butoxyethanol (BE) and water at 20°C and 40°C. The absolute values of all the G_{ij}'s are much larger than those so far reported and increase with the temperature. It was shown that these results reflect the existence of two kinds of large clusters; water-rich and BE-rich clusters in the concentration range of $0.02 < x_{BE} < 0.2$. The concentration dependences of sizes of these clusters were determined from the observed G_{ij} values at each temperature by using a simple model. Figure 1 shows the sizes ($2r_c$) of water-rich (○) and BE-rich (●) clusters at 20°C and 40°C.

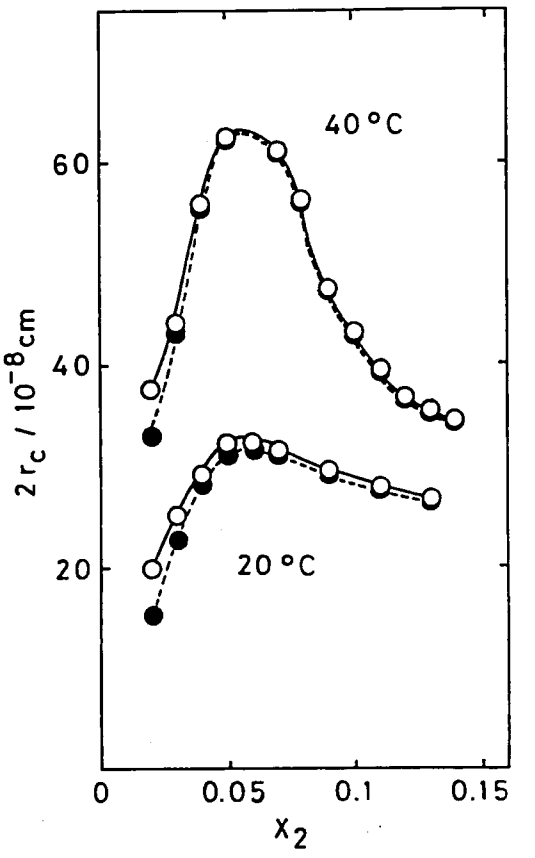

Figure 1. Concentration dependences of sizes ($2r_c$) of water-rich (○) and BE-rich (●) clusters at 20°C and 40°C. X_2 is the mole fraction of BE.

II-D-11 Dispersed Fluorescence Spectra of Hydrogen-Bonded Phenols in a Supersonic Free Jet

Haruo ABE, Naohiko MIKAMI, Mitsuo ITO *(Tohoku Univ.)*, **and Yasuo UDAGAWA**

[*J. Phys. Chem.*, **86**, 2567 (1982)]

Dispersed fluorescence spectra are reported for

Table I. Intermolecular Vibrational Frequencies of Hydrogen Bonded Phenols in the Ground State and the First Excited Electronic State (in cm^{-1})

	ground state		excited state	
proton acceptor	bending ν_β	stretching ν_σ	bending ν_β	stretching ν_σ
methanol	22	162	27	175
ethanol	22	153	24	150
diethyl ether	21,38		31	
dioxane	19	128	23	137
benzene	26		20	50

hydrogen-bonded complexes of phenol with various proton-accepting molecules prepared in a supersonic free jet. The spectra show a well-resolved structure characteristic of intermolecular vibrations from hydrogen bonding in the ground state. All the proton acceptors studied give two kinds of new frequencies; one is due to hydrogen bond stretching vibration and the other is due to bending vibration. The frequencies are listed in Table I. The possibility of excitation energy redistribution in the excited state leading to different conformational isomers is also suggested.

II—E Structures of Liquids and Noncrystalline Solids

Structures of liquids and noncrystalline solids still remain to be determined. Spectroscopic method employed in II—D can supply only indirect knowledge on the geometrical structures. Since the majority of chemical reaction in real life is taken place in liquids and many noncrystalline solids have properties of chemical interests, it is important to establish the method to determine the structure of liquid and noncrystalline solid. Toward this goal, a new project has started by the use of X-ray. Although the experimental equipments are largely used in common, the project can be divided into two. One is X-ray diffraction study and the other is extended X-ray absorption fine structure (EXAFS). The former is mainly for the study of liquid structure and the latter is for the study of the structure of liquid and noncyrstalline materials.

II-E-1 Construction of an EXAFS Spectrometer with Conventional X-ray Source

Kazuyuki TOHJI and Yasuo UDAGAWA

[*submitted to Jpn. J. Appl. Phys.*]

An EXAFS spectrometer has been constructed by the use of a rotating anode X-ray tube, Ge(220) crystal and pure Ge solid state detector. The features of the system constructed are in the following.

(a) Common use for X-ray diffraction and EXAFS studies with only a little change in optical components
(b) Use of solid state detector (SSD) to obtain radiation purity by discriminating higher order diffraction
(c) Use of fast detector, amplifier and discriminater to achieve high count rate
(d) Use of accurate goniometer for the study of near edge structure

An EXAFS spectrum of Ni foil is shown in Figure 1 to show the quality of the data taken by this apparatus.

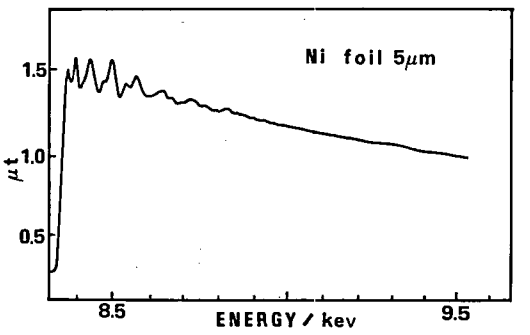

Figure 1. EXAFS spectrum of Ni foil.

RESEARCH ACTIVITIES III
Department of Electronic Structure

III-A-1 Photochemistry of the Lowest Excited Singlet State: Acceleration of *Trans-Cis* Isomerization by Two Consecutive Picosecond Pulses

Minoru SUMITANI and Keitaro YOSHIHARA

[*J. Chem. Phys.*, **76**, 738 (1982)]

One-photon photochemistry of molecules already in excited states can induce new photochemical reactions or accelerate oridinary ones. This two-photon method of initiating reactions has some advantages, since excited states can be populated for which direct transition from the ground state is forbidden.

In the case of the cis-trans isomerization of stilbene, the ^1A_g state, which is characterized by a double electron excitation, is strongly stabilized when the molecule rotates about the central double bond. Thus, if the ^1A_g level can be optically populated, the downhill reaction from this level would take place efficiently and does not require much thermal energy.

We found that the fluorescence intensity was suddenly ($\lesssim$10 ps) decreased by introducing the second pulse into the sample [Figure 1 (B)] (photobleaching).

The temperature dependence of photobleaching was compared with that of the ordinary one-photon isomerization. The quantum yield of the latter decreases at ~200 K whereas that of the former decreases at ~80 K. The photobleaching was explained in terms of chemical reaction of the ^1A_g state and the above temperature dependence is due to the highly reactive nature of this state.

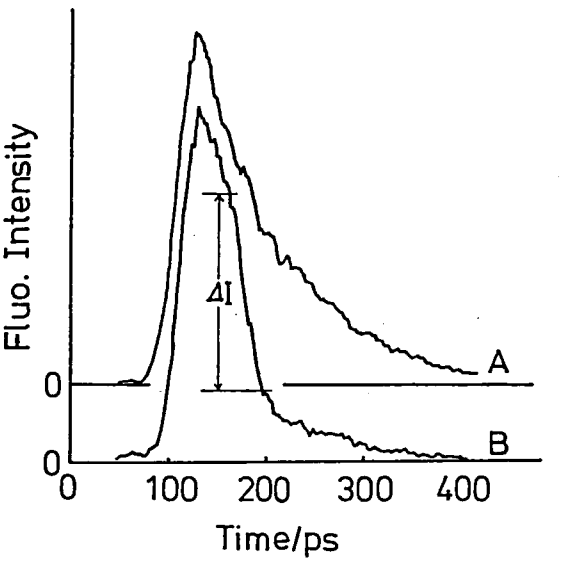

Figure 1. The normal fluorescence decay curve of trans-stilbene at room temperature (A). A sudden decrease of fluorecence intensity induced by a second laser pulse is shown by Fig. 1 (B). The second pulse (532 nm) is delayed by 90ps from the first pulse (266nm).

III—B Electronic Structures of Excited States

III-B-1 Laser Photolysis of Benzene. V. Formation of Hot Benzene

Nobuaki NAKASHIMA and Keitaro YOSHIHARA

[*J. Chem. Phys.*, **77**, in press]

Flash photolysis of gaseous benzene has been carried out with a KrF laser (248.4 nm) as an excitation source. Two new transients have been detected, one of which has a structured absorption in the wavelength region from 235 to 260 nm. It has a rise time of 80 ns and a long decay time (>25 μs). The precursor of this transient has also been detected. It appears as a shoulder at 225 nm and has a lifetime of 80 ns. This species is postulated to be a highly excited vibrational state of the ground electronic state, namely, a hot benzene molecule. This species is quenched by ground state benzene as well as by twelve different foreign gases, including oxygen and nitrogen, which have similar quenching rates. The decay of the hot benzene is accompanied by an increase in the temperature of the sample,

which leads in turn to formation of the species with the structured absorption. The temperature of the equilibrated sample was determined by comparing the thermalized spectra in the nanosecond time scale with the steady-state absorption spectra at higher temperatures. The temperature rises by about 50 degrees when 20 torr of benzene is excited with an energy of 33 mJ/cm^2. This temperature increase indicates that the yield of hot benzene is 0.6 ± 0.2. The $T_n \leftarrow T_1$ absorption spectrum has been measured and the intersystem crossing yield is estimated to be 0.2 ± 0.1. The major non-radiative channel in benzene is internal conversion, as shown in Figure 1.

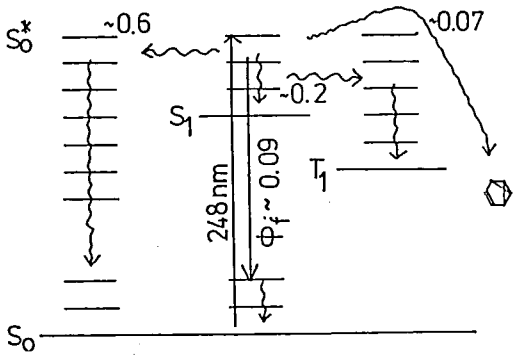

Figure 1. Energy balance in the photochemistry of benzene at 20 torr with a KrF laser (248.4 nm) irradiation of 33 mJ/cm^2.

III-B-2 Laser Flash Photolysis of Benzene. VI. Photolysis in Aqueous Solution

Nobuo SHIMO, Nobuaki NAKASHIMA, and Keitaro YOSHIHARA

[*Bull. Chem. Soc. Jpn.*, in press]

Three transient absorption spectra in aqueous solution were observed by irradiation of benzene with an excimer laser (KrF, 248 nm or ArF, 193 nm). A part of the time-resolved spectra are shown in Figure 1. A short-lived absorption with a peak at 275 nm is assigned to the $S_n \leftarrow S_1$ absorption. A long-lived absorption, which appears as a clear shoulder at 230 nm, stays longer than 500 ns and is not shortened by oxygen. This species is tentatively assigned to benzvalene, and the quantum yield is determined to be ca. 0.1. Solvated electron with a peak at 720 nm was formed *via* multiphoton processes at a power level of 60 mJ/cm^2 of an ArF laser. The $T_n \leftarrow T_1$ absorption was lower than our detection limit ($\Phi_T < 0.1$).

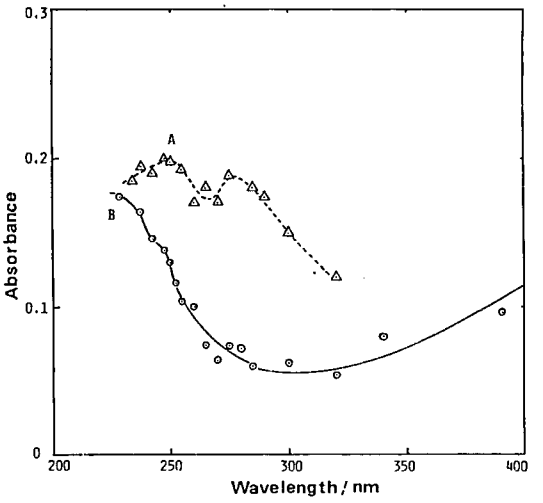

Figure 1. Transient absorption spectra of benzene in aqueous solution by excitation at 193 nm. (ArF). Absorbance is normalized at 230 nm. The spectrum of A is taken immediately after excitation, and the spectrum of B is taken at 100 ns after laser excitation.

III-B-3 Complex Fluorescence Decay in Fluorinated Benzenes

Desmond V. O'CONNOR, Minoru SUMITANI, and Keitaro YOSHIHARA

[*Chem. Phys. Lett.*, in press]

Fluorescence decay curves of pentafluorobenzene and hexafluorobenzene have been measured following excitation at 266 nm with the frequency quadrupled picosecond pulses of a mode-locked Nd:YAG laser. Both compounds exhibit double exponential decay kinetics even under isolated molecule conditions. One decay time is quite short, ca. 100 ps, while the other is in the region of 1 ns. The non-exponential behaviour persists over a wide pressure range and at temperatures from 22 °C to −35 °C. The intensity contribution of the longer lived component increases at lower temperatures or at higher pressures. Under these conditions the decay time of this component also increases.

Since these molecules, like benzene, are assumed to lie in the "statistical limit" the non-exponential decay kinetics cannot be attributed to "intermediate

case" behaviour. Rather, the complex decay is interpreted in terms of emission from a large number of vibrational levels, each having a characteristic decay time. These levels are populated directly upon excitation owing to the highly congested absorption of these molecules at normal temperatures. Other mechanisms, such as intermolecular vibrational redistribution, may also play a role in the dissipation of excess energy.

III-B-4 Nanosecond Laser Flash Photolysis of 1-Anilinonaphthalene

Hiroki NAKAMURA, Jiro TANAKA *(Nagoya Univ.)*, **Nobuaki NAKASHIMA, and Keitaro YOSHIHARA**

[*Bull. Chem. Soc. Jpn.*, **55**, 1795 (1982)]

The photoionization mechanism of 1-anilinonaphthalene (1-AN) was investigated by a nanosecond laser flash photolysis and the result was compared with that of 8-anilino-1-naphtalenesulfonate (ANS). The photoionization of 1-AN in polar solvent is shown to occur through a biphotonic process *via* a triplet state; the mechanism is different from those of ANS, in which an intermediate of a charge transfer to solvent (CTTS) state was observed. Thus the major deactivation process of the lowest excited singlet state is an intersystem crossing in 1-AN, while it is a transition to the CTTS state in ANS which might be stabilized by the sulfonate group. Transient absorption spectra upon excitation of 1-AN with a XeF excimer laser (351 nm) are given in Figure 1.

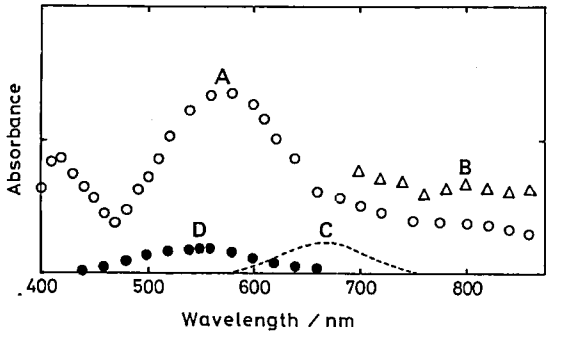

Figure 1. Transient absorption spectra of 1-AN A: 70 ns after the laser pulse in a degassed methanol-water (1 : 1) mixed solvent, B: the $S_n \leftarrow S_1$ absorption, C: the absorption spectrum of solvated electron, D: the $T_n \leftarrow T_1$ absorption in cyclohexane.

III-B-5 Temperature Dependence of Non-radiative Relaxation Process of the Lowest Excited Singlet States of Meso-Substituted Bromoanthracenes

Masanao TANAKA, Ikuzo TANAKA *(Tokyo Institute of Technology and IMS)*, **Shigeyoshi TAI, Kumao HAMANOUE** *(Kyoto Institute of Technology)*, **Minoru SUMITANI, and Keitaro YOSHIHARA**

[*J. Phys. Chem.*, in press]

Direct measurements of the temperature dependence of the fluorescence lifetimes of 9-bromoanthracene (BA) and 9,10-dibromoanthracene (DBA) have allowed the determination of the rate constant for intersystem crossing (isc) in the form $K_{isc} = A_{isc} \exp(-\Delta E/kT)$. This isc is attributed to that from the lowest excited singlet state S_1 to an adjacent higher excited triplet state T_n. The values of ΔE *i.e.*, 600 ~ 710 cm^{-1} for BA and 1100 cm^{-1} for DBA, are about 300 cm^{-1} larger than those deduced from the $T_n \leftarrow T_1$ fluorescence (TTF) measurement by Gillispie and Lim (*Chem. Phys. Lett.*, **63**, 355 (1979)). The consistent values of S_1 decay constants with those of the buildup times of triplet-triplet absorptions lead us to the suggestion that the T_n lifetimes are tens of picoseconds, and this estimate gives a good agreement of calculated and experimental Φ_{TTF} of DBA. Frequency factors and activation energies in various solvents are summarized in Table I.

Table I: Frequency Factors A_{isc} and Activation Energies ΔE in Various Solvents

Solute	Solvent [a]	A_{isc}/ ($10^{11}s^{-1}$)	ΔE_{exp}/ (cm^{-1})	Temperature/ (K)	Method	$\Delta\bar{\nu}(0,1)$/ [b] (cm^{-1})	ΔE_{cal}/ [c] (cm^{-1})
BA	3-MP	1.47±0.01	600±10	77, 104~296	k	480	1080
	MCH	0.93±0.01	710±30	77, 110~296	k	430	1110
	bromobenzene	6.1±0.1	1350±35	283~333	Φ_F	0	1350
	benzene	4.7±0.1	1220±30	283~333	Φ_F	150	1270
	95% ethanol	5.8±0.07	1110±20	283~333	Φ_F	430	1110
	hexane	6.8±0.1	1010±20	283~333	Φ_F	530	1040
DBA	3-MP	1.39±0.01	1100±20	77, 173~296	k	530	1430
	bromobenzene	9.0±0.4	1750±75	283~333	Φ_F	0	1750
	benzene	10.1±0.4	1710±70	283~333	Φ_F	170	1650
	95% ethanol	9.1±3.5	1590±50	283~333	Φ_F	450	1480
	hexane	9.9±3.5	1560±50	283~333	Φ_F	500	1450

a. The values of A_{isc} and ΔE_{exp} except for those in 3-MP and MCH are given in reference.
b. Spectral shifts of the second emission band relative to that in bromobenzene. All spectra were taken using a Shimadzu RF 502 fluorescence spectrometer.
c. Calculated values taking bromobenzene as a reference solvent.

III-B-6 Picosecond Study of Energy Transfer between Rhodamine 6G and 3,3'-Diethylthiacarbocyanine Iodide in the Premicellar Region: Förster Mechanism with Increased Local Concentration

Hiroyasu SATO *(Mi'e Univ.)*, **Yoshihumi KUSUMOTO** *(Kagoshima Univ.)*, **Nobuaki NAKASHIMA, and Keitaro YOSHIHARA**

[*Chem. Phys. Lett.*, **71**, 326 (1980)]

The mechanism of enhancement in the energy transfer between rhodamine 6G and 3,3'-diethylthiacarbocyanine iodide (DTC) by sodium lauryl sulfate (SLS) in the premicellar region was studied by a picosecond laser technique. Förster mechanism with an increased local concentration suggesting dye-rich induced micelle formation was concluded from the shape of the decay curve. Excitation energy of rhodamine 6G in aqueous solution with SLS transfered to DTC with a high efficiency even at low acceptor concentrations, as shown in Figure 1.

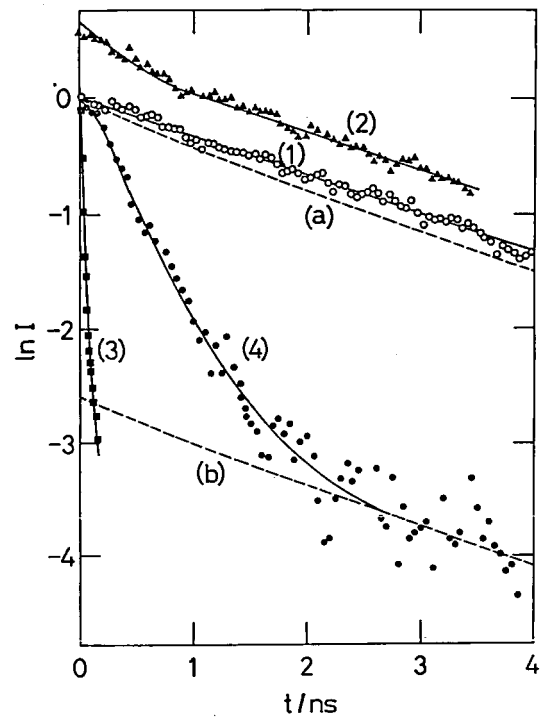

Figure 1. Observed fluorescence decays. (1): aqueous solution (R6G 1.0×10^{-7}M), (2), (3) and (4): aqueous solution with SLS (5.0×10^{-3}M) of R6G (1.0×10^{-7}M), of DTC (5.0×10^{-5}M), and of R6G (1.0×10^{-7}M) plus DTC (5.0×10^{-5}M), respectively. The curve (a) is the calculated decay curve for an aqueous solution (R6G 1.0×10^{-7}M, DTC 5.0×10^{-7}M) assuming a Förster-type decay with R_0 = 86Å. The curve (b) is drawn parallel to the curve (a).

All intensities except (2) are normalized to ln I = 0 at t = 0. The curve (2) is shifted upward for clarity. The data in (4) were measured with a wider slit width than the other ones.

III-B-7 Picosecond Fluorescence Lifetimes of Anthraquinone Derivatives; Radiationless Deactivation *via* Intra- and Inter-molecular Hydrogen Bonds

Haruo INOUE, Mitsuhiko HIDA *(Tokyo Metropolitan Univ.)*, **Nobuaki NAKASHIMA, and Keitaro YOSHIHARA**

[*J. Phys. Chem.*, **86**, 3184 (1982)]

Radiationless deactivations from the $S_1(^1CT)$ states of seven 1- and 2-substituted aminoanthraquinones were investigated by measuring picosecond fluorescence lifetimes and fluorescence quantum yields in benzene, acetonitrile, and ethanol. The $S_1(^1CT)$ states of all derivatives were largely deactivated in ethanol. Deuterium isotope effect of the sovlent were observed on the nonradiative rate constants (k_{nr}(in EtOH/k_{nr}(in EtOD) = 9.0 (1-NH_2); 2.1 (2-NH_2); 1.7(2-piperidino). The fluorescence quantum yield in ethanol was not affected by temperature (278 K − 343 K). In benzene the excited 1-aminoanthraquinones were deactivated faster than those of 2-aminoanthraquinones. These observations were interpreted in terms of the radiationless deactivations of $S_1(^1CT)$ through the intra- and inter-molecular hydrogen bonds. The fluorescence quantum yields (Q_f), fluorescence lifetimes, calculated radiative rate constants, and rate constatns of radiationless transition are summarized in Table I.

Table I. Properties of the Excited States of 1- and 2-Substituted Anthraquinones

Anthraquinones	Solvent	Q_f	τ_{obs}	Q_f/τ_{obs}	k_f(calcd)	k_{nr}
		10^{-2}	10^{-12}·s	10^9·s^{-1}	10^9·s^{-1}	10^9·s^{-1}
	C_6H_6	1.7	410	0.042	0.047	2.4
1-$NHCOCH_3$	CH_3CN	0.82	320	0.026	0.035	3.1
	C_2H_5OH	0.41	66	0.063	0.036	15
	C_6H_6	5.8	1750	0.033	0.040	0.54
1-NH_2	CH_3CN	1.0	660	0.015	0.029	1.5
	C_2H_5OH	0.82	460	0.018	0.030	2.2
	C_6H_6	0.76	330	0.023	0.039	3.0
1-$NHCH_3$	CH_3CN	0.16	190	0.0084	0.030	5.3
	C_2H_5OH	0.14	94	0.015	0.026	11
	C_6H_6	0.32	190	0.017	0.038	5.3
1-$NHCH_3$-4-B_r	CH_3CN	0.11	190	0.0058	0.031	5.3
	C_2H_5OH	0.087	53	0.016	0.050	19
	C_6H_6	21	6500	0.032	0.030	0.12
2-NH_2	CH_3CN	0.80	850	0.0094	0.021	1.2
	C_2H_5OH	0.059	54	0.011	0.024	19
	C_6H_6	15	9800	0.015	0.039	0.087
2-$N(C_4H_9)_2$	CH_3CN	0.33	680	0.0049	0.027	1.5
	C_2H_5OH	0.021	76	0.0028	0.031	13
	C_6H_6	8.5	7700	0.011	0.035	0.095
2-Piperidino	CH_3CN	0.12	300	0.0040	0.024	3.3
	C_2H_5OH	0.012	40	0.0030	0.029	25

III-B-8 A Novel Effect of Man-made Molecular Assemblies on Photoinduced Charge Separation. Sensitized Photoreduction of Zwitterionic Viologen in the Presence of Cationic Surfactants

Toshihiko NAGAMURA, Takashi KURIHARA, Taku MATSUO *(Kyushu Univ.),* **Minoru SUMITANI, and Keitaro YOSHIHARA**

[*J. Phys. Chem.*, in press]

Addition of cationic surfactant at concentrations above CMC drastically increased the efficiency of photoreduction of zwitterionic propylviologen sulfonate as sensitized by tris(2,2'-bipyridine)-ruthenium complex, $Ru(bpy)_3^{2+}$, in the presence of triethanolamine. The efficiency of net electron transfer in the quenching process was slightly improved by the addition of cationic surfactants. The lifetime of reduced viologens remarkably increased with increasing the concentrations of cationic surfactants as shown in Figure 1. The electrostatic fields due to the positively charged molecular assembly such as micelles or bilayers were concluded to trap the reduced viologens and to prevent thermodynamically favored back electron transfer reactions.

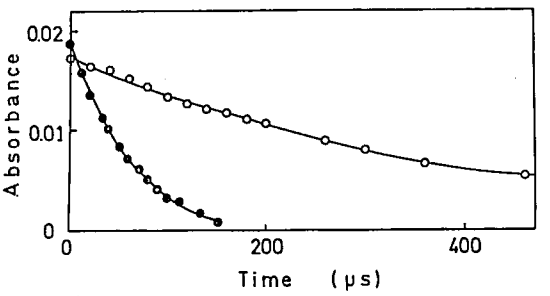

Figure 1. Absorbance at 632.8 nm as a function of time after flash for aqueous solutions of $Ru(bpy)_2^{2+}$ (4.0×10^{-5}M) and $PS^{-2}V^{2+}$ (2 mM) in the absence (●) and presence (○) of CTAC micelles (10 mM).

III—C Solar Energy Conversion by Using Photocatalytic Effects of Semiconductors —Decomposition of Water and Hydrogen Evolution

III-C-1 Dynamical Studies of Photocatalytic Reactions

Kazuhito HASHIMOTO, Tomoji KAWAI, and Tadayoshi SAKATA

The purpose of this study is to elucidate the mechanism of photocatalytic reactions on platinized semiconductor powders. In order to know the dynamical processes of these reactions, we have set up an Ultra-High-Vaccum system equipped with a pulsed molecular beam source. An overall scheme of the apparatus is shown in Figure 1. A molecular beam of mixed methanol and water vapor was injected onto a photocatalyst (Pt/TiO_2 powder) and the photocatalyst was excited by a ns N_2 laser. Formaldehyde and formic acid were detected as the oxidation products of methanol in the time of flight spectra of the reaction products from the Pt/TiO_2 surface. However, the reduction product, hydrogen, could not be observed in the same time region. This seems to suggest that the rate of hydrogen production is slower than that of the oxidation of methanol.

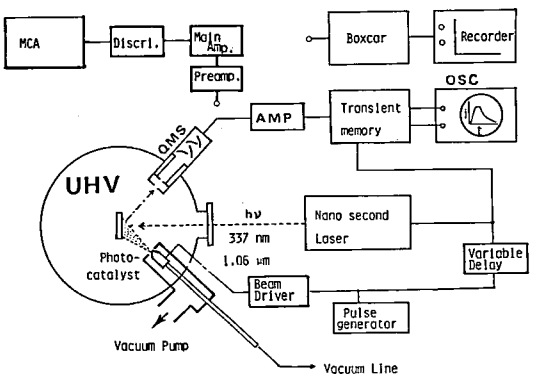

III-C-2 Transient Photo-Current in Ag/Merocyanine/Al sandwich Cells

Kazuhito HASHIMOTO, Tomoji KAWAI, Tadayoshi SAKATA, Yukihiro OZAKI,* Masahiko YOSHIURA,* and Keiji IRIYAMA* *(*Jikei Univ. School of Medicine)*

Organic photo-diodes with sunlight efficiencies of order 1% have been reported.[1] These diodes consist of evaporated dye film sandwiched between two different metals such as Al and Ag. Each dye film behaves like a p-type semiconductor with a rectifying barrier at the Al interface and an ohmic contact at the Ag electrode. The open circuit photovoltage for one of the derivaties of merocyanine dye is as high as $V_{oc} \simeq 1.5$ V, and the short circuit current, I_{sc}, $\simeq 20$ μA. We have studied the transient photocurrent in these diodes by using a ns dye laser as an exciting light source. The theory so far developed does not explain the observed initial photocurrent, although this theory is usually used for the analysis of photocurrents inorganic single crystals. The ovserved transit time is several orders longer than that predicted by this theory. This result suggests that the charge carriers are produced by a bulk process probably involving collision with traps, defects or grain boundaries.

Reference

1) K. Iriyama, *et al. Jpn. J. Appl. Phys.*, Supplement 19-2, 173 (1980).

III-C-3 Hydrogen Evolution by the Photocatalytic Reaction of Several Organic Acids and Water

Tadayoshi SAKATA, Tomoji KAWAI, and Kazuhito HASHIMOTO

The photocatalytic reactions of organic acids are interesting from the view point of hydrocarbon production similar to the methane fermentation in nature. Until now water has not been considered to be involved in these reactions. However our recent experiment showed that the quantity of hydrogen evolved cannot be neglected compared with hydrocarbon production and that only hydrogen is evolved in an alkaline medium. The product analysis carried out by using a steam gascharomatography showed the production of CH_3OH, CH_3CHO, C_2H_5OH, CH_3COOCH_3 and C_2H_5-COOH in aqueous medium for the photocatalytic reaction of acetic acid with powdered TiO_2 (rutile or anatase)/Pt. From these results we could conclude that there exist new reaction paths including the reaction with water as shown schematically in Figure 1 in the case of acetic acid.

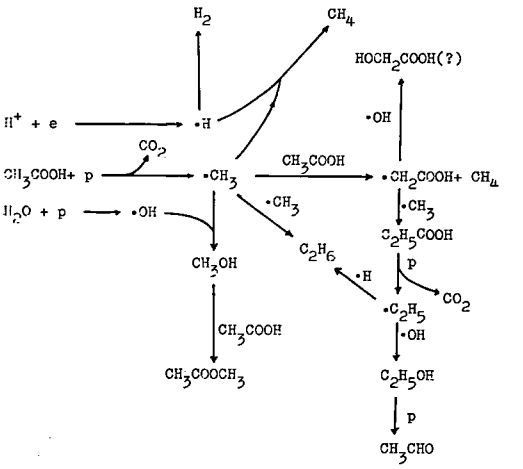

Figure 1. Reaction scheme of photocatalytic reactions of acetic acid in aqueous medium with TiO_2/Pt powdered photocatalyst.

III-C-4 The Catalytic Properties of RuO_2 on n-type Semiconductor under Illumination

Tadayoshi SAKATA, Tomoji KAWAI, and Kazuhito HASHIMOTO

RuO_2 is well known as a good oxidation catalyst for oxygen or chlorine evolution. For the last few years RuO_2 has often been used in photocatalytic water splitting systems. In these systems RuO_2 has been always considered intuitionally to play a role as an oxidation catalyst. In order to elucidate the catalytic role on n-type semiconductors, we measured the photoelectrochemical behaviors of single crystal TiO_2 and CdS by depositing a small amount of RuO_2 and Pt. Figure 1 shows the effect of RuO_2 on the current-voltage curve of TiO_2 single crystal electrode. A remarkable decrease of photoanodic-current and the increase of the cathodic current were observed by depositing RuO_2 on TiO_2 surface as shown in this figure. These results suggest that RuO_2 becomes a recombination center and that RuO_2 works as a hydrogen evolution catalyst. This conclusion was also supported by the photovoltage measurement of a TiO_2 single crystal on which RuO_2 and Pt were deposited separately in two regions. Interestingly, the potentials of RuO_2 and Pt shifted into the negative direction under illumination. Similar negative shift of the potential was also observed under illumination for FuO_2 and Pt

on a syngle crystal CdS. A good photocatalytic activity of particulate RuO_2/TiO_2 was also observed for H_2 evolution from an ethanol-water mixture. All these results suggest that RuO_2 works as a reduction catalyst as well as Pt also on the fine particle RuO_2/TiO_2(or CdS)/Pt photocatalyst, when it is used for water splitting reaction.

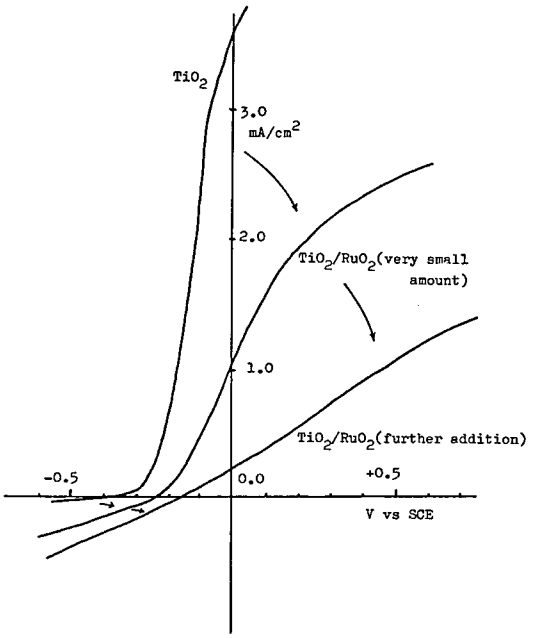

Figure 1. The effect of RuO_2 deposition on the current-voltage curve of a TiO_2 single crystal electrode under illumination.

III-C-5 Photoinduced Decomposition of Organic Acids by Cupric Oxides

Kohichi MIYASHITA,* Kenichiro NAKAMURA* *(Tokai Univ.)*, **Tomoji KAWAI, and Tadayoshi SAKATA**

Photophysical and photocatalytic characteristics of copper oxide (II) are investigated. This study aims to find effective doping conditions of CuO in photocatalytic decomposition of organic acids, mainly pyruvic acid.

The CuO catalyzers are prepared by heating CuO powder with doping metal oxides at about 800°C approximately for 5 hours. Eelctronic conductivity measurements were carried out by CuO doped with 1 − 10% impurity. It has been found that the conductivity of CuO doped with impurities shows a minimum near at 1 mol % of trivalent oxides concentration, and increases by adding univalent oxide or trivalent oxides more than 1 mol %.

Production of CO_2 was observed by irradiating with visible light an aqueous pyruvic acid solution with the CuO catalyzer. The production rate is much higher for CuO doped by Sb and B than undoped CuO. The maximum points for producing CO_2 against various impurity concentration are fairly good coincident with the minimum points for the conductivity described above. In solution, no production of acetoin was observed in the CuO catalytic system, though acetoin is a main product in direct decomposition of pyruvic acid or in other system using catalyzer such as Pd, CdS and M_oS_2.

It has been concluded that CuO doped with some of trivalent metals has effective photocatalytic characteristics for decomposition of pyruvic acid.

III—D Dynamical Processes in Eelctronically and/or Vibrationally Excited Molecules

III-D-1 Infrared Photodissociation of Benzene and Methanol Dimers

Iwao NISHIYAMA and Ichiro HANAZAKI

Infrared photodisssociation of benzene and methanol dimers was investigated using a supersonic molecular beam apparatus. A dissociation probability was determined by measuring the decrease of molecular beam intensity with a Q-pole mass spectrometer. Laser fluence dependence of the dissociation probability was measured in the range of 0.005-1 Jcm^{-2} for the laser lines of CO_2 9 μm band. The threshold fluence for dissociation was observed in the range of 0.005-1 Jcm^{-2} for both

dimers. Dissociation of monomer molecules was not observed in the present fluence range. In Figure 1, the dissociation probability of benzene dimer was plotted as a function of excitation wavelength together with an IR absorption spectrum of benzene monomer. Although the IR absorption spectrum of benzene dimer is different from that of monomer, the peak of absorption band is expected to be not so different because the liquid absorption spectrum has a peak at almost the same wavelength. Therefore, Figure 1 implies that the dissociation probability of benzene dimer has a maximum at the peak of the absorption band. On the other hand, a significant blue shift, ca. 15 cm^{-1}, was found for the methanol dimer. This fact may be explained by the number of photons necessary to dissociate a dimer. The benzene dimer can be dissociatd by a single photon and the methanol dimer needs two photons. Futhermore, it should be noted that dissociation probability seems to reach unity for all laser lines if the laser fluence incereases sufficiently.

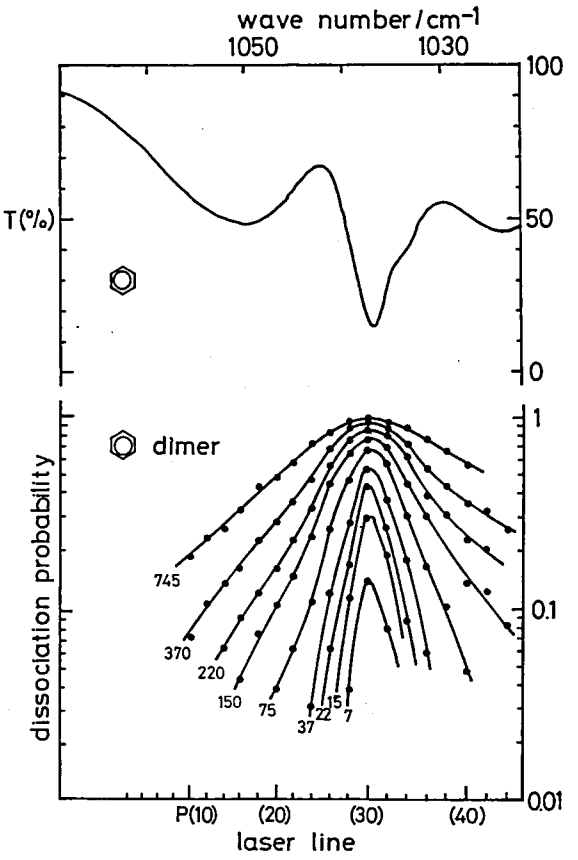

Figure 1. Excitation wavelength dependence of the dissociation probability of benzene dimer. The figures are laser fluences in $mJcm^{-2}$. Infrared absorption spectrum of benzene monomer is also shwon. Within the present wavelength region, monomeric benzene has a single absorption band due to the CH in-plane bending vibration.

III-D-2 Fluorescence Excitation Spectrum of Acetone in a Supersonic Nozzle Beam

Masaaki BABA and Ichiro HANAZAKI

The absorption and emission spectra of gaseous polyatomic molecules are generally not well resolved because of highly overlapping vibrational and rotational structures. However, recent molecular beam studies using a supersonic free jet have revealed that the spectra could be simplified drastically to give well resolved structure even for large molecules.

We have recently started a study on the relaxation and chemical reaction of carbonyl compounds in the $S_1{}^1A_2(n, \pi^*)$ state using a pulsed supersonic molecular beam apparatus described elsewhere (See "Special Research Project"). In Figure 1. are shown the fluorescence excitation spectra of acetone under various conditions. The gas phase absorption spectrum of acetone is known to show no clear fine structure and, to our knowledge, there is no well resolved spectrum for this molecule. Acetone in the molecular beam is excited by the second harmonics of YAG laser pumped dye laser output with the power of 2~3 mJ/pulse. The band width is nominally 0.07 cm^{-1} and the maximum repetition rate is 10 Hz. Figure 1 (a) is the absorption spectrum of acetone in the gas phase at room temperature, (b) is the fluorescence excitation spectrum in a supresonic beam of neat acetone (260 Torr) and in (c) acetone was seeded in 2.5 atm He gas. (b) and (c) were measured from 310 to 325 nm using R-640 dye. We can see that each vibrational band becomes sharper as the temperature becomes lower on going from (a) to (c). In (c) is observed a progression with a spacing of 250 cm^{-1} due to the C = O out-of-plane mode. This spectrum does not agree with the assignment based on the absorption spectrum.[1] A detailed vibrational analysis is now being undertaken.

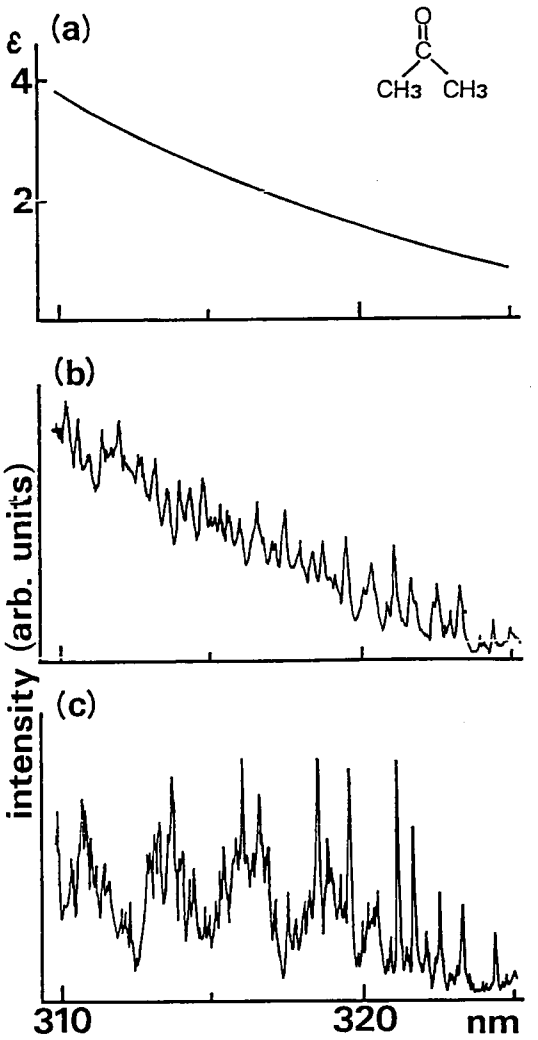

Figure 1. (a) Absorption spectrum of acetone in the gas phase at room temperature. (b) Fluorescence excitation spectrum in a supersonic beam of neat acetone (260 Torr). (c) Fluorescence excitation spectrum in a supersonic beam of acetone seeded in 2.5 atm He gas.

Reference

1) W. A. Noyes, Jr., A. B. F. Duncan and W. M. Manning, *J. Chem. Phys.*, **2**, 717 (1934).

III-D-3 Overtone Spectra of CH Stretching Vibrations in Acetone and Acetaldehyde

Ryoichi NAKAGAKI and Ichiro HANAZAKI

[*J. Phys. Chem.*, **86**, 1501 (1982)]

CH stretching overtone spectra of acetone and acetaldehyde were measured in the liquid phase up to $\Delta v = 5$ as shown in Figure 1. It was found that the methyl CH stretching overtones exhibit a splitting due to non-equivalent sites with respect to the skeletal plane of the acetyl group. Aldehydic CH stretching overtones were also observed.

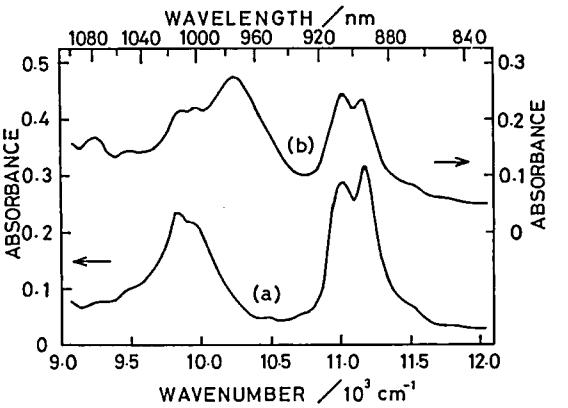

Figure 1. Liquid-phase overtone spectra of (a) acetone and (b) acetaldehyde at room temperature in the region Δv (CH) = 4 (10 cm pathlengh).

III-D-4 Inequivalent Methyl CH Oscillators in Methyl-Substituted Conjugated Compounds as Revealed by Higher Overtone Spectra

Ryoichi NAKAGAKI and Ichiro HANAZAKI

[*Chem. Phys.*, in press]

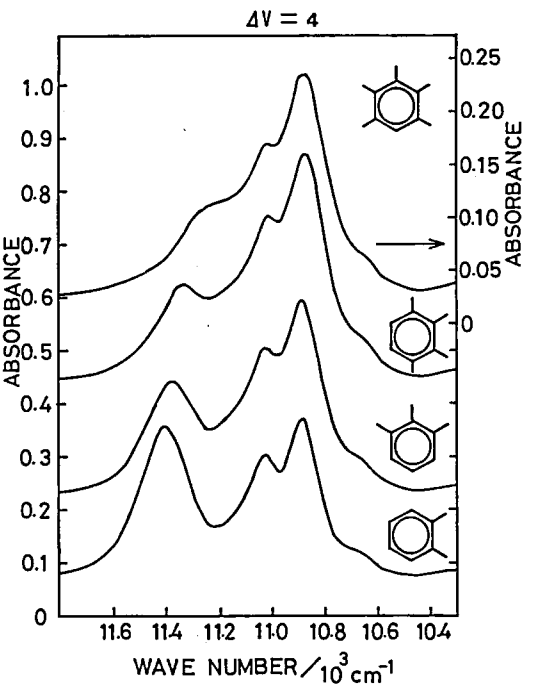

Figure 1. Liquid-phase overtone spectra at room temperature in the region of $\Delta v = 4$ (10 cm pathlength). From the top to the bottom: pentamethylbenzene (carbon tetrachloride solution, 2.71 mol. l^{-1}), prehnitene (pure liquid), hemimellitene (pure liquid), and o-xylene (pure liquid). The offset of absorbance scale is 0.2 for hemimellitene, and 0.4 for prehnitene.

CH stretching overtone spectra of methyl groups in aklylated aromatic and heterocyclic compounds were measured in the liquid phase up to $\Delta v = 5$ as shown in Figure 1. A large splitting of methyl CH stretching overtones is observed for methyl groups with relatively high rotational barriers (V_3), whereas quasi-free methyl internal rotors show a small splitting on account of rotational averaging. The splitting is shown to be confined to methyl groups directly bonded to conjugated systems and attributed to the inequivalence of local methyl CH oscillators caused by the non-bonded interaction with the molecular conjugated plane.

III-D-5 Substituent Effects in Benzene Derivatives —A Local Mode Analysis of Ring CH Stretching Overtone Spectra of Methylated and Chlorinated Benzenes

Ryoichi NAKAGAKI and Ichiro HANAZAKI

Methylation and chlorination of benzene induce red and blue shifts, respectively, in overtone spectra of the ring CH stretching vibrations. Except for the distinctly different sign of spectral shifts, both substitutions exhibit similar effect on the magnitude of A terms in the Birge-Sponer relationship, $\Delta E(v\text{-}0) = (A+Bv)v$. The observed changes in the A terms (see Figure 1) are due to the polar effect and quantitatively analyzed by the use of a simple model based upon the local mode asuming additivity of the substituent effects.

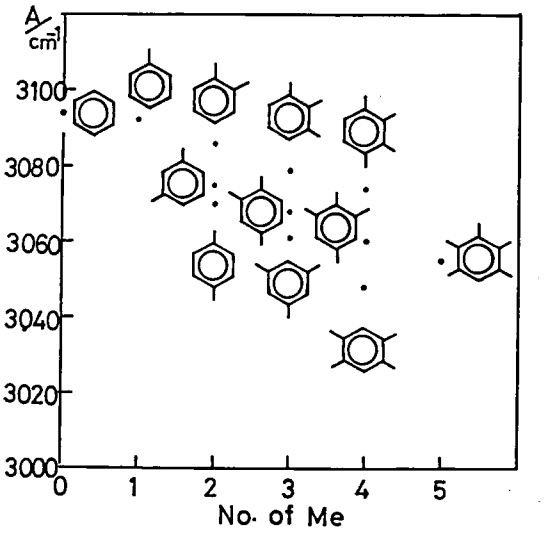

Figure 1. Effect of methylation on the magnitude of A terms for the ring CH stretching vibrations.

III—E Study on Photochemical Processes Related to Planetary Space Chemistry

Photochemical events on comet surface or icy satellites of outer planets are of great interest since the chemistry initiated by high energy photons (*i.e.* UV and VUV light) under the extreme conditions is expected to include unknown pathways yielding simple organic molecules. We have found that the 6.4 eV (and/or 12.8 eV) photon impact on ammonia-containing water ice at 130 K produces hydrazine($H_2N{\cdot}NH_2$), diimide(HN=NH), and hydroxylamine(NH_2OH) in the solid. These compounds have been known to produce amino acids after the "incubation" with formaldehyde in hot water. The formation mechanism is well explained by a photochemical bimolecular condensation reaction in the solid cage. Ammonia and simple amines have been found to undergo the condensation reaction efficiently with methyl compounds such as CH_3CN, CH_3OH, etc. This reaction yields molecular hydrogen, or methane, or hydrogen cyanide, or water as a by-product together with a condensed bigger molecule.

In the space of outer planet or intersteller region, a large amount of molecules are expected to excist as clusters. Knowledge of the structure and composition of water-ammonia binary clusters is necessary to the understanding of condensation processes of these molecules. Application of the two-photon ionization mass spectroscopy coupled with a pulsed molecular beam technique has given us successful results for the study of stable composition of the larger water-ammonia clusters.

III-E-1 A Mechanism of UV Laser Photosputtering of Molecular Condensate Surface

Nobuyuki NISHI, Hisanori SHINOHARA, and Tohru OKUYAMA

Icy objects in space, such as Saturn's ring or comets, are known to release surface molecules into vacuum by UV photon impact on the surface. Here, we propose a new photosputtering mechanism for UV photon impact on icy materials based on VUV laser photosputtering experiments of H_2O ice containing NH_3.

Experimental apparatus consists of two UHV chambers. Premixed sample gas was deposited on a cold quartz plate in a sample chamber ($P \lesssim 6 \times 10^{-9}$ Torr). Sputtered molecules and photofragments were detected by a high resolution quadrupole mass spectrometer situated in a detection chamber ($P \lesssim 5 \times 10^{-10}$ Torr). Expanded light from an excimer laser at 248 nm or 193 nm (5 mJ/cm^2) was irradiated on the sample at 130 K.

The time-of-flight signal of parent H_2O molecules was twelve times as strong as that of NH_3, indicating photochemical breaching of NH_3 molecules. The translational energies of H_2O and NH_3 are thermalized at 625 and 655 K for 193 nm and 730 and 580 K for 248 nm, respectively. The energies are almost independent of photon density. The H_2O signals (I) increased nearly quadratically with the increment of laser power (E) ($n = 2.2 \pm 0.2$ at 248 nm, $n = 1.7 \pm 0.3$ at 193 nm; $I = E^n$). While the NH_3 signals showed the signal increment with $n = 1.5 \pm 0.3$ for the 248 nm excitation and that with $n = 1.0 \pm 0.2$ for 193 nm. The observed facts lead us to conclude that the photosputtering occurs due to electronic excitation of a constituent molecule through one- or two-photon absorption in a time shorter than the intermolecular energy transfer period. A surface molecule is considered to have Rydberg excited states with higher energies than the gas molecule. The surface molecule in a Rydberg state could be repelled by surrounding molecules due to increased exchange repulsive force. Figure 1 shows the sputtering mechanism propsoed here.

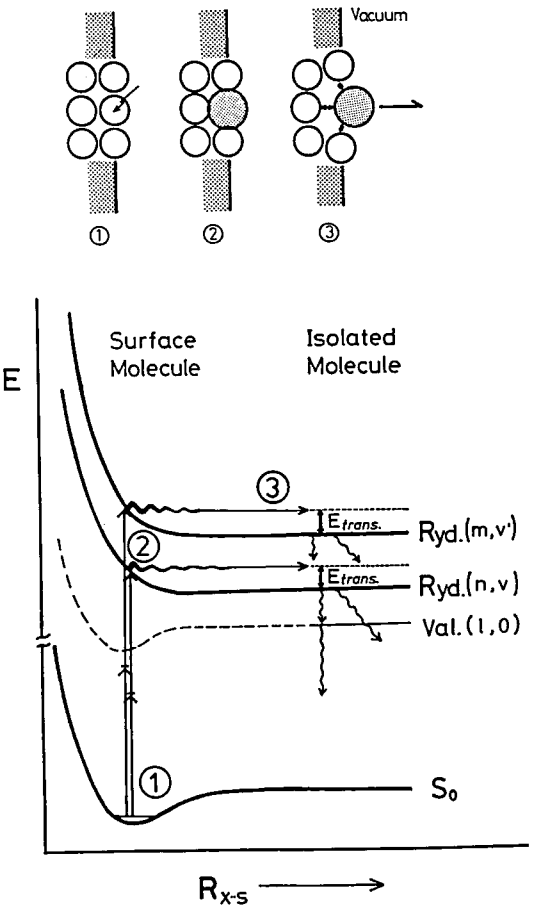

Figure 1. Surface molecule ejection through the excitation of an electron from a valence orbital to a Rydberg-type large orbital. Rydberg-type excited states of a surface molecule locate at energies higher than those of an isolated molecule. The translational energy of a sputtered molecule is related to intermolecular interactions of the surface molecule in the excited state with nieghbor molecules.

III-E-2 Bimolecular Photochemical Condensation Reaction in a Low Temperature Solid Containing Water and Ammonia

Nobuyuki NISHI, Tohru OKUYAMA, and Hisanori SHINOHARA

An 193 nm laser (5 mJ/cm^2~100 mJ/cm^2) was irradiated on an ice containing H_2O and NH_3 at 130 K. This light excites an ammonia molecule electronically in the solid but does not excite any water molecules. A quadrupole mass spectrometer analyzes mass numbers and kinetic energies of the particles ejected from the surface by the photon impact at 248 nm or 193 nm. 248 nm photons stripped off surface molecules from the ice mainly through two-photon excitation, although photo-

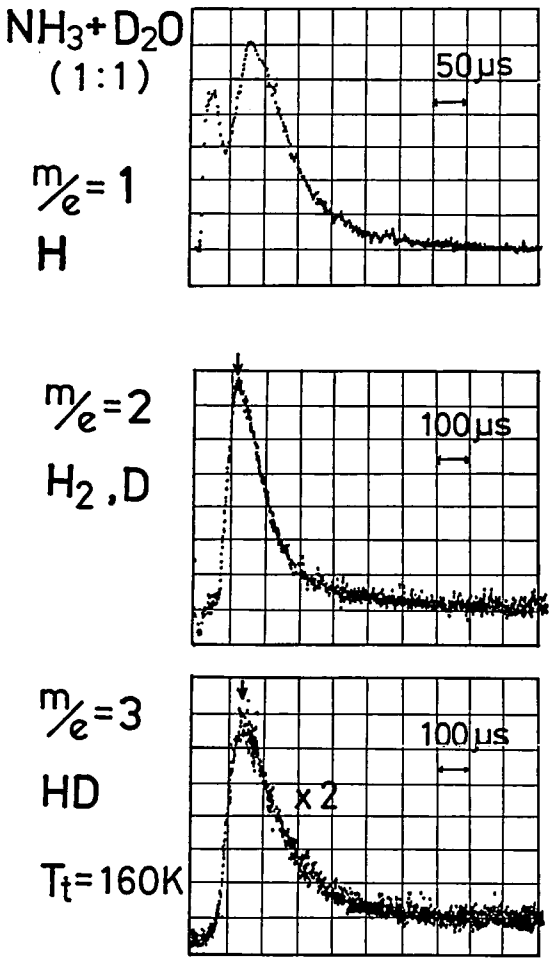

Figure 1. Time-of-flight signals of atomic and molecular hydrogen ejected from the ice surface containing NH_3 and D_2O by 193 nm photon impact.

chemical reaction could not be detected under the same condition as that of the 193 nm photolysis of this solid. Time-of-flight (TOF) signal of atomic hydrogen was observed showing two distinct translational energy components ($\bar{E}_t^1$ = 14 kcal/mol, $\bar{E}_t^1$ = 0.7 kcal/mol). The higher translational energy is slightly smaller than that observed for the 193 nm photolysis of an isolated ammonia in a molecular beam. The hydrogen with this average energy is attributed to a photofragment of a surface ammonia excited by 193 nm light. Photosputtering by 248 nm or 193 nm photons stripped off surface molecules, and the occluded hydrogen *molecules* appeared on the new surface and then escaping to vacuum. The observed translational temperature is in the range of 130 ~ 160 K. In the system of NH_3 + D_2O, the ratio of H_2 to HD(m/e = 3) was found to be ~2. The presence of HD molecule as a product indicates that the hydrogen is not generated by the recombination of hydrogen atoms. TOF signals at m/e = 32, 33, 34 were observed and attributed to $H_2N{\cdot}NH_2$, NH_2OH or NH_2NHD,and NH_2OD, respectively. It is concluded that a new type of photochemical condensation reactions occur in the 193 nm photolysis of water-ammonia mixed ice in the following ways.

$$NH_3^* + NH_3 \longrightarrow NH_2{\cdot\cdot}H + NH_3 \longrightarrow H_2N{\cdot}NH_2 + H_2 \quad (1)$$

$$NH_3^* + D_2O \longrightarrow NH_2{\cdot\cdot}H + D_2O \longrightarrow NH_2OD + HD. \quad (2)$$

III-E-3 Photosputterig Analysis of 193 nm Laser Induced Reactions in a Low Temperature Solid Containing Ammonia and Acetonitrile

Tohru OKUYAMA, Hisanori SHINOHARA, and Nobuyuki NISHI

Study on photochemical bimolecular condensation reactions in solids, which was first investigated in the ammonia containign water ice (**III-G-2**), has been extended to a more complex system of NH_3 + CH_3CN (or CD_3CN) (1:4) at 130 K. As expected from the previous study, time-of-flight (TOF) signals of atomic and molecular hydrogen were detected upon 193 nm laser irradiation (20 mJ/cm^{-2}, 10 ns). After 1~3 × 10^4 pulse irradiation, photoproducts were sputtered by 248 nm laser photons and analyzed *directly* by a high resolution mass spectrometer. Figure 1 shows TOF spectra of molecules ejected from the solid. Relative product yield changed depending on the total number of irradiated laser pulses. Besides the reactions of an ammonia pair ($2NH_3 \xrightarrow{h\nu} H_2NNH_2 + H_2 \xrightarrow{h\nu} HN = NH + 2H_2$), the following condensation reactions between ammonia and acetonitrile appear to be dominant in the solid.

$$NH_3 + CH_3CN \xrightarrow{h\nu} NH_2{\cdot\cdot}H + CH_3CN \longrightarrow NH_2CH_2CN + H_2 \quad (1)$$

$$\xrightarrow{h\nu} NH_2{\cdot\cdot}H + CH_3CN \longrightarrow NH_2CN + CH_4 \quad (2)$$

$$\xrightarrow{h\nu} NH_2{\cdot}H + CH_3CN$$
$$\longrightarrow NH_2CH_3 + HCN. \quad (3)$$

The produced amino compunds are photolyzed succesively and methane is subject to the attack by an atomic hydrogen yielding a methyl compound. The dimer of acetonitrile absorbs an 193 nm photon. Photosputtering analysis of photolyzed pure acetonitrile solid at 193 nm indicates the occurence of the following disproportionation reaction.

$$2CH_3CN \longrightarrow (HCN)_2 + C_2H_4. \quad (4)$$

The direct detection of photoproducts also showed us the existence of stable radicals on the surface and probably in the solid at 130 K.

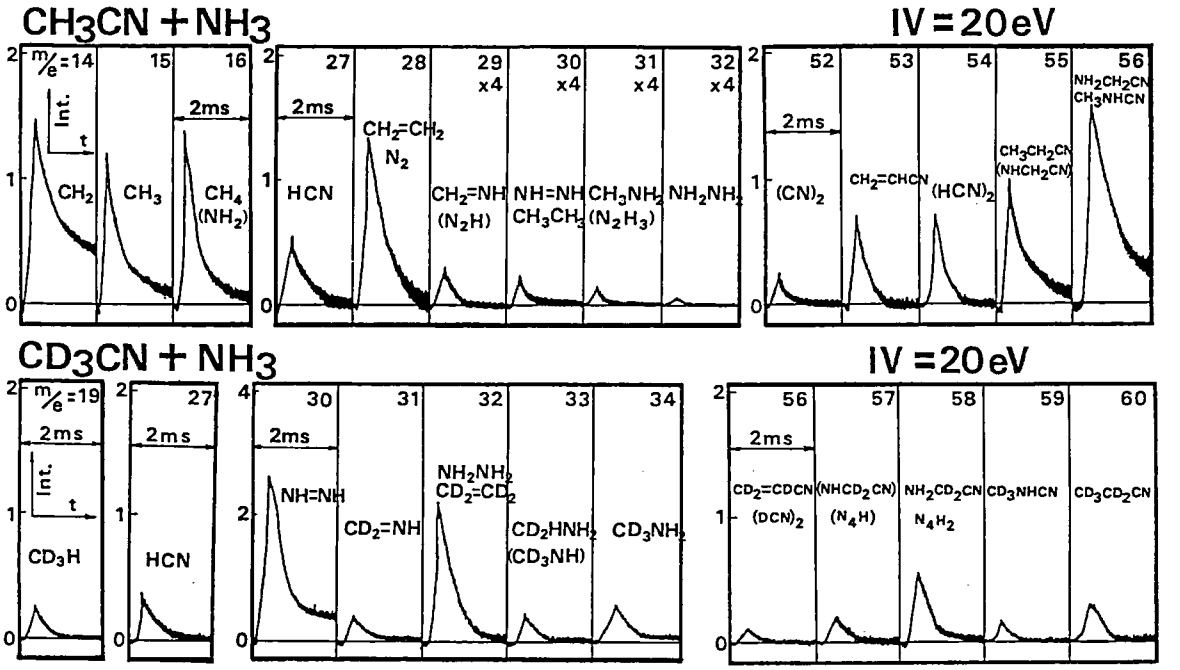

Figure 1. Time-of-flight signals obtained by 248 nm laser pulse (10 ns) irradiation on the solids of (a) $CH_3CN + NH_3$ (4:1) photolyzed by 1.5×10^4 shots of 193 nm laser pulse, and (b) $CD_3CN + NH_3$ (4:1) photolyzed by 3×10^4 shots of 193 nm pulse.

III-E-4 Detection of Ammonia Clusters by Two-Photon Ionization Mass Sepctroscopy

Hisanori SHINOHARA and Nobuyuki NISHI

Ammonia clusters and their photochemistry are especially interesting because ammonia is a constituent of the Jovian atmosphere and it will condense into a layer of cloud at some tropospheric level. The clusters may undergo photochemical processes in the atomosphere. We have recently shown[1] that UV two-photon ionization (TPI) method is suitable for "soft" detection of ammonia clusters due to a strong resonance two-photon absorption of ammonia molecules of ArF (193 nm) photons.

A typical TPI mass spectrum of ammonia clusters that are generated by the ArF laser irradiation of a supersonic nozzle beam at several different stagnation pressures is depicted in Figure 1. The amount of observed clusters increased with increasing the nozzle stagnation pressure. A KrF laser (248 nm) irradiation of the ammonia clusters, on the other hand, gives only very weak TPI signals, since an ammonia molecule does not absorb a 248 nm photon. This is indicative of the necessity of selectively photon-absorbing moiety for

the "soft" generation of the ammonia cluster ions. The selectivity and softness of TPI method could be seen most drastically for the ionization of clusters, as shown in this work, on account of their weak intermoleuclar bonds.

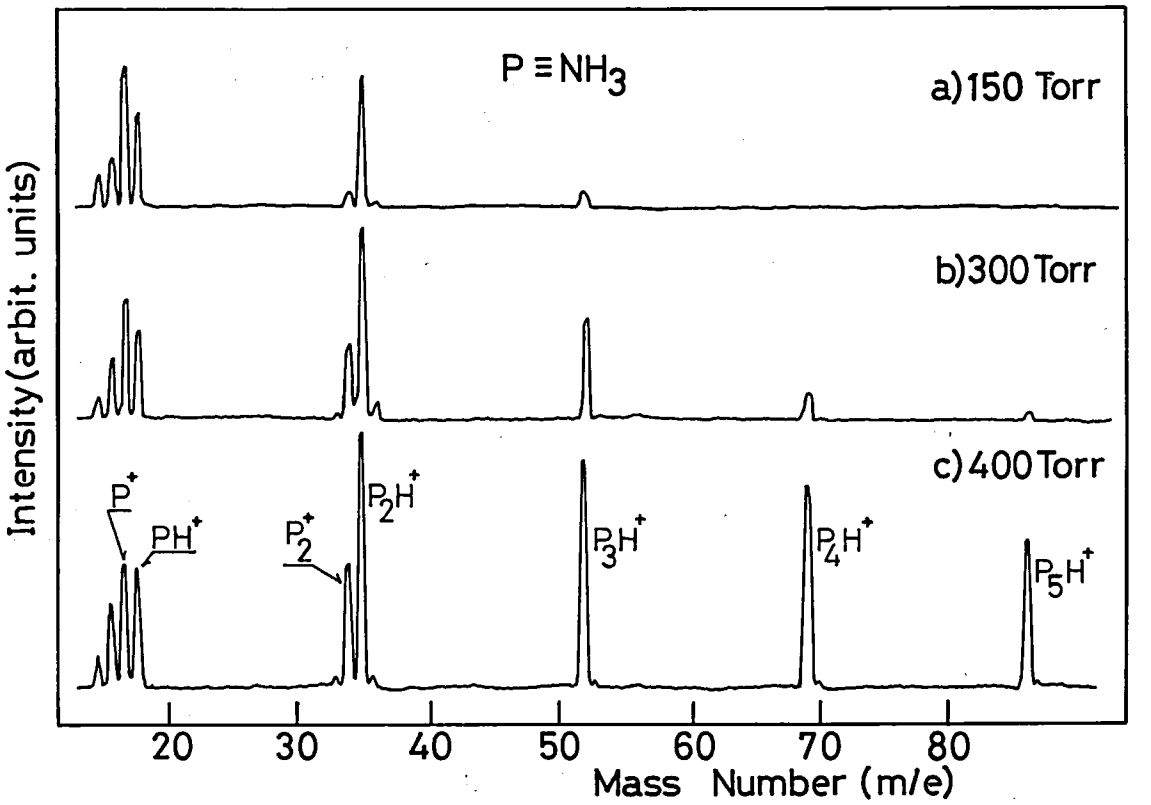

Figure 1. An 193 nm two-photon ionization mass spectrum of ammonia clusters at three different nozzle stagnation pressures. P represents ammonia monomer in the clusters.

Reference

1) H. Shinohara and N. Nishi, *Chem. Phys. Lett.*, **87, 561 (1982).**

III-E-5 Molecular Beam Two-Photon Ionization Studies on Ammonia-Water Binary Clusters

Kwang Y. CHOO *(Seoul National Univ. and IMS)*, **Hisanori SHINOHARA, and Nobuyuki NISHI**

Ammonia and water are known to be two of the most important molecules in chemical evolution studies and also interstellar chemistry. We have detected ammonia-water binary clusters by means of two-photon ionization (TPI) mass spectroscopy. All the major ions detected for the binary clusters are classified into three categories according to the following general expressions, (i) $H^+(NH_3)_m$ ($1 \leqq m \leqq 8$) (ii) $H^+(H_2O)_n$($n=3$, 4) (iii) $H^+(NH_3)m(H_2O)_n$ ($1 \leqq m$, $n \leqq 7$ and $1 \leqq m+n \leqq 8$). A typical TPI mass spectrum of the binary clusters is shown in Figure 1. Each peaks in the TPI spectrum were identified by replacing water-^{16}O in the mixture with water-^{18}O. The results show the necessity of photon-absorbing moiety (ammonia molecules in this case) in the cluster ions. On account of its "softness", the TPI experiment reveals that the intensities of the ion clusters are approximately related to the concentration of neutral clusters, which makes it possible to elucidate the stability of the neutral clusters. From different mixing-ratio experiments, it is concluded that the most stable inner shell consists

of ammonia moleucles and water molecules are bound with the shell.

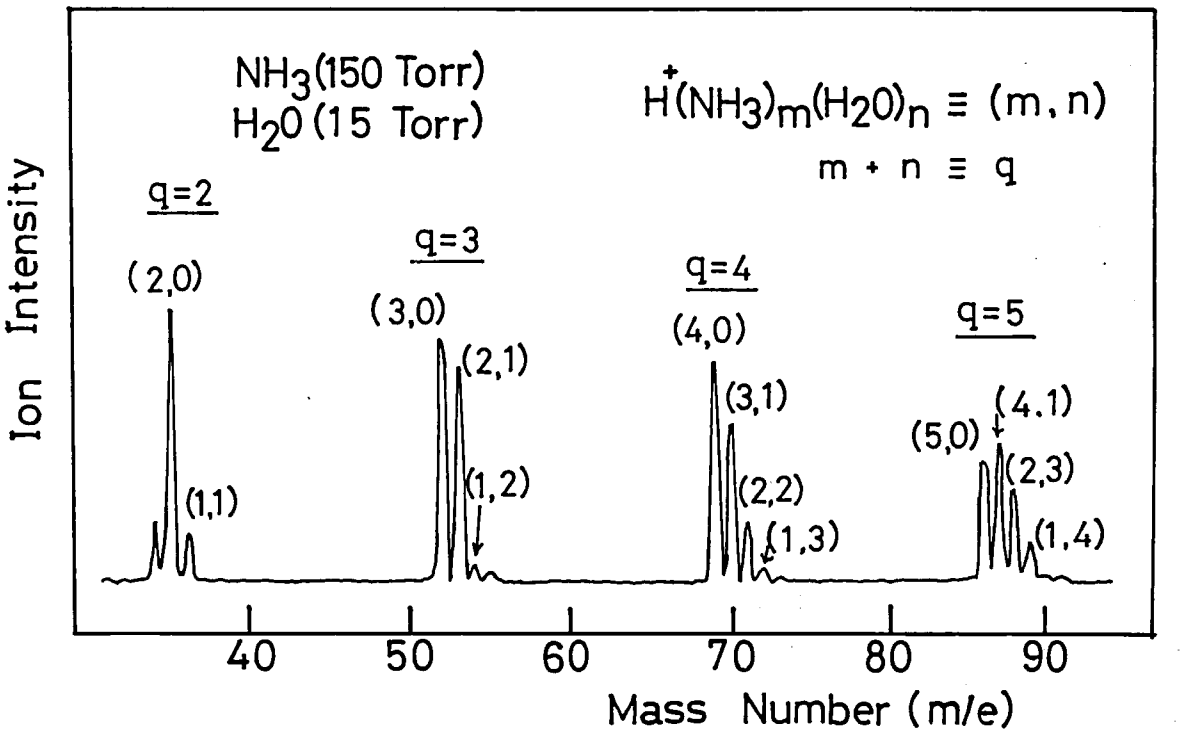

Figurer 1. Two-photon ionization mass spectrum of ammonia-water binary clusters generated by ArF excimer laser (193 nm). q stands for the total number of molecules in the clusters.

III—F Photodissociation and Multiphoton Ionization Dynamics of Molecular Beams Initiated by UV Excimer Lasers

It has been recognized that knowledge of mechanisms and excess energy partitioning of photofragments is important to our understanding and modeling such diverse problems as chemical processes in interstellar space, the composition and kinetics of planetary atmospheres, and laser chemistry in general. Strong VUV lasers, together with technology of supersonic nozzle beams, make the so-called photofragment spectroscopy a promising candidate for elucidating photodissociation dynamics. A photofragment spectrometer equipped both with a high peak power VUV excimer laser and a pulsed supersonic moleuclar beam enables us to characterize experimentally dissociation channels. The UV excimer lasers are also well suited for multiphoton ionization (MPI) mass spectrometry study. Since most species absorb light somewhere in these wavelength regions and only two or three UV photons are required to reach molecular ionization thresholds, efficient resonant-enhanced processes can occur. In many cases, single-photon photodissociations and two-photon ionization steps at the UV region are mutually competing processes. Thus, an understanding of the extent of ionization along with photofragmentation is necessary for all future experiments in UV laser induced chemistry.

III-F-1 Translational Energy Distribution in the 193 nm Photo-elimination Reactions of Chloroethylenes

Masayuki UMEMOTO, Hisanori SHINOHARA, Nobuyuki NISHI, and Ryoichi SHIMADA
(Kyushu Univ.)

Upon the $\pi^* \leftarrow \pi$ excitation of chloroethylenes at 193 nm, photofragments of Cl and HCl were detected with different translational energy distributions by a photofragment spectrometer.[1] These fragments originate from the following reactions.

$$C_2H_nCl_{4-n} \longrightarrow C_2H_nCl_{3-n} + Cl \quad (1)$$

$$\longrightarrow C_2H_{n-1}Cl_{3-n} + HCl, \quad (n=1,2) \quad (2)$$

Table I summarizes the translational energies for four chloroethylenes. Mean fraction of translational energy to available energy ($E_{avl} \simeq h\nu - \Delta H^0_f$) is also shown. The observed translational energy for the Cl atom detachment process of cis-dichloroethlene is much less than that of trans-dichloroethylene. This fact indicates that *cis-trans* isomerization does not occur in a time domain of the photodissociation. The observed laboratory angular distribution of the recoiling Cl atom suggests that the dissociation occurs in a time scale shorter than the vibrational period ($10^{-12} \sim 10^{-14}$s). The degree of rotational excitation of fragment molecule in reaction (1) is qualitatively explained by the rigid radical impulsive model. It is concluded that 40% of the available energy is converted to vibrational excitation of molecular fragments in reaction (1).

Table I. Photofragmentation energetics of chloroethylenes.

	Cl atomic detachment			HCl molecular elimination		
Parent	E_{avl}	E_{Tmax}	f_T	E_{avl}	$\bar{E}_T$	f_T
CH_2=CHCl	62.5	23.4	0.374	124	23.0	0.185
cis-CHCl=CHCl	58.2	13.6	0.231	120	15.2	0.127
trans-CHCl=CHCl	59.4	26.1	0.439	120	16.6	0.138
CH_2=CCl_2	58.5	21.2	0.362	120	15.3	0.128

Energies are given in kcal/mol.

Reference
1) H. Shinohara and N. Nishi, *J. Chem. Phys.*, **77**, 234 (1982)

III-F-2 Photodissociation of Molecular Beams of SO_2

Masahiro KAWASAKI,* Kazuo KASATANI,* Hiroyasu SATO,* *(*Mi'e Univ.)*, Hisanori SHINOHARA, and Nobuyuki NISHI

The $\tilde{C}^1B_2 \leftarrow \tilde{X}^1A_1$ band system of SO_2 starts near 235 nm and extends down to 165 nm, although predissociation begins at the threshold of 219.5 nm. The c.m. translational energy distribution $f(E_T)$ is given in Figure 1. As the dissociation energy of SO_2 is 546 kJ/mol, the available energy ($E_{AVL} = \hbar\omega + E_p - D_0$) at 193 nm (620 kJ/mol) is 78 kJ/mol. The spin-forbidden process, if it occurs, producing the $SO(a^1\Delta)$ (ΔH = 76 kJ/mol) is barely accessible.

$$SO_2 \longrightarrow SO(X^3\Sigma^-) + O(^3P) \quad \Delta H = 546 \text{ kJ/mol}$$

$$SO_2 \not\longrightarrow SO(a^1\Delta) + O(^3P) \quad \Delta H = 622 \text{ kJ/mol.}$$

According to phase space theory, the prior distribution $P(E_T)$ is given by,

$$P(E_T) \propto \sqrt{E_T - \alpha}(E_{AVL} - E_T)^n$$

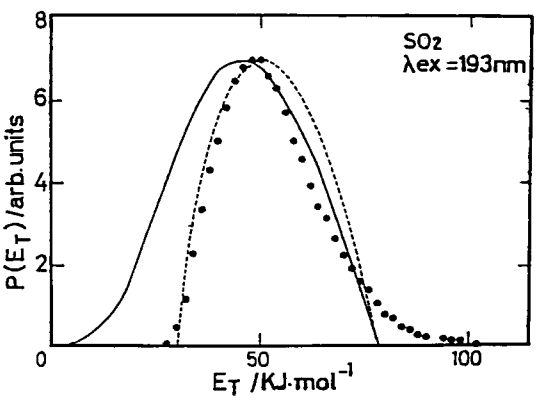

Figure 1. Translational energy distrtibution in SO_2 photolysis at 193 nm: ●, obtained from the time-of-flight distribution of the SO fragments; solid line, prior distribution assuming that both the vibrational and rotational levels are continuous and that the potential barrier (α) equals zero; broken line, assuming α = 30 kJ/mol.

where n is the number of normal modes of the photofragments and α the potential barrier. Using n = 1 and α = 30 kJ/mol, the theoretical distribution is in good agreement with experimental one. This distribution is well characterized as being most statistical subject. Actually, the angular distribution $g(\theta)$ was nearly isotropic and is consistent with slow predissociation mechanism,

$$SO_2 + \hbar\omega(193\ nm) \rightarrow SO_2^*(\tilde{C}) \rightarrow SO_2(\tilde{X}) \rightarrow SO + O.$$

III-F-3 Photodissociation of Molecular Beams of N_2O_4

Masahiro KAWASAKI,* Kazuo KASATANI,* Hiroyasu SATO,* *(*Mi'e Univ.),* **Hisanori SHINOHARA, and Nobuyuki NISHI**

The N_2O_4 absorption increases sharply to what appears to be a maximum in the region of ~190 nm. Structures in the spectrum are absent in the entire region. Figure 1 shows $P(E_T)$ obtained in 193 nm photolysis. Observed fragments were NO_2. Since the maximum E_T observed was ~300 kJ/mol, the possible photodissociation processes are as follows.

$$N_2O_4 + \hbar\omega \longrightarrow 2NO_2^*(\tilde{A}^2B_2) \quad 330 \text{ kJ/mol} \quad [1]$$

$$\longrightarrow NO_2^*(\tilde{A}^2B_2) + NO_2(\tilde{B}^2B_1) \quad 271 \text{ kJ/mol} \quad [2]$$

$$\longrightarrow 2NO_2^*(\tilde{B}^2B_1) \quad 211 \text{ kJ/mol} \quad [3]$$

Actually the visible emission from NO_2^* ($\tilde{A}$ or $\tilde{B}$) was observed in the photolysis of N_2O_4 at 193 nm. Since β = 1.1 in angular distribution, the photoexcited state has a parallel transition moment and the lifetime is estimated to ~0.9 ps. Photodissociation processes at 193 nm must be direct or quite fast predissociative ones

From symmetry consideration, the planar N_2O_4 (D_{2h}) which has a transtion dipole along N-N axis does not correlated with the formation of $2NO_2^*$

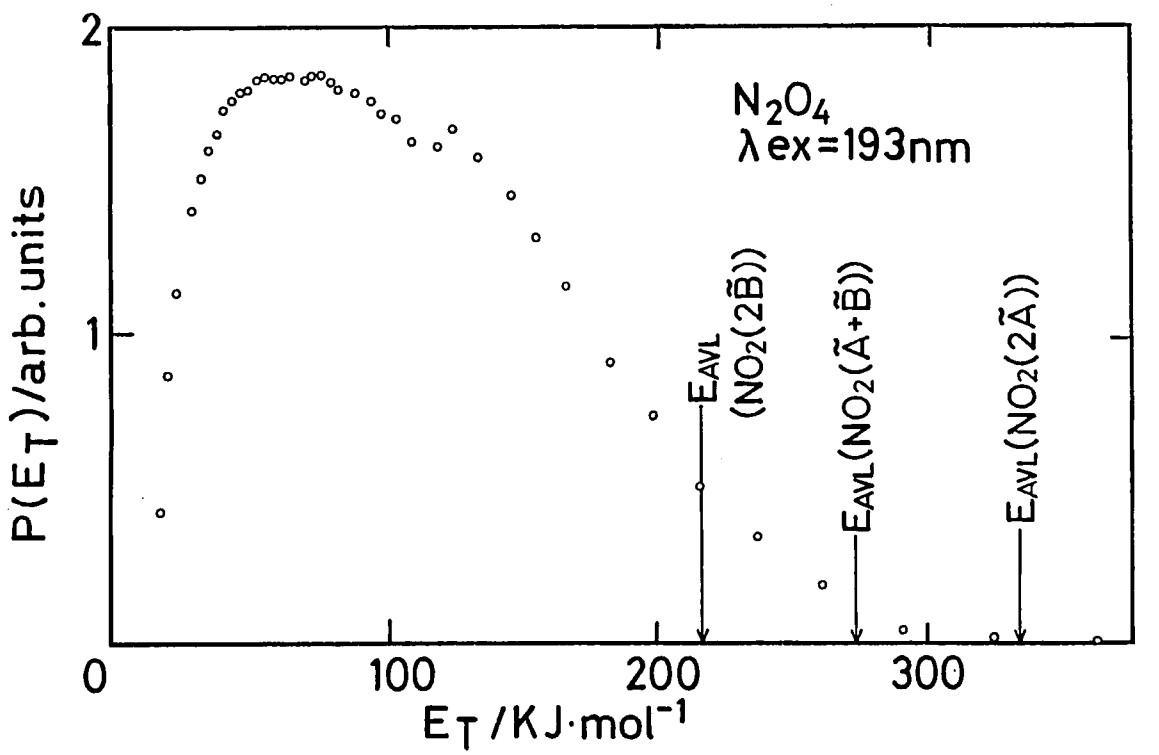

Figure 1. Translational energy distribution in N_2O_4 photolysis at 193 nm. E_{AVL} is the available energy for the formation of the excited states of NO_2.

($2\tilde{A}$, A + $\tilde{B}$, or $2\tilde{B}$). Since absorption coefficient at 193 nm is more than 10,000 and also the transition dipole is along N-N axis, this absorption may be attributed to the CT band.

III-F-4 Multiphoton Ionization Mass Spectroscopy of Acetone

Masaaki BABA, Hisanori SHINOHARA, and Nobuyuki NISHI, and Noboru HIROTA *(Kyoto Univ.and IMS)*

Acetone is a particularly interesting molecule in that KrF (248 nm, 5.0 eV) and ArF (193 nm, 6.4 eV) lasers correspond to different intermediate states, the first singlet (n, π^*) and the (n, 3s) Rydberg states, respectively, and that the two ionization processes should reflect these intermediate states' character. An acetone molecule has been found to dissociate into methyl and acetyl radicals by a KrF photon while the molecule is relatively stable at the (n, 3s) Rydberg state. At both excitation wavelengths the parent ion can be formed by resonance enhanced two-poton processes. At 193 nm the measured power dependence for the parent ion exhibits quadratic dependence on intensity, which coincides with the energetical consideration. The observed power index for $CH_3COCH_3^+$ at 248 nm is, however, much less than the expected quadratic dependence. The 248 nm power data might reveal a complex process consisting of single-photon photodissociation and two-photon ionization steps. To the extent that molecular dissociation competes with ionization, four level system —— a gound state, the resonant intermediate ^{1}(n, π^*) state, an ionization continuum, and polulation trapping state —— provides a satisfactory model for the 248 nm two-photon ionization. The four-level model for acetone two-step ionization is presented in Figure 1.

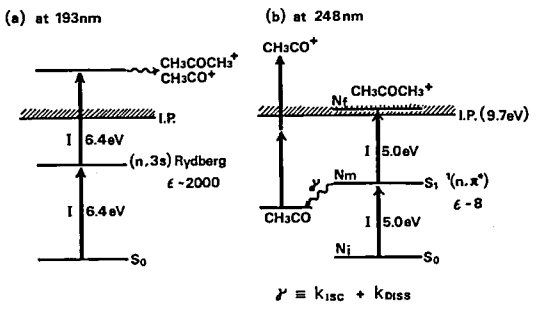

Figure 1. Three- and four-level model for acetone two-step ionizations.

III-F-5 Multiphoton Ionization Mass Sepctroscopy of Aliphatic Ketones in a Supersonic Beam

Masaaki BABA, Hisanori SHINOHARA, and Nobuyuki NISHI, and Noboru HIROTA *(Kyoto Univ. and IMS)*

Knowledge of the primary photochemical processes of aliphatic ketones under collision free conditions is clearly lacking in spite of several studies[1] in the past. Multiphoton ionization (MPI) experiments with a supersonic nozzle beam would provide good information for such processes.

The aliphatic ketones have weak $\pi^* \leftarrow$ n absorption at 4.98 eV and relatively strong 3s $\leftarrow$ n Rydberg absorption at 6.42 eV. The ^{1}(n, π^*) and (n, 3s) states serve as resonant intermediate states for the MPI processes at 248 and 193 nm, respectively. Then the MPI spectra obtained at 248 and 193 nm may reflefct the characters of the resonant intermediate states directly. Generally, the MPI spectra at 193 nm are similar to the electron impact ionization spectra. At 248 nm have, however, much weaker signal intensities of the parent ions. These results stem from the stability of the one-photon resonant states. Various laser power dependence on ion intensities of the ketones is indicative of the fact that at the ^{1}(n, π^*) states two-photon ionization steps (leading to the parent ion formations) and single-photon photodissociation are competing with each other while the molecules are relatively stable when they are excited to the Rydberg states. A typical 193 nm MPI mass spectrum of cyclobutanone is presented in Figure 1.

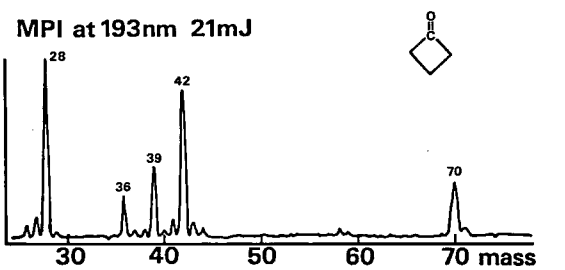

Figure.1. An 193 nm MPT mass spectrum of cyclobutanone

Reference
1) D. A. Hansen and E. K. C. Lee, *J. Chem. Phys.*, **63**, 3272 (1975).

III—G UV Laser Induced Hot-Hydrogen-Initiated Chemistry

The production of hot hydrogen atoms on interstellar grains or cometary surfaces may be of relevance to interstellar chemistry. This project deals with hot hydrogen atom initiated chemistry both in the gas phase and on low temperature surfaces of interstellar molecules. Because of technical difficulties involved in introducing atoms with known translational energy in the range of tenths of an electron volt to 5 eV into a reaction system, relatively little is known about chemical reactions of atoms in this energy range. UV excimer laser photolyses of diatomic and triatomic hydrides exactly provide hydrogen atoms with translational energies in this region. If this UV laser technique for hot hydrogen atom productions were coupled with the so-called photofragment mass spectroscopy, where both the magnitude and direction of the velocities of the recoiling fragments are determined, then the details of the energy disposal accompanying a hot hydrogen reaction, hence the distribution of hot hydrogen energies *at reaction* would be determined.

Since atomic hydrogen is the most cosmically abundant species, reactions of H atom with interstellar molecules will be an important process affecting the chemical composition of comets and also interstellar clouds.

III-G-1 Construction of a Photofragment Mass Sepctrometer for the Sutdy of Hot Hydrogen Atom Chemistry

Toshio HORIGOME, Shinji KATO, Hisanori SHINOHARA, and Nobuyuki NISHI

We have constructed an aluminum alloy, ultra-high-vacuum, molecular beam apparatus which can investigate (V)UV laser initiated hot hydrogen atom reactions by measuring both mass and emission spectra of the products.

One of the salient features of the present vacuum apparatus is that ordinary stainless steel vacuum chamber is replaced by aluminum alloy vacuum system. The aluminum alloy vacuum system contains several advantages over the conventional stainless steel apparatus. As a vacuum material, aluminum alloy is preferred by virtue of its ease of manufacture with high machining precision, lightness, and low material cost. A bakable vacuum system (200°C) consists of aluminum alloy main chamber (6061-T6) and a couple of aluminum alloy flanges (7075-T6) with a metal seal [Helicoflex: pure aluminum (1050) O-ring with an elastic core (Ni base super alloy Inconel 750) which supplies the sealing force]. Such a system can withstand many 200°C bakeouts without leaking.

An overall schematic of the apparatus is depicted in Figure 1. The main aluminum chamber is shaped by miller octagonally suitable for three axes: a laser beam, a molecular beam, and a quadrupole mass filter axes. The laser and molecular beam axes are crossed perpendicularly while the mass filter may have three different angles (90, 135, 180°) relative to the molecular beam axis. A liquid nitrogen (or helium) cryostat is used for preparing a low temperature surface in a temperature controllable manner.

The construction of the present apparatus was achieved in collaboration with the Equipment Development Center of IMS.

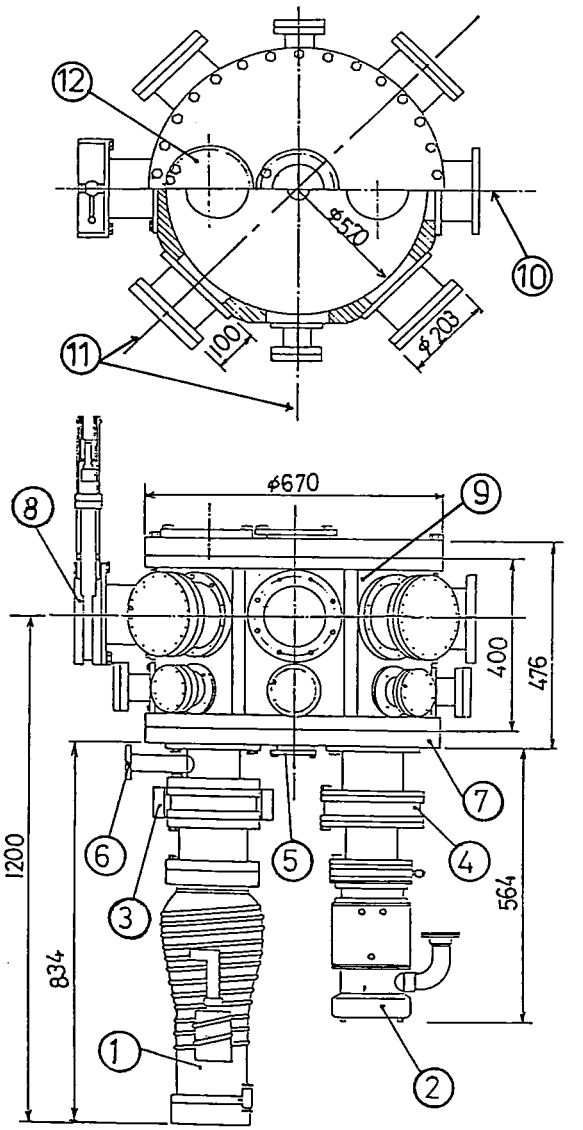

Figure 1. Schematic of apparatus.
① "diffstak" (700 l/s)
② 6" diffusion pump (1500 l/s) with a water baffle
③ UHV gate valve
④ HV gate valve
⑤ suprasil window for laser inlet
⑥ roughing pump port
⑦ aluminum alloy (7075-T6) bottom flange
⑧ HV gate valve
⑨ aluminum alloy (6061-T6) main chamber
⑩ molecular beam axis
⑪ detector axes
⑫ liquid N_2(He) cryostat setting position

III—H Studies on Eelctronic Structure, Energy Transfer, Dissociation and Recombination of Small Molecules

III-H-1 Laser Induced Fluorescence of the RbCs Molecule

Hajime KATÔ *(Kobe Univ. and IMS)* **and Hiromi KOBAYASHI**

Laser-induced fluorescence of RbCs has been observed when a mixture of rubidium and cesium is irradiated by the 5682 Å line of Kr^+ laser. A series of fluorescence lines of transitions to the vibrational levels of up to $v'' = 22$ has been observed and a continuous spectrum with banded diffraction structure has been contiguous to it. Analysis of the fluorescence allows us to determine the spectroscopic constants of the $X^1\Sigma^+$ ground state, and the potential curve is constructed by the RKR-procedure. The dissociation energy D_e is determined to be 3833 ± 1 cm^{-1}. The value of the asymptotic long-range potential constant C_6 is estimated to be 8.75 $cm^{-1}Å^6$. The potential curve of the excited state is estimated from the analysis of the flurescence intensity.

III-H-2 Fluorescence of the $C^1\Sigma^+ - X^1\Sigma^+$ Transition of NaK and the Dissociated Atoms

Chifuru NODA *(Kobe Univ.)* **and Hajime KATÔ** *(Kobe Univ. and IMS)*

[*Chem. Phys. Lett.*, **86**, 515 (1982)]

The $C^1\Sigma^+ - X^1\Sigma^+$ transition of NaK following excitation by the Kr^+ 5309 Å laser lines is observed. The molecular constants and the potential curve of the $C^1\Sigma^+$ state are determined. It is shown that the $C^1\Sigma^+$ state lies above the $B^1\Pi$ state. The mechanism responsible for Na and K D-line fluorescence is discussed.

III—I Picosecond Coherent Spectroscopy

III-I-1 Amplification System for High Power Tunable Picosecond Pulse

Shuji ASAKA,* Hiroki NAKATSUKA,* Masayuki FUJITA,* and Masahiro MATSUOKA *(Kyoto Univ. and IMS)*

[*Rev. Laser. Engineering.*, **10**, 71 (1982)]

A mode-locked cw dye laser synchronously pumped by a mode locked Ar^+ laser was amplified by three stages of dye amplifiers which were pumped by second harmonics of a Q-switched YAG laser. By this system we obtained output pulses of 7 ps pulse width, 0.5 mJ pulse energy and a spectral width close to transform limit at a repetition rate of 10 Hz. The first and second amplifier cells were transversely pumped, and the gains were 10^3 and 25, respectively. The third cell was pumped longitudinally for a better output beam profile, and the gain was 5. To suppress the amplified spontaneous emission (ASE) in the course of amplification, a saturable absorber was inserted between the first and the second cell. The ratio of the peak intensity between the output pulse and the ASE was 2000 : 1.

III-I-2 The Backward Photon Echoes in Na and Na_2 in the Nanosecond and Picosecond Regions

Masayuki FUJITA,* Shuji ASAKA,* Hiroki NAKATSUKA,* and Masahiro MATSUOKA *(Kyoto Univ. and IMS)*

[*J. Phys. Soc. Jpn.*, **51**, 2582 (1982)]

Backward generation of echoes with three-pulse excitation is discussed in solid and gaseous systems. The backward echo in gases is possible as in solids but with different combinations of incident

pulse directions. The first experiments in a gas were performed on the atomic sodium D_1 line in both the nanosecond and the picosecond region. Furthermore, we have observed the first backward echo in a molecular system, that is, in both of the $X\Sigma-A\Sigma$ and $X\Sigma-B\Pi$ transitions of Na_2. Decays of the echoes were measured as a function of buffer gas (Ar) pressure, and collisional cross sections due to phase interrupting collisions were evaluated for each of the above cases.

RESEARCH ACTIVITIES IV
Department of Molecular Assemblies

IV—A Photoelectric and Optical Properties of Organic Solids/Liquids in Vacuum Ultraviolet Region

Photoelectron spectra were measured on various types of organic solids — neat molecular crystals, charge-transfer complexes, vinyl aromatic polymers, and 1 : 1 alternant copolymers. Also molecular orbital calculations were performed to help the understanding of the observed photoelectron spectra.

IV-A-1 Ultraviolet Photoemission Spectroscopic Studies of Six Nanocyclic Aromatic Hydrocarbons in the Gaseous and Solid States

Naoki, SATO, Hiroo INOKUCHI, Kazuhiko SEKI, Junji AOKI *(Toho Univ.)*, **and Satoshi IWASHIMA** *(Meisei Univ.)*

[*J. Chem. Soc., Faraday Trans. 2*, in press]

Applying various synthetic methods, six nanocyclic aromatic hydrocarbons, violanthrene A (VEA), isoviolanthrene A (IsoVEA), violanthrene B (VEB), isoviolanthrene B (IsoVEB), tetrabenzoperylene (TBP), and tetrabenzopentacene (TBPA), have been prepared. Four of them, VEA, IsoVEA, VEB, and IsoVEB, have coplanar or fairly coplanar structures, whereas the other two, TBP and TBPA, have non-planar structures.

Ultraviolet photoemission spectra of the six compounds were measured in the gaseous and solid states and the ionization potentials and polarization energies were determined as shown in Table I. The gas-phase ionization potentials were related to their molecular structures whereas the polarization energies[1] reflected the small molecular polarizability and the reduced molecular packing density of overcrowded molecules in the solid state.

Table I. Ionization potentials, polarization energies, and relaxation shifts of the six nanocyclic aromatic hydrocarbons (in eV).

compound	I_g^a	I_s^{th}	P_+	I_g^{vl}	I_s^{pl}	R_+
VEA	6.42	4.8_6	1.5_6	6.54	5.5	1.0
IsoVEA	6.36	4.9_2	1.4_4	6.42	5.5	1.0
VEB	6.36	4.8_2	1.5_4	6.44	5.3	1.1
IsoVEB	6.54	4.9_6	1.5_8	6.63	5.6	1.1
TBP	6.58	5.3_4	1.2_4	6.69	5.8	0.9
TBPA	6.13	4.9_8	1.1_5	6.28	5.7	0.6

g, gas; s, solid; a, adiabatic; th, threshold; vl, 1st vertical; pl, 1st peak; P_+, polarization energy; R_+, relaxation shift.

Reference

1) N. Sato, K. Seki, and H. Inokuchi, *J. Chem. Soc., Faraday Trans. 2*, 77, 1621 (1981).

IV-A-2 UV Photoelectron Spectroscopy of Several One and Two Component Organic Photoconductors

Norbert KARL *(Univ. of Stuttgart and IMS)*, **Naoki SATO, Kazuhiko SEKI, and Hiroo INOKUCHI**

[*J. Chem. Phys.*, 77, 4870 (1982)]

Solid state photoelectron spectra have been measured at several UV wavelengths for vapor-deposited films of the organic photoconductors, phenothiazine, anthracene, and carbazole and for the 1 : 1 donor-acceptor complexes of phenothiazine, carbazole, and acridine with the common acceptor, pyromellitic dianhydride (PMDA).

Differences in photoemission threshold energies of the one-component photoconductors are used to estimate hole trap depth energies for systems where

one of the compounds is doped with another one. Further, the photoemission threshold values are used for predicting the energy differences of charge transfer transitions in donor-acceptor crystals with a common acceptor. The reliability of this kind of estimation for the above mentioned substances is tested.

In addition, by comparing the threshold values obtained for the D-A complexes with those of the neat donors, it is found (in confirmation of an earlier result[1]) that complex formation with PMDA tends to increase the ionization threshold of the respective donor by 0.2 − 0.3 eV.

Reference

1) K. Ishii, K. Sakamoto, K. Seki, N. Sato, and H. Inokuchi, *Chem. Phys. Lett.*, **41**, 154 (1976).

IV-A-3 Conformation Dependence of Ionization Potential and Electronic Structure of Long-Chain Alkanes by MO Calculations

Kazuhiko SEKI and Hiroo INOKUCHI

Long-chain alkane molecules form extended planar-zigzag chains in crystalline states, while they form random coils in gas, liquid, and amorphous solid states. Therefore, the elucidation of the conformational dependence of electronic structure is important in understanding the electronic properties of the amorphous part of polyethylene solid and also in extracting meaningful informations on the extended chain from the experimental results on random coil states. In order to examine this dependence, *ab initio* molecular orbital calculations with minimal basis set were performed on various conformers of alkanes from n-C_4H_{10} to n-$C_{15}H_{32}$ in rotational isomeric states (RIS) model, in which a trans(t)- and two gauche(g)-states are allowed for each C-C band. A considerable conformation dependence was found for both the gross electronic structure and the value of threshold ionization potential I^t. As shown in Table I, the value of I^t is smallest for all-t conformer among realistic conformers of each alkane (strictly staggered g^+g^- conformers have much steric hindrance). This means that I^t of a mixture of random coils is determined by that of the all-t conformer, although its statistical weight is very small for long-chain alkanes. Thus the experimentally observed I^t of random coils gives the upper limit of an extended chain.

Table I. Ionization potentials of various conformers of alkanes obtained assuming Koopmans' theorem.

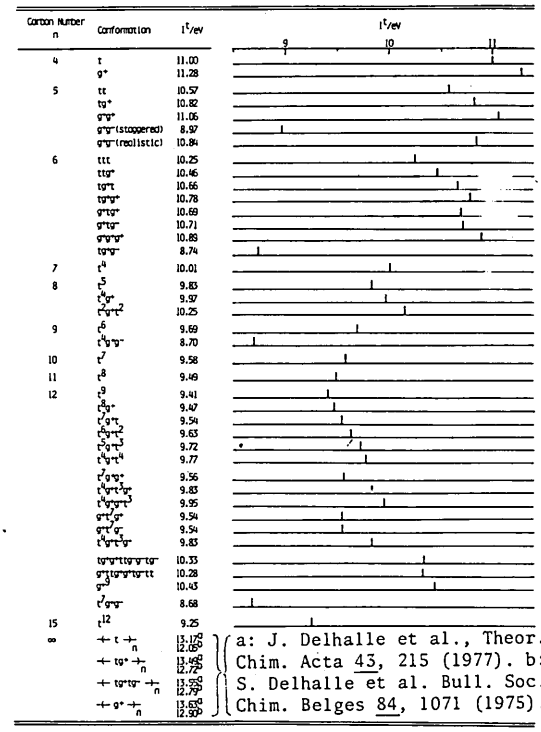

IV-A-4 UV Photoelectron Spectroscopy of Vinyl Aromatic Polymers and 1:1 Alternating Copolymers

Yasuhiko SHIROTA *(Osaka Univ. and IMS)*, **Yasuyo MATSUMOTO** *(Osaka Univ.)*, **Hiroshi MIKAWA** *(Osaka Univ.)*, **Kazuhiko SEKI, and Hiroo INOKUCHI**

Ultraviolet photoelectron spectroscopic studies have been made on thin films of homopolymers of N-vinylcarbazole (VCz), vinylferrocene (VFe), and 2-vinylnaphthalene (VNa), their copolymers with styrene (St) the composition of which is rich in St, and 1:1 alternating copolymers with diethyl fumarate (DEF), fumaronitrile (FN), and maleic anhydride (MAn) to determine and compare the threshold ionization potentials (I_s^{th}) of these polymers. Table I summarizes the values of I_s^{th} determined for these polymers from their photoelectron spectra. Small, but distinct differences in

the I_s^{th} values between the corresponding homopolymers, copolymers with St, and 1 : 1 alternating copolymers were reproducibly observed from repeated measurements using different incident photon energies. The I_s^{th} values of the copolymers with St were *ca.* 0.1 eV greater relative to those of the homopolymers except for the ferrocene polymers, and the I_s^{th} values of the 1 : 1 alternating copolymers were up to 0.3 eV greater than those of the homopolymers. The greater I_s^{th} values for the copolymers are ascribed partly to a decrease in stabilization energies of the ionized chromophores due to the surrounding pendant aromatic groups and partly to the inductive effect by the electron-withdrawing groups in the comonomers.

Table I. Threshold ionization potentials (I_s^{th}) [eV] of polymers

PVCz	5.8_5	PVFe	5.3_5	PVNa	6.3_5
Copoly(VCz-St)	5.9_5	Copoly(VFe-St)	5.3_5	Copoly(VNa-St)	6.4_5
Copoly(VCz-DEF)	6.0_5	Copoly(VFe-DEF)	5.4_0	—	—
Copoly(VCz-FN)	6.1_5	Copoly(VFe-FN)	5.5_0	Copoly(VNa-FN)	6.5_5
Copoly(VCz-MAn)	6.1_5	Copoly(VFe-MAn)	5.4_5	Copoly(VNa-MAn)	6.5_5

IV—B Photoconduction in Organic Solids

Using an ultra-high vacuum photoconduction apparatus (UHV-PCA), we have observed a photoconductive behaviour of organic semiconductores: The behaviour depends strongly on purity, crystallinity, temperature, surface states, and atmosphere, in particular oxygen. In cooperation with joint research group (p.131) and Chemical Materials Centre of IMS, very high purity polycyclic aromatic compounds, tetrabenzo-[*a,cd,j,lm*]perylene, tetrabenzo[*de,hi,op,st*]pentacene, and flavanthrene, are employed to observe their intrinsic photoconductive characters.

IV—C Electron Transfer in Cytochrome c_3

The unusual behaviour of electronic conduction in cytochrome c_3 has been analysed by the percolation theory.

IV—D Physics and Chemistry of Graphite Intercalates

By means of ESR and electrical resistivity measurements, the catalytic activity for hydrogen dissociation and/or chemisorption of the graphite-alkali metal intercalation compounds as function of alkali metal components are being studied.

As host material, graphite filament prepared from purified graphite in argon flame is being used.

IV—E Organic Metal

IV-E-1 Two-Dimensionality and Suppression of Metal-Semiconductor Transition in a New Organic Metal with Alkylthio Substituted TTF and Perchlorate

Gunzi SAITO, Toshiaki ENOKI, Koshiro TORIUMI, and Hiroo INOKUCHI

[*Solid State Commun.*, **42**, 557 (1982)]

Single crystals of a new organic cation radical salt; [BEDT-TTF(1)]$_2$ClO$_2$(1,1,2-trichloroethane)$_{0.5}$,

were prepared by the electrocrystallization technique. This complex is the first organic metal which exhibits two-dimensional transport properties ($\rho_\perp : \rho_{//} : \rho_b = 1 : 1\sim2 : 10^2\sim10^3$, where $\rho_\perp$ is along the elongated direction of a leaf-like crystal and $\rho_{//}$ is normal to it in the a-c plane and is nearly parallel to the stacking axis, Figure 1). Moreover, a remarkable suppression of a metal to semiconductor transition is achieved and a quasi-metallic character is observed down to 1.4K.[1] These facts indicate that a chemical modification such as the extension of TTF (or TSF) moiety with alkylcharcogenide substituents has an appropriate effect to increase the interchain interactions leading to a "low temperature" organic metal and hopefully to an organic superconductor. The increased dimensionality in a complex is one of the requirements for an organic metal to become an organic superconductor of the $[TMTSF(2)]_2X$ type.

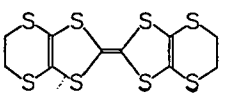

1 **BEDT-TTF**

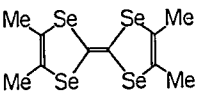

2 **TMTSF**

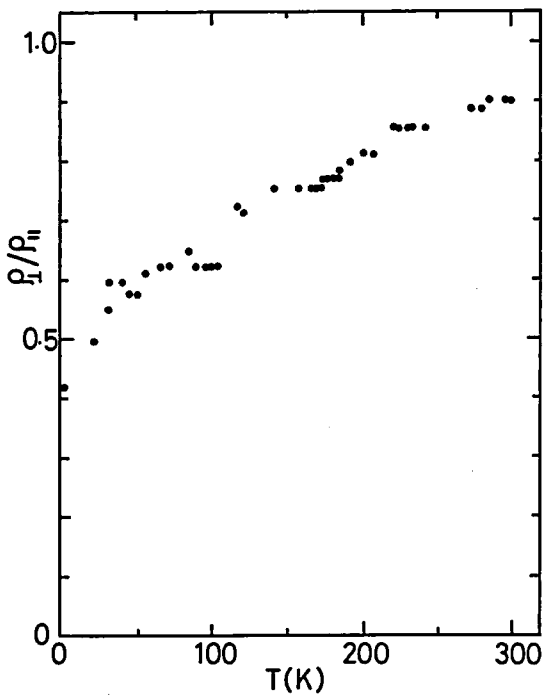

Figure 1. The anisotropy $\rho_\perp/\rho_{//}$ vs temperatures by the Montgomery method. $\rho_\perp/\rho_{//}$ for a different single crystal was 0.5 at room temperature.

Reference

1) G. Saito, T. Enoki, K. Toriumi, and H. Inokuchi, *IMS Ann. Rev.*, 96 (1981).

IV-E-2 A Novel Behavior of Electrical Resistivity in a New Two-Dimensional Organic Metal, $(BEDT\text{-}TTF)_2ClO_4(1,1,2\text{-}Trichloroethane)_{0.5}$

Gunzi SAITO, Toshiaki ENOKI, and Hiroo INOKUCHI

[*Chem. Lett.*, 1345 (1982)]

An unusual temperature dependence of the resistivity along the elongated axis (~a axis) of a single crystal of the BEDT-TTF complex was observed (Figure 1). It was ascribed to the inclusion of the ρ_b component in $\rho_\perp$ due to the thermally produced microfissures. This observation deduces a quite abnormal feature of ρ_b; ρ_b is in semiconductive region down to 180K followed by a

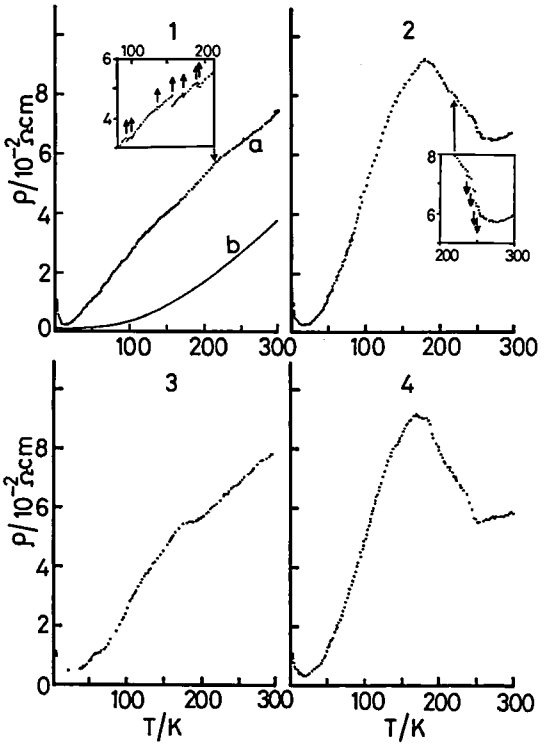

Figure 1. Hysteresis of the temperature dependence of the observed $\rho_\perp$ after the rectification; 1-a) the first cooling, 2) the first heating, 3) the second cooling, and 4) the second heating process. The inserts are the observed resistivity before the rectification and arrows indicate the resistance jumps due to the formation of microfissures. Curve 1-b) represents $\rho_\perp$ of the best sample free from the microfissures.

metallic region down to *ca.* 15K, indicating some phase transition at around 180K. This transition may be caused by an ordering and/or freezing of motion of the counter ions or the trichloroethane molecules. Other possibility is a stop of vibration of the methylenes of BEDT-TTF. These changes reduce the scattering process and increase the carrier mobility, so that ρ_b will result in a metallic behavior.

IV-E-3 The Crystal Structure of $(TMTSF)_2BF_4$

Hayao KOBAYASHI,* Akiko KOBAYASHI, Gunzi SAITO, and Hiroo INOKUCHI** *(*Toho Univ., **Univ. of Tokyo)*

[*Chem. Lett.*, 245 (1982)]

Although $(TMTSF)_2X$ compounds ($X=PF_6$, ClO_4, ReO_4, BF_4, etc.) are isomorphic, their physical properties differ from one another. $(TMTSF)_2PF_6$ has an antiferromagnetic ground state (SDW) and transforms to a superconductive state at high pressure.[1] $(TMTSF)_2ClO_4$ is a "zero pressure" organic superconductor ($T_c=1.0-1.4K$),[2] $(TMTSF)_2ReO_4$ has a metal-insulator transition (176K) due to the ordering of the counter ion, but becomes a superconductor at high pressure,[3] and $(TMTSF)_2BF_4$ undergoes a metal-insulator transition(39K) and remains insulator even at high pressure.[4]

We have determined the crystal structure of $(TMTSF)_2BF_4$ at room temperature. The crystals belong to the triclinic system. The space group is $P\bar{1}$ and the lattice constants are: $a=7.255(1)$, $b=7.647(1)$, $c=13.218(3)$ Å, $\alpha=82.23(2)$, $\beta=87.15(2)$, $\gamma=70.36(1)°$, $Z=1$, $V=688.10$ Å^3. The nearly planar TMTSF groups stack in diadic columns along the a-axis. The intra- and interstack contacts between Se atoms show the two-dimensional nature of the crystal (Figure 1).

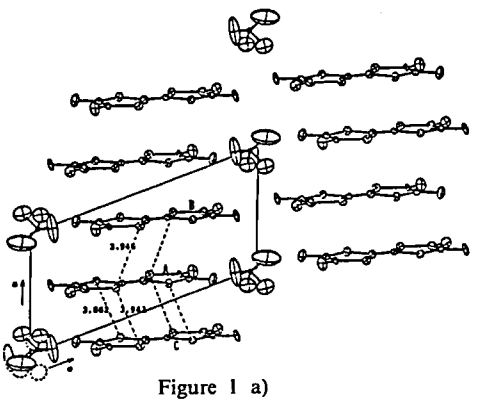

Figure 1 a)

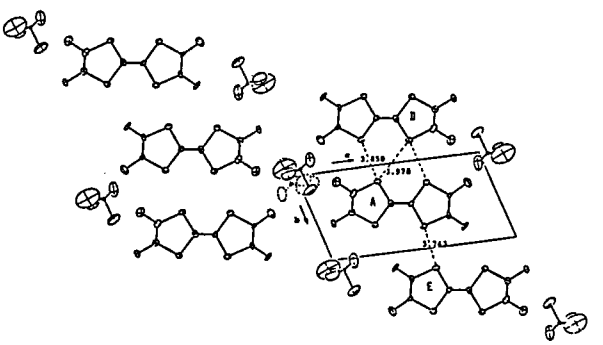

Figure 1 b)

Figure 1.

a) Side-view of stack (tilted 10°) showing shorter distances (Se ... Se) (Å) within a stack. Each contact between two TMTSF units occurs twice because of the inversion center midway between the units. The BF_4 anions show disorder, taking one of the two possible positions randomly.

b) View along the a-axis showing shorter interchain distances (Se ... Se) (Å).

References

1) K. Mortensen, Y. Tomkiewicz, T. D. Schultz, and E. M. Engler, *Phys. Rev. Lett.*, **46**, 1234 (1981), and H. J. Schultz, D. Jerome, M. Ribault, A. Mazaud, and K. Bechgaard, *J. Phy. Lett.*, **42**, 51 (1981).

2) K. Bechgaard, K. Carneiro, F. B. Rasmussen, M. Olsen, G. Rindorf, C. S. Jacobsen, H. J. Pedersen, and J. C. Scott, *J. Am. Chem. Soc.*, **103**, 2440 (1981).

3) C. S. Jacobsen, H. J. Pedersen, K. Mortensen, G. Rindorf, N. Thorup, J. B. Torrance, and K. Bechgaard, J. Phys C: *Solid State Phys.*, **15**, 2651 (1982).

4) K. Bechgaard, C. S. Jacobsen, K. Mortensen, H. J. Pedersen, and N. Thorup, *Solid State Commun.*, **33**, 1119 (1980), and K. Bechgaard, *Mol. Cryst. Liq. Cryst.*, **79**, 1 (1982).

IV-E-4 Evidence for Three Dimensional Ordering of Superconductivity in Highly Anisotropic Organic Conductor, $(TMTSF)_2ClO_4$

Keizo MURATA,* Hiroyuki ANZAI,* Gunzi SAITO, Koji KAJIMURA,* and Takehiko ISHIGURO* *(Electrotechnical Laboratory)*

[*J. Phys. Soc. Jpn.*, **50**, 3529 (1981)]

The anisotropy of the conductivity of $(TMTSF)_2ClO_4$ at room temperature is high ($\sigma_a:\sigma_b:\rho_{c^*}=900:40:1$), and σ_{c^*} at 300K is $3\times10^{-2}\Omega^{-1}cm^{-1}$. Along the least conductive c*-axis, superconductivity is also observed by conductivity measurement (Figure 1), showing evidently three dimensional ordering of superconductivity. The critical current density along the c*-axis at 0.5K is 0.1 ± 0.05 A/cm^2, and is about an order of magnitude smaller than that along the a-axis, showing the superconductivity in the c*-axis is weak. The finite resistance along the c*-axis is not detectable in the superconducting state, in contrast to the appearance of finite resistance along the a-axis.

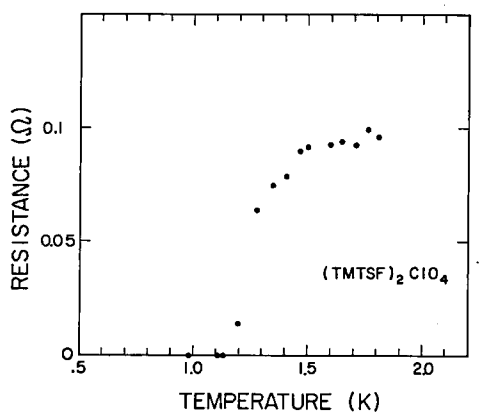

Figure 1. Transition in resistance to superconducting state in $(TMTSF)_2ClO_4$. The resistance was measured along the c*-axis, with currents, 50 μA.

IV-E-5 Superconducting Transition of $(TMTSF)_2ClO_4$ in Magnetic Fields

Keizo MURATA,* Hiroyuki ANZAI,* Koji KAJIMURA,* Takehiko ISHIGURO,* and Gunzi SAITO *(*Electrotechnical Laboratory)*

[*Mol. Cryst. Liq. Cryst.*, **79**, 283 (1982)]

Superconducting transition of $(TMTSF)_2ClO_4$ was studied by conductivity measurements along the most conductive a-axis in magnetic fields applied along three different principal crystallographic axes. The temperature dependence of the upper critical field H_{c2} for three different directions is shown in Figure 1. By using the relations,

$$dH_{c2i}/dT|_{T=Tc} = \phi_0/[2\pi\xi_j(0)\xi_k(0)T_c], \quad (1)$$

$$\xi(T) = \xi(0)[T_c/(T_c-T)]^{1/2}, \quad (2)$$

where ϕ_0 is a flux quantum and i, j, and k denote different axes, we obtained the GL coherence lengths at 0K along the a-, b-, and c*-axes, to be $\xi_a(0)>600$ Å, $\xi_b(0)\cong540$ Å, and $\xi_{c^*}(0)\cong60$ Å, respectively.

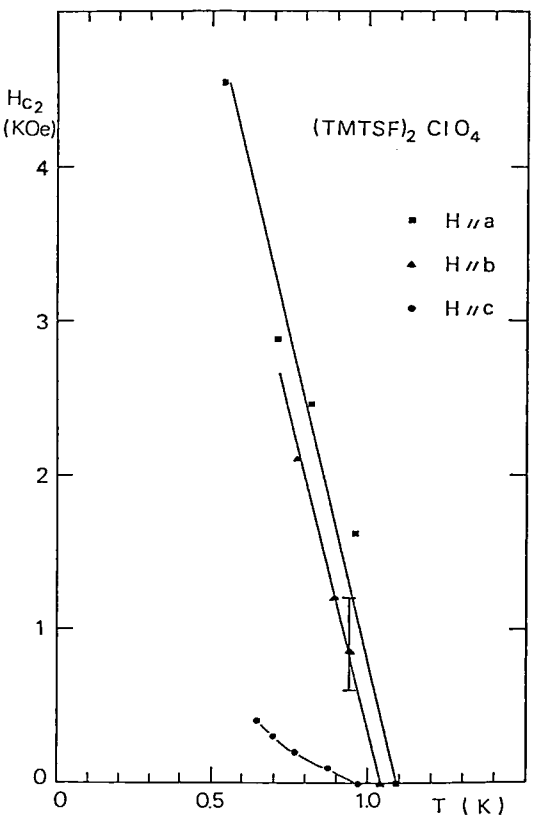

Figure 1. Upper critical field, H_{c2}, as a function of temperature. The GL coherence lengths, $\xi_a(0)$, $\xi_b(0)$, and $\xi_{c^*}(0)$, are estimated from the curves using Eqs. (1) and (2).

IV-E-6 Nonlinear Effect above the Superconducting Critical Current in $(TMTSF)_2ClO_4$

Keizo MURATA,* Takashi UKACHI,* Hiroyuki ANZAI,* Koji KAJIMURA,* Gunzi SAITO, and Takehiko ISHIGURO* *(Electrotechnical Laboratory)*

[*J. Phys. Soc. Jpn.*, **51**, 695 (1982)]

A novel nonlinear characteristics of the resistivity above the superconducting critical current was observed along the a-axis of $(TMTSF)_2ClO_4$ by measuring the voltage-current characteristics (Figure 1). The nonlinearlity has close relations with the appearance of the semiconducting phase (so called SDW) just above the superconducting phase.

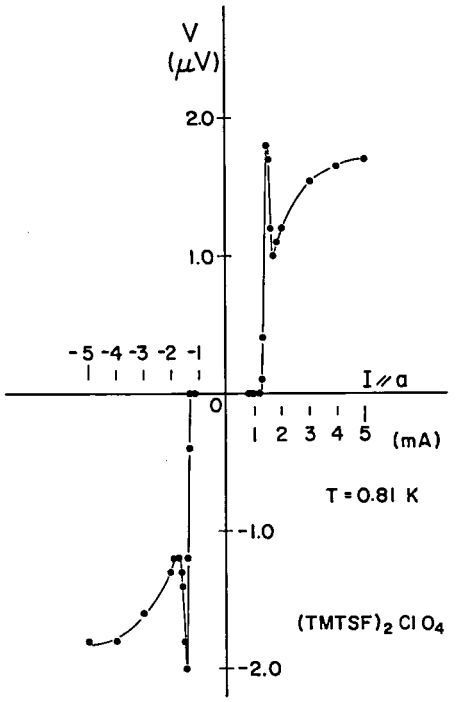

Figure 1. Voltage-current characteristic along the a-axis. at 0.81K.

IV-E-7 Nonlinear Effects near the Superconducting Transition of Organic Synthetic Metal $(TMTSF)_2ClO_4$

Keizo MURATA,* Takashi UKACHI,* Hiroyuki ANZAI,* Gunzi SAITO, Koji KAJIMURA,* and Takehiko ISHIGURO* *(Electrotechnical Laboratory)*

[*J. Phys. Soc. Jpn.*, **51**, 1817 (1982)]

Two types of nonlinear effects in the electrical conductivity along the most conductive a-axis of $(TMTSF)_2ClO_4$ were observed near the superconducting transition temperature. Along the a-axis, the resistivity decreased as decreasing the temperature between 300K and 5.5K and turned to increase down to 1.07K below which the superconductivity appeared (Figure 1). One of the nonlinearities was the increase in resistance up to a value greater than the normal one at a current just above the superconducting critical current (Figure 2). Along the c*-axis such nonlinearity was not observed. The other is the decrease in resistance driven by the current much larger than the critical current, which seems to show the restoration of the metallic behavior.

The effects of thermally induced microcracks were examined. It was found that the resistive transition at the superconducting transition is very sharp only when the crack-free samples was studied. Further the semiconducting phase below 5.5K is easily smeared out by the microcracks.

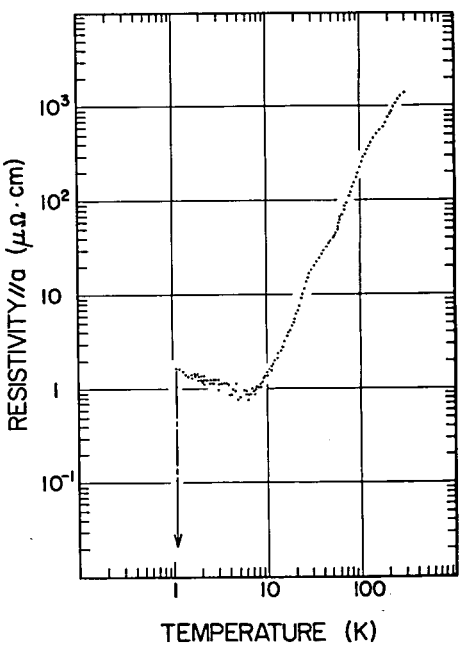

Figure 1. Temperature dependence of resistivity along the a-axis. Resistivity, R, shows a minimum at 5.5K, above which R behaves like $T^{2.1}$. Arrow indicates the superconducting transition.

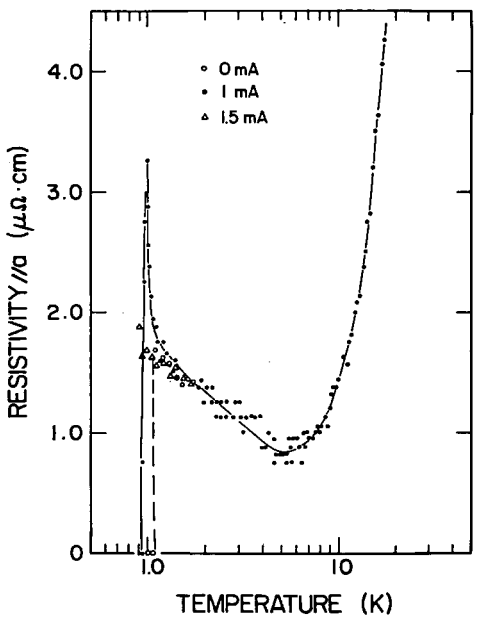

Figure 2. Temperature dependence of resistivity along the a-axis in the low current regime (1.5 mA), measured with three representative currents, 0 mA (○), 1 mA (●), and 1.5 mA (△). Lines are the guides to the eyes for 0 and 1 mA. The resistivity measured with a current of 1.5 mA shows an anomalous peak near the superconducting transition temperature.

IV-E-8 Shubnikov - de Haas Effect in $(TMTS)_2ClO_4$

Hiroshi BANDO,* Kokichi OSHIMA,* Mitsuru SUZUKI,* Hayao KOBAYASHI, and Gunzi SAITO** *(*Univ of Tokyo, **Toho Univ.)*

[*J. Phys. Soc. Jpn.*, **51**, 2711 (1982)]

Angular dependence of the transverse magneto-resistance in $(TMTSF)_2ClO_4$ was measured in a-plane down do 0.47K and H up to 13T. Two types of Schbnikov-de Haas oscillations were observed for the angle θ between H and the c*-axis less than 60 degrees: One with period $0.015\cos\theta T^{-1}$, comparable to that found in $(TMTSF)_2PF_6$[1], and newly observed one with $(0.0036\cos\theta+0.002)T^{-1}$ (Figure 1). If these correspond to electron- and hole Fermi surfaces respectively, they support the compensated as well as the quasi-two dimensional feature of this organic metal.

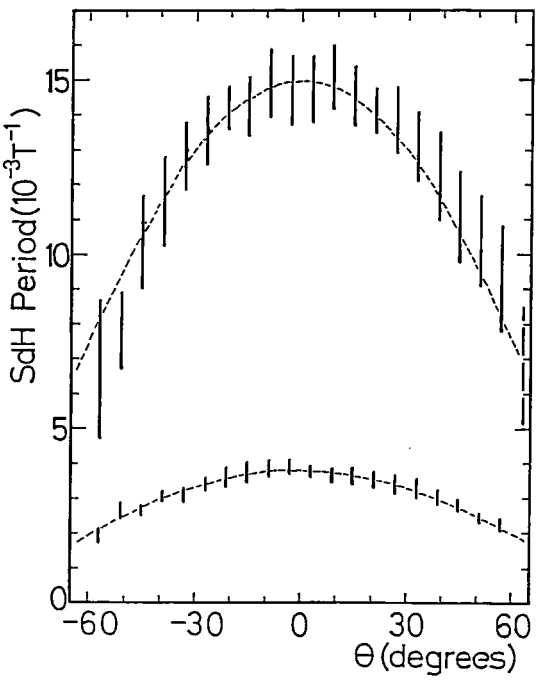

Figure 1. Angular dependence of the Shubnikov-de Haas (SdH) period. Fitted values of $0.015\cos\theta T^{-1}$ and $(0.0036\cos\theta+0.002)T^{-1}$ are shown as dashed curves.

Reference

1) J. F. Kwak, J. E. Schirber, R. L. Greene, and E. M. Engler, *Phys. Rev. Lett.*, **46**, 1296 (1981).

IV—F Studies of Ion-Molecule Reactions by a Threshold Electron-Secondary Ion Coincidence (TESICO) Technique

The knowledge of the microscopic reaction cross sections for evolution of a system in a single reactant quantum state (translational, rotational, vibrational, and electronic) to a single product quantum state is essential for a complete understanding of a chemical reaction. Ion-Molecule reactions are particularly suited for studying such microscopic cross sections since ions can readily be prepared in various internal states in the initial ionization processes, such as photoionization, and the emitted photoelectrons provide information on the distribution among these states.

In this project, we study state-selected ion-molecule reactions by the use of a photoionization technique

which utilizes the threshold photoelectron-secondary ion coincidence. The technique allows direct determination of $\sigma(i, v)$, *i.e.* the reaction cross section as a function of the internal and collisional energies of reactants. The selection of electronic, vibrational, rotational, and fine-structure states are possible by this technique.

IV-F-1 Vibronic-State Dependence of the Cross Sections in the Reactions $O_2^+(X^2\Pi_g, v; a^4\Pi_u, v) + H_2 \rightarrow O_2H^+ + H$, $H_2^+ + O_2$

Kenichiro TANAKA, Tatsuhisa KATO, Paul-Marie GUYON *(Univ. of Paris-Sud and IMS)*, **and Inosuke KOYANO**

[*J. Chem. Phys.*, 77, 4441 (1982)]

The threshold electron-secondary ion coincidence (TESICO) technique has been utilized to select the vibronic states of the O_2^+ reactant ions in the endoergic reactions $O_2^+ + H_2 \rightarrow O_2H^+ + H$ (1) and $O_2^+ + H_2 \rightarrow H_2^+ + O_2$ (2). The vibronic states selected were $X^2\Pi_g$, v=19, 20 and $a^4\Pi_u$, v=0−8, for each of which the relative reaction cross sections have been determined. Figure 1 summarized the experimental results obtained at the collision energy of 0.25 eV. It can be seen from the figure that while Reaction (1) indeed proceeds with the ground $X^2\Pi_g$ state ions by the vibrational excitation (at collision energies lower than the translational threshold), it is considerably (an order of magnitude) enhanced by the electronic excitation of the reactant ions to $a^4\Pi_u$. When vibrational energy is added to the $a^4\Pi_u$ state, the cross section of Reaction (1) further rises sharply (by a factor of 2) at v=2 and then decreases more slowly, reaching the original (v=0) value at v=4. After that, the cross section apparently decreases by about a factor of 2 at v=8.

The cross section of Reaction (2) behaves in a manner similar to that of Reaction (1) as a function of vibrational quantum number. The magnitudes of the cross sections for both electronic states are, however, consistently smaller than those of Reaction (1) by roughly a factor of 10.

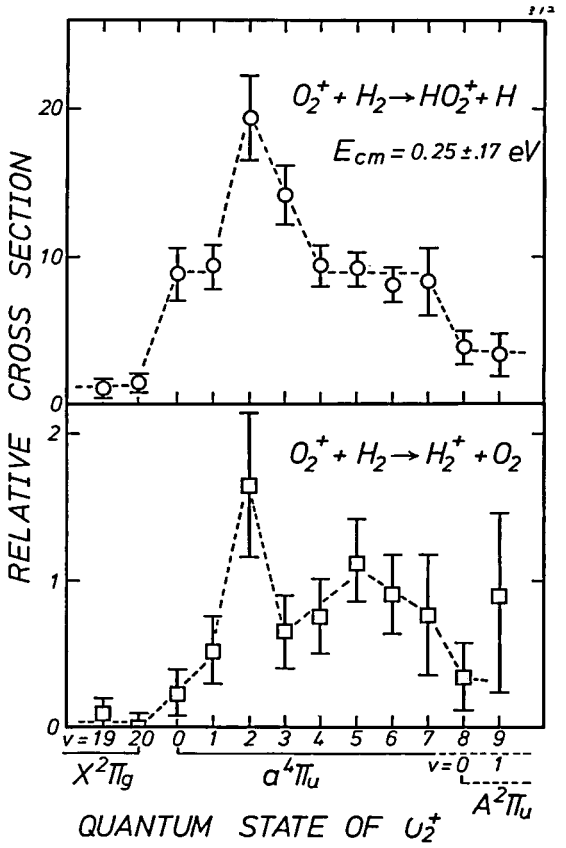

Figure 1. State selected cross sections of Reactions (1) and (2) for 12 vibronic states of O_2^+.

IV-F-2 Kinetic Isotope Effect in the Reactions of $O_2^+(X^2\Pi_g, a^4\Pi_u)$ with HD

Kenichiro TANAKA, Tatsuhisa KATO, Paul-Marie GUYON *(Univ. of Paris-Sud and IMS)*, **and Inosuke KOYANO**

In order to elucidate the reaction mechanism of Reaction (1) studied in the preceding paper (IV-F-1), we have performed two kinds of experiments on the isotope effect in the reaction $O_2^+ + HD \rightarrow O_2H^+ (O_2D^+) + D(H)$. One is a measurement of the product ion intensity ratio O_2D^+/O_2H^+ at two wavelengths, 956.1 and 584.2 A, without state selection. At 956.1 A, O_2^+ are produced only in the $X^2\Pi_g(v \leq 4)$ states, while at 584.2 A a mixture of the $X^2\Pi_g$ and $a^4\Pi_u$ states are produced. The results obtained at the collision energy of 2.5 eV show that the ratios O_2D^+/O_2H^+ are much larger than unity (~7) for 956.1 A but are smaller than unity (~0.7) for 584.2 A, indicating the different mechanisms operating in the reactions with the $X^2\Pi_g$ state (complex mechanism) and the $a^4\Pi_u$ state (direct mechanism).

The other experiment is a measurement of the state selected cross sections for the production of $O_2H^+(\sigma_H)$ and $O_2D^+(\sigma_D)$. Figure 1 shows σ_H, σ_D, and their ratio σ_D/σ_H as a function of the vibronic states of O_2^+ indicated. For v=0−4 of $O_2^+(a^4\Pi_u)$, σ_D and σ_H show exactly the same variation with vibrational quantum number. The ratio of the cross sections, σ_D/σ_H, is almost constant throughout v=0−4, and its values are slightly smaller than unity. These results are consistent with the expectation from a direct reaction mechanism.

For v=19 and 20 of $O_2^+(X^2\Pi_g)$, on the other hand, σ_D/σ_H also appear to be smaller than unity. This result is of particular interest because the complex mechanism deduced from studies with low v ions predicts the ratio to be considerably larger than unity. Thus, the present result may indicate that the mechanism of the $X^2\Pi_g$ reaction changes from complex to direct ones when a sufficient energy is supplied in the form of reactant vibration.

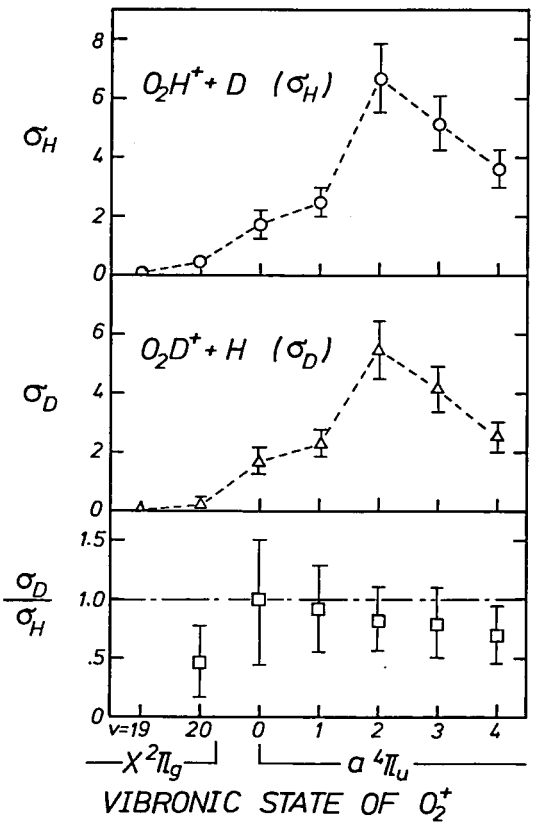

Figure 1. Relative cross sections for the production of O_2H^+ and O_2D^+ from the O_2^++HD reaction and their ratios.

IV-F-3 State Selected Charge-Transfer Reaction of $Ar^+(^2P_{3/2}, ^2P_{1/2})$ with NO

Tatsuhisa KATO, Kenichiro TANAKA, and Inosuke KOYANO

Low energy charge-transfer reactions have most often been discussed in terms of the energy resonance and Franck-Condon factors. In order to investigate the roles of these factors in charge-transfer process, we have studied the low energy charge-transfer reaction

$$Ar^+(^2P_J) + NO \rightarrow Ar + NO^+ \qquad (1)$$

with separation of the two spin-orbit states (J=3/2 and 1/2) of the reactant ion utilizing the TESICO[1] technique.

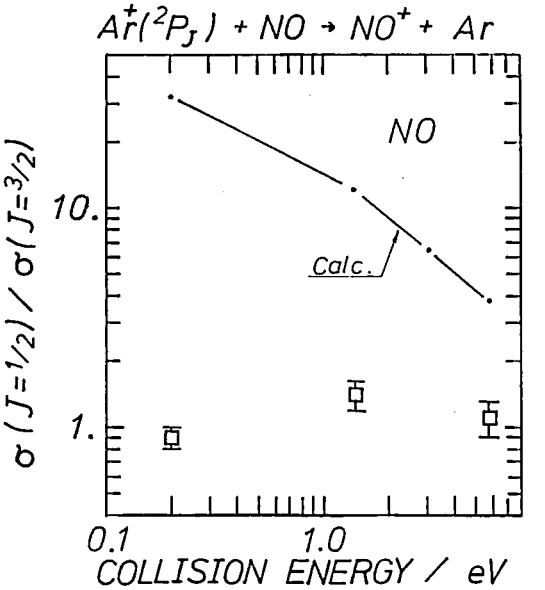

Figure 1. The ratios of cross sections of Reaction (1) for the two spin-orbit states (J=1/2, J=3/2). □: experimental results. −•−: calculated results.

The Ratios of the cross sections $\sigma(1/2)/\sigma(3/2)$ obtained at three different collision energies are shown in Figure 1. Since energy-resonance exists between the $Ar^+(^2P_{1/2})$+NO($X^2\Pi$, v=0) and Ar+ $NO^+(a^3\Sigma^+$, v=2) levels, the ratio $\sigma(1/2)/\sigma(3/2)$ in this system is expected to be much larger than unity, as can also be seen from the results of simple model calculation based on the energy defect and F-C factors (solid line curve). In contrast, the

experimental ratios are found to be very close to unity, indicating that the mechanism of this reaction is much more complicated than the simple model predicts. This is also contrasted with the results on the reverse reaction $NO^+(v)+Ar \rightarrow Ar^+ + NO$ (the following paper, IV-F-4).

Reference

1) I. Koyano and K. Tanaka, *J. Chem. Phys.*, **72**, 4858 (1980).

IV-F-4 Selection of Vibrational States of $NO^+(a^3\Sigma^+)$ in the Charge-Transfer Reaction with Ar

Tatsuhisa KATO, Kenichiro TANAKA, and Inosuke KOYANO

In order to further investigate the mechanism of the low energy charge-transfer reaction $Ar^+ + NO \rightarrow Ar + NO^+$ (see the preceding paper, IV-F-3), we have also studied the following reverse charge-transfer reaction

$$NO^+(a^3\Sigma^+, v) + Ar \rightarrow Ar^+(^2P_J) + NO \qquad (1)$$

with separation of each vibrational state ($v=0-5$) of the reactant ion $NO^+(a^3\Sigma^+)$.

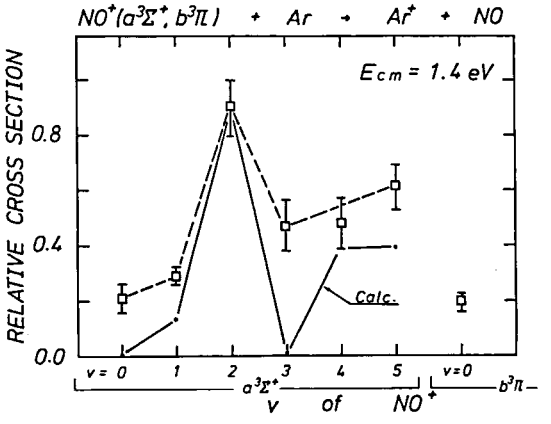

Figure 1. State selected cross sections for Reaction (1) as a function of vibrational quantum number v of NO^+ obtained at 1.4 eV of collision energy. □: experimental results. —•—: calculated results.

Experimental results obtained at a collision energy of 1.4 eV are summarized in Figure 1, together with the results of a simple model calculation based on the energy defect and Franck-Condon factors (solid line curve). As can be seen from the figure, a resonance-like enhancement of the cross section $\sigma(v)$ has been observed at $v=2$ of $NO^+(a^3\Sigma^+)$. In this connection, it is very interesting to note that the resonance effect was not observed in the reverse reaction $Ar^+ + NO \rightarrow Ar + NO^+$ (the preceding paper). This difference in the appearance of the resonance effect can be interpreted in terms of the difference in the reaction mechanism. Namely, in the $Ar^+ + NO$ reaction, the charge transfer at low collision energies is considered to proceed mainly by a complex mechanism through a singlet coupled state of $(Ar \cdot NO)^+$, whereas it mainly proceeds by a direct mechanism in the $NO^+(a^3\Sigma^+) + Ar$ reaction.

IV-F-5 State Selected Reactions of $N_2^+(A^2\Pi_u, v)$ with Ar

Inosuke KOYANO, Kenichiro TANAKA, and Tatsuhisa KATO

A requisite for successful application of our TESICO technique[1] to the reaction of an electronically excited ion is that the state of interest must have a sufficiently long lifetime compared with the time-of-flight of the ion between the ionization and reaction chambers. While such a condition is often met with metastable excited states, such as $O_2^+(a^4\Pi_u)$ (IV-F-1) and $NO^+(a^3\Sigma^+)$ (IV-F-4), it is not met with many other excited states of importance.

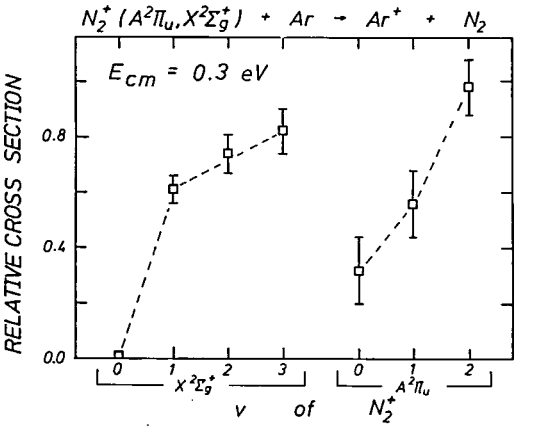

Figure 1. Relative charge-transfer cross sections with Ar for vibronic states $N_2^+(A^2\Pi_u, v=0-2)$, together with those for $N_2^+(X^2\Sigma_g^+, v=0-3)$.

We have found, however, that the TESICO experiment also works for excited states with a lifetime comparable to or somewhat shorter than the TOF, if we use the single chamber mode of operation.[1] This is the first report of such a study on $N_2^+(A^2\Pi_u, v)$, which have a lifetime of ~ 10 μs.

The relative reaction cross sections for vibrational states $v=0-2$ of $N_2^+(A^2\Pi_u, v)$ are determined from the coincidence signals at each threshold, taking into account the lifetimes and the Franck-Condon factors of the $A^2\Pi_u \rightarrow X^2\Sigma_g^+$ transitions, and the relative cross sections[2] of the resulting $(X^2\Sigma_g^+, v)$ ions. The preliminary results are shown in Figure 1.

References

1) I. Koyano and K. Tanaka, *J. Chem. Phys.*, **72**, 4858 (1980).
2) T. Kato, K. Tanaka, and I. Koyano, *J. Chem. Phys.*, **77**, 834 (1982).

IV—G Photoionization Processes in Small Molecules

Two techniques have generally been used for the study of molecular photoionization processes, *i.e.*, measurements of photoionization efficiency curves (PIEC) and photoelectron spectra (PES). While PIEC yields a wealth of information on the ionization processes and energy levels of ions and neutral molecules, difficulty is often encountered with this technique when autoionization obscures the step structure of the curve. In such a situation, we often resort to PES which provides precise locations of ionic states and transition probabilities of these states. However, ionic states that can be studied by the ordinary (constant wavelength) PES are largely limited to the states which combine with the ground state of the parent molecule with favorable Franck-Condon factors. Another type of photoelectron spectoscopy is the threshold electron spectroscopy (TES) which uses a variable wavelength light source and detects only the zero kinetic energy photoelectrons (threshold electrons). In this method, ionic states which are not favored by direct ionization are often observed through resonance autoionization.

In this project, we study photoionization processes in small molecules by simultaneous measurements of photoionization efficiency curves and threshold electron spectra. Furthermore, we find that the analysis of autoionizing transitions is often possible utilizing charge-transfer processes of the product ions. This technique is also incorporated.

IV-G-1 Photoionization Efficiency Curves of $^{16}O_2$, $^{16}O^{18}O$ and $^{18}O_2$. Re-examination of the Assignment of Autoionizing States of O_2

Eisuke NISHITANI *(Tokyo Inst. of Tech. and IMS)*, **Kenichiro TANAKA, Tatsuhisa KATO, Ikuzo TANAKA** *(Tokyo Inst. of Tech. and IMS)*, **and Inosuke KOYANO**

The absorption spectra of O_2 in the VUV region have been studied by many investigators. Price and Collins[1] found many Rydberg transitions in their photograph, and some of them were classified into several vibrational progressions (H, H′, M, M′ I, I′, etc.). This classification of vibrational progressions has been accepted by later investigators, but many absorption bands remain yet to be assigned, especially in the wavelength region longer than 740 Å.

The position of Rydberg absorption is observed to be shifted regularly in the spectra of the isotopic molecules. Thus, by measuring this isotope shift, we can re-examine the assignment of the Rydberg states. From this view point, we have measured the photoionization efficiency curves (PIEC) of $^{16}O_2$, $^{16}O^{18}O$, and $^{18}O_2$. In Figure 1 PIEC's of these isotopes are shown together with the band assignments for $^{16}O_2$. We have also calculated the isotope shifts for Rydberg states in three wavelength regions (660～740 Å, 780～860 Å, and 910～1010 Å) using the previous assignments. Comparison of the observed and calculated isotope shifts has revealed that while the previous assignments in the first two regions (660～740 Å and 780～860 Å) are correct, those in the last region (910～1010 Å) seem to be questionable. More detailed analysis of the isotope shifts obtained is in progress.

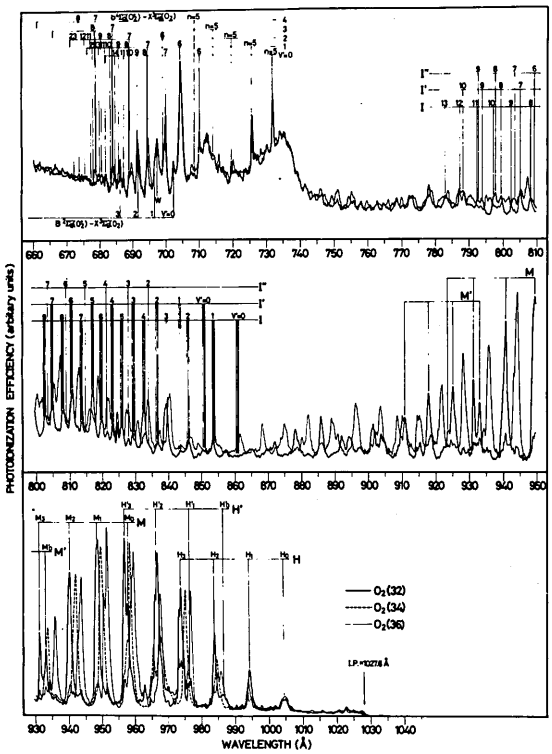

Figure 1. Photoionization efficiency curves of $^{16}O_2$, $^{16}O^{18}O$, and $^{18}O_2$.

Reference

1) W. C. Price and G. Collins, *Phys. Rev.*, **48**, 714 (1935).

IV—H Spectroscopy and Chemical Dynamics Using Supersonic Nozzle Beams

The usefulness of supersonic nozzle beams has increasingly been recognized in both spectroscopy and chemical dynamics. The capability of cooling internal degrees of freedom of molecules and the possibility of producing various kinds of molecular clusters are important properties of the technique. In this project, we aim at high resolution absorption and Raman spectroscopy, dynamical studies of cluster reactions, and their combination, utilizing the above properties of supersonic nozzle beams.

IV-H-1 Further Characterization of the Ar_2 and $(H_2)_2$ Beam for Ion-Cluster Reactions

Koji TESHIMA *(Kyoto Univ.)*, **Kenichiro TANAKA, Tatsuhisa KATO, and Inosuke KOYANO**

[*Uchuken Hokoku, Suppl., 3*, 85 (1982) (in Japanese)]

As a continuation of a previous study,[1] a detailed characterization has been performed of the Ar_2 and $(H_2)_2$ beams produced in a supersonic expansion. A time-of-flight technique combined with mass spectrometric detection has been used. It has been found that sufficiently narrow velocity spreads (high speed

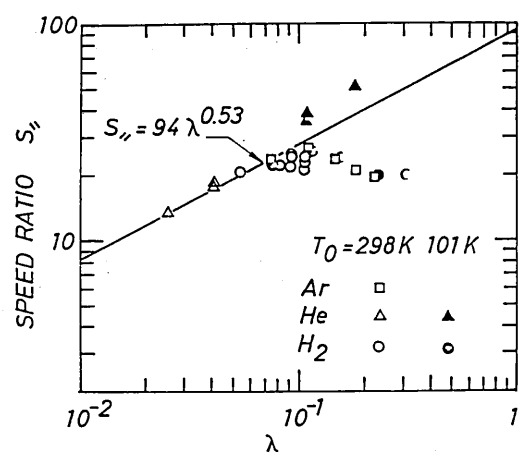

Figure 1. Speed ratio of Ar, He and H_2 beams obtained by supersonic expansion through a nozzle of 30 μm olifice diameter. For λ, see text.

ratios) for crossed beams experiments with ions are obtained for both monomers and dimers of Ar and H_2, utilizing a liquid nitrogen cooled nozzle with 30 μm olifice diameter. Figure 1 shows the speed ratio for monomer beams of Ar, He, and H_2 as a function of the parameter $\lambda(\equiv p_0 d\varepsilon^{1/3} R_m^{2} T_0^{-4/3})$ introduced by Toennies and Winkelmann.[2] Here, p_0, d, and T_0 are gas pressure at the nozzle, olifice diameter, and nozzle temperature, respectively. ε and R_m are the depth and position, respectively, of the Lennard-Jones (12, 6) potential well. With the cold source, it has been found that the relative population of $(H_2)_2$ up to $\sim$2% is obtained at the source pressure of 5 atm.

References

1) K. Tanaka, T. Kato, K. Teshima, and I. Koyano, *IMS Ann. Rev.*, 101 (1981).
2) J. P. Toennies and K. Winkelmann, *J. Chem. Phys.*, **66**, 3965 (1977).

IV—I Determination of Intensity-Normalized HeI Photoelectron Spectra of Molecules

Molecular photoelectron spectroscopy with the 584 Å HeI resonance line is a well-established technique to determine ionization potentials of valence electrons for molecules in the gas phase. However, subjects on photoelectron intensities have not been fully studied yet. Quantitative measurements of photoelectron intensities of molecules are important from both physical and chemical points of view. Intensity-defined photoelectron spectra should be quite useful for analytical purposes, while the photoelectron band intensities are closely related to photoionization cross sections associated with specific ionic states. We have continued to develope our system of photoelectron intensity measurements by further improving the mole fraction determination of a binary gaseous mixture in the ionization region.

IV-I-1 Further Improvement of Mole Fraction Determination of Gaseous Binary Mixture in Photoelectron Intensity Measurements

Yohji ACHIBA, Katsumi KIMURA, Noriyoshi KAKUTA,* and Koshiro MIYAHARA* *(*Hokkaido Univ.)*

[*J. Electron Spectrosc.*, **28**, 139 (1982)]

Recently, Kimura and his co-workers[1,2] have proposed an experimental method for determining the real mole fraction of a binary gaseous mixture (A and B) in the ionization chamber of HeI photoelectron spectrometer, in order to determine intensity-normalized photoelectron spectra as well as differential and partial photoionization cross-sections. In this paper a further modification of our photoelectron-intensity processing system is reported, by putting a special emphasis on a more refined method of the mole fraction determination. With the system modified here, we have been able to reduce the standard deviation in the mole fraction determination from 10% to 5%.

References

1) K. Kimura, Y. Achiba, M. Morishita, and T. Yamazaki, *J. Electron Spectros.*, **15**, 269 (1979).
2) Y. Achiba, T. Yamazaki, and K. Kimura, *Bull. Chem. Soc. Jpn.*, **54**, 408 (1981).

IV—J Studies of Molecular Complexes and Dimers by HeI Photoelectron Spectroscopy

Various inter-molecular species such as van der Waals molecules, hydrogen-bonded species and electron-donor-acceptor complexes in the gas phase are interesting species to be studied by HeI photoelectron spectroscopy, since changes in ionization potentials due to the molecular association may directly be measured. It is however difficult to detect such inter-molecular species by ordinary photoelectron measurements, since the concentration is usually too low. For an EDA complex formed between $(CH_3)_2O$ and BF_3, we have measured photoelectron spectra with a conventional HeI photoelectron spectrometer using a gas

inlet system of effusive nozzle type.

On the other hand, for hydrogen bonded species such as dimers of water and methanol, we have constructed a supersonic molecular beam photoelectron spectrometer with a high-speed pumping system.

IV-J-1 Photoelectron Spectrum of the Water Dimer

Shinji TOMODA, Yohji ACHIBA, and Katsumi KIMURA

[*Chem. Phys. Lett.*, **87**, 197 (1982)]

In this work, we have successfully obtained the HeI photoelectron spectrum of the gas-phase water dimer produced in a supersonic nozzle beam in the energy region below 13.5 eV, by subtracting a monomer spectrum from a monomer-dimer mixed spectrum. The spectrum of the water dimer is shown in Figure 1. The first and the second vertical ionization energies have been found to be 12.1 ± 0.1 and 13.2 ± 0.2 eV. According to an electric resonance spectroscopy by Dyke *et al.*[1], the water dimer has a trans configuration with a linear hydrogen bond. From *ab initio* SCF MO calculations, the following assignments may be deduced. The highest occupied MO (2a″) is mainly due to the out-of-plane non-bonding orbital of the proton donor, while the second occupied MO (8a′) is due to a mixture of the in-plane non-bonding orbital of the proton donor and the out-of-plane non-bonding orbital of the proton acceptor. Furthermore, the lower bound of the dissociation energy of the ground-state dimer cation with respect to $H_2O^+ + H_2O$ has been estimated to be 1.7 eV from the bond energy of the water dimer.

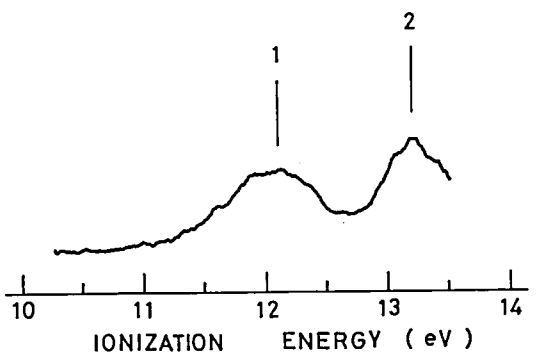

Figure 1. The difference spectrum attributed to the water dimer.

Reference

1) T. R. Dyke, K. M. Mack, and J. S. Muenter, *J. Chem. Phys.*, **66**, 498 (1977); J. A. Odutola, and T. R. Dyke, *J. Chem. Phys.*, *J. Chem. Phys.*, **72**, 5062 (1980).

IV-J-2 Photoelectron Spectroscopic Study of Simple Hydrogen-Bonded Dimers. I. Supersonic Nozzle Beam Photoelectron Spectrometer and the Formic Acid Dimers

Shinji TOMODA, Yohji ACHIBA, Katsunori NOMOTO, Kenji SATO, and Katsumi KIMURA

[*Chem. Phys.*, in press]

In the present work, we have constructed a supersonic nozzle beam photoelectron spectrometer for studying hydrogen bonded dimers in the gas phase by HeI (58.4 nm) radiation. With this apparatus we have re-investigated the HeI photoelectron spectrum of the formic acid dimer $(HCOOH)_2$ which is well known as a fairly strong doubly hydrogen bonded dimer. The spectra for the dimer and the monomer deduced from the mixture spectra are shown in Figure 1. It was found that the $(HCOOH)_2$ spectrum deduced here from the spectrum of the monomer-dimer mixture considerably differs from that reported by Carnovale *et al.*[1]

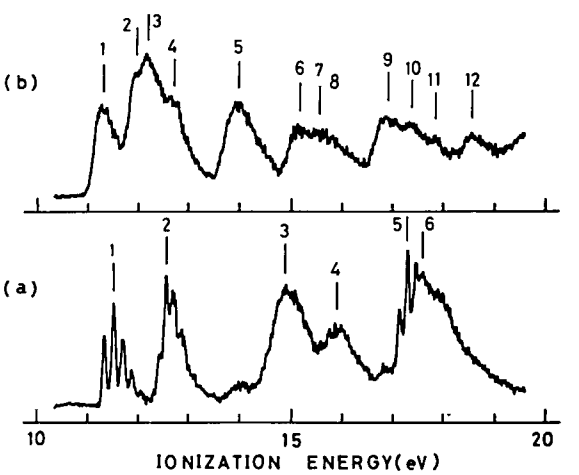

Figure 1. The HeI photoelectron spectra for the formic acid dimer and the monomer deduced from mixture spectra by stripping.

in the region beyond 16.5 eV. New spectrum assignments are given for four ionization bands beyond 16.5 eV. It is also indicated that the lower bound of the dissociation energy of $(HCOOH)_2^+$ is estimated to be 1.0 ± 0.1 eV on the basis of the experimental data. This value is considerably smaller than the value of 1.7 ± 0.2 eV recently reported for the water dimer.[2)]

References

1) F. Carnovale, M. K. Livett, and J. B. Peel, *J. Chem. Phys.*, **71**, 255 (1979).
2) S. Tomoda, Y. Achiba, and K. Kimura, *Chem. Phys. Lett.*, **87**, 197 (1982).

IV-J-3 Photoelectron Spectroscopic Study of Simple Hydrogen-Bonded Dimers. II. The Methanol Dimer

Shinji TOMODA and Katsumi KIMURA

[*Chem. Phys.*, in press]

HeI photoelectron spectra of a supersonic jet of methanol vapor have been obtained by using a temperature-controlled supersonic-nozzle-beam photoelectron spectrometer recently constructed in our laboratory (see IV-J-2). A HeI spectrum attributable to the methanol dimer has been deduced by spectrum stripping from monomer-dimer mixed spectra. The equilibrium structure of the methanol dimer has been obtained by *ab initio* SCF MO calculations assuming a configuration with a linear hydrogen bond analogous to the water dimer. The vertical ionization energies obtained from the stripped spectra have been compared with the calculated values based on the Koopmans' theorem. The lower bound of the dissociation energy of the methanol dimer has been estimated to be 1.2 ± 0.2 eV from the adiabatic ionization energies of the monomer and dimer.

IV-J-4 A Simple Temperature-Controlled Supersonic Nozzle Beam Source for Use in Photoelectron Spectroscopy

Shinji TOMODA, Toshio HORIGOME, and Katsumi KIMURA

A temperature-controlled supersonic nozzle beam system suitable for photoelectron spectroscopy has been produced and used to measure HeI photoelectron spectra of the hydrogen bonded dimers, namely the water dimer (IV-J-1), the formic acid dimer (IV-J-2) and the methanol dimer (IV-J-3). A schematic drawing of the system is shown in Figure 1. In the present system the temperature of the top of the nozzle has been controlled by circulating a relevant fluid from the temperature-regulated bath circulator. Very stable operation with a temperature fluctuation within ± 0.3K in the temperature range 290~370K has been achieved.

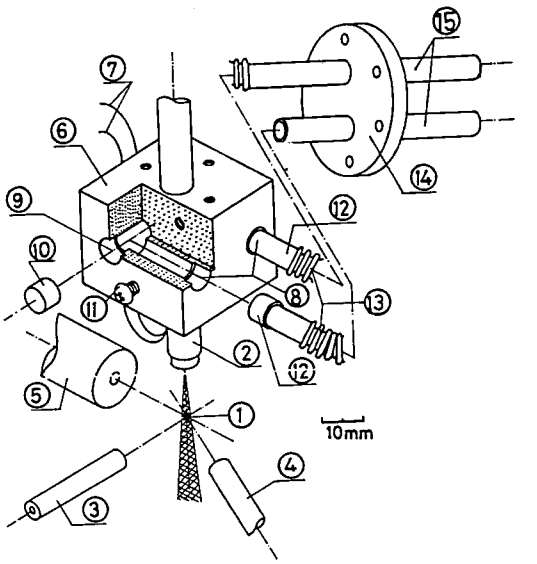

Figure 1. A schematic drawing of the construction of the temperature-controlled supersonic nozzle beam source: (1) the ionization region, (2) the nozzle pipe, (3) the glass capillary for the light beam, (4) the copper tubing for the effusive source, (5) the first piece of an electrostatic lens system, (6) the copper block heat bath, (7) the copper-constantan thermocouple, (8) the two parallel holes, (9) the hole which connects the two parallel holes, (10) the plug, (11) the screw to fasten the nozzle pipe with the heat bath, (12) the braze adopters, (13) the bellows, (14) the vacuum flange and (15) the tubings connected with the fluid circulator.

IV-J-5 Ionization Energies of the Water Dimer and Clusters

Shinji TOMODA and Katsumi KIMURA

["IONS AND MOLECULES IN SOLUTION"-Proceeding of the 6th IS$_4$I, 1982, ed. by N. Tanaka, H. Ohtaki, and R. Tamamushi, Elsevier, in press]

Ionization energies recently determined for the water dimer from HeI (58.4 nm) photoelectron spectrum by Tomoda *et al.*[1] are compared with "modified" Koopmans' theorem ionization energies based on *ab initio* SCF MO calculations. Calculations have been extended for various model clusters of water from the trimer up to the octamer. The calculated first vertical ionization energies of the model clusters are compared with available experimental data on ice as well as for the monomer and the dimer in Figure 1. The results of calculation for the pentamer and the octamer show good agreement with the experimental results. The stable character of the pentamer and the octamer is also suggested from the "hydrogen bond strength" per bond evaluated from the total energies.

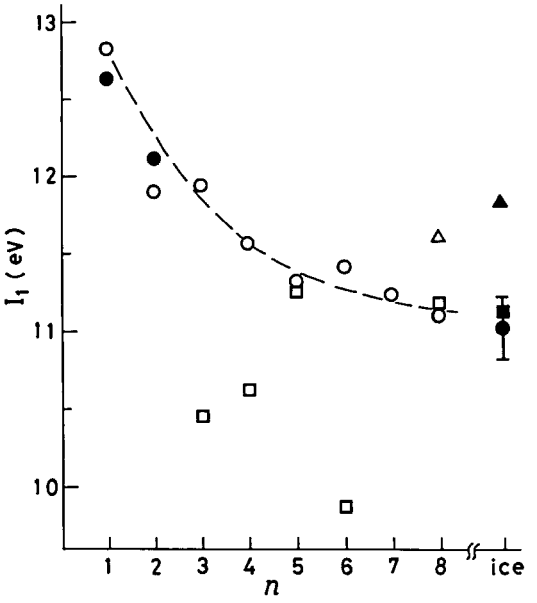

Figure 1. The first vertical ionization energy of the model water clusters as a function of the cluster size (n). Calculated values (open symbols) show good agreement with the experimental values for ice (solid symbols) at n = 5 and 8.

Reference

1) S. Tomoda, Y. Achiba, and K. Kimura, *Chem. Phys. Lett.*, **87**, 197 (1982).

IV-J-6 Theoretical Study of the Water Dimer Cation: Molecular Structure and Electronic Structure

Kenji SATO, Shinji TOMODA, Katsumi KIMURA, and Suehiro IWATA* *(*Keio Univ.)*

Ab initio CI calculations have been carried out for the water dimer cation to study the two lowest electronic states which correspond to the first and the second ionization energies of the water dimer recently determined by Tomoda *et al.*[1] Calculated results indicate that (1) the ground state of the water dimer cation has $^2A''$ symmetry and the second ionic state has $^2A'$ symmetry (trans linear conformation), and (2) these ionic states may be regarded as molecular complexes formed between H_3O^+ and OH. Total energies of the water dimer cation in the lowest two states are shown in Figure 1 as a function of the angle between the hydrogen bond O ... H axis and the hydroxyl radical O-H bond.

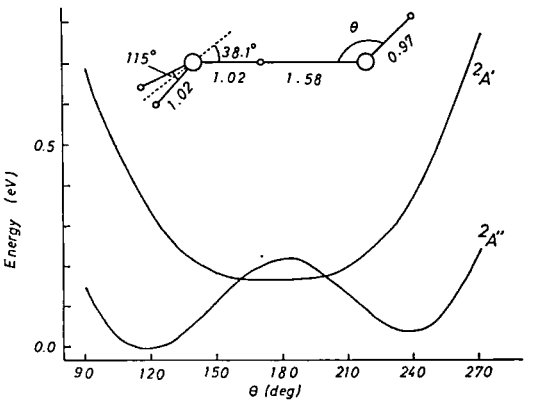

Figure 1. The potential energy curves of the two lowest states of the water dimer cation.

Reference

1) S. Tomoda, Y. Achiba, and K. Kimura, *Chem. Phys. Lett.*, **87**, 197 (1982).

IV—K Development of Multiphoton Ionization Photoelectron-Mass Spectroscopy and Its Application to Photochemistry of Molecular Clusters

Selective excitation and ionization of molecules by UV and visible lasers are now important subjects to be studied from photophysical and photochemical points of view. The ion current and the mass-spectrometric detection of ions produced by resonantly enhanced multiphoton ionization of molecules have recently been

carried out by many workers to study ionic photofragmentation. However, energy analysis of photoelectrons emitted in these experiments has scarcely been performed, in spite of its importance for identifying both the excited and the ionic states associated with the multiphoton ionization.

In the present project, we have constructed a supersonic-molecular beam photoelectron spectrometer capable of multiphoton ionization photoelectron measurements as well as ion current and mass spectrometric measurements. (IMS Annual Review, 100 (1980); 105 (1981)).

IV-K-1 The Mechanism for Photofragmentation of H_2S revealed by Multiphoton Ionization Photoelectron Spectroscopy

Yohji ACHIBA, Kenji SATO, Kosuke SHOBATAKE, and Katsumi KIMURA

[*J. Chem. Phys.*, **77**, 2709 (1982)]

Multiphoton ionization photoelectron measurements for H_2S were carried out at several laser wavelengths in the 422-475 nm region to obtain a direct evidence for the mechanism of ionic fragmentation which takes place by resonantly enhanced multiphoton ionization (REMPI). An ion current spectrum of multiphoton ionization was also measured for H_2S in the this wavelength region, indicating that the ionization takes place *via* three-photon resonant Rydberg states. From photoelectron spectra obtained here, it has been found that the main peaks are attributed to the H_2S^+ ion in the ground state with $v = 0$. Other photoelectron bands due to $v = 1$ have also been obtained. It should be mentioned that no photoelectron band above 1.3 eV has been found. These experimental evidences directly support the parent ion fragmentation mechanism that the formation of HS^+ and S^+ ions mainly results from the ground state of H_2S^+ ion with $v = 0$ and $v = 1$, respectively, by additional photon absorption.

IV-K-2 Multiphoton Ionization Photoelectron Spectroscopy of NO for (3 + 1) and (2 + 2) processes

Yohji ACHIBA, Kenji SATO, Kosuke SHOBATAKE, and Katsumi KIMURA

Photoelectron spectra have been measured for ionization of NO molecule by four photons through three-photon resonant Rydberg states, F($v = 0$ and 1) and H,H'($v=0$ and 1). The photoelectron spectra obtained are shown in Figure 1, indicating single peaks due to $\Delta v = 0$ transition. Such (3 + 1) MPI processes are confirmed also by photoelectron angular distribution measurements.

On the other hand, photoelectron spectra obtained by (2+2) processes through the resonant A Rydberg state show two kinds of photoelectron peaks, one of which is explained by $\Delta v=0$ transition and the other may be explained in terms of vibrational autoionization.

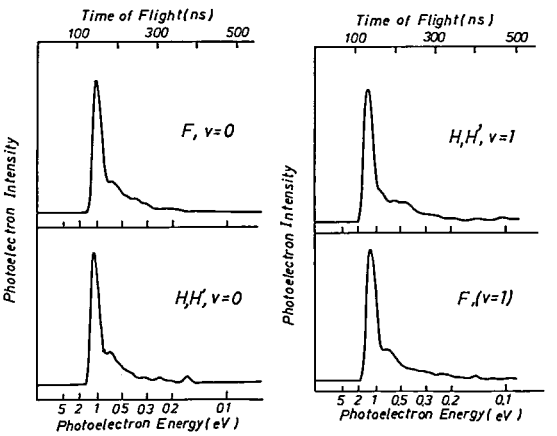

Figure 1. Photoelectron spectra obtained for NO by ionization of (3 + 1) process.

IV-K-3 Photoelectron Spectra and Angular Distribution in Resonant Three-Photon Ionization of Atomic Iron: J Dependence

Yatsuhisa NAGONO,* Yohji ACHIBA, Kenji SATO, and Katsumi KIMURA *(*Osaka Univ.)*

[*Chem. Phys. Lett.*, in press]

In the present work we have carried out measurements of kinetic energies and angular distributions of photoelectrons emitted by three-photon ionization of atomic iron through two-photon resonant states, using light from a tunable dye laser in the 447-466 nm region. Atomic iron

was produced initially by decomposition of $Fe(CO)_5$ with the same laser. In ionization through e^7D_J resonant states (J=4, 3, and 2), photoelectron bands attributable to the a^6D_J ionic states were observed, resolved into J components (9/2, 7/2, 5/2, 3/2, and 1/2). On the other hand, strong satellite bands due to the a^4F_J ionic states (J = 9/2, 7/2, 5/2, and 3/2) were obtained by ionization through the e^5D_J resonant levels, in addition to the bands due to the a^6D_J ionic states. Spectra obtained at the $e^5D_{J=3}$ level are shown in Figure 1.

Photoelectron asymmetry parameters (β) have also been determined, indicating considerably large J dependences. The J dependences of the β values and the difference of yield among ionic J components have been found to be interpreted in terms of the angular momentum conservation rule.

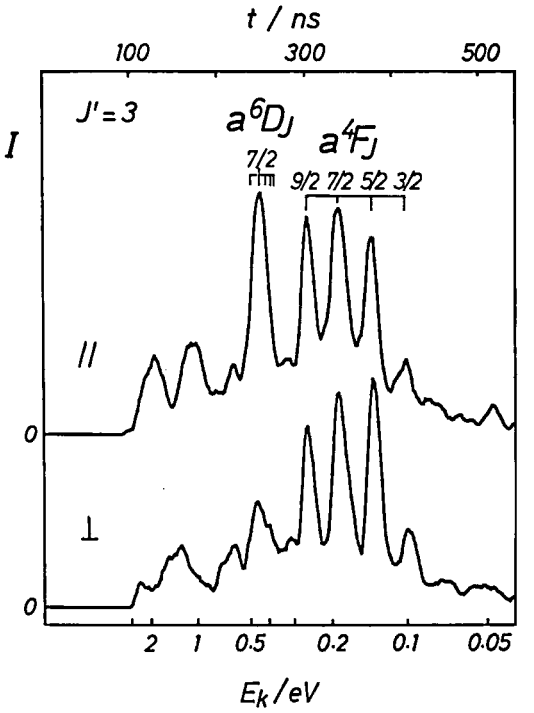

Figure 1. MPI photoelectron spectra obtained at the laser wavelength of 448.0 nm for polarized light (paralled // and parpendicular ⊥), corresponding to the ionization through the $a^5D_{J=3}$ resonant state.

IV—L Production, Characterization, and Spectroscopic Studies of Molecular Complexes and Clusters

Kosuke SHOBATAKE, Kiyohiko TABAYASHI, Yohji ACHIBA, Kenji SATO, Katsumi KIMURA, and Yoshihiro MORI* *(*Toyama Med. and Pharmaceut. Univ.)*

There are several techniques to investigate the physics and chemistry of molecular complexes and clusters. One of the most powerful techniques for the production of such weakly bound complexes is the supersonic expansion of a high pressure gas through a small nozzle hole, by which one can produce a very large number of exotic complexes. However, the characterization of these complexes is hard because of its weak bonding character.

In the present project we have constructed several types of supersonic nozzle beam sources including a variable low temperature nozzle beam source which can be cooled from room temperature to −165K, in order to investigate IR absorption spectroscopy, laser induced fluorescence spectroscopy, and electron bombardment and multiphoton ionization mass spectroscopy of van der Waals complexes, molecular complexes and clusters. We pay here a great interest in finding what would happen after weakly bound molecular complexes are brought to vibrationally and/or electronically excited states and especially in obtaining information on the predissociation dynamics of these molecules in relation to the intermolecular potential between the component molecules.

IV—M Molecular Beam Studies of Reaction Dynamics Involving Chemically Reactive Atoms and Free Radicals

In this project we investigate the dynamics of chemical reactions involving reactive species such as N, B, C, CH, etc. using a crossed molecular beams technique. For the production of supersonic nozzle beams of these reactive species we have constructed an arc-heated beam source and the beam characterization has been made using a TOF technique. A crossed molecular beams apparatus with a rotatable mass spectrometer (MBC-I) to measure the angular distribution and velocity distributions of the scattered species has been under construction and is near completion. For the measurement of the internal state distributions of the scattered species another molecular beam apparatus with optical spectroscopic detection (MBC-II) is used, in which laser induced fluorescence and chemiluminescence dispersion spectroscopy are presently applied.

IV-M-1 Production of Supersonic Nozzle Beams of Atomic Nitrogen and Argon Using an Arc-Heated Source

Kiyohiko TABAYASHI, Kosuke SHOBATAKE, Toshio HORIGOME, and Norio OKADA

An arc-heated beam source has been constructed to carry out the reactive scattering experiments involving high intensity supersonic nozzle beams of chemically reactive atoms and free radicals, such as N, B, C, CH. So far we have produced stable supersonic beams of atomic nitrogen and argon.

The arc-heated beam source was constructed based on the design of Young *et al.* as is shown in Figure 1a. The sample gas (either pure Ar or a mixed gas of 10% N_2 in Ar) heated in the plasma-arc between the tungsten cathode (WC) and the nozzle tip (N) is allowed to expand into a vacuum chamber through a nozzle (0.5 to 1.0 mm in diameter). The arc-current ranged from 35 to 100A and the source pressure applied was about 1 atm. The magnetic field was applied to effectively heat the plasma arc using the magnet coil (MC). The core flow was skimmed by a cooled Cu skimmer into a vacuum chamber (MBC-II).[2]

One-shot time-of-flight measurements were carried out to obtain the velocity distributions of atomic Ar and N beams. Typical TOF-Mass spectra obtained using a gas mixture of 10% N_2 in Ar are shown in Figure 1b. Nitrogen beam with kinetic energy E_N = 1.40 eV and the speed ratio R = 2.5; Ar beam with E_{Ar} = 3.19 eV and R = 3.6 were obtained at 60A arc-current (Ia) and 5A magnet coil current (Im).

Reactive scattering experiments using the N atomic beam thus produced is now underway.

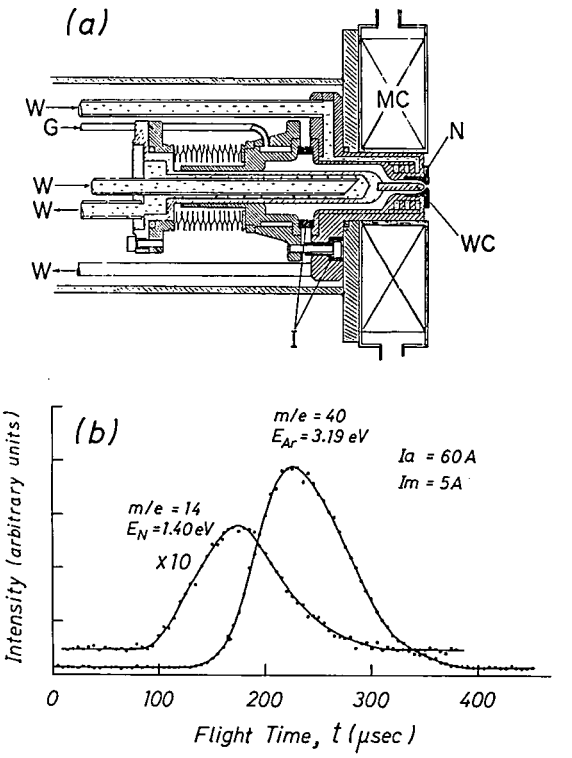

Figure 1. (a) Partially sectioned view of the arc-heated beam source. WC, 2% thoriated tungsten cathode; N, anode nozzle tip; I, electric insulator; MC, magnet coil; G, gas inlet; W, cooling water. (b) TOF spectra of N and Ar nozzle beams. Sample gas, 10% N_2 in Ar; stagnation pressure P_0 = 1.0 atm.; stagnation temperature T_0 = 18800K. The neutral flight length was 104. cm.

References

1) W. S. Young *et al. Rev. Sci. Instrum.*, **40**, 1346 (1969).
2) K. Tabayashi and K. Shobatake, *IMS Ann. Rev.*, 108 (1981).

RESEARCH ACTIVITIES V
Department of Applied Molecular Science

V—A Molecular Design of Bridged Aromatic Compounds and Organic Compounds with High Spin Multiplicity

Electronic interactions in the ground as well as excited states between the benzene rings in a fixed three dimensional molecular framework are the subject of our continued interest. As a chemical consequence of the excitonic interaction between the three benzene rings held at an angle of 120° each other, triptycenes undergo photochemical bridging between the two benzene rings to give the monocentric diradical species, *i.e.*, carbenes and nitrenes, due to one of the bridgehead atoms. Spectroscopic studies of a new carbene of the anthracen-9(10H)-ylidene family have been carried out. Our carbene chemistry has now been extended to molecular design of aromatic hydrocarbons in the ground quintet, septet and nonet states.

V-A-1 Charge-Transfer Complexation with a New Class of Electron Acceptors Made of Triptycenequinone Unit

Ewa LIPCZYNSKA-KOCHANY[1] and Hiizu IWAMURA

[*Chem. Lett.*, 1075 (1982)]

There is an interesting transannular interaction between the benzoquinone rings incorporated in a molecular framework of triptycene.[2] The electrochemical reduction potential of the benzoquinone unit is lowered and the trapped electron is found to be rapidly jumping from one site to the other in the mono- and trianion radicals of triptycenebisquinone I(n = 1).[3] The charge-transfer complex formation has now been examined in CH_2Cl_2 solutions with I(n = 1) and I(n = 3) as electron acceptors. When a solution of I(n = 3) ($C_A°$ = 4.45 mM) was mixed with TTF ($C_D°$ = 0.018 M), an increase of the absorbance at 456 nm and an appearance of new bands at 543 and 774 nm were observed. The band at 543 nm disappeared gradually on raising the TTF concentration. In the donor concentration range: $C_D°$ = 0.04 ~ 0.1 M with constant $C_A°$(= 0.445 mM), the absorbance (A_{CT}) at 774 nm followed Eq. 2.

$$A + 2D \overset{K}{\rightleftharpoons} D_2A \quad (1)$$

$$\frac{C_A° C_D°^2}{A_{CT}} = \frac{1}{K\varepsilon_{CT}} + \frac{C_D°(C_D° + 4C_A°)}{\varepsilon_{CT}} \quad (2)$$

From the determination of the formation constants at several temperatures, the enthalpies and entropies of formation of the CT complex were obtained (Table I).

At higher TTF concentrations, $C_D° > 0.1$ M, the observed absorbance was better analyzed in terms of 1:3 and even 1:4 stoichiometry.

Table I. Thermodynamic constants for 1:2 I(n = 1)-TTF and I(n=3)-TTF complexes in CH_2Cl_2

	λ_{CT}/nm	$-\Delta H$/kJmol^{-1}	$-\Delta S$/Jdeg^{-1}mol^{-1}	$-\Delta G$/kJmol^{-1}[a)]
I(n=1)·2TTF	760	37.7±0.4	90.0±1.5	10.4±0.1
I(n=3)·2TTF	774	45.1±2.0	104.6±6.5	13.5±0.6

a) at 303K

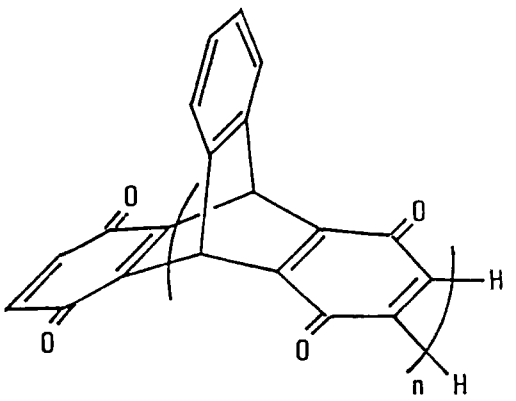

I(n=1,2,3, ...)

References

1) JSPS Invited Foreign Scholar 1981 ~ 1982 from Warsaw Technical University.
2) H. Iwamura and K. Makino, *J.C.S., Chem. Commun.*, 720 (1978); *IMS Ann. Rev.*, 106 (1980).
3) G. A. Russel, N. K. Suleman, H. Iwamura, and O. W. Webster, *J. Am. Chem. Soc.* **103**, 1560 (1981); *IMS Ann. Rev.*, 106 (1980).

V-A-2 10,10-Dimethyl-10-silaanthracen-9(10H)-ylidene and 10,10-Dimethylanthracen-9(10H)-ylidene

Akira SEKIGUCHI *(Univ. of Tsukuba)*, **Wataru ANDO** *(Univ of Tsukuba)*, **Tadashi SUGAWARA, Hiizu IWAMURA, and Michael T. H. LIU** *(Univ. of Prince Edward Island)*

[*Tetrahedron Lett.*, **23**, 4095 (1982)]

Title carbenes **2b** and **3b**, the first members of the anthracen-9(10H)-ylidene family **1**, have been generated by photolysis of the corresponding diazo compounds **2a** and **3a**.[1] The reaction products with 2-butenes were **4** ~ **9** which were accounted for by the hydrogen abstraction-recombination mechanism of the triplet carbenes. No cyclopropane derivative due to addition of **2b** and **3b** to the C = C bond was found.

The results are quite in contrast with typical diaryl-substituted carbenes; diphenylcarbene, 9H-fluoren-9-ylidene and dibenzocycloheptenylidene all give the corresponding cyclopropane products in which stereoselectivity is reasonably well kept. One precedent which shows similar reactivity as **2b** and **3b** is dihydrodibenzocycloheptenylidene.[2] In these cases, reactivity of the singlet state carbenes with olefins is considered to be somehow retarded and

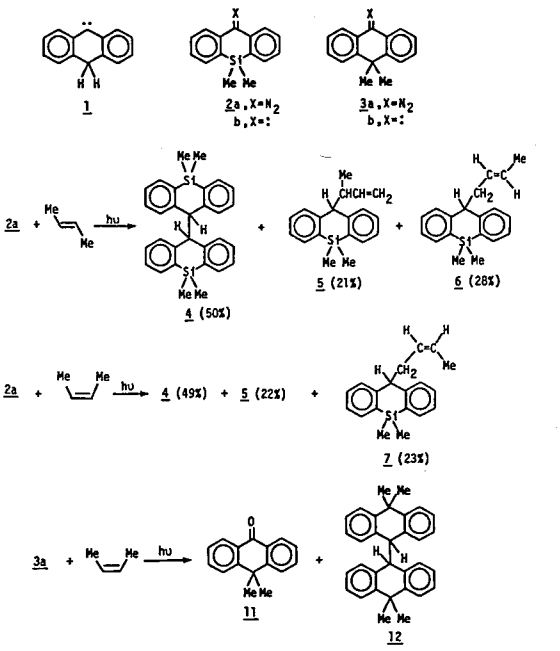

the triplet reactivity must have dominated the reaction pattern.

References

1) A. Sekiguchi and W. Ando, *Bull. Chem. Soc. Jpn.*, **55**, 1675 (1982).
2) I. Moritani, S. Murahashi, H. Ashitaka, K. Kimura, and H. Tsubomura, *J. Am. Chem. Soc.*, **90**, 5918 (1968).

V-A-3 ESR Characterization of the Ground Triplet State of 10,10-Dimethyl-10-silaanthracen-9(10H)-ylidene

Tadashi SUGAWARA, Hiizu IWAMURA, Akira SEKIGUCHI *(Univ. of Tsukuba)*, **Wataru ANDO** *(Univ. of Tsukuba)*, **and Michael T. H. LIU** *(Univ. of Prince Edward Island)*

Since the title carbene (**1**) showed the unexpected reactivity toward olefins,[1] we became interested in

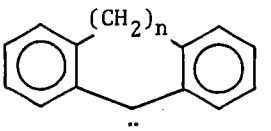

0 (n = 0)

1 (n = 1, $(CH_3)_2Si$ instead of CH_2)

2a (n = 2)

2b (n = 2, -CH=CH- instead of $(CH_2)_2$)

its ground state spin multiplicity. Irradiation of the corresponding diazo compound in an EPA matrix with a high pressure mercury lamp at *ca.* 20K in an ESR cavity (microwave frequency of 9.173 GHz) gave a set of signals characteristic of triplet carbenes (Figure 1). The triplet nature of the ground state **1** was confirmed by the linear Curie-Weiss plots of the intensity of the triplet signal at 1135 G *vs.* temperature^{-1}. The *D* and *E/D* parameters which are regarded to represent the delocalization of the odd electron in the π-type orbital and the s-character of the n-type orbital, respectively, lie between the lower (**0**) and higher (**2a, 2b**) homologs and do not appear to be unusual. The anomalous reaction pattern has to be ascribed to the unusually slow reactivity of the singlet state.

Reference

1) See the preceeding article.

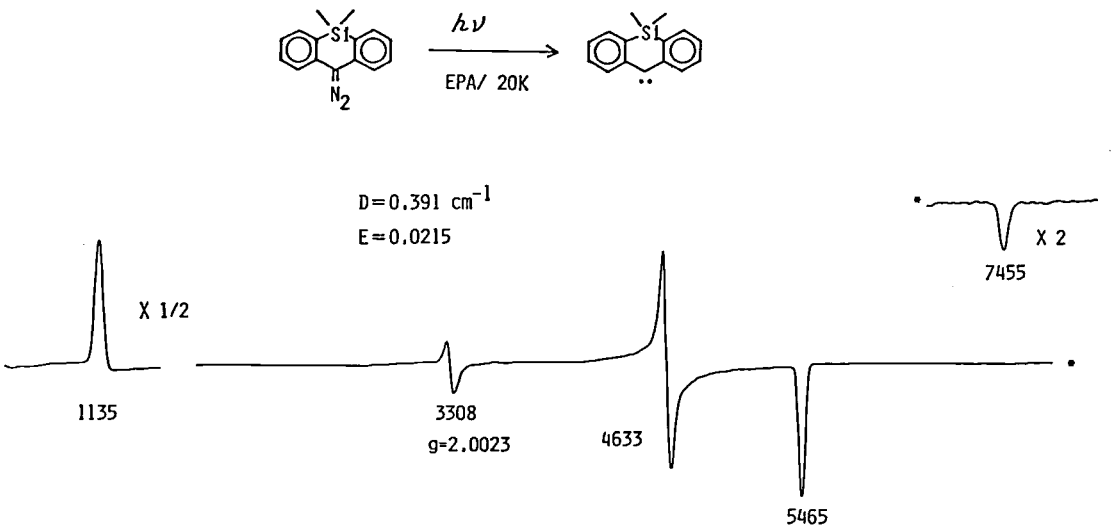

Figure 1. ESR spectra obtained on irradiating the diazo compound in EPA glass at 20K.

V-A-4 Time-Resolved Spectroscopic Study on 10,10-Dimethyl-10-silaanthracen-9(10H)-ylidene. Absorptions due to the Carbonyl Oxide

Tadashi SUGAWARA, Hiizu IWAMURA, Hisaharu HAYASHI *(Inst. Phys. Chem. Res.)*, **Akira SEKIGUCHI** *(Univ. of Tsukuba)*, **Wataru ANDO** *(Univ. of Tsukuba)*, **and Michael T. H. LIU** *(Univ. of Prince Edward Island)*

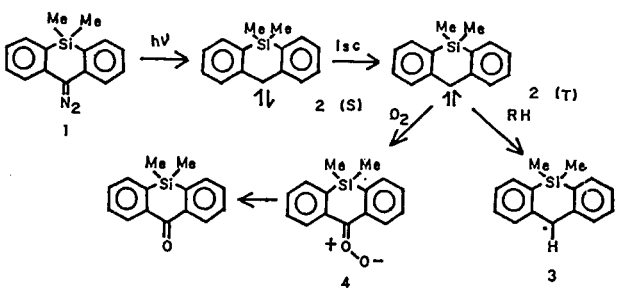

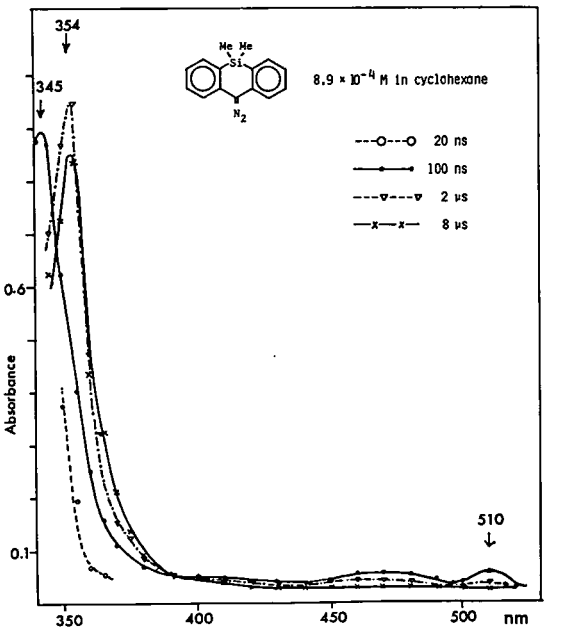

Figure 1. Absorption spectra of the transient products in the irradiation of **1** in degassed cyclohexane.

Laser photolysis studies have been carried out on a solution of diazo compound **1** in cyclohexane to obtain a series of UV absorptions due to transient species, *e.g.*, title carbene **2** and the corresponding radical **3** (Figure 1). The spectrum (λ_{max} at 345 and 510 nm) due to triplet **2** was independently obtained by the stationary photolysis of **1** in an EPA matrix at 77K, supporting the assignment of the transient absorptions. Deconvolution analyses of the growth and decay traces of the absorption spectra gave the lifetimes of the singlet and triplet **2** and radical **3** as 23 ± 4 ns, 870 ± 50 ns, and 29 ± 3 μs, respectively. Effect of the added quenchers was analyzed to give the rate constants of the singlet **2** with methanol as $1.5 \times 10^8 M^{-1}s^{-1}$. Those of triplet **2** with methanol, 2-methyl-2-butene, 2-methyltetrahydrofuran and oxygen were 6.9×10^6, 4.2×10^6, 2.8×10^7 and $2 \times 10^9 M^{-1}s^{-1}$, respectively. In the last case, a characteristic absorption appeared at 425 nm at the expense of the absorptions due to triplet **2** and was assigned to the carbonyl oxide **4**.

V-A-5 Molecular Design of Organic Compounds in the Ground Multiplet State

Kazumasa KOBAYASHI *(Yamaguchi Univ.)*[1] **and Hiizu IWAMURA**

Setting the development of organic ferromagnetism by aligning all the electron spins in parallel in molecule **I** as an ultimate goal, we have undertaken the preparative work of a series of basic intermediates **II** ~**IV** of n = 2 and 3.

Benzophenone was brominated to give **V** which was then converted through dicyanide **VI** to dicarboxylic acid **VII**. The Friedel-Crafts reaction of diacid dichloride **VIII** with benzene gave **II**, n = 2. The reaction of *m*-tolylmagnesium bromide with isophthalonitrile followed by hydrolysis gave diketone **IX** which was then oxidized stepwise to give dicarboxylic acid **X**. Tetraketone **II**, n = 3 was obtained as in **II**, n = 2. Hydrazones **III**, n = 2 and 3 were prepared by the standard method from the corresponding ketones and converted to wine-red crystals of diazo compounds **IV**, n = 2 and 3 by oxidation with active manganese dioxide in ether under basic conditions.

Both diazo compounds (see Table I) were found to generate **I**, n = 2 and 3 under uv irradiation.[2]

References

1) IMS Graduate Student from Yamaguchi University for 1980.
2) **I**, n = 1 has been characterized as a quintet species. See: K. Itoh, *Chem. Phys. Lett.*, **1**, 235 (1967); *Pure and Appl. Chem.*, **50**, 1251 (1978).

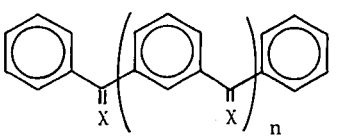

I (X = :)
II (X = O)
III (X = NNH_2)
IV (X = N_2)

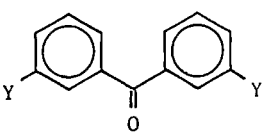

V (Y = Br)
VI (Y = CN)
VII (Y = CO_2H)
VIII (Y = COCl)

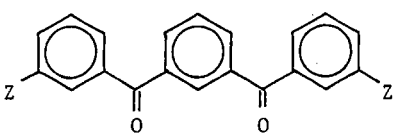

IX (Z = CH_3)
X (Z = CO_2H)

Table I. Some Properties of Polydiazo Compounds **IV**

n	mp	IR/cm^{-1}	λ_{max}/nm(logε) in $CHCl_3$	ϕ_{dec}
2	84~86°C (dec.)	2040	293(4.83) 519(2.55)	0.51±0.02 (at 254 nm in MeOH) 0.02±0.01 (at 520 nm in Et_2O)
3	113°C (dec.)	2040	294(4.91) 518(2.65)	0.42±0.05 (at 254 nm in MeOH) 0.02±0.01 (at 520 nm in $CHCl_3$)

V-A-6 Stepwise *vs.* Spontaneous Cleavages in the Photolysis of Polydiazo Compounds to give Aromatic Hydrocarbons with High Spin Multiplicity

Kazumasa KOBAYASHI *(Yamaguchi Univ.)*,[1] **Makoto INADA** *(Ehime Univ.)*,[2] **Tadashi SUGAWARA, and Hiizu IWAMURA**

Photolysis of polydiazo compounds **I** in EPA matrices has been shown by ESR and UV absorption spectroscopy to give the ground quintet, septet and nonet state species **II**, n = 1, 2 and 3.[3] Irradiation of **I**, n = 1 with a low-pressure mercury lamp in isopropyl alcohol-ether (8 : 1 v/v) at room temperature gave **III**, **IV** and **V** in a ratio of 32 : 9 : 1, indicating that each carbenic center has both the singlet and triplet reactivities in a ratio of *ca.* 5.5 : 1. When the photolysis was stopped at the 25% conversion and the remaining diazo group was quenched by *p*-nitrobenzoic acid, the products were mostly the bis(*p*-nitrobenzoate) and mono(*p*-nitrobenzoates). Elimination of only one nitrogen molecule by one photon was established. This result in solution is in contrast with the photolysis in a matrix at 77K in which the rate of formation of the quintet species shows the 1st order dependence on the incident light intensity and therefore two nitrogen molecules are eliminated by a single photon.[4] The different photolytic behaviors are under investigation.

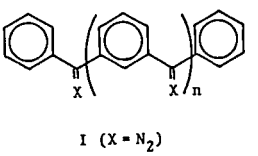

I (X = N_2)

II (X = :)

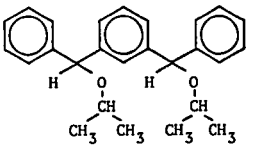

III

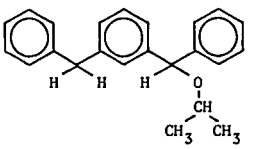

IV

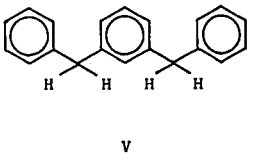

V

References

1) IMS Graduate Student from Yamaguchi University for 1980.
2) IMS Graduate Student from Ehime University for 1982.
3) The work in collaboration with Prof. K. Itoh of Osaka City Univ.
4) K. Itoh, T. Takui, and Y. Teki, presented at the 46th National Meeting of the Chemical Society of Japan, Niigata, October, 1982.

V—B Stereochemical Consequences of the Non-bonded Interaction in Overcrowded Molecules

We have been interested in the unexpectedly high potential energy barrier to rotation around the bond extending out of the bridgehead carbon of triptycene molecules. The uniqueness of the molecules lies in the high s-character of the bond and the ideal disposition of the peri hydrogens on the benzene rings serving as an effective picket for the three-fold barrier. In order to see how far the internal rotation around the two or more bonds within a molecule can be coupled and what stereochemical consequences would be brought about from the correlated rotation, a series of two-top molecules Trip-X-Trip in the shape of a bevel gear has been designed. As a result of perfectly correlated rotation around the two bridgehead-X bonds, the new stereoisomers of the gear shaped molecules were born in which the phase relationship of the labeled cogs was different. An extreme example of recognition of a minute difference in molecular shapes has now been obtained.

V-B-1 Correlated Rotation in Ditriptycyl-X Type Compounds. VI. To What Extent Can "Phase Isomers" be Differentiated in Practice?

Yuzo KAWADA *(Ibaraki Univ. and IMS)* **and Hiizu IWAMURA**

[*Tetrahedron Lett.*, in press]

Di-(monosubstituted 9-triptycyl)methanes and ethers show "phase isomerism", since internal rotation around the two bonds extending out of the bridgehead is perfectly correlated.[1] The dl and meso isomers thus produced were previously separated by HPLC on a μ Porasil column.[1] The former isomer has now been separated into the optical antipodes by HPLC on a column of

microsilica coated with chiral (+)-poly(triphenylmethyl methacrylate).[2] The optical resolution was easily achieved for the 2,2′-dichloromethane (**1**) ($[\alpha]_D^{25°}$ $-8 \pm 1.5°$ (c 0.27, CH_2Cl_2)) and very difficult for the 3,3′-dichloroether (**2**). CD spectra were obtained for the resolved isomers.

When di-(9-triptycyl)-X molecules are made of a chiral 9-triptycyl unit, they are expected to have meso and dl isomers under the uncorrelated rotation of the two C-X bonds. When the internal rotation is correlated, the meso isomer is predicted to give birth to meso and dl isomers. Three dl pairs are formed from the original dl isomer. The 2,2′,6,6′-tetrachloromethane (**3**) was prepared starting from 9-bromo-2,6-dichloroanthracene. Repeated HPLC on μ Porasil and polystyrene gel columns allowed us to obtain three pure and two not fully separated fractions. Works are in progress to assign which fraction is which isomer.

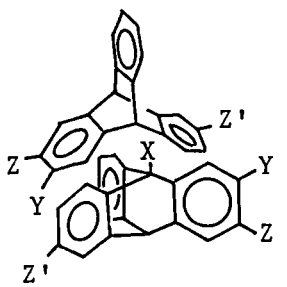

	X	Y	Z	Z'
1	CH_2	Cl	H	H
2	O	H	Cl	H
3	CH_2	Cl	H	Cl

References

1) Y. Kawada and H. Iwamura, *J. Am. Chem. Soc.*, **103**, 958 (1981); Y. Kawada and H. Iwamura, *Tetrahedron Lett.*, **22**, 1533 (1981); *IMS Ann. Rev.*, 112, 113 (1981).
2) H. Yuki, Y. Okamoto, and I. Okamoto, *J. Am. Chem. Soc.*, **102**, 6356 (1980).

V-B-2 Equilibria and Barriers to Interconversion between the *syn* and *anti* Conformers in 9-(*o*-Substituted Phenyl)fluorenes Obtained by Photorearrangement of Triptycenes

Hideyuki TUKADA, Michiko IWAMURA *(Toho Univ.)*, **Tadashi SUGAWARA, and Hiizu IWAMURA**

[*Org. Magn. Reson.*, **19**, 78 (1982)]

The population ratios of the *syn* and *anti* conformers in 9-(*o*-substituted phenyl)fluorenes have been determined by ^{1}H NMR spectroscopy to range from 0.25 to $\geq$20. They appear to increase, firstly, with the steric bulk of the 2′-substituents and, second, with the electronic repulsion between the substituent and the π-electrons on the fluorene ring. Whereas the substituents on the fluorene ring do not affect the population of the two isomers in 9-(2-tolyl)fluorenes, the same series of substituents exhibit a positive slope in the Hammett plots of the equilibrium constants in 9-(2-methoxymethylphenyl)-fluorenes. Through-space interaction between the methoxymethyl group and the π-donating fluorene ring is postulated. The free energy of activation ($\Delta G^{\neq}$) for the interconversion between the two conformers has been obtained from the line-shape dependence on temperatures. The $\Delta G^{\neq}$ values range from 56.8 (for 2′-NH_2) to 78.6 kJmol^{-1} when there is no fluorene ring substituent. Introduction of a methyl group at position 1 of the fluorene ring raises $\Delta G^{\neq}$ by *ca.* 13 kJmol^{-1}.

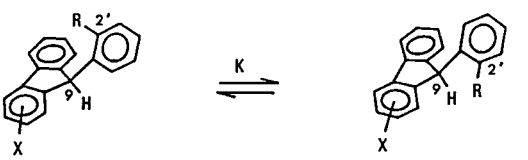

V—C Structural and Mechanistic Studies by Means of NMR of the Less Common Nuclei

Structural and mechanistic studies with the aid of NMR of ^{17}O, ^{35}Cl and ^{119}Sn have been carried out on a Varian FT-80A spectrometer. ^{17}O chemical shift data in several solvents together with pH titration enabled us to solve the long-standing puzzle of the tautomeric structures of hydroxamic acids and hydroxamate ions in

solution. Information as to the ion pairing and solvation derived from ^{35}Cl NMR line widths was critically evaluated. A new exchange reaction of the organotin compounds was analyzed. The ^{17}O isotope labeling technique has now been applied to the study of the electron spin distribution of the carbonyl group in the $^3(n\pi^*)$ state.

V-C-1 ^{17}O NMR Studies on the Structures of Benzohydroxamic Acids and Benzohydroxamate Ions in Solution

Ewa LIPCZYŃSKA-KOCHANY[1] and Hiizu IWAMURA

[*J. Org. Chem.*, in press]

The ^{17}O NMR chemical shifts of the carbonyl oxygens have been determined for benzohydroxamic acid (**1**) and its methyl derivatives **2** ~ **4** in dioxane, benzene and methanol and as functions of pH in the last solvent. The observed chemical shift values in dioxane (330 ~ 350 ppm downfield from external H_2O as a standard) are in the range characteristic of benzamides, supporting the amide structure A. Upfield shifts of *ca.* 31 and 57 ppm were observed for the *N*-methyl (**2** and **4**) and N-H compounds (**1** and **3**), respectively, in methanol solutions. Stronger hydrogen bonding with the solvent molecules in the latter compounds was suggested. From the ^{17}O chemical shift titration curves of these compounds, the pK_a values were obtained as 10.1, 9.8 and 10.8 for **1**, **2** and **3**, respectively.

On deprotonation, the carbonyl oxygen of **1** suffers an upfield shift of 72 ppm which corresponds better to that of **3** (83 ppm), namely N-H deprotonated structure D ↔ D'. A smaller but significant upfield shift for **2** indicated unexpectedly large charge delocalization on OH dissociation as given by canonical structure E'. Stabilization of structures A and D by intramolecular hydrogen bonding and dipole stabilization of the terminal O-anion have been supported by the *ab initio* MO theoretical calculations.[2]

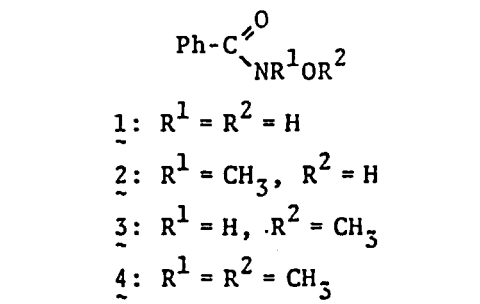

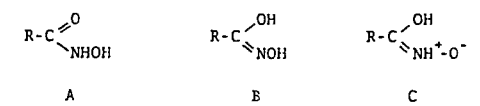

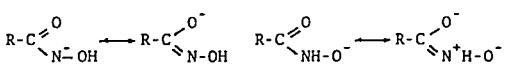

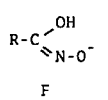

Table I. ^{17}O NMR Chemical Shift Data for **1**, **2**, **3** and **4** under different conditions

	dioxane	benzene	methanol	alkaline methanol[a]
1	333	—[b]	277	204.5
2	330	303	298.5	263.5
3	341	344	283.5	201
4	347	351	316	317

[a]pH > 12. [b]Solubility was too low to obtain data.

References

1) JSPS Invited Foreign Scholar 1981 ~ 1982 from Warsaw Technical University.
2) Joint work with K. Morokuma of Department of Theoretical Studies.

V-C-2 On the Viscosity Correction of Line Width in ^{35}Cl NMR

Tadashi SUGAWARA, Masako YUDASAKA,[1] Katsuo TAKAHASHI *(Inst. Phys. Chem. Res.)*, **Reita TAMAMUSHI** *(Inst. Phys. Chem. Res.)*, **Hiizu IWAMURA, and Tsunetake FUJIYAMA[2]**

[*Bull. Chem. Soc. Jpn.*, **55**, 1959 (1982)]

In order to see the validity and limitation of the viscosity correction treatment on the line width of ^{35}Cl NMR, line widths were measured in the aqueous solutions of sodium chloride (0.1 mol kg^{-1}) in the presence of polyethylene glycol (PEG) with

various molecular weights, the macroscopic viscosity of which ranged from 0.9 to 138 cP. The electrical conductivity, κ, of the solution was also determined as the measure of microscopic viscosity. From the correlation in Figure 1, the following criterion for the viscosity correction treatment was proposed. If the Walden product of aqueous sodium chloride in the presence of additives (PEG in the present case) is close to that of the aqueous solution in the absence of additives, microscopic viscosity can be replaced with macroscopic one in this solution. The idea obtained here would be quite useful for analyzing NMR line width on ionic species of quadrupolar nuclei.[3]

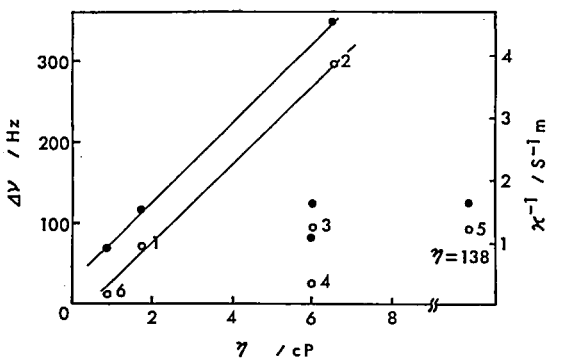

Figure 1. Plots of the ^{35}Cl NMR line width (○) and the inverse of electrical conductivity (●) *vs.* macroscopic viscosity η for the sodium chloride solutions in aqueous polyethylene glycol. 1: PEG 200 (20 wt%), 2: PEG 200 (50 wt%), 3: PEG 4000 (20 wt%), 4: PEG 20000 (5 wt%), 5: PEG 20000 (20 wt%), and 6: none.

References

1) Present address: Department of Applied Chemistry, Faculty of Engineering, Yokohama National University.
2) Department of Molecular Structure.
3) T. Sugawara, M. Yudasaka, Y. Yokoyama, T. Fujiyama, and H. Iwamura, *J. Phys. Chem.*, **86**, 2705 (1982); *IMS Ann. Rev.*, 118 (1981).

V-C-3 Reaction of Trialkylstannyllithium and Hexaalkyldistannane. ^{1}H and ^{119}Sn NMR Studies

Kazuko KOBAYASHI *(Kyoto Univ.)*, **Mituyoshi KAWANISHI** *(Kyoto Univ.)*, **Sinpei KOZIMA** *(Kyoto Univ.)*, **Torazo HITOMI** *(Kyoto Univ.)*, **Hiizu IWAMURA, and Tadashi SUGAWARA**

[*J. Organometal. Chem.*, **217**, 315 (1981)]

The reaction of hexamethyldistannane ($Me_3SnSnMe_3$) with metallic lithium in THF has been studied by ^{1}H and ^{119}Sn NMR spectroscopy. All spectra displayed a single peak which moved gradually from the chemical shifts (0.22 ppm in ^{1}H and −108.7 ppm in ^{119}Sn NMR) of $Me_3SnSnMe_3$ into those of trimethylstannyllithium (Me_3SnLi, −0.37 ppm and −182.7 ppm) in 2 h. There was a linear relationship between the chemical shift of the peak and the amount of lithium per a trimethylstannyl group. The equilibration of the Me_3Sn group between the two species was proposed as a plausible explanation for the apparent equivalency of Me_3Sn and was supported by investigating two mixed alkyl systems. Both the Me_3SnLi-$Et_3SnSnEt_3$ and Et_3SnLi-$Me_3SnSnMe_3$ systems showed single Me_3Sn and Et_3Sn group resonances each in the NMR spectra. The chemical shift of Me_3Sn *vs.* (Li/R_3Sn) plots deviated to higher field from the linear relationship, while that of Et_3Sn shifted to lower field. A rapid exchange between Me_3Sn and Et_3Sn in the following two equilibria is proposed.

$$Me_3SnLi + Et_3SnSnEt_3 = Et_3SnLi + Me_3SnSnEt_3$$
$$K_1 = 0.5$$

$$Me_3SnLi + Me_3SnSnEt_3 = Et_3SnLi + Me_3SnSnMe_3$$
$$K_1 = 0.2$$

V-C-4 Optically-Detected Electron-Nuclear Double Resonance and Electron-Nuclear-Nuclear Triple Resonance Studies of Oxygen-17 Hyperfine Coupling in the Lowest $n\pi^*$ Triplet State of Benzil

Yoshio TEKI *(Osaka City Univ.)*, **Takeji TAKUI** *(Osaka City Univ.)*, **Mitsuru HIRAI** *(Osaka City Univ.)*, **Koichi ITOH** *(Osaka City Univ.)*, **and Hiizu IWAMURA**

[*Chem. Phys. Lett.*, **89**, 263 (1982)]

^{17}O Hyperfine coupling is expected to provide direct information as to the electron spin distribution in the carbonyl group in the $^{3}(n\pi^*)$ state. The ^{17}O enriched (15 atom %) sample (PhCOCOPh) was prepared by the base-catalyzed exchange reaction of the unlabelled benzil with water-^{17}O (20

atom %). Optically-detected ENDOR and electron-nuclear-nuclear triple resonance (ODTRIPLE) of ^{17}O have been detected for the first time through phosphorescence from $^3(n\pi^*)$ benzil in benzophenone-d_{10} crystals at high magnetic field.

The observed ^{17}O-ODENDOR spectra are explicable in terms of a superposition of the calculated ENDOR transitions of benzil molecules ^{16}O-^{17}O (26%) and ^{17}O-^{17}O (2%). The assignment was confirmed by the ^{17}O ODTRIPLE measurements (Figure 1).

The n and π^* spin densities on the oxygen atom were found to be 0.201 and 0.092, respectively, the angle between the two C=O bond planes being 150°.

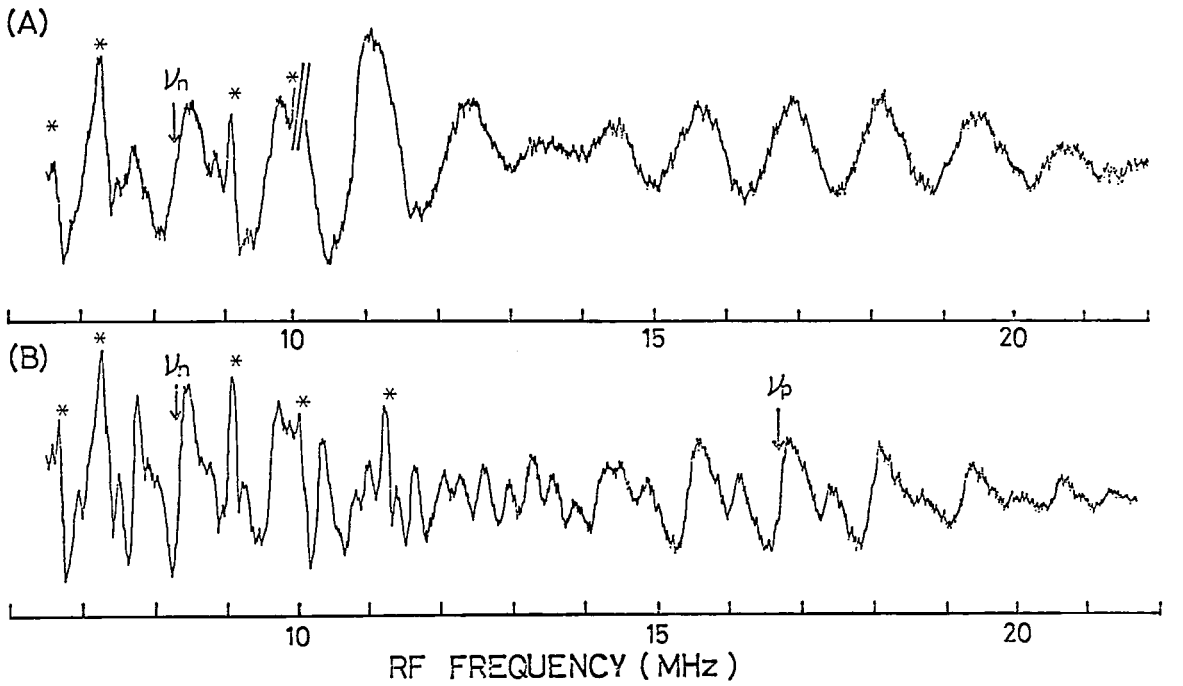

Figure 1. ^{17}O-ODENDOR spectrum (A) and ^{17}O-ODTRIPLE spectrum (B) of $^3(n\pi^*)$ benzil at 4.2K. The magnetic field is along the *Z* axis. The modulation amplitude was 70 KHz except the range over 10 MHz where 175 KHz was used to increase the sensitivity by 2.5 times without signal distortion. The asterisk indicates the ^1H-ODENDOR signal, ν_n the free proton frequency, and ν_p the pumping frequency.

V—D Application of the CD Exciton Chirality Method in Organic Stereochemistry, and Intramolecular Charge Transfer Transition in Triptycene Systems

The circular dichroic exciton chirality method, a nonempirical method based on the coupled oscillator theory, has been successfully used for determination of absolute configrations of various organic chiral compounds. In this project, the absolute stereochemistries of 2,2′-spirobi-indane-1,1′-diol and 2,2′-spirobibenz(e)indane systems were definitely determined. Furthermore, the mechanism of the intramolecular charge transfer transition of 1,4-dihydro-1,4-bis(dicyanomethylene)triptycene was clarified by the SCF-CI-DV molecular orbital calculation.

V-D-1 Absolute Stereochemistry of 2,2′-Spirobi-indane-1,1′-diols as determined by the CD Exciton Chirality Method

Nobuyuki HARADA *(Tohoku Univ. and IMS)*, **Tomoyoshi AI** *(Tohoku Univ.)*, **and Hisashi UDA** *(Tohoku Univ.)*

[*J. Chem. Soc. Chem. Commun.*, 232 (1982)]

The absolute configurations of *cis,trans*- and *trans,trans*-2,2′-spirobi-indane-1,1′-diols were non-empirically determined by applying the c.d. exciton chirality method to their bis(*p*-dimethylamino-benzoates). The CD spectrum of the *cis,trans*-dibenzoate (**4c**) clearly exhibits exciton split Cotton effects of negative exciton chirality, which lead to a left-handed screw relationship between the two benzoate groups (Figure 1). The (1*R*,1′*S*,2*S*) absolute configuration of (**4a**) was thus determined in a non-empirical manner. Since oxidation of (**4a**) gave (+)-(1), the (2*S*) absolute configuration of (+)-(1) was established.

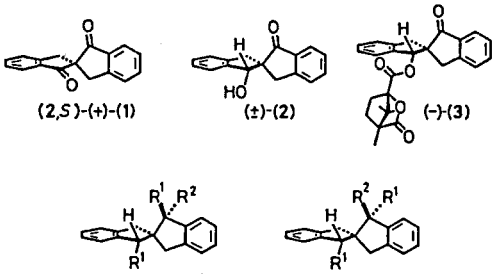

For (4) and (5):	R^1	R^2
a	OH	H
b	$OCOC_6H_4$-*p*-Cl	H
c	$OCOC_6H_4$-*p*-NMe_2	H
d	OH	D
e	$OCOC_6H_4$-*p*-Cl	D

V-D-2 Optical Resolution of 2,2′-Spirobibenz-(e)indane Derivatives by Means of Liquid Chromatography and Determination of Absolute Configuration

Nobuyuki HARADA *(Tohoku Univ. and IMS)*, **Jun IWABUCHI** *(Tohoku Univ.)*, **Yoichi YOKOTA** *(Tohoku Univ.)*, **Hisashi UDA** *(Tohoku Univ.)*, **Yoshio OKAMOTO** *(Osaka Univ.)*, **Heimei YUKI** *(Osaka Univ.)*, **and Yuzo KAWADA**

The spiro compounds with two naphthalene chromophores, 1,1′,3,3′-tetrahydro-2,2′-sporobi-(2H-benz(e)indene)-1,1′-dione (**3**) and (*cis,trans*)-1,1′,3,3′-tetrahydro-2,2′-spiro(2H-benz(e)indene)-1,1′-diyl diacetate (**4**), were synthesized. Optical resolution of each compound was successfully accomplished by means of liquid chromatography using a chiral packing material of (+)-poly(triphenylmethyl methacrylate) coated on macroporous silica gel.

The CD spectrum of diketone **3** exhibits negative first and positive second Cotton effects in the ^1B_b transition region. From the negative sign of the first Cotton effect, the (2*S*) absolute configuration was deduced.

On the other hand, diacetate **4**, which has no homoconjugation effect, exhibits very strong exciton split Cotton effects of negative chirality as shown in Figure 1. From the sign of the Cotton effects, the (1*R*,1′*S*,2*S*) absolute configuration was determined in a nonempirical manner.

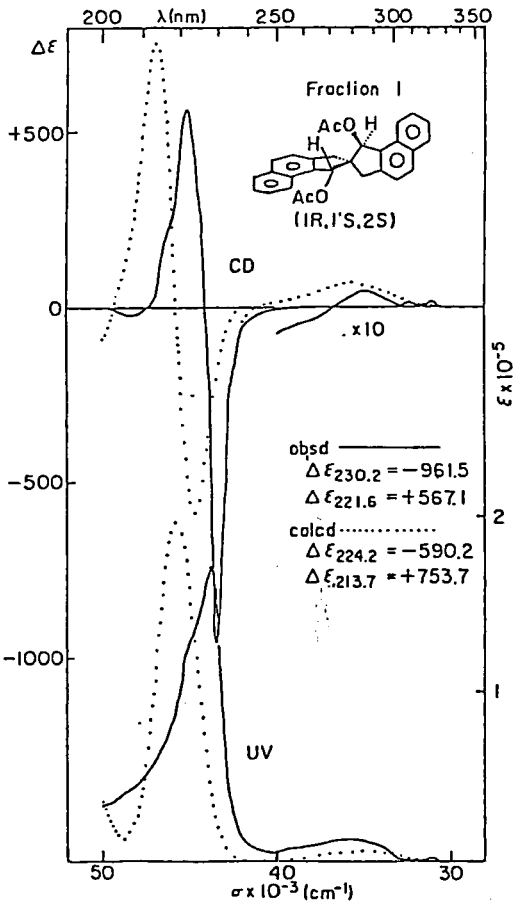

Figure 1. CD and UV spectra of (1*R*,1′*S*,2*S*)-1,1′,3,3′-tetrahydro-2,2′-spiro(2H-benz(e)indene)-1,1′-diyl diacetate (**4**) in EtOH. The dotted curves are the calculated spectra.

V-D-3 Interchromophoric Homoconjugation Effect and Intramolecular Charge Transfer Transition

Nobuyuki HARADA *(Tohoku Univ. and IMS)*, **Hisashi UDA** *(Tohoku Univ.)*, **Kazuhiro NAKASUJI** *(Osaka Univ.)*, **and Ichiro MURATA** *(Osaka Univ.)*

The mechanism of the intramolecular charge transfer transition (λ_{max} 535 nm, log ε 3.40) of 1.4-dihydro-1.4-bis(dicyanomethylene)triptycene (**5**) was clarified by the SCF-CI-DV MO calculation. The TCNQ chromophore exhibits a very strong $\pi \rightarrow \pi^*$ transition, λ_{max} 409 nm, log ε 4.66, from which the CT transition borrows the absorption intensity, as follows. The HOMO of TCNQ group mix with the HOMO of two benzene groups to build up the HOMO of the total system. The transition from the resultant HOMO to the LUMO of TCNQ is partially allowed because the transition includes a part of the allowed TCNQ transition. Therefore, the intensity of the CT transition depends on the degree of mixing of the HOMO of TCNQ and benzene chromophores.

The SCF-CI-DV MO calculation corroborated the above mechanism; when β(homo)/β(arom) is 35%, the calculated curve is in good agreement with the observed electronic spectrum. From the calculation results, the interchromophoric homoconjugation effect β(homo) of triptycene system was estimated to be about 30% of a regular aromatic conjugation β(arom).

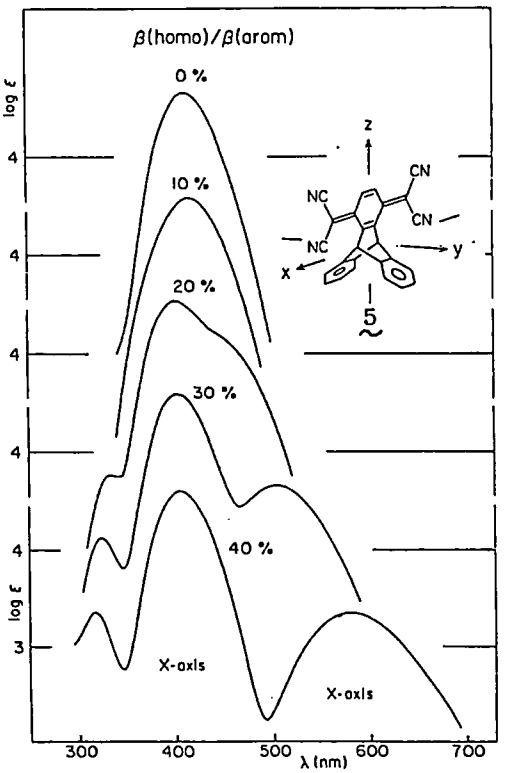

Figure 1. Calculated electronic spectrum curves of 1,4-dihydro-1,4-bis(dicyanomethylene)triptycene (**5**).

V—E Correlation between Axial and In-plane Coordination Bond Lengths in *trans*-MX_2N_4 Type Complexes and its Electronic Origin —Metal Ion Characteristics—

In complexes of the *trans*-MX_2N_4 type, —where a metal ion (M) is surrounded octahedrally by four nitrogens in plane and by two X, halide or pseudo-halide ions, occupying the axial positions—, is there any relation between axial (M-X) and in-plane (M-N) coordination bondlengths? Earlier structural studies of Ni(II) complexes suggested the possibility of the presence of such a correlation (*IMS Ann. Rev.*, 127-129 (1981)). In this study, we aimed at a systematic investigation of the correlation: whether the correlation generally exist or not? Is the correlation characteristic of a metal ion? How about an effect of the ligand field strengths on the correlation? Recent developments both in the accuracy of X-ray analysis and in coordination chemistry in a sense that appropriate compounds are now available made the present study possible.

V-E-1 Correlation between Axial and In-plane Coordination Bond Lengths in *trans*-MX_2N_4 Type Complexes (M = Co^{3+}, Ni^{2+}, and Zn^{2+})

Tasuku ITO, Masako SUGIMOTO, and Haruko ITO

In order to investigate the titled correlation experimentally, we have carried out X-ray analyses of a series of complexes of the *trans*-MX_2N_4 type. In all, 13 structures have been determined. As in-plane ligands, we used mainly the tetraazacycloalkanes shown below. By going from smaller to larger rings, the average M-N bond distances can be varied

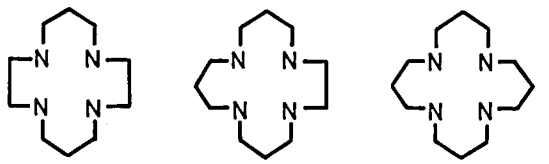

[14]aneN$_4$ [15]aneN$_4$ [16]aneN$_4$

systematically. As axial ligands (X), we used Cl^- and NCS^-, which have relatively weak and strong ligand field strengths, respectively. Figure shows the observed correlation for the Co^{3+}, Ni^{2+}, and Zn^{2+} complexes. Co^{3+} shows almost no correlation, Zn^{2+} the strongest among these three metal ions, and Ni^{2+} is intermediate. A stronger axial ligand gives rise to weaker correlation [compare the slopes for the Cl^- and NCS^- complexes of Ni(II)]. Generally speaking, the M-X bondlength decreases as the M-N distance increases. A negative correlation exists. There is no doublt that the nature of this phenomenon is electronic in origin and the correlation is characteristic of each metal ion, since the structure analyses show no obvious intramolecular steric effects which might cause these correlations.

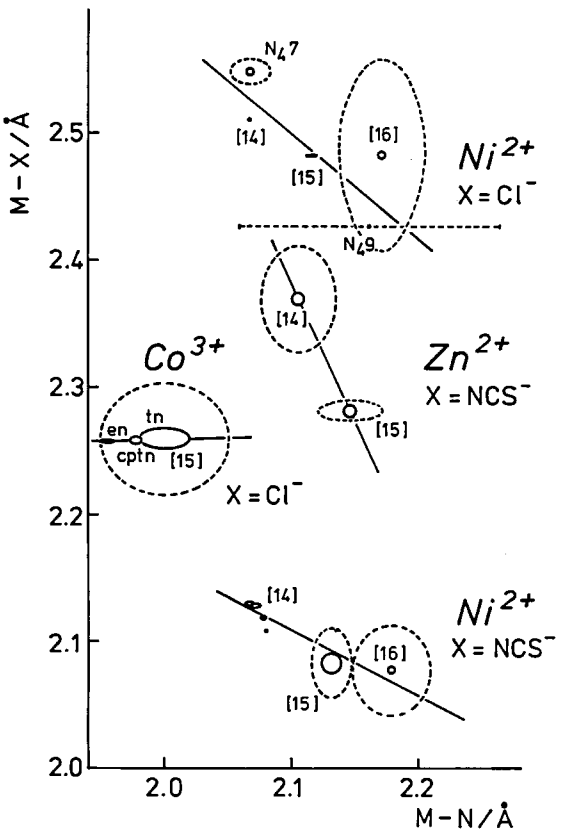

Figure 1. Correlation between axial and in-plane coordination bondlengths in Ni^{2+}, Co^{3+}, and Zn^{2+} complexes of *trans*-MX_2N_4 type.

V-E-2 Correlation between Axial and In-plane Coordination Bond Lengths in *trans*-MX_2N_4 Type Complexes and Its Electronic Origin —*Ab Initio* MO study—

Haruko ITO and Tasuku ITO

In order to investigate theoretically the metal ion characteristics which bring about the correlation of coordination bondlengths described in a preceding paper, we carried out *Ab Initio* MO calculations on model compounds, *trans*-[$MCl_2(NH_3)_4$], where M = Co^{3+}, Ni^{2+}, and Zn^{2+}. Figure shows the potential energy surfaces along M-N and M-Cl bonds. Each contour is an ellipse elongated in the M-Cl direction

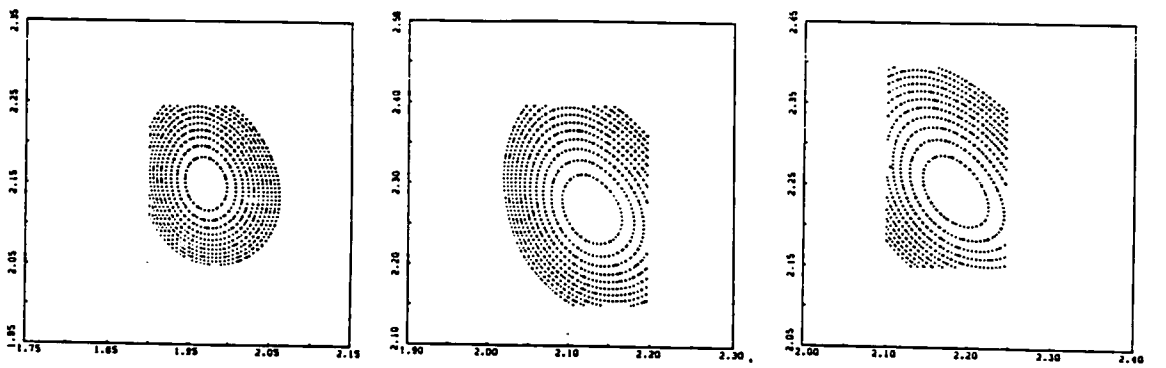

trans-[$CoCl_2(NH_3)_4$]$^+$ *trans*-[$NiCl_2(NH_3)_4$] *trans*-[$ZnCl_2(NH_3)_4$]

Figure 1. Potential energy surfaces along M-Cl (vertical axis) and M-N (horizontal axis) coordination bonds. Contours are at intervals of 0.5 kcal/mol. Ratio of the short to the long axis of contour ellipse and tilt of the ellipse are 0.76, 0.70, and 0.60, and 14°, 30.5°, and 41° for the Co^{3+}, Ni^{2+}, and Zn^{2+} complexes, respectively.

with an anticlockwise tilt. The tilt of the ellipse is the smallest for Co^{3+}, intermediate for Ni^{2+}, and the largest for Zn^{2+}. The ellipse for Co^{3+} is the most close to a circle, whereas the ratio of the long to the short axes is the largest for the Zn^{2+} ellipse. The contour lines are the most congested for Co^{3+}, and the furthest apart for Zn^{2+}. When a contour is an ellipse with an anticlockwise tilt, the line connecting energy minimum points at each M-N distance has a negative slope. The M-Cl distance decreases with an increase in the M-N distance. In terms of the potential surface, a stronger negative correlation between these two quantities would be expected under the following requirements: (1) The ratio of the long axis to the short axis of the ellipse is larger. The closer the ellipse is to a circle, the weaker the correlation. (2) The ellipse has a larger tilt. (3) The contour lines are less congested, *i.e.* the slope of the potential surface is more gentle. The calculated maps agree very well with the experimentally observed results. These results may give a quantitative measure for Hard and Soft — Acid and Base concept for metal ions.

V-E-3 The Structures of *trans*-Diisothiocyanato-(1,4,7,10-tetraazacyclo-tetradecane, -pentadecane, and -hexadecane)nickel(II) Complexes

Masako SUGIMOTO, Haruko ITO, and Tasuku ITO

Molecular structures of a series of titled compounds, *trans*-[Ni(NCS)$_2$(L)], L = [14]aneN$_4$ (**1**) [15]aneN$_4$ (**2**), [16]aneN$_4$ (**3**), have been determined in order to investigate the correlation of intramolecular coordination bond lengths (*cis* effect) in Ni(II) complexes (see V-E-1). Perspective views of the structures of these complexes are shown in Figure. The average axial bond length decreases as the average in-plane bond length increases (see Figure in V-E-1). Interestingly enough, in the crystal structure of the complex **1**, the negative correlation was observed even for chemically the same but crystallographically inequivalent molecules. In the complex **2**, significant disorder was observed between gauche five-membered and skew form six-membered chelate rings. This arises from the fact that the bite angle (∠N-Ni-N) of skew form six-membered chelate ring is similar to that of gauche five-membered ring. The chelate ring conformations of the complexes **1**, **2**, and **3** are chair-gauche-chair-gauche, chair-chair-skew-gauche, and chair-chair-skew-skew, in these sequences. In the compound **3**, there exists an intramolecular steric effect which makes the *cis* effect small.

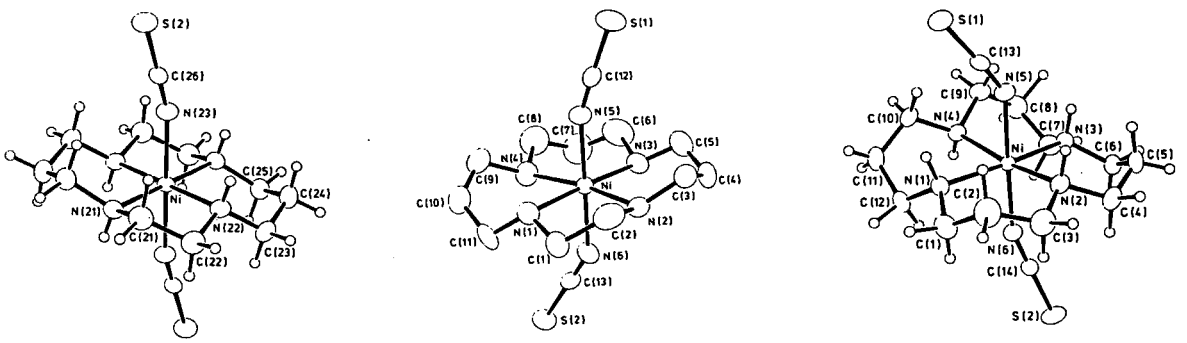

(a) (b) (c)

Figure 1. Perspective views of the structures of *trans*-[Ni(NCS)$_2$[14]aneN$_4$] (a), *trans*-[Ni(NCS)$_2$[15]aneN$_4$] (b), and *trans*-[Ni(NCS)$_2$[16]aneN$_4$] (c).

V-E-4 The Structures of *trans*-Dichloro-(1,4,7,10-tetraazacyclo-tetradecane, -pentadecane, and -hexadecane)nickel(II) Complexes

Masako SUGIMOTO, Haruko ITO, and Tasuku ITO

Molecular structures of a series of titled compounds, *trans*-[NiCl$_2$(L)], L = [14]aneN$_4$ (**1**), [15]aneN$_4$ (**2**), [16]aneN$_4$ (**3**), have been determined. Perspective views of the structures are shown in

Figure. This study was undertaken in order to investigate especially an effect of ligand field strength of the axial ligands on the correlation. Cl^- has much weaker ligand field strength than NCS^-. The results show that the weaker the axial ligand field is, the stronger the correlation. Chelate ring conformations of the compounds **1** and **3** are the same as those of the *trans*-diisothiocyanato analogues, respectively, while the 15-membered macrocycle in the compound **2** takes a conformation different from the *trans*-diisothiocyanato analogue and adopts a chair-skew(6)-chair-gauche form.

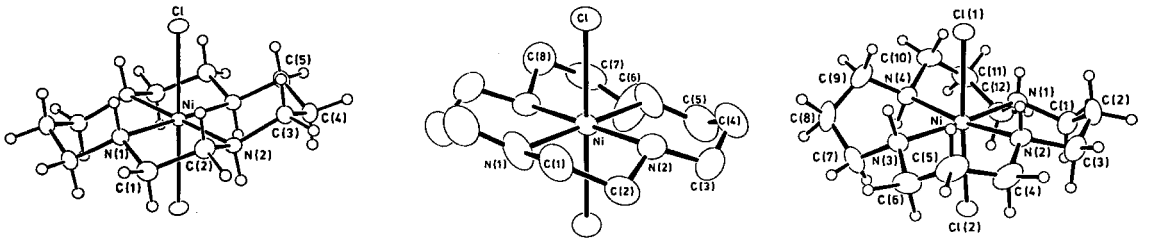

(a) (b) (c)

Figure 1. Perspective views of the structures of *trans*-$[NiCl_2[14]aneN_4]$ (a), *trans*-$[NiCl_2[15]aneN_4]$ (b), and *trans*-$[NiCl_2[16]aneN_4]$ (c).

V—F Electron Density Distribution in Crystals of $[Co(hexaen)]Cl_3$ Determined by X-ray Diffraction Method

Koshiro TORIUMI, Yuzo YOSHIKAWA *(Nagoya Univ.)*, **and Tasuku ITO**

Electron density distributions in transition-metal complexes can be directly determined by the accurate single crystal diffraction measurements. Molecular wavefunctions have been calculated to obtain the molecular energy levels, but now they can be compared with the spacial distribution of experimental electron density. It is particularly interesting to study the characteristic behavior of 3d electrons and the bond nature in inorganic compounds on the basis of electron density distributions.

The electron density distribution in crystals of $[Co(hexaen)]Cl_3$ (hexaen = 1,4,7,10,13,16-hexaazacyclooctadecane) has been determined by single crystal X-ray diffraction at 106 K. The crystal data are: rhombohedral, $R\bar{3}$, $Z = 1$, $a = 7.7163(1)$ Å, $\alpha = 73.684(1)°$, $U = 412.88(1)$ Å^3, μ(Mo $K\alpha$) = 1.567 mm^{-1} (at 106 K).[1] Data collected with Mo $K\alpha$ radiation up to $2\theta = 135°$ were refined by the full-matrix least-squares techniques to $R = 0.031$ and $R_w = 0.027$. The central cobalt atom of the complex cation at $\bar{3}$ site is surrounded octahedrally by six equivalent nitrogen atoms of hexaen ligand with the distance of 1.9962(2) Å, and the octahedron is trigonally compressed along its C_3 axis. Observed deformation density maps around the cobalt atom show the residual electron densities of 1.3 − 1.5 eÅ^{-3} at 0.40 Å from the cobalt nucleus directed into the faces of the octahedron as expected for a $(t_{2g})^6(e_g)^0$ electronic configuration. The positions of positive peaks on the pseudo C_3 axes, however, are shifted toward the plane perpencicular to the C_3 axis according to the trigonal compression of an octahedral ligand field. A bonding electron is also observed on the Co-N bond, which is elongated along the bond. Two peak-top positions of the peak are located at 0.50 and 0.90 Å from the nitrogen nucleus, indicating a significant covalency of the Co-N bond.

Reference

1) Y. Yoshikawa, K. Toriumi, T. Ito, and H. Yamatera, *Bull. Chem. Soc. Jpn.*, **55**, 1422 (1982).

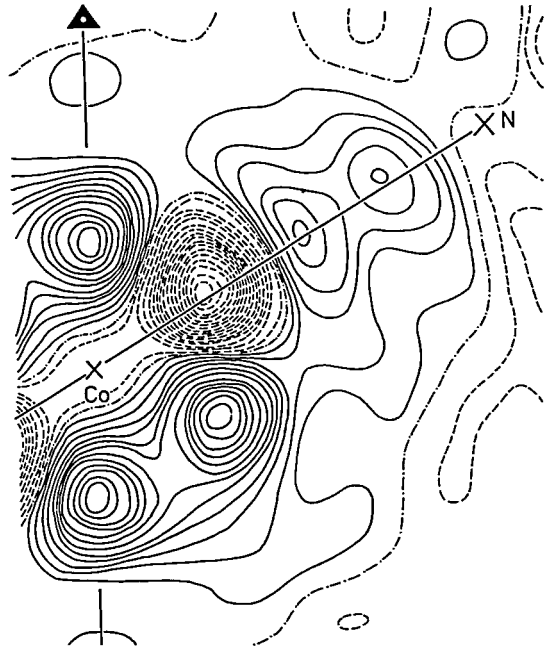

Figure 1. Section of the difference Fourier map through a Co-N bond and a C_3 axis. Coutours are at intervals of 0.05 eÅ^{-3}. Negative contours are dotted, and zero being chain-dotted. Resolution: $2\sin\theta_{max}/\lambda$ = 1.81 Å^{-1}.

V—G EXAFS Study of Amorphous Materials. Structure Determination of Mixed-Valence Complexes Having M-X···M Linear Chains

Koshiro TORIUMI, Masahiro YAMASHITA, and Tasuku ITO

Structural informations are essential to study physical and chemical properties of a compound. For structure determination, a conventional X-ray analysis is not always feasible in a case where suitable crystals are not available. Recent experimental and theoretical advances have made EXAFS a powerful new tool for a study of local structure around a specific absorbing atom in amorphous compounds.

Mixed-valence complexes having M^{IV}-X···M^{II} linear chains (M = Pt, Pd, Ni; X = I, Br, Cl) exhibit semiconductive behaviors along the chain directions, which are correlated with the distances of M^{II}···X and M^{IV}-X. In many cases, suitable crystals for X-ray analyses cannot be obtained for such compounds. Structural studies of the mixed valence palladium complexes containing tetraaza-macrocyclic ligands, [PdL][PdX_2L](ClO_4)$_4$ (X = Cl, Br; L = [14]aneN$_4$, [15]aneN$_4$), are now being carried out by using the EXAFS techniques. EXAFS spectra have been measured in a transmission mode by in-laboratory EXAFS system utilizing a rotating anode X-ray source, a Ge(220) flat crystal monochromator, and a solid state detector (see I- -). Analyses of the spectra so far obtained show that the contribution of the atom X in the M^{II}···X moieties to the EXAFS appears to be absent, or very weak if any.

V—H Structural Studies of Some Compounds of Interest

V-H-1 A Binuclear Copper(II) Complex with Both Metals Bound within a 22-Membered-tetraazacycloalkane

Masahiro YAMASHITA, Haruko ITO, and Tasuku ITO

There is a great current interest in binuclear metal complexes, particularly those of copper, in regard to metal-metal electron exchange interaction, electron transfer properties, and as synthetic analogues for some metalloproteins. In this study, a new type of binuclear copper(II) complex, in which two copper atoms are bound within a *tetraaza*-macrocycle, has been synthesized by the reaction of copper(II) perchlorate with 2,2,4,13,13,15-hexametyl-1,5,12,16-tetraazacyclodocosane prepared beforehand by the condensation of acetone and monohydroperchlorate of hexamethylenediamine. X-ray data: $Cu_2Cl_2O_{10}N_4C_{26}H_{58}$, M = 784.8, a = 16.734(3), b = 8.549(1), c = 13.103(2) Å, β = 111.05(1)°, U = 1749.4(5) Å^3, Z = 2, space group $P2_1/a$, R = 0.037 for 3806 observed reflections. Of particular interest is the fact that two alkoxo-bridged copper ions are bound within the tetraazamacrocycle (Figure). The copper ions are tetracoordinated with two N atoms of the macrocycle and two O atoms of the alkoxo groups, the dihedral angle between the NCuN- and OCuO-planes being 36.6°. Two copper ions and four N atoms of the macrocycle are coplanar within 0.001 Å. The Cu ··· Cu separation is 3.034(1) Å and the angle Cu-O-Cu is 102.50(8)°. The magnetic moments were 0.87 BM at 299°K and 0.19 BM at 81°K, indicating that a relatively strong antiferromagnetic interaction operates between the Cu(II) ions.

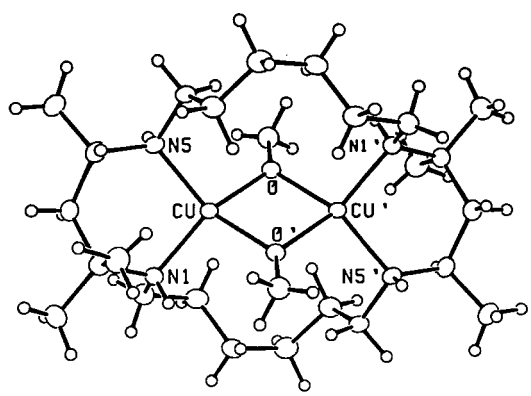

Figure 1. A perspective view of $[Cu_2L(OCH_3)_2]^{2+}$. A crystallographic center of symmetry is located at the midpoint of the line connecting two copper atoms. Bond lengths: Cu-Cu', 3.034(1); Cu-O, 1.952(2); Cu-O', 1.938(2); Cu-N(1), 2.006(2); Cu-N(5), 2.018(3)Å. Bond angles: Cu-O-Cu', 102.50(8); O-Cu-O', 77.50(8)°.

V-H-2 Crystal Structure of Tetrakis(trimethylsilyl)ethylene at −70° C

Hideki SAKURAI,* Yasuhiro NAKADAIRA,* Hiromi TOBITA,* Tasuku ITO, Koshiro TORIUMI, and Haruko ITO *(*Tohoku Univ.)*

[*J. Am. Chem. Soc.*, **104**, 300 (1982)]

An X-ray crystal structure determination at −70°C of tetrakis(trimethylsilyl)ethylene [monoclinic; space group $P2_1/n$; a = 17.841(3); b = 12.432(2); c = 9.598(1) Å; β = 92.88(1)°; Z = 4; final R = 0.045] revealed several unusual features for the very crowded olefin. The double bond is twisted by 29.5° with significant bond lengthening to 1.368(3) Å due to overcrowding. The Si-C(sp^2) bond is also lengthened to a rather unusual value of 1.915(4) Å. The olefin shows reversible thermochromism which may be related to temperature dependent variable nonplaner distortions around the double bond.

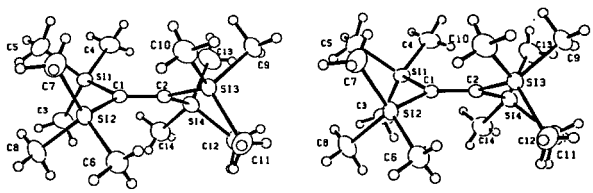

Figure 1. Stereoscopic view of the molecular structure of tetrakis(trimethylsilyl)ethylene at −70°C.

V-H-3 Mechanisms for a Chiral Recongnition of a Prochiral Center and for Asymmetric Induction in Asymmetric Synthesis of Amino Acids Using Chiral Co(III) Complexes — Crystal Structure of (−)$_{546}$-(α-Amino-α-methylmalonate) ((6*R*,8*R*)-6,8-Dimethyl-2,5,9,12-tetraazatridecane)cobalt(III) Bromide Trihydrate

Shigenobu YANO,* Morio YASHIRO,* Masanobu AJIOKA,* Sadao YOSHIKAWA,* Koshiro TORIUMI, and Tasuku ITO *(*Univ. of Tokyo)*

Recently we have developed an asymmetric synthesis of α-amino acids by using Co(III) complexes with (6*R*,8*R*)-6,8-dimethyl-2,5,9,12-tetraazatridecane (hereafter abbreviated as 1,5*R*,7*R*,11-Me$_4$-2,3,2-tet).[1] α-Amino-α-methylmalonic acid ($AMMH_2$) which has a prochiral center was used as an intermediary compound for synthesis of alanine. It reacted with the *trans*-dichloro complex to give

$(-)_{546}$-[Co(AMM) (1,5*R*,7*R*,11-Me_4-2,3,2,tet)]$^+$ stereospecifically. Decarboxylation of the AMM complex resulted in 83% *R*-alaninate and 17% *S*-alaninate. To elucidate machanisms for chiral recognition and for asymmetric induction we undertook an X-ray structure determination of the title AMM complex. Crystals of the compound are orthorhombic, space group $P2_12_12_1$, a = 14.041(2), b = 16.158(2), c = 9.997(1) Å, and Z = 4. The structure has been solved and refined to R = 0.051. The complex has the Λ-β_2-*S* geometry with the pro-*R* carboxyl group of the AMM (Figure). A hydrogen bond between

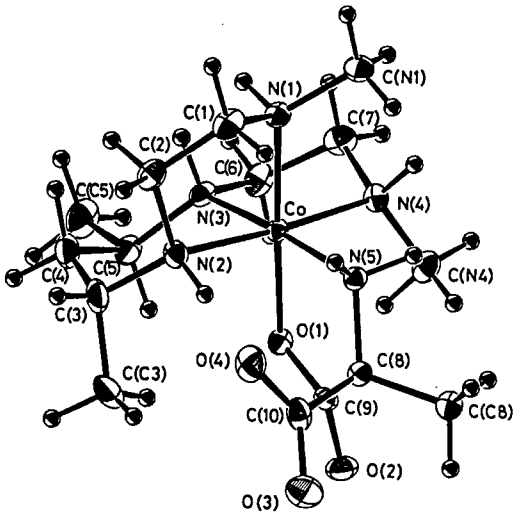

one carboxylate group of the AMM and the proton on a secondary nitrogen (N2) of the tetramine operates as is in the AMM complex with a trien derivative.[2] The present system provides an example of specific differentiation between prochiral functional groups which is commonly observed in enzyme reactions. The pro-*R* configuration of the AMM suggests that decarboxylation occurs mainly with retention of asymmetric carbon center.

References

1) M. Ajioka, S. Yano, K. Matsuda, and S. Yoshikawa, *J. Am. Chem. Soc.*, **103**, 2459 (1981).
2) J. P. Glusker, H. L. Carrell, R. Job, and T. C. Bruice, *J. Am. Chem. Soc.*, **96**, 5741 (1974).

V-H-4 Isolation and Characterization of Nickel(II) Complexes with N-Glycoside Ligands Derived from Amino Sugars

Shigenobu YANO,* Yuichi SAKAI,* Sadao YOSHIKAWA,* Koshiro TORIUMI, Haruko ITO, and Tasuku ITO *(*Univ of Tokyo)*

2-Amino-2-deoxyaldoses are combined in many polysaccharides and mucopolysaccharides of microbiological and animal origin, where they play an important role in physiological processes. Despite a wide interest in complexes with amino sugars, isolation of any transition metal complexes containing amino sugar moieties has not yet been reported. We recently found that monosaccharides reacted with $[Ni(en)_3]^{2+}$ to give octahedral Ni(II) complexes with N-glycosides.[1]

We have applied the similar method to the synthesis of Ni(II) complexes with amino sugar residues. The hydrochloride salts of *D*-glucosamine, *D*-galactosamine, or *D*-mannosamine reacted with $[Ni(en)_3]^{2+}$ to yield Ni(II) complexes. The compounds have been characterized by elemental analyses, magnetic susceptibilities, electronic absorption, and circular dichroism spectra. To elucidate the detailed stereochemistry of this system, we have undertaken an X-ray structure determination of the *D*-glucosamine complex $[Ni(D\text{-N-gl-en})_2]Br_2 \cdot 4H_2O$. Crystals of the compound are orthorhombic, space group $P2_12_12_1$, a = 16.461(2), b = 23.371(3), c = 15.965(3) A, and Z = 4. The structure was solved by the direct method to give an R value of 0.052 for 4102 observed reflexions. The geometry around the nickel atom is distorted octahedron with two N-glycosides being tridentate (Figure). One nitrogen atom of en binds to carbon 1 of sugar. The pyranose ring of sugar is in the $^4C_1$ form. This crystal structure suggests that some of the coordination pattern of aldoses are predictable.

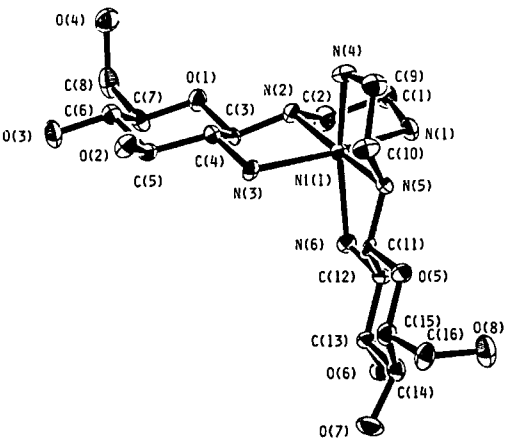

Reference

1) S. Tokizawa, H. Sugita, S. Yano, and S. Yoshikawa, *J. Am. Chem. Soc.*, **102**, 7969 (1980).

V-H-5 Synthesis of (*R*)-(−)- and (*S*)-(+)-2,2'-(2, 2-Dimethyl-2-silapropane-1,3-diyl)-1, 1'-binaphthalene, an Axially Dissymmetric Organosilicon Compound

Ryoji NOYORI,*[1] Norimichi SANO,*[1] Shizuaki MURATA,*[1] Yoshio OKAMOTO,*[2] Heimei YUKI,*[2] and Tasuku ITO (*[1]*Nagoya Univ.*; *[2]*Osaka Univ.*)

[*Tetrahedron Lett.*, **23**, 2969 (1982)]

The first, expeditious synthesis of an axially dissymmetric organosilicon compound is disclosed. Synthesis of a racemate of the title compound followed by optical resolution with a chiral poly(triphenylmethyl methacrylate) column has led to the both enantiomers in optically pure form. The structure including the absolute configration has been established by spectroscopic and single crystal X-ray diffraction methods.

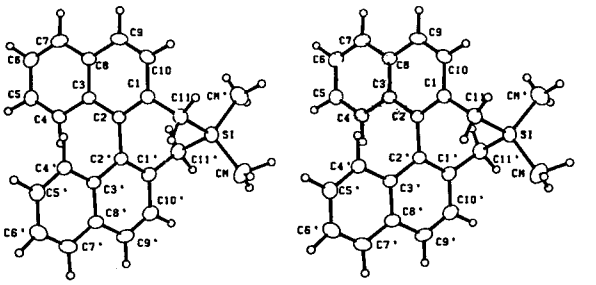

Figure 1. Stereoscopic view of the structure.

V—I The Electronic Structures of Transition-metal Cyanide Complexes

Transition-metal ions have long been known to form cyanide complexes of various symmetries, O_h, D_{4h}, T_d, and $D_{\infty h}$. Their electronic structures are of particular interest from both experimental and theoretical points of view, because the cyano ligand are capable of both donating σ electrons to the metal ion and accepting π electrons from the metal $d\pi$ orbital. The complexes have been the subject of extensive experimental studies in relation to the electronic structures in the ground and excited states, while theoretical approaches to the electronic structures have been carried out in terms of the Wolfsberg-Helmholz method by many workers. However, the detailed electronic structure, orbital interaction, charge distribution, etc., are left unknown. The present project is to study the electronic structures of transition-metal cyanide complexes by means of the MO theory.

V-I-1 An *Ab Initio* Calculation of the Electronic Structure of the $[Co(CN)_6]^{3-}$ Ion

Mitsuru SANO (*Nagoya Univ.*), **Yasuyo HATANO** (*Nagoya Univ.*), **Hiroshi KASHIWAGI, and Hideo YAMATERA** (*Nagoya Univ. and IMS*)

[*Bull. Chem. Soc. Japan*, **54**, 1523 (1981)]

Ab initio LCAO MO SCF calculations were carried out on $[Co(CN)_6]^{3-}$. Figure 1 shows the map of the electron-density difference between $[Co(CN)_6]^{3-}$ and a system of Co^{3+} ($d\pi^6$) plus six free CN^- ions. The positive value in the region of the cobalt σ orbitals represents that the electron density is increased there by σ donation from the ligands. The decreased electron density in the $d\pi$ orbital indicates π back-donation. The increase in the cobalt charge accompanied by σ donation is larger than the decrease accompanied by π back-donation; thus the positive charge of the cobalt atom is decreasd. The map also shows that the cyanide ion is polarized by the positive charge of cobalt and that, in the carbon atom, the 2s population is decreased and the 2p population is increased. In effect, the nitrogen atom donates an electron density to the cobalt atom through the carbon atom; π back-donation from cobalt to nitrogen is of small importance in this complex. The calculated radial distribution of charge density was compared with that obtained from X-ray experiments. The calculated ionization and exciting energies showed a qualitative correspondence with

the spectra.

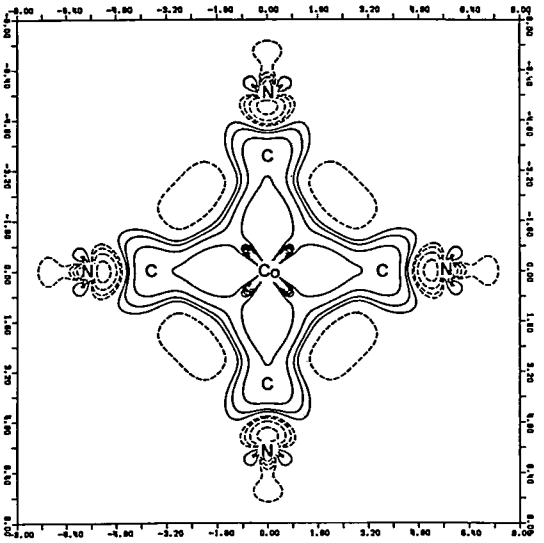

Figure 1. The electron density difference between $[Co(CN)_6]^{3-}$ and Co^{3+} (with $d\pi^6$ configuration) plus six free CN^- ions. The first solid and dotted contours show ± 0.0025 e(a.u.)$^{-3}$, respectively, and neighboring contours differ by a factor of two.

V-I-2 An *Ab Initio* MO Calculation for the Bonding Structure of $[Ni(CN)_4]^{2-}$

Mitsuru SANO *(Nagoya Univ.),* **Hiroshi KASHIWAGI, and Hideo YAMATERA** *(Nagoya Univ. and IMS)*

[*Bull. Chem. Soc. Japan*, **55**, 750 (1982)]

An *ab initio* MO computation of $[Ni(CN)_4]^{2-}$ has been undertaken to clarify the metal-cyanide bonding structure in $[Ni(CN)_4]^{2-}$ and the electronic change occurring on the coordination of CN^- to Ni^{2+} on the basis of the MO contours and the electron-density maps. Figure 1 shows the maps (for xy and xz planes) of the electron density difference between $[Ni(CN)_4]^{2-}$ and a system of Ni^{2+} (d^8 configuration with an unfilled $d_{x^2-y^2}$ orbital) and $(CN^-)_4$. The decrease of the electron density in the nickel d_{xy} region results from π back-donation. This π back-donation increases the nitrogen π_x and π_y populations by the combination of 1π-$d\pi$-2π (Figure 1a). As can be seen from the decrease in the d_{xy} electron density, the extent of π back-donation from d_{xy} is as large as that in $[Fe(CN)_6]^{4-}$ and is larger than that in $[Co(CN)_6]^{3-}$.[1,2] There is no indication of the decrease in electron density in the

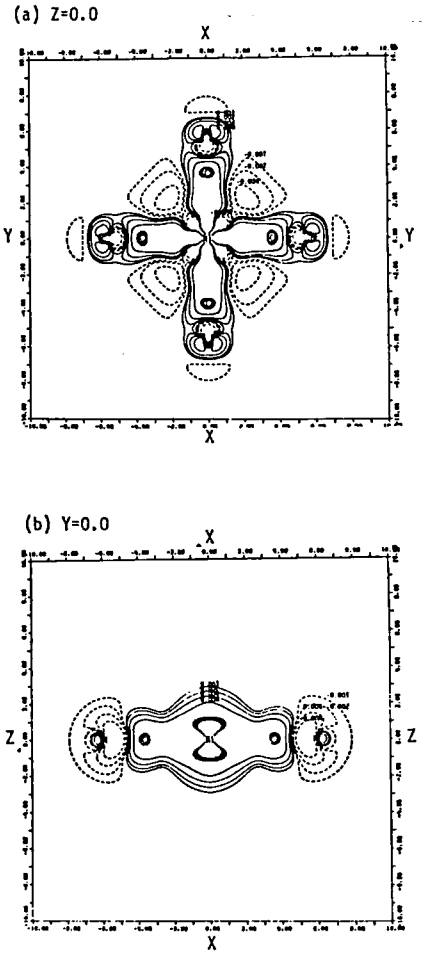

Figure 1. The electron density difference between $[Ni(CN)_4]^{2-}$ and a cluster of Ni^{2+} (d^8 configuration with unfilled $d_{x^2-y^2}$ orbital) and $(CN^-)_4$: (a) on the xy plane and (b) on the xz plane. The first solid and dotted contours show ± 0.001 e(a.u.)$^{-3}$, respectively, and neighboring contours differ by a factor of two.

region of d_{zx} (Figure 1b), suggesting little π back-donation from d_{yz} and d_{zx}.

References

1) M. Sano, Y. Hatano, H. Kashiwagi, and H. Yamatera, *Bull. Chem. Soc. Japan*, **54**, 1523 (1981).
2) M. Sano, H. Kashiwagi, and H. Yamatera, *Inorg. Chem.*, in press.

V-I-3 The DV-Xα MO Study of the Electronic Structures of $[M(CN)_6]^{3-}$ (M = Cr, Mn, Fe, and Co) and $[Fe(CN)_6]^{4-}$

Mitsuru SANO *(Nagoya Univ.),* **Hirohiko ADACHI** *(Osaka Univ.),* **and Hideo YAMATERA** *(Nagoya Univ. and IMS)*

[*Bull. Chem. Soc. Japan*, **54**, 2898 (1981)]

The discrete-variational Xα (DV-Xα) calculations are made on the hexacyano transition-metal complexes, $[M(CN)_6]^{3-}$ (M = Cr, Mn, Fe, and Co) and $[Fe(CN)_6]^{4-}$ in order to obtain a deeper understanding of the coordinate bond by comparing the electronic structures of a series hexacyano complexes. The difference between the N1s and C1s orbital energies of the complexes showed a trend similar to that observed in the X-ray photoelectron spectra. The 3d Mulliken population increases from 1.28 to 1.89 with the increase in the carbon-to-metal σ donation in going from Cr^{3+} to Co^{3+}. The 3dπ population, of course, increases with the increase in the atomic number; the net population of 3dπ, however, is lower than the formal population, and the deficiency increases from 0.12 to 0.52, showing an increase in the π back-donation with an increase in the atomic number. The C2s and C2pσ populations decrease from 1.28 and 1.15 (for Cr) to 1.20 and 1.10 (for Co) respectively with an increase in the σ donation from C to metal, while the C2pπ population remains approximately constant. The N population remains unchanged for 2s, slightly decreases for 2pσ, and increases for 2pπ, in going from Cr to Co.

V-I-4 The Electronic Structures of Linear Dicyano Complexes

Mitsuru SANO *(Nagoya Univ.)*, **Hirohiko ADACHI** *(Osaka Univ.)*, **and Hideo YAMATERA** *(Nagoya Univ. and IMS)*

[*Bull. Chem. Soc. Japan*, **55**, 1022 (1982)]

MO calculations in the DV-Xα scheme have been made on linear dicyano complexes, $[Ag(CN)_2]^-$, $[Au(CN)_2]^-$, and $[Hg(CN)_2]$ to clarify their electronic structures. The main features of the NC-M-CN bonding were deduced from the calculated overlap populations, MO contours, and energy-level diagrams. The greatest contribution to the stabilization of the complexes is made by the bonding interaction of the metal dσ orbital and the (4σ+5σ)-type ligand orbital (dominantly consisting of the C2s and C2p orbitals); the (dσ+s)-type mixing of the (n+1)s with the ndσ orbital also occurs to add a minor contribution to the stabilization of the M-C bond. On the other hand, the (dσ−s)-type metal orbitals interact with the (5σ−4σ)-type ligand orbital (dominantly consisting of the N2p orbital) to form an antibonding orbital, in which the (n+1)s orbital is considerably mixed with the ndσ orbital to reduce the antibonding character of the orbital. The situation mentioned above is in contrast to Orgel's simplified theory,[1] according to which the dσ-s orbital is stablized while the destablized dσ+s orbital is empty.

Reference

1) L. E. Orgel, *J. Chem. Soc.*, **1958**, 4186.

V—J The Electronic Structures of Dithiolate Complexes

The metal dithiolate compounds, such as *cis*-1,2-dicyano-1,2-ethenedithiolate (maleonitriledithiolate, mnt), have been of great interest to inorganic chemists because of their remarkable oxidation-reduction behavior, including the formation of abnormal oxidation states of the metal. For example, nickel forms complexes such as $[Ni(mnt)_2]$, $[Ni(mnt)_2]^-$, and $[Ni(mnt)_2]^{2-}$. The formal oxidation state of Ni in $[Ni(mnt)_2]^-$ may be +3, on the assumption that mnt is a dinegative ion. However, the determination of the oxidation state of the metal in such a way is questionable. Experimental and computational studies were made on a series of mnt complexes including $[Ni(mnt)_2]^-$.

V-J-1 The Electronic Structures of Bis(*cis*-1,2-dicyano-1,2-ethenedithiolate)nickel Complexes

Mitsuru SANO *(Nagoya Univ.)*, **Hirohiko ADACHI** *(Osaka Univ.)*, **and Hideo YAMATERA** *(Nagoya Univ. and IMS)*

[*Bull. Chem. Soc. Japan*, **54**, 2636 (1981)]

In order to clarify the electronic structures of $[Ni(mnt)_2]^{2-}$ and $[Ni(mnt)_2]^-$, the X-ray photoelectron spectra of $[M(mnt)_2]^{2-}$ (M = Co, Ni, Cu, and Zn) and $[M(mnt)_2]^-$ (M = Fe and Ni) were

obtained in the N1s, S2s, and Ni2p regions and discrete-variational (DV) Xα MO calculations were made on $[Ni(mnt)_2]^{2-}$ and $[Ni(mnt)_2]^{-}$. Both the experimental and computational results consistently showed that the oxidation state of the nickel atom is +2 for both nickel mnt complexes and that the ligands are collectively oxidized in $[Ni(mnt)_2]^{-}$.

RESEARCH ACTIVITIES VI

COMPUTER CENTER

VI—A Theoretical Investigations of Metalloporphyrins by the *Ab Initio* SCF MO Method

Metalloporphyrins and CoF_6 complexes are interesting polyatomic systems because of their complicated electronic structure and because of their catalytic function. Heme and chlorophyll are prominently important as an active center of energy conversion processes in biological systems. In this project the electronic structure and the fundamental functions are studied for several complexes by performing *ab initio* MO computations.

VI-A-1 Reaction Center of Photosynthesis

Fumihiko HIROTA *(Shizuoka Univ.)*, **Hiroshi KASHIWAGI, Unpei NAGASHIMA and Toshikazu TAKADA** *(Chicago Univ.)*

An *ab initio* LCAO SCF MO calculation was perfomerd on the model of a chlorophyll-water system with a basis set including 169 CGTO's. The wavefunctions of the neutral, cationic and anionic states were obtained. The structure of the special pair of the system in the reaction center of photosynthesis was investigated by employing the atom-atom interaction model for intermolecular interaction,[1] where the calculated net charges in the three states were used. The obtained potential surfaces are illustrated in Figure 1. The equilibrium distance between chlorophyll planes in the cationic state was 3.7 Å in agreement with the expectation by Shipman,[2] though in the neutral state the distance was fairly large. This change makes the forward electron transfer to be more effective than the backward transfer. The energy level of the $\pi - \pi$ charge-transfer state was estimated, using the above result and including the effect of the surroundings, to be 1.7 − 2.3 eV. The possibility that the CT state works as the intermediate state for charge separation was suggested.

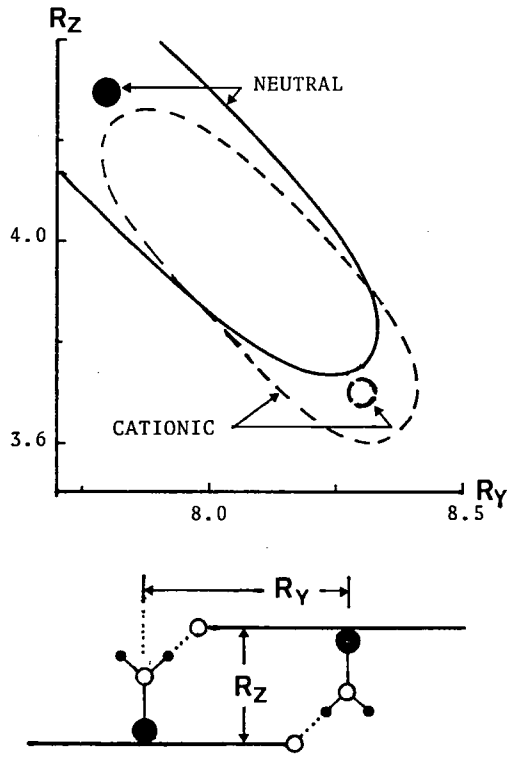

Figure 1. Potential Surface for formation of the special pair

References

1) J. Caillet and P. Claverie, *Acta Cryst.*, **A31**, 744 (1979).
2) L. L. Shipman, T. M. Cotton, J. R. Norris, and J. J. Katz, *Proc. Natl. Acad. Sci. USA.*, **73**, 1791 (1976).

VI-A-2 Theoretical Study of Charge-Transfer States of High-Spin Fe(III)-Porphyrin Complex

Shigeyoshi YAMAMOTO and Hiroshi KASHIWAGI

Ab initio calculations have been carried out on Fe(III)-porphine-pyridine-fluoride, FeP(py)F, whose molecular symmetry is C_{2v}. The main purpose of the present study is to elucidate the electronic structure of charge-transfer states corresponding to the transition from porphine π-orbitals to iron d-orbitals.

The ground state obtained by the calculation is the high-spin state $^6A_1$ $(d_{x^2-y^2})^1(d_{xz})^1(d_{yz})^1(d_{z^2})^1(d_{xy})^1$. This result agrees with observations. Since there exist the two highest occupied orbitals which consist of porphine π-orbitals and are nearly degenerate, the candidates of symmetry-allowed charge-transfer states are following.

(1) $\pi(A_1) \rightarrow d_{xz}(B_1)$ (2) $\pi(A_1) \rightarrow d_{yz}(B_2)$
(3) $\pi(A_2) \rightarrow d_{xz}(B_1)$ (4) $\pi(A_2) \rightarrow d_{yz}(B_2)$
(5) $\pi(A_1) \rightarrow d_{z^2}(A_1)$

Nozawa *et al.* observed MCD and absorption spectra of metmyoglobin fluoride (metMbF) (Figure 1, reference 1). From the shape, the MCD spectra can be regarded as Faraday A term. The origin of A term is the transition from non-degenerate ground state to doubly-degenerate excited states. Therefore, the observed spectra in Figure 1 can be assigned to coupled transitions (1) – (2) and/or (3) – (4). The calculated energy difference between these transitions is about 3kK. This is in good agreement with the energy difference between the main peak and the shoulder in the absorption spectra of Figure 1.

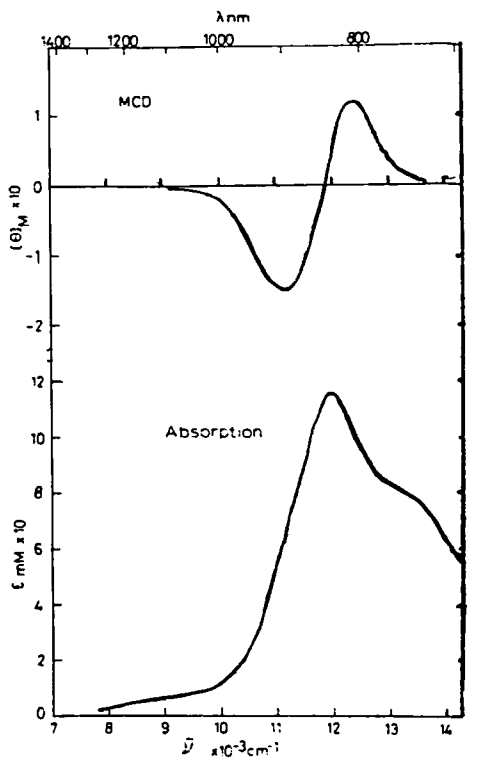

Figure 1. MCD and absorption spectra of metMbF[1].

Reference

1) T. Nozawa, T. Yamamoto, and M. Hatano, *Biochim. Biophys. Acta.*, **427**, 28 (1976).

VI-A-3 Theoretical Study of Equilibrium Co-F Bond Distance of CoF_6^{n-} Complexes (n=4, 3, and 2) in Crystals

Eisaku MIYOSHI *(Fukuoka Dental Coll.)* **and Hiroshi KASHIWAGI**

Theoretical studies on the excitation energies and the degree of covalency of the Co-F bond in the CoF_6^{n-} complexes (n=4, 3, and 2) were recently reported.[1,2] In the present research, the equilibrium Co-F bond distance and the a_{1g} vibrational frequency of CoF_6^{n-} complexes in crystals were investigated from a theoretical point of view. *Ab initio* SCF MO calculations were performed for the isolated CoF_6^{n-} complexes in order to obtain the potential energy curves against the Co-F distance. The potential energy curves were improved by considering the effects of the surrounding ions in crystals, which included the exchange energy caused by overlapping of charge clouds between ions.

For the ionic $KCoF_3$ crystal, which contains the CoF_6^{4-} complex, a considerable improvement in the equilibrium Co-F distance R_e and the a_{1g} vibrational frequency ω_e has been achieved by taking into account the potentials from the next nearest neighbor $8K^+$ ions and the next nearest neighbor 6 Co^{2+} ions, comparing with the result of the SCF calculations for the isolated CoF_6^{4-} complex, as shown in Table I. On the other hand, for the K_3CoF_6 and Cs_2CoF_6 crystals, in which the Co-F bond has some degree of covalency, the potentials from the surrounding ions affect the R_e and ω_e less than the case of the $KCoF_3$ crystal. The shape of

Table I. Equilibrium Co-F bond distance R_e and a_{1g} vibrational frequency ω_e in the $KCoF_3$ crystal.

system	R_e(Å)	ω_e(cm^{-1})
CoF_6^{4-}	2.40	202
CoF_6^{4-} + $8K^+$	2.08	436
CoF_6^{4-} + $8K^+$ + $6Co^{2+}$	2.09	504
CoF_6^{4-} + $8K^+$ + $6Co^{2+}$ + $23F^-$	2.07	513
crystal[a]	2.035	—

a) observed value for the $KCoF_3$ crystal.

the potential energy curves for these crystals are almost determined by the intramolecular interaction of the isolated CoF_6^{3-} and CoF_6^{2-} units.

References

1) E. Miyoshi, T. Takada, S. Obara, H. Kashiwagi, and K. Ohno, *Int. J. Quantum Chem.*, **19**, 451 (1981).
2) E. Miyoshi, S. Obara, T. Takada, H. Kashiwagi, and K. Ohno, *Int. J. Quantum Chem.* in press.

CHEMICAL MATERIALS CENTER

VI—B Reaction of 1-Cyanobicyclo[1.1.0]butane with Pt(II) Complexes. Isolation and Characterization of 2-[Bis(pyridine)dichloroplatina]-1-cyanobicyclo[1.1.1]-pentane

Akira MIYASHITA and Hidemasa TAKAYA

We have reported the first isolation of novel 2-platinabicyclo[1.1.1.]pentane complexes from the reaction of bicyclo[1.1.0]butane with Pt(II) complexes and revealed their unique chemical behaviors.[1] This time we have examined the reaction of 1-cyanobicyclo[1.1.0]butane (**1**) with Zeise's dimer (**2**) (eq. 1 and 2). The new platinacycle complex **4** was characterized by elemental analyses and ir, ^1H, and ^{13}C NMR spectra. Products derived from the reductive decomposition of **4** with $LiAlH_4$ and $LiAlD_4$ were also examined. The substituent effects on the mode of the reactions and the stability of the complex **4** have been discussed.

Reference

1) A. Miyashita, M. Takahashi, and H. Takaya, *J. Am. Chem. Soc.*, **103**, 6257 (1981).

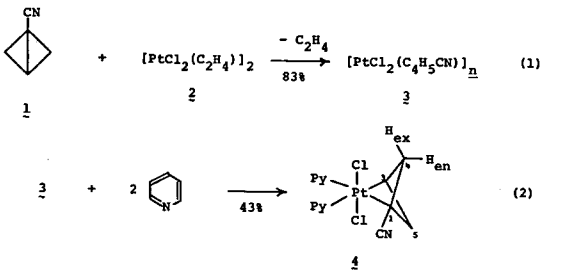

INSTRUMENT CENTER

VI—C Intramolecular Electronic Relaxation and Photochemical Reaction in Organic Compounds

A study of the vapor-phase fluorescence characteristics especially under a collision-free condition allows us to examine the nature of the intramolecular electronic relaxation. Azabenzenes such as pyridine, pyrazine and pyrimidine are the molecules of special significance in view of a dynamical aspect of the electronic structure in the excited state. The present study is designed for the two problems of the azabenzenes; (1) variation of the intramolecular non-radiative decay rate upon excitation into different vibronic levels in the S_1 vibrational manifolds; and (2) dynamical aspects of the intramolecular photoisomerization that occurs in the S_2 excitation. The final goal is to get a general picture of the intramolecular photoisomerization of azabenzenes in relation to the third channel problem of the parent hydrocarbon, benzene.

VI-C-1 Subnanosecond Fluorescence Lifetimes of Pyrazine-h_4 and -d_4 Vapor for Photoselected Vibrational Levels in the $S_1(n, \pi^*)$ State

Iwao YAMAZAKI, Toshiro MURAO, and Keitaro YOSHIHARA

[*Chem. Phys. Lett.*, **87**, 384 (1982)]

Subnanosecond fluorescence decays of pyrazine-h_4 and -d_4 vapor were measured by exciting selected vibrational levels in the $S_1(n, \pi^*)$ state. A combination of a synchronously pumped, cavity-dumped dye laser and a time correlated photon-counting system was used and enabled us to measure the lifetime down to ~10 ps.[1] The lifetime values for pyrazine-h_4 are shown in Figure 1, along with the $S_1 - S_0$ absorption spectrum. The fluorescence lifetime is significantly long for the vibronic levels involving the non-totally symmetric ν_{10a} vibration. By reference to the quantum yields of fluorescence and intersystem crossing,[2] the radiative (k_F) and intersystem crossing (k_{ISC}) rate constants are derived. It is found that k_F's for $10a^n$ (n = 1, 2 and 3) levels are increased owing to a strong vibronic coupling between S_1 and S_2 through ν_{10a} vibration. On the other hand, k_{ISC} for these levels are fairly small, indicating that the Franck-Condon overlap integral is small resulting from a distortion of the S_1 potential.

References

1) T. Murao, I. Yamazaki, and K. Yoshihara, *J. Spectrosc. Soc. Japan* **31**, 96 (1982).
2) I. Yamazaki, M. Fujita, and H. Baba, *Chem. Phys.*, **57**, 431 (1981).

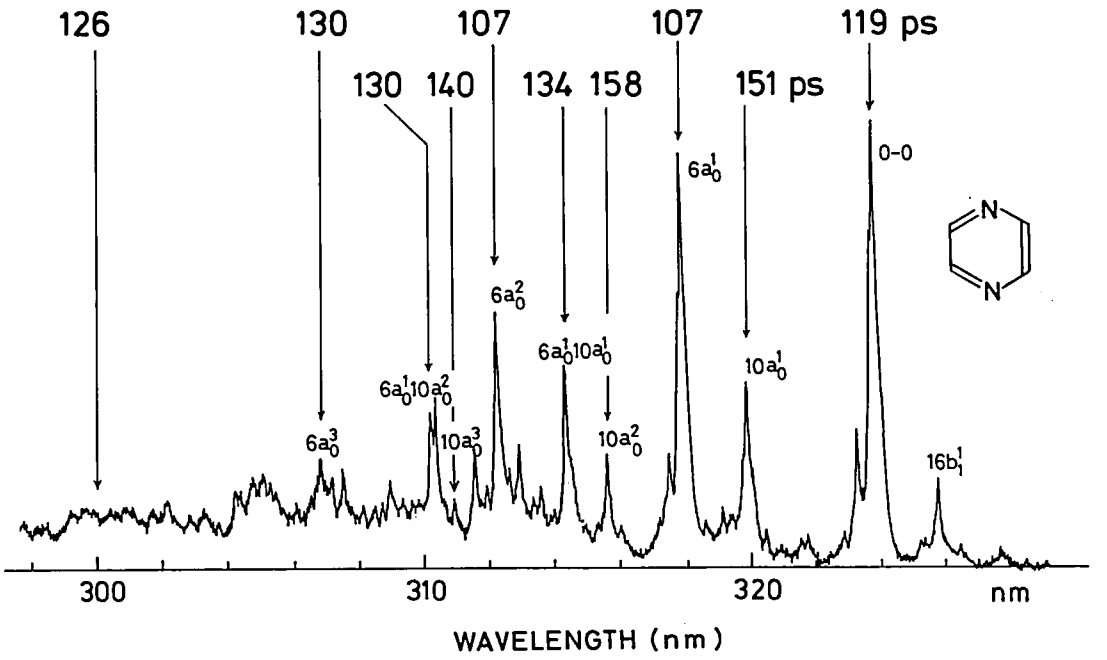

Figure 1. Fluorescence lifetimes and $S_1(n, \pi^*) - S_0$ absorption spectrum of pyrazine-h_4 vapor, in the presence of SF_6 100 Torr.

VI-C-2 Picosecond Fluorescence Decays from Vibrational Levels in the $S_1(n, \pi^*)$ State of Pyridine Vapor

Iwao YAMAZAKI, Toshiro MURAO, Keitaro YOSHIHARA, Masahisa FUJITA *(Hokkaido Univ.)*, **Kazuyoshi SUSHIDA** *(Hokkaido Univ.)*, **and Hiroaki BABA** *(Hokkaido Univ.)*

[*Chem. Phys. Lett.*, **92**, 421 (1982).]

For the simplest azabenzene, pyridine, insufficient data have been obtained to allow discussion as to the intramolecular electronic relaxation. In this study, fluorescence lifetimes of pyridine vapor were measured by exciting at various vibrational bands

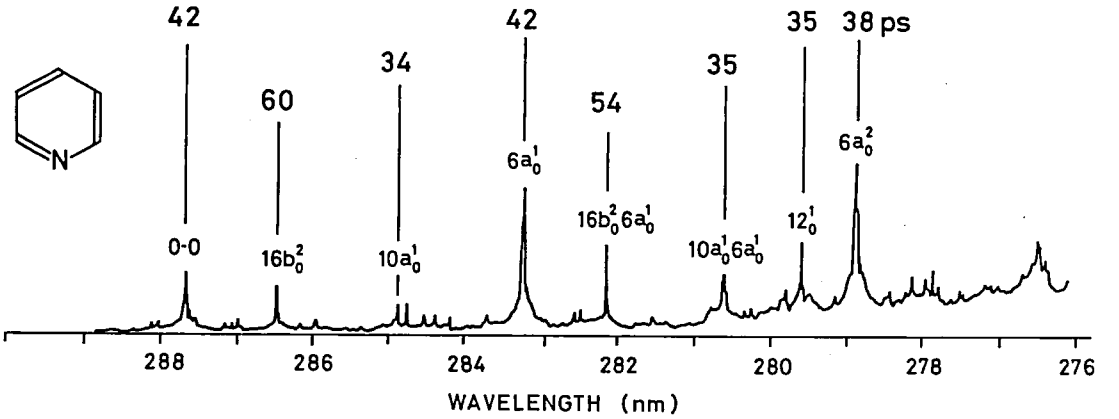

Figure 1. $S_1(n, \pi^*) \leftarrow S_0$ absorption spectrum of pyridine vapor obtained with an excitation bandwidth of 0.5 cm^{-1}. The values of fluorescence lifetimes (ps) are shown above the absorption bands at which the sample is excited.

in the lower energy region of $S_1(n, \pi^*) \leftarrow S_0$ transition. The lifetime (Figure 1) varies between 35 – 60 ps, depending on the vibronic level excited. The lifetime for the vibrational levels involving ν_{16b} (out-of-plane CC bending), *i.e.* $16b^2$ and $16b^26a^1$, are 1.3 – 1.4 times as large as that for the zero-point vibrational level, while those for levels involving ν_{10a} (out-of-plane CH bending), *i.e.*, $10a^1$ and $10a^16a^1$ are fairly small. It is found that the non-radiative decay from S_1 in pyridine is characterized by a particularly fast $S_1 \rightarrow S_0$ internal conversion. This is in marked contrast to other azabenzenes such as pyrazine and pyrimidine. With respect to the fluorescence decay kinetics, we reached a conclusion that pyridine cannot behave as an "intermediate case" molecule.

VI-C-3 Fast Non-Radiative Decay Channel and Intramolecular Photoisomerization of Pyrazine Vapor

Iwao YAMAZAKI, Toshiro MURAO, Takaya YAMANAKA, and Tomoko YAMAZAKI

[*Faraday Discuss. Chem.* Soc., in press]

For pyrazine vapor under a collision-free condition, quantum yields of the fluorescence and the intersystem crossing have been measured as a function of the excitation energy ranging from the zero-point level of $S_1(n, \pi^*)$ to the higher vibrational levels of $S_2(\pi, \pi^*)$. The fluorescence lifetimes in ps and ns time scale were also measured

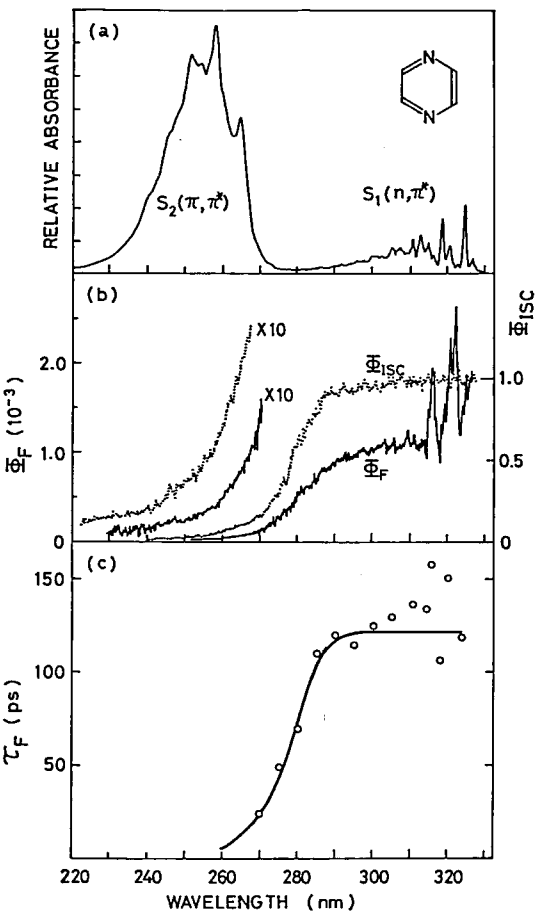

Figure 1. (a) Absorption spectrum, (b) quantum yield spectra of fluorescence (solid line) and intersystem crossing (dotted line), and (c) variation of fluorescence lifetime, for pyrazine vapor (1 Torr) in the presence of SF_6 (50 Torr).

by exciting the molecules at various wavelengths. The results are shown in Figure 1. New dynamical aspects of the intramolecular electronic relaxation

were found: (1) There exists an energy threshold in which a particularly fast non-radiative channel ($10^{11}s^{-1}$) opens; and (2) in the excitation energy of $S_2 \leftarrow S_0$ transition region, this decay channel is predominant, whereas in the $S_1 \leftarrow S_0$ region the radiationless transition is governed by the inter-system crossing to the triplet state. The fast non-radiative channel may probably be an intramolecular photoisomerization process. Discussion is made in relation to the third channel problem of the parent hydrocarbon, benzene.

VI—D Picosecond Time-Resolved Fluorescence Spectroscopy of Photosynthetic Organisms

Iwao YAMAZAKI, Toshiro MURAO, Keitaro YOSHIHARA, Mamoru MIMURO *(NIBB)*, **and Yoshihiko FUJITA** *(NIBB)*

[*Photochem. Photobiol.*, in press]

Photosynthetic organisms have evolved a light harvesting antenna system for light absorption and energy transfer to the reaction center. In blue-green and red algae, the system consists of phycobiliproteins and chlorophyll *a*; the former forms an aggregate, phycobilisome, on the surface of thylakoid membrane, and the latter is derectly connected to the reaction center. The light energy absorbed by phycobiliproteins is transferred to the reaction center in thylakoid membrane. In the course of energy transfer processes, fluorescence is emitted from each pigment, and is used as a probe of the energy transfer.

The present study has been initiated with purposes of getting detail information on the energy transfer processes by means of a time-resolved spectroscopic technique.[1] Figure 1 shows a typical example of time-resolved fluorescence spectra for *Porphyridium cruentum*. The variation of the spectrum with time indicates that the photon energy initially absorbed by phycoerythrin migrates ultimately to the reaction center within 400 ps. A kinetic analyses of the spectra provides us with information on the structure of the pigment system of algae.

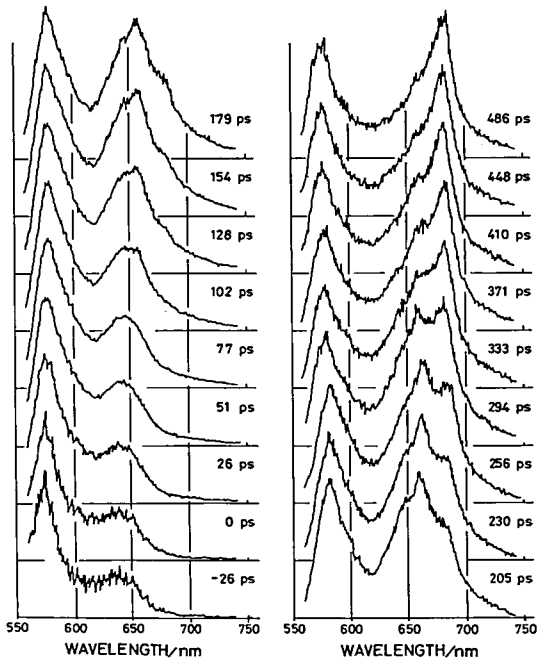

Figure 1. Time-resolved fluorescence spectra of a red alga intact cell, *Porphyridium cruentum*. The spectrum is changed successively with time. The spectrum of each pigment component appears in the order of pycoerythrin (λ_{max} = 570 nm), phycocyanin (λ_{max} = 645 nm), allophycocyanin (λ_{max} = 660 nm) and chlorophyll *a* (λ_{max} = 683 nm).

Reference

1) T. Murao, I. Yamazaki, and K. Yoshihara, *App. Opt.*, **21**, 2297 (1982)

VI—E A New Formalism of Chemical Exchange Near the Region of Intermediate Rate

Keisaku KIMURA

The Bloch equation incorporating chemical exchange between two environments is solved and is expanded in a power series of the exchange rate τ. The expansion near the fast exchange region is given by a power series in τ of which the first term corresponds to the fast exchange limit. The second term together with the first term difines the "*boundary*" intermediate exchange region. In the slow exchange region, the expansion is conducted in a power series of $1/\tau$. The conditions of convergence of the expansion of both exchange regions are examined and as a result the chemical exchange is devided into five regions (Table I): fast limit, fast intermediate, pure intermediate, slow intermediate and slow limit. In the "*pure*" intermediate region, we need a conventional simulation procedure in order to determine the exchange rate. On the other hand, we have derived an analytical form for the line width in the other regions. The line width as a function of exchange rate, transverse relaxation time, content of component species and chemical shift difference between two environments is examined in the light of the proposed formula.

Table I. Classification of Exchange Rate Region

Exchange rate region	Definition	Spectrum
Fast limit	$n < 0.01$	Single narrow resonance, the line width and the shift of which are the weighted average of the two environments.
Fast intermediate	$0.01 < n < 1$	Single broad resonance, the shifts of which is the weighted average of the two environments. The line width is broader than that of the fast limit region.
Pure intermediate	$n < 1$ and $m < 1$	Very broad single or broad double resonances
Slow intermediate	$0.01 > m > 1$	Double broad resonances, the shifts of which do not change with the environments. The line width is broader than that of the slow limit case.
Slow limit	$m < 0.01$	Two resonances, the shifts of which do not change with the environments. The line width is constant which equals to each environment.

$n = p_A p_B(\omega_A - \omega_B)^2 \tau T_2$.
$m = p_A p_B T_{2A} T_{2B}(\omega_A - \omega_B)^2/\tau\omega_{obs}$.

VI—F Electron Paramagnetic Resonance Study of Cytochrome c_3

Keisaku KIMURA and Hiroo INOKUCHI

Cytochrome c_3 is an electron carrier in *Desulfovibrio vulgaris* and is found to have four hemes in a single polypeptide chain. Electrochemical measurement shows that this molecule undergoes very fast electron exchange between electrode/solution interface. The four heme structure of cytochrome c_3 is reflected in its ESR spectra for which g-values were analyzed. It was found that four hemes have different g_x and g_z values but the same for all g_y's. From these g-tensors, two energy parameters, axial distorsion energy and rhombic distorsion energy of porphyrin skeleton are derived using Griffith theory.[1)]

In the redox titration of cytochrome c_3 molecule, NMR study has revealed that the existence of the intermediate of cytochrome c_3 in the course of reduction. Therefore ESR redox titration was conducted in order to examine whether the same state is observed in ESR spectrum or not. Ferrocytochrome c_3 is not ESR active that it is very difficult to detect the weak signal from the expected intermediate state. An unusual spectrum was observed near the region of reduced state.

Reference
1) K. Kimura and H. Inokuchi, *IMS Ann. Rev.*, 150 (1981).

VI—G Development of Experimental Devices and Techniques

The Instrument Center is equipped with various types of instruments relevant to the research fields of molecular spectroscopy, solid-state chemistry and magnetic spectroscopy. In view of efficient use of these instruments, the Center staffs attend to development of new experimental devices and techniques.

VI-G-1 Fluorescence Spectrofluorimeter with Nanosecond Time Resolution by Means of a Transient Digital Memory

Takaya YAMANAKA, Yoshio SHINDO *(Hokkaido Univ.)*, **and Iwao YAMAZAKI**

For the purpose of measuring the decay curves and the time-resolved spectra for fluorescence and phosphorescence, a spectrofluorimeter with nanosecond time resolution has been constructed. The system consists of a transient digital memory (Biomation 6500) and a microcomputer system. A schematic diagram is shown in Figure 1. The photoelectric signal associated with emission signal is recorded on the transient digital memory (1024 channels) in which the time history of emission intensity can be recorded with 2 ns/channel time resolution. The data are transferred to the computer and accumulated for successive excitations. The wavelength of the monochromator is driven under the control of the computer. After a series of rise and decay curve measurements at various wavelengths, time-resolved spectra are obtained for the minimum time difference of 2 ns. All these measurements and data processing are performed automatically with the aid of the computer. This system is applicable to the time-dependent molecular spectroscopy and the molecular dynamics in photochemical reactions.

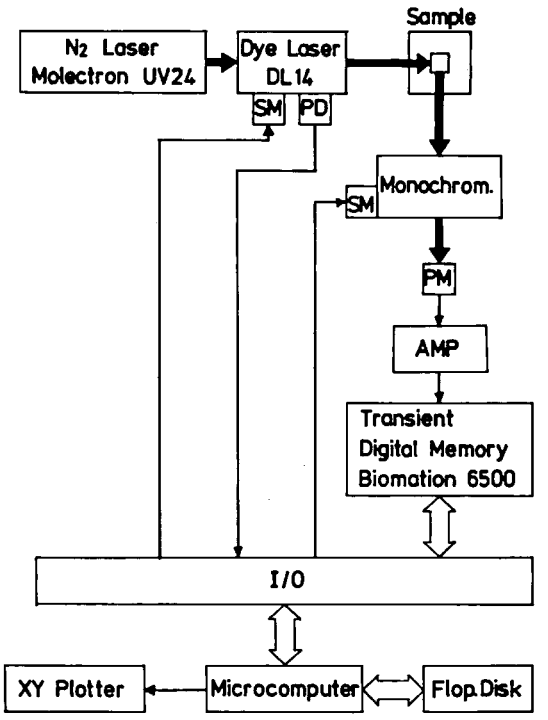

Figure 1. Schematic diagram of the spectrofluorimeter. PD, photodiode; SM, stepping motor; PM, photomultiplier.

VI-G-2 Apparatus for the Preparation of Finely Dispersed Particles

Keisaku KIMURA and Shunji BANDOW

A gas evaporation method is one of the useful technique for making ultra fine particles in which we expect different physical properties from the bulk state. It is conventionally engaged to evaporate materials onto the metal wall such as stainless steel or copper following the collection of it by brushing. By this method, however the surface of the particles stick each other forming chained particles. It is thus sometimes pointed out that the chain formation of the fine particles obscures the true characteristics of the fine particles due to size effect and/or surface effect. In order to avoide this problem, the actual particles must be coated with the stable chemical species. Dispersion of fine particles or the matrix isolation method is the promising technique to overcome this problem.

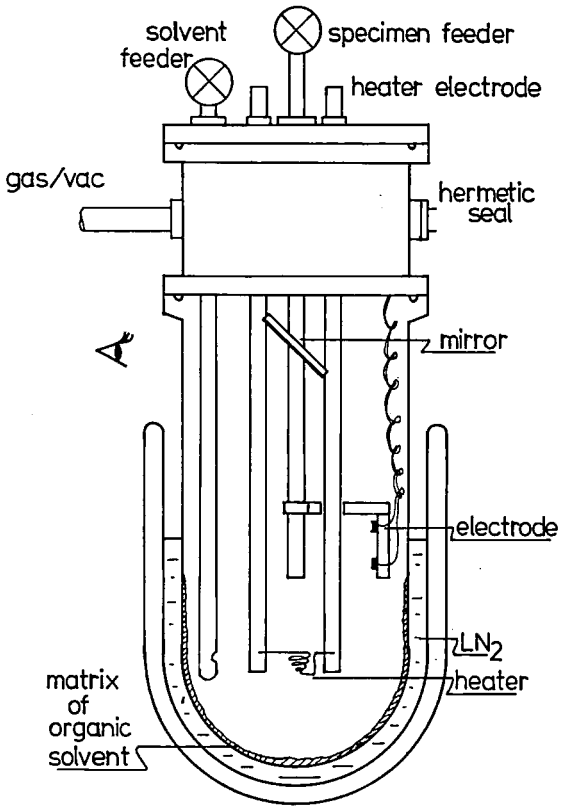

Figure 1 shows glass apparatus which is the modification of those reported by Wada.[1] Mirror enables us to monitor the condition of heater and melting sample. Conductivity measurement plate supplies the data of the thickness of the deposited fine particles. By this contrivance, we can avoide the sticking of fine particles. Other apparatus which traps the fine particles directry into liquid phase is also designed and constructed by us.

Reference

1) N. Wada, *J. Phys.* C-2, suppl. 7 (1977).

LOW TEMPERATURE CENTER

VI—H Physical Chemistry of Polyvalence Compounds

VI-H-1 Synthesis and ESR Study of Tetrabenzopentacence-Cesium Complexes

Kenichi IMAEDA, Toshiaki ENOKI, Hiroo INOKUCHI, Junji AOKI *(Toho Univ.)*, **and Satoshi IWASHIMA** *(Meisei Univ.)*

It has been reported that nanocyclic aromatic hydrocarbon, isoviolanthrene (isoVEA), has charge transfer complex with potassium, which has various compositions isoVEA-K_x between x = 0 and 4.55.[1] Tetrabenzopentacene(TBPA) is a nonplanar nanocyclic aromatic molecule with bay structures unlike a planar molecule isoVEA. It is interesting to know what compositions TBPA-alkali metal complex has. We synthesized TBPA-Cs complexes and investigated their magnetic properties.

TBPA-Cs complexes were prepared by using a double furnance and we found that they had three phases of TBPA-$Cs_{0.6}$(I), TBPA-$Cs_{1.1}$(II) and TBPA-$Cs_{2.4}$(III). The correlation between the linewidth ΔH of ESR and cesium concentrations is shown in Figure 1. ΔH is considered to be caused mainly by dipole-dipole interactions among electron spins on TBPA molecules. The spin concentration of the complexes increases as the raising of cesium concentration. In the phase (I), ΔH is narrow due to weak interaction as there exists one spin per two TBPA molecules. In the phase (II), ΔH becomes broad with increasing this interaction because a TBPA molecule has one spin. In the phase (III), ΔH begins to be narrow by the effect of spin-spin exchange interaction because a TBPA molecule has about two spins.

Reference

1) N. D. Parkyns and A. R. Ubbelohde, *J. Chem. Soc.*, **1961**, 2110.

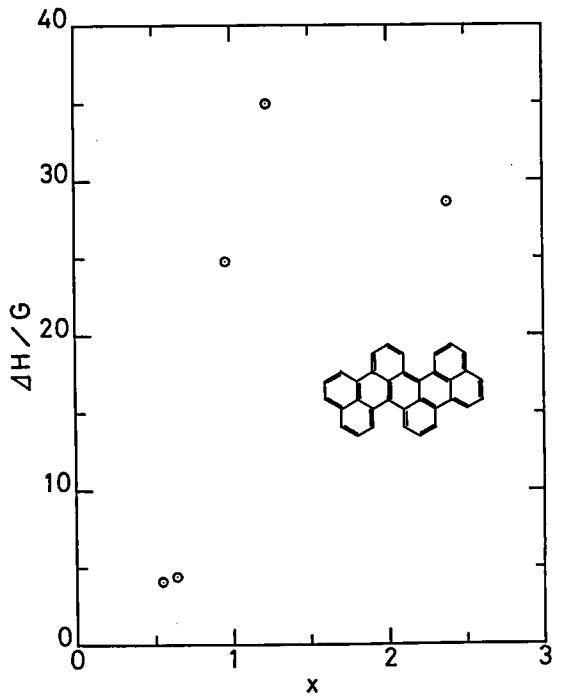

Figure 1. Linewidth for various cesium concentrations of TBPA-Cs_x complexes at 295K. The inset illustrates the molecular structure of TBPA.

VI-H-2 Electron Spin Resonance of Hydrogen-Absorbed Graphite-Potassium Intercalation Compounds

Toshiaki ENOKI, Mizuka SANO *(Univ. Electro-communications)*, **and Hiroo INOKUCHI**

[*Chem. Phys. Lett.*, **86**, 285 (1982)]

The conduction electron spin resonance (CESR) of the graphite-potassium intercalation compounds, C_8K and $C_{24}K$, was studied in hydrogen gas. An enhancement of CESR absorption and a decrease in an asymmetry parameter were observed for C_8K in the initial stage of hydrogen absorption, which is attributed to paramagnetic hydrogen atoms stabilized in the matrix of the compound.

VI-H-3 Physical Properties of a Quasi One-Dimensional Conductor $Pt_6(NH_3)_{10}Cl_{10}(HSO_4)_4$: Partially Oxidized Salt of the Magnus Green Salt

Ryozo INOUE *(Kyoto Univ.)*, **Toshiaki ENOKI, and Ikuji TSUJIKAWA** *(Kyoto Univ.)*

The salt $Pt_6(NH_3)_{10}Cl_{10}(HSO_4)_4$ with the average valence of Pt 2.33 was prepared by means of partial oxidation of $[Pt(NH_3)_4][PtCl_4]$. The electrical conductivity σ has a maximum at about 230K and a minimum at about 280K which indicate two M-I transitions. The thermal analyses by a DSC show three anomalies only on heating, G at ~150K and A at ~200K and B at ~250K. The exothermic anomaly A succeeding to the weak anomaly G indicates that a glass transition takes place, which is supported by a.c. calorimetry. The endothermic anomaly B corresponds to a structural transition. The result by adiabatic calorimetry at low temperatures is expressed as $C(T) = \delta T + \beta T^3$. The β value leads to the Debye temperature of 188K and the presence of the T-linear term also supports the glassy state. The results of X-ray powder patterns at low temperatures are given. The M-I transitions are discussed.

EQUIPMENT DEVELOPMENT CENTER

VI—I Fine Engineering for the Construction of He-Gas Flow Cryostat

Toshio HORIGOME, Kusuo SAKAI, and Tadaoki MITANI

By making use of the technological and engineering skills present at Equipment Development Center, we have constructed helium gas flow cryostat used for optical measurements in ultra-high vacuum. Improvements in design of the temperature control system provide a clean surface of a sample necessary for the surface study, such as the photoelectron spectroscopy at low temperature. All component parts of the cryostat are manufactured from copper and stainless steel welded by the electron-beam method and the TIG welding method. The principle of design of the cryostat is illustrated in Figure 1. The coolant from a helium transfer

syphon is introduced into the separate heat exchangers through the needle valves. Temperatures of the heat exchangers are independently controlled so that the outer heat exchanger can be used as a helium cryopump during pumping procedure as well as a radiation shield for the inner heat exchanger. By this cooling method, it is easy to achieve fine temperature control of the inner heat exchanger and also to keep samples mounted in it to be free from the contamination due to the adsorption of residual gas. The cryostat has satisfied the strict requirements of cooling ability and routine leak-testing.

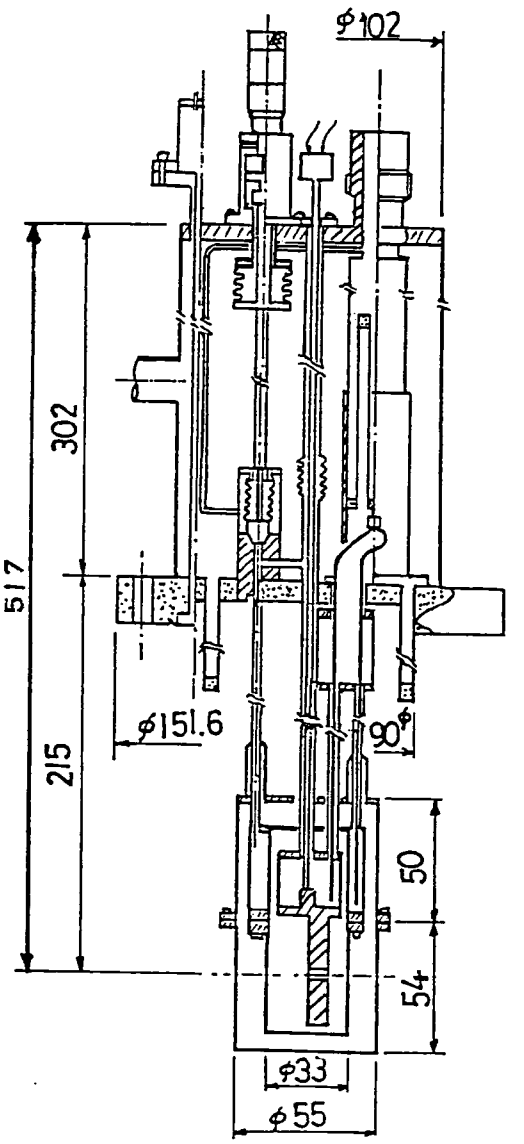

Figure 1. Sectional view of He-gas flow cryostat.

VI—J Study of Neutral-Ionic Phase Transition in Charge-Transfer Solids

Tadaoki MITANI, Yoshinori TOKURA,* Gunzi SAITO, and Takao KODA* *(*Univ. of Tokyo)*

The organic charge-transfer solid tetrathiafluvalene(TTF)·p-chloranil undergoes a phase transition from a predominantly neutral to an ionic phase with decreasing temperatures. This phase transition, which is essentially induced by thermal contraction, provides an unique oppotunity to elucidate the fluctation effect of charge density in the mixed valence compounds.

With a purpose to grow highly pure and sizable single crystals, we make an effort to improve the sublimation method instead of preparing crystals by reaction in solution. Crystals of TTF·p-chloranil and its derivatives have been grown from purified components by the modified plate sublimation method.[1] Thickness of single crystals can be controlled by the vapor pressures of each components. Typically, bulky crystals grow out up to $5 \times 3 \times 1$ mm^3 in size.

The physical properties of these crystals have been investigated with a wide variety of experiments: conductivity, photoconductivity, dielectric, optical,[2] infrared, X-ray diffraction and ESR measurements. All of the experimental data indicate that the neutral-ionic phase transition in TTF·p-chloranil takes place at a well-defined critical temperature, $T_c = 84$K. For example, we show the temperature dependence of the spin susceptibility obtained by the ESR measurements in Figure 1. Below T_c, paramagnetic spins are additionally induced. It should be noted here that the induced spin density is much smaller than the theoretically predicted values.[3] These behaviours can be account for by a formation of soliton kinks induced by lattice dimerizations at the phase transition.

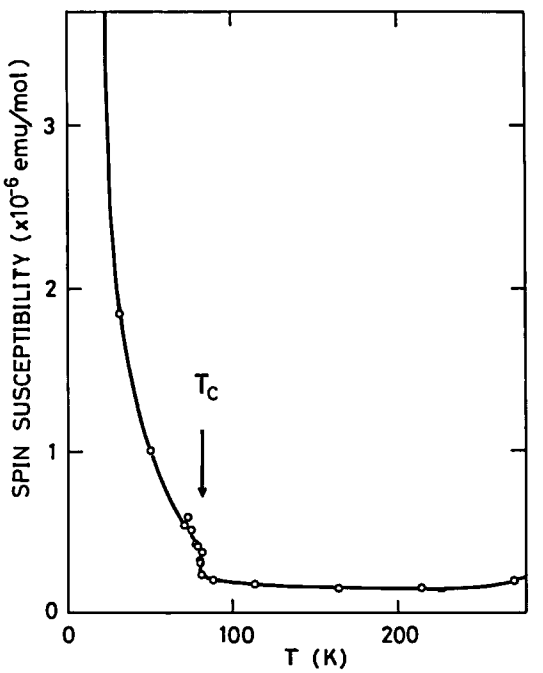

Figure 1. Temperatufe dependence of spin susceptibility for TTF·p-chloranil single crystals.

References

1) N. Karl, in Crystals, Growth, Properties and Applications, Vol. IV (Springer, Berlin, 1980) pp.1—100.
2) Y. Tokura, T. Koda, T. Mitani, and G. Saito, *Solid State Commun.*, **43** 757 (1982).
3) P. J. Strebel, and Z. G. Soos, *J. Chem. Phys.*, **53** 4077 (1970).

VI—K Fast Transient Digitizer System Using a TV Camera for the Measurement of Optically Induced Spin Polarization

Yoshihiro TAKAGI

[*Rev. Sci. Instrum.*, in press]

A fast digitizer for single transient analysis has been developed which is composed of a microcomputer-based image processor and an ordinary TV camera attached to an 1 GHz oscilloscope. It functions first as an equivalent storage oscilloscope which latches a fast single transient signal. Temporal resolution of the system is limited only by the bandwidth of the oscilloscope used. Using a fast oscilloscope (TEKTRONIKS 7104) having a bright screen we latched subnanosecond single transient. The second funcition is an averaging of successively latched signals.

The image processor consists of two NIM modules: one contains a circuit for the data-acquisition, while the other includes five circuit boards: for CPU and address decoders, 8-kbyte ROM, 16-kbyte RAM, parallel I/O ports, and a video controller. The CPU prepares some conditions prior to data acquisition, corrects and accumulates raw data. The software is written in the 8-kbyte ROM in machine language.

The combination of oscilloscope — TV camera — image processor was arranged as an experimental system for the observation of laser-induced spin polarization in paramagnetic materials. By the use of the second function of this instrument we overcame law signal-to-noise ratio due to strong radio frequency noises and found clear signals of the optically induced magnetizations in about 50 species of transition metal complexes in solution. The spin-lattice relaxation time of most of these materials at room temperature was of the order of 1 ns. Detail of the study on the spin-lattice relaxation and some interesting results will be published elsewhere.

VI—L Laser-Induced Magnetization in Transition Metal Complex Ions and Aromatic Molecules

Yoshihiro TAKAGI

Transient behavior of laser-induced spin polarization in transition metal complex ions and aromatic molecules has been studied by using a powerful picosecond laser and an effective data-aquisition technique for single transient analysis. The circularly polarized second or third-harmonic (532 or 355 nm) of a mode-locked YAG laser was used to excite these materials. A population difference in the ground state Zeeman levels can be produced as a result of the Zeeman-selective optical transition. The signal due to the magnetization was detected by a pick-up coil around the sample and a wide-band amplifier. The spin-lattice relaxation time was about 1 ns or less for most of the transition metal ions in solution ($VOSO_4$, Cr-alum, $MnSO_4$, Fe-alum, $NiSO_4$, $CuSO_4$, etc.). Some of them showed a magnetic field dependence of the spin-lattice relaxation time. For example, the spin-lattice relaxation time in $CuSO_4$ increased from less than 1 ns to 3 ns by applying a magnetic field of about 100G. This effect can be understood as a decrease of cross relaxation with increase of the magnetic field.

Creation of magnetization due to linearly polarized light in $Cr(CH_3COO)_3$ and $Cu(CH_3COO)_3$ in CH_3COOH and Fe-alum was found in aqueous solution. These compounds are known to form dimers. Therefore we assumed that the signal of the magnetization is due to the Boltzmann population difference in the triplet state. The dimer in the singlet state is excited to a higher singlet state and *via* fast intersystem crossing the population difference between three sublevels in the triplet state is produced under the magnetic field. To verify this assumption we examined some aromatic molecules having fast intersystem crossing rates. We found clear signals in benzene solution of benzophenone, benzaldehyde, and acetophenone. The decay time of the magnetization was about 1 ns or less. If the decay time corresponds directly to the life time of the

triplet state, a means of obtaining information about the triplet state or intersystem crossing is available. The details of the study will be published elsewhere.

VI—M Generation of High-Power Picosecond Tunable UV Light by Mixing of H_2 Raman with Optical Parametric Light

Yoshihiro TAKAGI, D.V.O'CONNOR, Minoru, SUMITANI, Nobuaki NAKASHIMA, and Keitaro YOSHIHARA

High-power picosecond tunable light ranging between 227 and 244 nm has been generated by using efficient frequency mixing of H_2 Raman with optical parametric light. A single pulse from a stable passively mode-locked Nd-YAG laser was amplified and split into two lines. The first line was converted to the fourth harmonic and was used to generate high-pressure (50 atm) H_2 Raman light at 299 nm. The second line was used for optical parametric oscillation. In the latter, two deuterated KDP single crystals (TYPE 2, 61° cut) were pumped by a tightly focused second-harmonic beam. As a result of efficient optical parametric oscillation and amplification in the two crystals, infrared light in the range 900 to 1350 nm (see IMS Ann. Rev. 1981) was generated. The energy of each incident beam was about 1 mJ. The conversion efficiency of mixing exceeded 20%, and the energy of the resultant UV light isolated with a dispersive prism, was 50 to 250 μJ in the wavelength range 227 − 244 nm, as shown in Figure 1.

We have obtained another tunable UV light in the shorter wavelength region (214 − 221 nm) by mixing the optical parametric light with the fourth harmonic light (266 nm). The energy was about 50 μJ. We have previously reported the generation of picosecond tunable light at 250 − 380 nm using frequency mixing of the optical parametric light with its pumping light (see IMS Ann. Rev. 1981). The present work extends the tunability of the UV light to the interesting shorter wavelength region where important photochemical reactions of organic molecules can be induced.

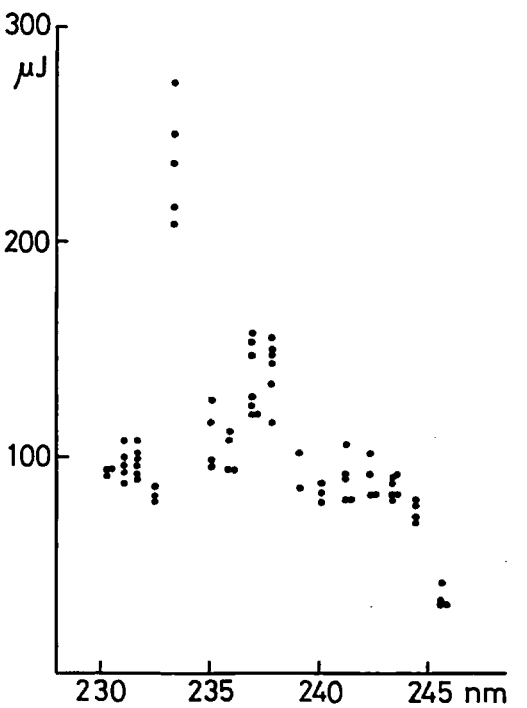

Figure 1. Wavelength dependence of the energy of tunable UV light.

ULTRAVIOLET SYNCHROTRON ORBITAL RADIATION FACILITY

VI—N Construction of UVSOR (Ultraviolet Synchrotron Orbital Radiation) Light Source

Makoto WATANABE, Toshio KASUGA, Akira UCHIDA, Osamu MATSUDO, Masami HASUMOTO, Hiromichi YAMAMOTO,* Kusuo SAKAI, Kiyoshi TAKAMI, Takeshi KATAYAMA,*** Katsuhide YOSHIDA,*** and Motohiro KIHARA,****** *(*Fukui Univ. and IMS, **Kyoto Univ., ***Univ. of Tokyo, ****Nat. Lab. High Energy Phys. and IMS)*

UVSOR light source is a 600 MeV electron storage ring dedicated to synchrotron radiation research, the injector of which is a 600 MeV synchrotron with a 15 MeV linac. In 1981, its construction was started. At present, the synchrotron is under construction. The present status of the UVSOR light source is given in "Ultraviolet Synchrotron Orbital Radiation Facility" in this issue.

VI—O Design of a Plane-Grating Monochromator

Kazuhiko SEKI *(Dept. of Molecular Assemblies)*, **Makoto WATANABE, Eiji ISHIGURO** *(Osaka City Univ.)*, **and Riso KATO** *(Kyoto Univ.)*

A vacuum-uv monochromator with two plane gratings was designed for the experiments of photoelectric

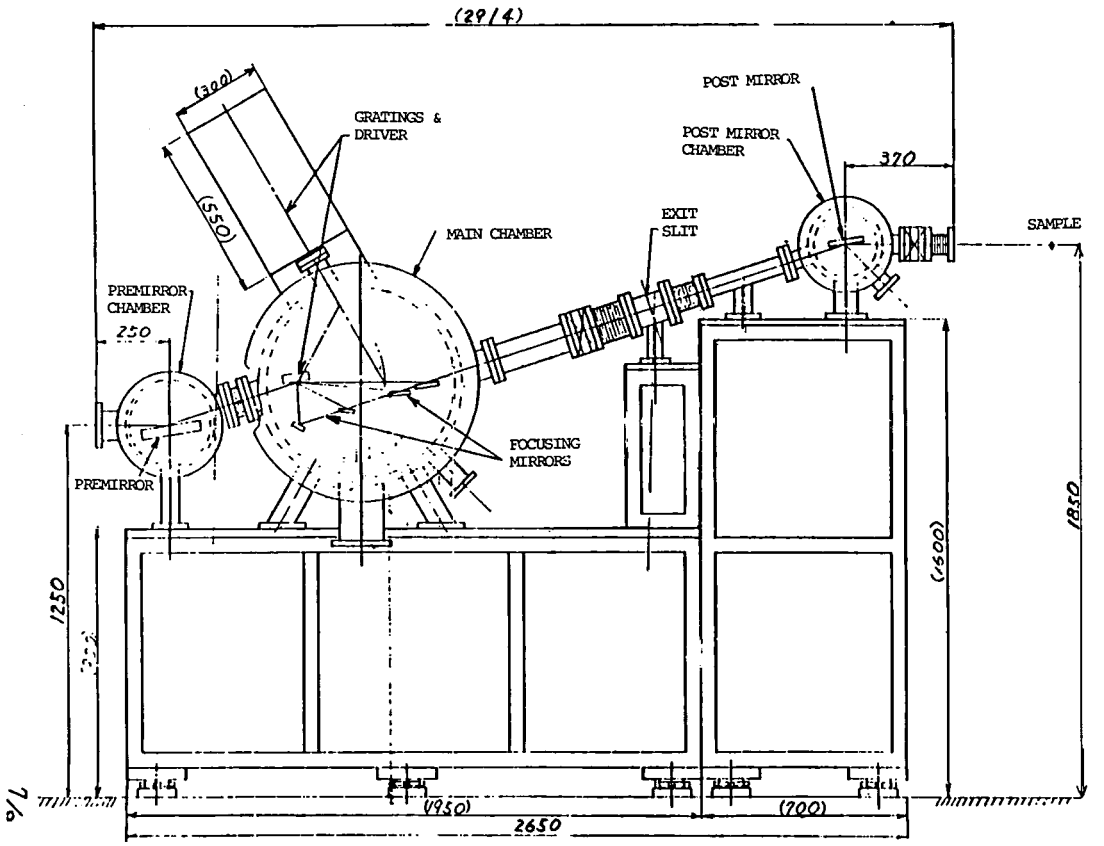

Figure 1. The plane-grating monochromator.

effects of organic and inorganic solids at the UVSOR storage ring. The principal idea of the optical design is similar to that of Miyake *et al.*,[1] Eberhardt *et al.*,[2] and Williams *et al.*,[3] with interchangeable two plane gratings and five focusing mirrors. It covers a fairly wide wavelength range of 10 − 400 nm with a resolution of 0.1 − 0.2 eV and a spot size of 1 − 2 mm diameter on the sample. A sketch of the monochromator is shown in Figure 1.

References

1) K. P. Miyake, R. Kato, and H. Yamashita, *Sci. Light*, **18**, 39 (1969).
2) W. Eberhardt, G. Kalkoffen, and C. Kunz, *Nucl. Instrum. Methods*, **152**, 81 (1978).
3) G. P. Williams, M. R. Howells, and R. McKinney, *Nucl. Instrum. Methods*, **172**, 379 (1980).

RESEARCH FACILITIES

For the sake of brevity of the present issue are included only the newly installed facilities and the activities since September 1981. Concerning the activities and facilities before September 1981, please refer to IMS Annual Review (1981).

Computer Center

The Computer Center began its service in January 1979 with two HITAC M-180 computers. They were replaced by HITAC M-200H computers in April 1980 and in April 1982, M-200H has a processing capacity of over 10 million instructions per second. The processors uses 32 bit words and are essentially IBM-compatible at both the hardware and software levels. They have 12×2 mega byte main memory and 12 giga byte disk memory. Unattended operation of the Computer Center in the night and on holidays has been carried on since September 1979, using the automated operation system developed by the Center and Hitachi Ltd. The computers are used not only by the research staff at IMS but also by the staff at nearby National Institutes as well as by scientists outside the Institutes in the related fields. As of March 1982, the number of project groups was 193 consisting of 458 users. In the twelve month period ending March 1982, 214847 jobs were processed with 6320 hours of the CPU time (The base of speed is M-200H).

A program library for molecular science has been established under a unique library management system, with which users can search on their TSS terminal whereabouts and guides of wanted programs. Until March 1982, 84 programs have been registered on the disk memory and are being used frequently. All of the QCPE programs has been obtained and will be so on the continued basis. The center is in service of QCLDB (Quantum Chemistry Literature Data Base), a file of references of *ab initio* molecular orbital calculations from 1977 to 1981.

Low-Temperature Center

In January, 1982, Mr. Hayasaka moved to this center from the Inst. for Solid State Physics at the Univ. of Tokyo. He is developing cryostats to be operated at the intermediate temperatures between the liquid helium and liquid nitrogen temperatures for the experimental studies of the molecular science.

Instrument Center

Three instruments have been newly equipped for general use.

1) Picosecond time-resolved fluorescence spectrophotometer

The spectrophotometer consists of a synchronously pumped, cavity-dumped dye laser, a time-correlated photon counting detector and a computer system. For very weak fluorescence emissions, decay curves and time-resolved spectra can be measured with a time resolution of 10 − 50 ps.

2) High-energy photo-irradiation system

The system consists of a 1.2 kW xenon lamp, an f/2 monochromator and a microcomputer. Wavelength scanning and data acquisition are automatically performed with the aid of the computer.

3) Electrochemical analyzer

A PAR 370 electrochemistry system, consisting of a polarographic analyzer, a potentiostat-galvanostat, a universal programmer and a lock-in analyzer, has been installed. As standard uses, the system is applicable to polarography, voltammetry and coulombmetry.

Equipment Development Center

The staff of the Equipment Development Center has designed and constructed every variety of research instruments applying the mechanical, electrical and glass-blowing technology available at this facility. Major instruments constructed during the fiscal year of 1981 are as listed below:

1) Acoustic delay line installed in the UVSOR Facility.
2) Several high-vacuum chambers for molecular beam experiments.
3) Helium gas flow cryostat (see Research Activities VI—I).
4) Multi-channel scaler for the determination of TOF velocity distributions of molecular beams.
5) Microcomputer-controlled picture analyzer II for a picosecond streak camera.
6) A microcomputer interface for an OMA equipment.
7) Absorption cell for IR diode laser operated at low temperatures.
8) Arc-heated atomic beam source (see Research Activities IV-M-1).

Ultraviolet Synchrotron Orbital Radiation Facility

On the first of April, 1982, Ultraviolet Synchrotron Orbital Radiation (UVSOR) Facility which had been proposed since 1974, was established at the south-wing of Instrument Center as the sixth research facility of IMS. A plane view (B2F) of the UVSOR Facility is shown in Figure 1. The light source is a 600 MeV (maximum, 750 MeV) electron storage ring whose injector is a 600 MeV synchrotron with a 15 MeV linac.[1] Spectral distribution of photon flux is shown in Figure 2. Under the regular operation at 600 MeV, photons above 10 Å can be used. Optical instruments combined with this light source have been made since 1980 and at present four monochromators have been completed. Construction of the light source was started in 1981 and the main parts of the injector synchrotron comprising magnets, rf system, vacuum doughnuts and a linac have been installed. At present, the checkup operation is underway. A building accomodating the synchrotron has been completed. The operation of the whole facility will be started at the beginning of 1984.

The storage ring consists of eight bending magnet sections, four short straight sections, and four long straight sections (see Figure 1). The circumference is 53.2 m. The orbit radius in the bending magnet is 2.2 m. The maximum current at 600 MeV is 500 mA with 1 hour Touschek lifetime. One wavelength shifter and two undulators can be installed in long straight sections. Pulsed light with a width of 0.2 ns and an interval of 180 ns will be available. Detailed parameters are given in Table I. Electrons are extracted from the synchrotron, transported under the floor of the storage ring room, and injected into the ring from the inside.

At each bending section, two outlets of synchrotron radiation are attached. Each outlet subtends 80 mrad of arc, which can be split into two beams by a premirror for two simultaneous experiments. The outlet consists of a water cooled shutter, a slow closing valve and a fast closing valve with finite conductance. Acoustic delay lines which can delay the speed of propagation front of leaked air will be attached between outlets and monochromators. About ten monochromators will be installed in 1980 ~ 1983. Two 1 m Seya-Namioka monochromators[2] and two plane-grating monochromators[3] were already completed. Use of almost all kinds of gases will be allowed at the storage ring site under the severe regulations on the quantity and the handling method. Carefully designed ventilation systems are present.

The building has total floor space of 2837 m^2. Inner floor area of the storage ring room is 1225 m^2 and that of the synchrotron room is 184 m^2. Besides these rooms, the building includes small rooms, such as a control

room, an electronics shop and offices. The storage ring and synchrotron rooms are completely underground for radiation safety.

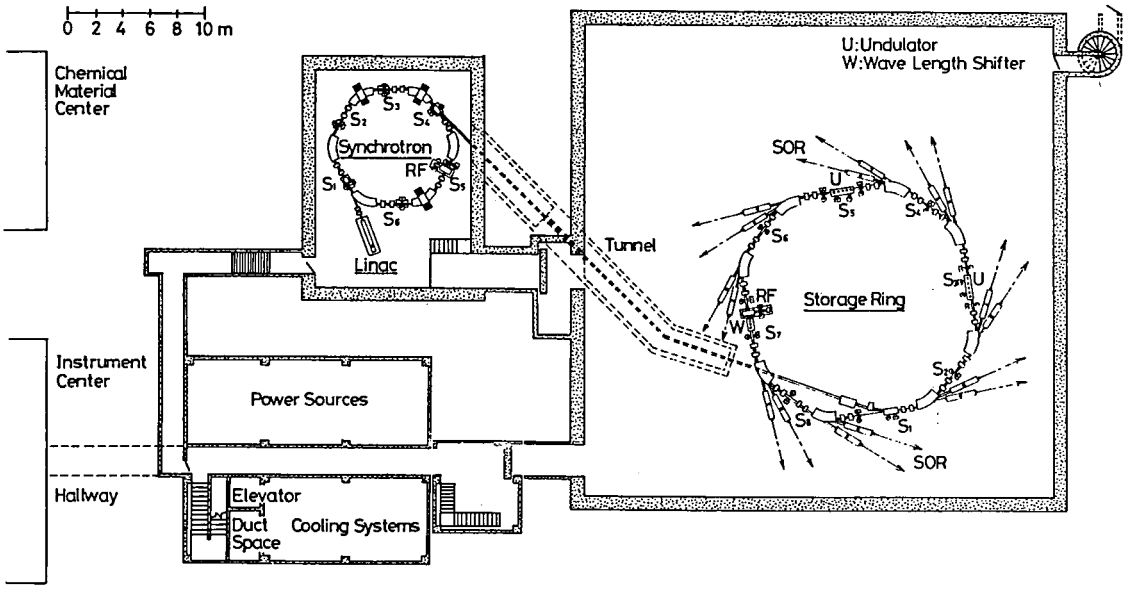

Figure 1. Plane view of UVSOR Facility (B2F).

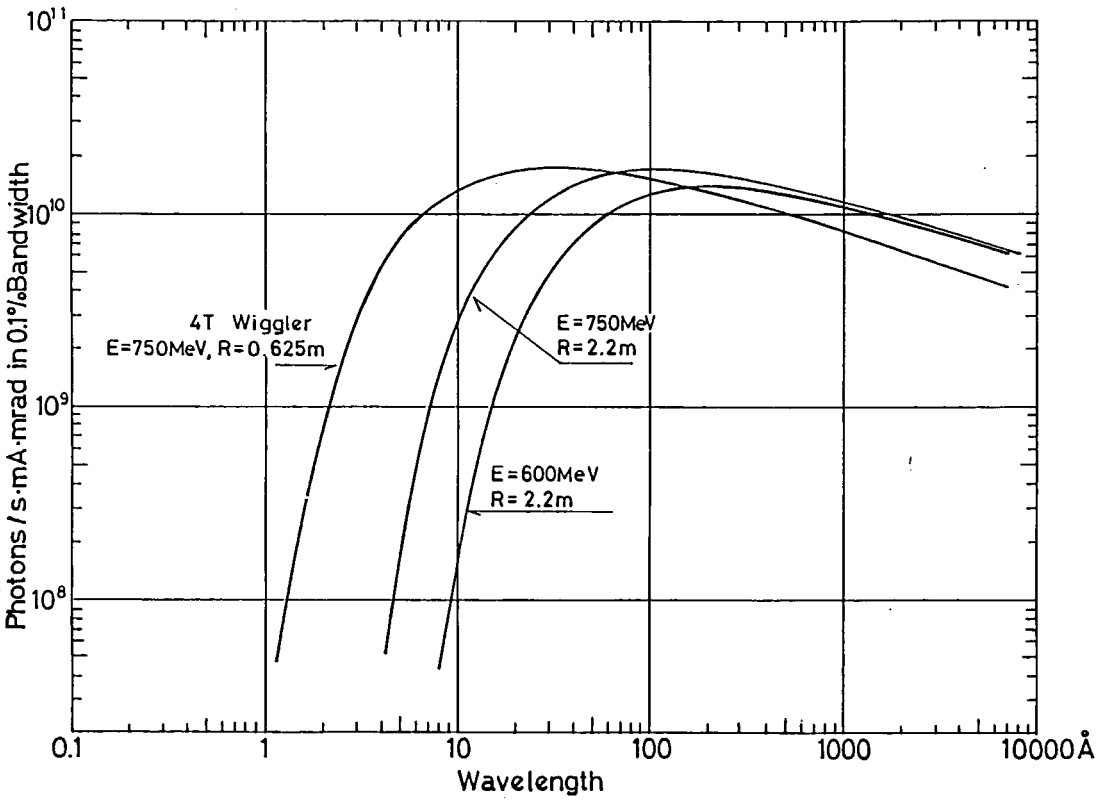

Figure 2. Spectral distribution of photon flux from UVSOR.

Table I. Design Parameters of the UVSOR Storage Ring

Energy		600 MeV (max. 750 MeV)
Critical Wavelength		56.9 Å
Current		500 mA ($\simeq 5.5 \times 10^{11}$ electrons)
Lifetime		1 h (500 mA)
Circumference		53.2 m
Periodicity		4
Bending Magnet	No.	8
	Radius	2.2 m
	Central Field	9.09 kgauss
	n-Value	0
Quadrupole Magnet	No.	28
	Length	0.2 m, 0.4 m
	Field Gradient	1 kgauss/cm
Sextupole Magnet	No.	12
	Length	0.1 m
Betatron Number	ν_x	3.25
	ν_z	2.75
Natural Chromaticity	ξ_x	−4.96
	ξ_z	−3.83
RF Frequency		90.2 MHz
Harmonic Number		16
Momentum Compaction Factor		0.026
Radiation Loss/turn/el.		5.21 keV
Radiation Loss/sec		2.6 kW (500 mA)
RF Voltage		75 kV
RF Power (Amplifier)		20 kW
Pressure (at 500 mA)		1×10^{-9} Torr
Total Pumping Speed		2×10^4 *l*/sec
Radiation Damping Time	τ_{β_x}	45.4 msec
	τ_{β_z}	40.9 msec
	τ_ε	19.5 msec
Emittance	ε_x	$8\pi \times 10^{-8}$ m·rad
	ε_z	$8\pi \times 10^{-9}$ m·rad*
Beam Size at the Center of Bending Section	σ_x	0.32 mm
	σ_z	0.23 mm
Injection Rate		1 ~ 3 Hz

*10% coupling is assumed.

References

1) M. Watanabe, A. Uchida, O. Matsudo, K. Sakai, K. Takami, K. Katayama, K. Yoshida, and M. Kihara, *IEEE Trans.* **NS-28**, 3175 (1981).
2) I. Koyano, Y. Achiba, H. Inokuchi, E. Ishiguro, R. Kato, K. Kimura, K. Seki, K. Shobatake, K. Tabayashi, Y. Takagi, K. Tanaka, A. Uchida, and M. Watanabe, *Nucl. Instrum. Methods*, **195**, 273 (1982).
3) K. Seki, M. Watanabe, E. Ishiguro, and R. Kato, *IMS Ann. Rev.*, (1982).

SPECIAL RESEARCH PROJECT

IMS has special research projects supported by national funds. Two projects presently in progress under the second five year plan (1980–1985) are:
(1) The development and control of molecular functions,
(2) Energy transfer and energy conversion through molecular processes.
These projects are being carried out with close collaboration between research devisions and facilities. Collaborators from outside also make important contributions. Research fellows join these porjects. In this report, the results in 1981 are reviewed.

(1) The Development and Control of Molecular Functions

Dynamical Molecular Structure and Control of Reactive Molecules

Eizi HIROTA,* Shuji SAITO,* Chikashi YAMADA, Yasuki ENDO, Kentarou KAWAGUCHI, and Tetsuo SUZUKI

Special attention has been given to metastable species among reactive molecules, *i.e.* species that have spin multiplicity different from that of the ground state. Famous examples are singlet and triplet carbenes; the reaction behaviors of carbenes are quite different for the two states. However, knowledge on such metastable states has been rather limited from spectroscopic point of view, because the transition from the ground state to the metastable state is forbidden. Furthermore, for simple carbenes (*e.g.* HCF and HCCl) and HNO the lowest triplet state is often expected to be located in the near-infrared region, where spectroscopic techniques have been much less developed than in the neighbor regions, visible and infrared. Fortunately needs for large scale communication transfer have prompted developments of high-quality diode lasers in the near infrared. We have set up a near-infrared absorption spectrometer using these diodes as sources, which is similar to the one in the infrared. We have tested its performance by observing the $3\nu_3$ band of N_2O, and have obtained 2.5×10^{-10} cm^{-1} as the minimum detectable absorption coefficient.

Local Structure in the Liquid State

Kazuyuki TOHJI, Yasuo UDAGAWA, and Tsunetake FUJIYAMA*

Majority of chemical reactions take place in the liquid state and it is well known that the yield and sometimes even reaction product changes in different solvent. The knowledge of the structure of liquid from the molecular standpoint is indispensable to understand what is going on in the liquid. However, the structure of liquids still remains unknown. X-ray analysis has been carried out for only a few very simple molecular liquids such as Ar, CH_4, and CCl_4.

In this project an energy-dispersive X-ray diffractometer for liquid is being constructed. It is composed of the following components.
(1) Rotating anode X-ray source (60 kV, 200 mA).
(2) High precision goniometer (0.3').
(3) SSD of high resolving power (200 eV).
(4) High speed ADC (5 μsec).

The goniometer, detector, ADC and memories are all controlled by a microcomputer through CAMAC bus, and accurate data for structure analysis of liquids can be accumulated. The system can be improved so that it can follow fast changes such as freezing, melting, and other phase transitions. Almost all the components are also used in the EXAFS measurement described in II-E.

Study on the Photochemical Reactions in the Surface Region of Gas Condensates at Low Temperatures

Nobuyuki NISHI,* Hisanori SHINOHARA, and Tohru OKUYAMA

VUV laser photolyses of small molecules have been studied in the solid state at a temperature as low as 130K. 193 nm light produced active hydrogen atom from ammonia or amines. This hydrogen atom attacks a neighbor molecule to abstract another hydrogen or methyl group, and forming a hydrogen molecule or methane in the solid. This reaction yields an unsaturated bigger molecule as a result. Primary reactions between different molecules are dominated by condensation processes and those between the same molecules by disproportionation reactions.

Ethylene solid containing ammonia or methylamine is highly reactive for the irradiation of 193 nm laser. Main photoproducts are polyacetylenes, amino or cyano compounds. Pure acetonitrile solid absorbs 193 nm light due to excitonic stabilization in the excited state. The acetonitrile dimer exhibits a disproportionation reaction yielding hydocyanic acid($H_2C_2N_2$) and ethylene primarily.

Since the recombination processes between radicals in the solid seem to be also efficient, quantum yields of respective processes are not so large at that temperature. However, the efficiency of molecular condensation reactions is apparently large in the solid. Some systems produced polymerized products.

Ground State Multiplet Species Based on the Molecular Design of Bridged Aromatic Compounds

Hiizu IWAMURA* and Tadashi SUGAWARA

We have found that there is excitonic interaction between the three benzene rings held at an angle of 120° each other in the triptycene molecule. As a result of the interaction, photochemical bridging between two of the three benzene rings takes place to give the monocentric diracial species due to one of the bridgehead atoms. A series of carbenes and nitrenes were generated in this way and found by ESR spectroscopy to be present in the ground triplet state. An extension of these studies enabled us to design a series of polycarbenes which was predicted to be in ground multiplet state and promised to open the way anew for organic ferromagnetism. Novel tris and tetrakis(diazo) compounds were prepared (see V-A-5) and the corresponding tri- and tetracarbenes were generated by uv irradiation in low temperature matrices. They were found to be in the ground septet and nonet states, respectively (see V-A-6).

Studies on the Mechanism of the Transition Metal Catalyzed Activation of Strained Carbon —Carbon σ Bonds

Akira MIYASHITA and Hidemasa TAKAYA*

We have been studying the transition metal-catalyzed isomerization of highly strained hydrocarbons in order to get insights into the mechanism of the catalysis. Our effort has been focused on the isolation of unstable strained hydrocarbon—transition metal complexes and the elucidation of their structures and chemical behaviors. The strained hydrocarbons studied are bicyclo[1.1.0]butane and its derivatives, bicyclo[2.1.0]pentane, and quadricyclane. A part of our results are presented in VI–B.

Synthesis and Solid State Properties of Superconductive Fine Particles with Chemically Modified Surface

T. ENOKI,* G. SAITO, K. KIMURA, and N. WADA *(Nagoya Univ.)*

It is known that the superconductive transition temperature of fine particles is enhanced a little when the surface of the particles is oxidized. Little suggested that the interaction between conduction electrons and molecules with large polarizable moiety caused high T_c superconduction.[1)]

We are investigating the electronic properties of superconducting fine particles with chemically modified surface by organic molecules and biological substances with large polarizability. In this year, we synthesized the organic modifiers, prepared measuring systems for solid state properties and performed preliminary investigation of electronic properties of the chemically modified fine particles, as follows. (1) TTF and TSF derivatives with carboxyl groups were synthesized in order to modify the surface of Sn fine particles. (2) An AC

calorimeter and an electrical conductivity measurement system were prepared to measure the solid state properties between liquid helium and room temperatures. (3) The superconductive transition of Sn fine particles with modified surface by undecahemepeptide was measured and found to be slightly higher than that of original Sn fine particles.

Reference
1) W. A. Little, *Phys. Rev.*, **134A**, 1416 (1964).

Development of Electric Field Modulation Spectrometer

Tadaoki MITANI* and Kazuo HAYAKAWA

In general, modulation spectroscopy has a great advantage to reveal fine structures out of a broad background spectrum. An application of electric field modulation spectroscopy to organic compounds is particularly interesting because the field induced responces should be selectively sensitive to the charge-transfer transitions more than the intramolecular transitions.

We have been constructing the field modulation spectrometer, which is available in the wavelength region from infrared to vacuum ultra-violet. In order to improve an experimental accuracy, we used a microcomputer based data-acquisition system. Temperature control of samples is made by heat exchange gas or by heat conduction and the variable temperature range is from about 2K to 300K. The modulation RF field applied to samples is up to about 5×10^4 V/cm. Preliminary measurements have been sucessfully made on 9,10-dichloroanthracene crystals at a liquid helium temperature, indicating that the charge-transfer excitons are clearly admixtured with the Frenkel excitons by applied modulation field.

(2) Energy Transfer and Energy Conversion through Molecular Processes

Theoretical Studies of Photosynthesis Systems and Solid Surface as Energy Conversion Systems

Hiroshi KASHIWAGI,* Fumihiko HIROTA *(Shizuoka Univ.)*, **Masaru TSUKADA** *(Univ. of Tokyo and IMS)*, **and Chikatoshi SATOKO**

In the primary process of the photosynthesis in green plants, a reaction center, which consists of a chlorophyll dimer, traps energy and induces electron transfer. We have performed *ab initio* SCF MO calculations on neutral, cationic, and anionic states of chlorophyll monomer. Using the results, we estimated the molecular structure of the reaction center and the energy level of a charge-transfer state which should play an important role in the charge separation. Several kinds of Fe-porphine complexes also have been investigated on the basis of the *ab initio* MO theory.

The surface of compound crystals is the place suitable for energy conversion through molecular processes. The electronic structures of the polar surfaces of ZnO, MgO, and TiC have been investigated by the use of the DV-Xα cluster calculations. The local electronic structure of the inner ions of MgO cluster is almost the same as that of the bulk. On the other hand the local electronic structures of the ions on the polar surface show metallic character. Static and/or dynamic chemisorption mechanism has been studied as well as basic electronic properties of solid surfaces.

Photocatalytic Decomposition of Water with Visible Light and the Dynamic Process on the Photocatalyst Surface

Tomoji KAWAI, Kazuhito HASHIMOTO, and Tadayoshi SAKATA*

We have demonstrated an efficient hydrogen production from water and various organic materials by using surface modified semiconductor (mainly TiO_2) photocatalysts. The photocatalytic redox reactions of carbohydrates, organic acids, alcohols, etc. were being investigated from the view point of organic synthesis. To exploit a new photocatalyst which works efficiently with visible light, the photocatalytic activity of various kinds of semi-

conductors was examined extensively.

By using dynamic mass spectroscopic technique we have investigated following processes, (1) neutral particle emission from semiconductor single crystals (ZnO, TiO_2, GaP) with high density electronic excitation, (2) photoinduced desorption and photocatalytic reaction on platinized TiO_2. The reactants are H_2O, CH_3OH, C_2H_5OH and CO_2.

Construction of a Pulsed Supersonic Nozzle Beam Apparatus

Masaaki BABA and Ichiro HANAZAKI*

A supersonic molecular beam is of great advantage to study the photochemical process of relatively large molecules with high optical resolution. In addition to the collision-free condition, a supercooling due to free expansion enhances the resolution drastically. With the object of investigating the relaxation and chemical reaction processes of excited molecules, we have constructed a pulsed supersonic molecular beam apparatus. A schematic diagram is shown in Figure 1.

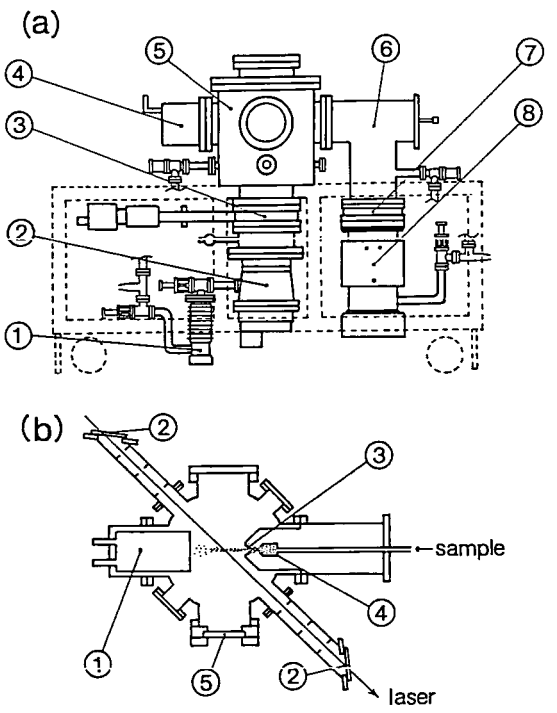

Figure 1.
(a) Vaccum pumping system for the supersonic nozzle beam. 1. oil diffusion pump (100 *l*/sec.), 2. turbo molecular pump (Sargent-Welch 1500 *l*/sec.), 3. gate valve, 4. liq. N_2 trap, 5. main chamber, 6. beam source chamber, 7. gate valve, 8. oil diffusion pump (1500 *l*/sec.)
(b) Schematic diagram of the main chamber. 1. liq. N_2 trap, 2. quartz window, 3. skimmer, 4. nozzle, 5. detection window

The main chamber (stainless steel, volume ~40*l*) was designed and machined at the IMS development workshop. It is equipped with five optical windows, one for optical detection and the others for laser irradiation. The chamber is pumped by a turbo molecular pump (Sargent-Welch, 1500 *l*/sec.) with the ultimate pressure of 8×10^{-9}Torr. An automobile EFI is used as a beam source with a differential pumping system (oil diffusion pump 1500 *l*/sec.).

As the excitation source we use a YAG laser pumped dye laser and a CO_2 TEA laser. Together with a quadrupole mass analyzer system, the apparatus is expected to give detailed informations on the molecular photochemical processes.

Multiphoton Ionization Photoelectron Spectroscopy and Its Application to Photochemistry of Molecular Clusters

Katsumi KIMURA,* Yohji ACHIBA, and Kenji SATO

In order to study photochemistry of molecules and molecular clusters from a new spectroscopic point of view, we have been developing a multiphoton ionization photoelectron spectroscopic technique with a tunable dye laser since 1979. Very recently, the construction of the apparatus has almost been completed, and preliminary tests have been carried out for measurements of photoelectrons and ions produced from various molecules by resonantly enhanced multiphoton ionization. The apparatus constructed in this project consists of (1) a supersonic molecular beam source, (2) an ionization chamber (main tault), (3) a time-of-flight electron analyzer, (4) a mass spectrometer, (5) an ion current spectrometer, (6) a Nd-YAG pumped dye laser system. The main part of the photoelectron spectrometer has previously been schematically shown in the 1980 Annual Review of IMS, and the detection system has been schematically shown in the 1981 Annual Review of IMS.

Intramolecular Energy Transfer in Vibrationally Excited Molecular Clusters and Molecular Beam Studies of Reaction Dynamics of Chemically Reactive Atoms and Free Radicals

Kosuke SHOBATAKE* and Kiyohiko TABAYASHI

The present project consists of two seemingly different subjects but has a common approach to study the dynamics of atomic and molecular interactions in that the energy transfer processes and reaction dynamics in the gaseous phase strongly depend on the potential surface(s) on which the system moves and the initial conditions of motion for the interacting systems. Techniques of supersonic nozzle expansion are applied for the production of molecular clusters, van der Waals molecules and chemically reactive free radicals (see IV–L and IV–M).

We have purchased a Kr ion laser (Spectra Physics: Model 165-01) to pump an F-center laser (Burleigh: Model FCL-20) which is used to vibrationally excite van der Waals molecules and clusters and to obtain infrared spectra of these compounds. In order to study the photodissociation dynamics of vibrationally excited molecular complexes and reaction dynamics involving chemically reactive atoms and free radicals a crossed molecular beams apparatus equipped with a rotatary mass spectrometer detector has been under construction for the last one year and a half and is near completion.

OKAZAKI CONFERENCES

"Okazaki Conferences" are principal symposia at IMS, which are held on the subjects related to the "Special Research Projects". They are held usually twice a year, with a moderate number of participants around 50, including several invited foreign speakers. The formal language for the conference is English. Outlines of the thirteenth and fourteenth conferences are as follows:

The Thirteenth Okazaki Conference

Transient Molecules and Ions, and their Roles in Interstellar Processes

(September 8—10. 1981)

Organizer: S. Saito *(IMS)*
Invited Speakers: G. Herzberg *(Herzberg Institute of Astrophysics, NRC)*, **T. Oka** *(Univ. of Chicago)*, **and G. Winnewisser** *(Univ. of Köln)*

Short-lived molecules such as unstable molecules, free radicals, and molecular ions, have now been studied by high-resolution spectroscopy. This has become possible with recent considerable improvements of molecular spectroscopy in both resolution and sensitivity. These transient molecules and molecular ions are widely distributed in cold and sparse interstellar space. Really some of them have been found to exist in interstellar space by recently developed radioastronomy and infrared astronomy. Their behaviors have revealed detailed physical and chemical processes in interstellar space. The Conference was organized so as to report and discuss recent activities in astronomy and molecular spectroscopy with exphasis on interstellar molecules, and then to pursue cooperative and mutual developments of both the fields in the future. The first day was dedicated to astronomical and laboratory spectroscopy in optical region. Dr. Herzberg reported his latest beautiful studies in

The Thirteenth Okazaki Conference, September 8–10, 1981

NRC on the H_3 and NH_4 radicals. The second day was mainly devoted to studies in infrared region. Professor Oka gave a talk on the recent detection of the H_3^+ ion by difference frequency infrared spectroscopy. H_3^+ is the most fundamental molecular ion in the ion-molecule reaction theory for molecular formation in space. Eight lectures were given on the final day including radioastronomical and laboratory microwave spectroscopy. Professer Winnewisser showed how the 100 m radio telescope in Effelsberg was effective in elucidating the detailed processes in star formation.

The Fourteenth Okazaki Conference

The Primary Processes in Photochemical Reactions

(October 20—22, 1981)

Organizers: N. Mataga *(Osaka Univ.)*, **and K. Yoshihara** *(IMS)*
Invited Speakers: G. Porter *(Royal Institution)*, **R. M. Hochstrasser** *(Univ of Pennsylvania)*, **A. Weller** *(MPI für Biophysik. Chem)*, **and J. K. Thomas** *(Univ. of Notre Dame)*

Dynamic properties of molecular excited states have long been studied with particular interest in relation to photochemistry. Recently a deeper understanding has been obtained due to the developments of laser spectroscopy in the picosecond and nanosecond timescale.

More sophisticated organized molecular systems, which have been developed recently, added many varieties in organic photochemical reactions.

The conference was composed of the following four sessions; 1) dynamics of molecular motions in solution, 2) elementary processes from excited states, 3) electron transfer and related processes, and 4) photochemical reactions in organized systems. About seventy scientists, including ten from abroad, actively engaged in this field.

Professor M. Ito *(Tohoku Univ.)* organized a half-day discussion on coherent molecular spectroscopy as a satellite meeting. Professor R. M. Hochstrasser was the invited speaker. Interesting discussions were presented from both sides of physics and chemistry.

The Fourteenth Okazaki Conference, October 20–22, 1981

JOINT STUDIES PROGRAMS

As one of the important functions of an inter-university research institution, IMS undertakes joint studies programs for which funds are available to cover research expenses as well as travel and living expenses of individuals. The proposals from domestic scientists are reviewed and controlled by the inter-university committee. The programs are carried out under one of four categories:

1) Joint Studies on special projects (a special project of significant relevance to the advancement of molecular science can be carried out by a team of several groups of scientists).
2) Research Symposia (on timely topics in collaboration with both outside and IMS scientists).
3) Cooperative Research (carried out in collaboration with both outside and IMS scientists).
4) Use of Facility (the Computer Center, Instrument Center and other research facilities at IMS are open to all researchers throughout the country).

In the fiscal year 1981, numbers of joint studies programs accepted amounted to 6, 10 and 165 for categories 1) ~ 3), respectively.

1) Joint Studies

Multiple Resonance and Multi-photon Process

Coordinators: **Eizi HIROTA** *(Department of Molecular Structure)*
Shuji SAITO *(Department of Molecular Structure)*

The present program has intended to develop new spectroscopic methods such as multiple resonance as an extension of double resonance. Visible and infrared lasers, microwave, and rf can be used for such purposes. It was also encouraged to investigate molecules and/or molecular systems from more dynamical points of view. However, the main results of the present program were obtained from double resonance spectroscopy. It is perhaps because there are still many problems of interest that can be attacked by double resonance methods. Prof. K. Takagi *(Toyama Univ.)* collaborated with S. Saito and T. Suzuki in extending MODR experiments on HNO. They could explain anomalous K splittings of $\tilde{A}(020)$ $K_a = 2$ levels in terms of Coriolis interaction with $\tilde{A}(100)$ $K_a = 1$ levels. Infrared-optical double resonance experiments of NH_2 were continued by K. Kawaguchi *et al.*, and a few so-called "u" levels were found by pumping infrared transitions $\tilde{A}(0,12,0)$ $N_{1,N-1} \leftarrow \tilde{A}(0,11,0)$ $N_{0,N}$ with N = 3 and 5. Dr. M. Takami (IPCR) continued microwave (rf)-infrared diode laser double resonance on the $^{13}CF_4$ ν_3 band, and could definitely show that perturbations observed for both ^{12}C and ^{13}C species were due to interactions with $2\nu_4$.

Electrical and Anionic Conductivities of Novel Crown Ether Complexes

Coordinators: **Hiroo INOKUCHI** *(Department of Molecular Assemblies)*
Hiroshi MIKAWA *(Osaka University)*

Macrocyclic polyethers called crown ethers have specific properties of coordinating metal cations into their cavities. We applied these properties of crown ethers to the developments of new types of electrical conductors and anionic conductors.

Electrical Conductors. TCNQ-complexes have been known to give a large number of organic conductors. We have synthesized novel TCNQ-complexes containing crown ethers. Two types of complexes were synthesized: one is called simple salt expressible as $[M^{n+}(TCNQ^-)_n]_m$(crown ether)$_i$, and the other is called complex salt expressible as $[M^{n+}(TCNQ^-)_n]_m TCNQ_i$(crown ether)$_j$. Here, M^{n+} denotes metal cation. Complex salts were much more conductive than simple salts and original TCNQ salts, $M^{n+}(TCNQ^-)_n$. The electronic reflection spectra and the ultraviolet photoelectron spectra of these complexes gave interesting informations on the electronic interaction between TCNQ molecules in the solid.

Anionic Conductors. The Coulomb attraction

force between metal cation and halide anion is much more reduced for the crown ether-metal halide complex than for the original metal halide. Thus, crown ether-metal halide complexes are expected to be a new type of anionic conductors. We have found 18-crown-6-KI complex and related complexes to be iodide ion conductors. Iodine concentration cell could be constructed by use of these crown ether complexes as the solid electrolytes.

Development of Variable Temperature Molecular Beam Sources For Spectroscopic Studies of Gaseous Molecular Complexes

Coordinator: **Katsumi KIMURA** *(Department of Molecular Assemblies)*

In the last several years, great interest has been aroused in gaseous molecular clusters and cooled molecules. Since 1981, in this project, we have designed and constructed a variable temperature supersonic nozzle beam source to form molecular complexes and van der Waals molecules efficiently.

A low temperature nozzle beam source constructed can be cooled down to the liquid nitrogen temperature by thermal conduction to a liquid nitrogen reservoir. The desired temperature is obtained and controlled by resistively heating the beam source. Various kinds of test experiments have been carried out by Shobatake and Tabayashi with this beam source using Ar and NO.

Since a large number of workers had shown great interests in applications of this beam source, we held an informal meeting on the titled subject on March 12 and 13, 1982, about 40 participants attending.

UVSOR

Coordinator: **Katsumi KIMURA** *(Department of Molecular Assemblies)*

The UVSOR light source consists of a 600 MeV storage ring, a 0.6 eV synchrotron and a 15 MeV linac. The layout of the UVSOR source and beam channels has been shown in the 1981 Annual Review of IMS (p. 167). 1) The following main parts of the synchrotron which were designed in 1980 have been constructed during the 1981 fiscal year: the 15 MeV linac, the RF cavity, the vacuum doughnut system, the radiation protection system and the control system. All these systems have been installed in early April of 1982. 2) The magnet lattice and RF system of the storage ring have been designed. 3) Preliminary tests have been carried for the beam outlet system. A test of the delay line has indicated that its delay time is about 30 msec at 1 atm. 4) Two plane-grating monochromators (PGM) for studying solid samples have been designed and constructed (the wavelength region 100 − 4000 Å, the resolution 0.1 − 0.2 eV).

Dynamical Behaviour and Chemical Reaction of Highly Excited Vibrational States

Coordinator: **Ichiro HANAZAKI** *(Department of Electronic Structure)*

The project was aimed to study the role of highly excited vibrational states in the dynamical behavior and chemical reaction of molecules both in the ground and electronically excited states. Following three items have been main subjects of the project; (1) Dynamical and spectroscopic behaviour of local mode, (2) Vibrational distribution and chemical reaction in the infrared multiphoton process, and (3) Contribution of vibrational levels in the relaxation and chemical reaction from electronically excited states. As described in "Research Activities", we have studied the infrared multiphoton process of normal molecules and molecular clusters with a supersonic molecular beam technique. This work has been done in collaboration with Prof. Y. Kitagawa *(Toyama Med. and Pharmaceut. Univ.)*. Dr. R. Nakagaki, who worked as an IMS fellow for 1980 − 1982, performed an extensive work on the local mode problem. In this study, we have clarified spectroscopically the nature of methyl C-H stretching overtones in various kind of molecules. Frequent discussions with Prof. B. R. Henry *(Univ. of Manitoba)*, Prof. M. Katayama *(Univ. of Tokyo)* and Prof. N. Yamamoto *(Osaka Univ.)* have been helpful throughout the period.

As a part of activities in the joint research, we had a small symposium on the same subject in July,

1981. About 30 attendants including Prof. Henry participated in active discussions on the nature of highly excited vibrational states.

Photochemistry of Fundamental Organic Molecules

Coordinator: **Keitaro YOSHIHARA** *(Department of Electronic Structure)*

In the past decade understandings on the primary photochemical processes in molecules have improved in a great extent. Under the present program, we intend to analyse the present knowledge on intra-molecular energy redistribution of molecules in both liquid and gas phase and to discuss the most current studies by the members of the program on the subject. We also promote actual experimental studies at IMS by the members. The fundamental organic molecules in concern are benzene, halogenated benzenes, aza-aromatic benzenes etc.

A one-day meeting was held on general discussion. Experiments on the reaction of halogenated benzenes by nanosecond flash photolysis with an excimer laser and on the single-vibronic-level fluorescence decays of aza benzenes were performed.

The members of the program are H. Baba and H. Ohta *(Hokkaido Univ.)*, I. Tanaka, Y. Mori, and T. Ichimura *(Tokyo Inst. Tech.)*, and K. Yoshihara, N. Nakashima, M. Sumitani, I. Hanazaki, I. Yamazaki, and T. Murao *(IMS)*.

2) Research Symposia

1. Effective Charge Separations in Photochemical Energy Conversion
   (July 7th — 8th, 1981)
   Organizer: A. Fujishima (Univ. of Tokyo)
2. Dynamical Structures in Liquids and Solutions
   (July 20th — 22nd, 1981)
   Organizers: Y. Kataoka (Kyoto Univ.), and M. Doi (Tokyo Metropolitan Univ.)
3. Collision Theoretical Approach to Chemical Reactions
   (September 3rd — 5th, 1981)
   Organizer: K. Ohno (Hokkaido Univ.)
4. Communication Between Theoretical Chemistry and Physics in Molecular Science
   (November 24th — 26th, 1981)
   Organizer: H. Nakamura (IMS)
5. UVSOR-Design of Storage Ring and Experiment System
   (December 3rd — 4th, 1981)
   Organizer: K. Kimura (IMS)
6. Resonant Secondary Emission Processes in Vibronic Systems
   (December 10th — 12th, 1981)
   Organizer: T. Azumi (Tohoku Univ.)
7. Intra- and Intermolecular Interactions in Metal Complexes
   (December 19th — 21st, 1981)
   Organizer: Y. Sasaki (Tohoku Univ.)
8. Syntheses and Reactions of Novel Organotransition Metal Complexes
   (January 19th — 20th, 1982)
   Organizer: H. Takaya (IMS)
9. Mechanistic Aspects of the Chemistry of Organic Derivatives of Metallic and Non-Metalic Elements
   (February 9th — 10th, 1982)
   Organizer: K. Akiba (Hiroshima Univ.)
10. Supercomputer and Its Applications to Molecular Science
    (February 17th — 18th, 1982)
    Organizer: H. Kashiwagi (IMS)
11. Symposium on Reaction Dynamics
    (June 11th — 12th, 1981)
    Organizers: K. Shobatake (IMS), I. Koyano (IMS), and T. Kondow (Univ. of Tokyo)
    No. of Participants: 65
    No. of Overseas Participants: 14

This one and a half day symposium was held as a satellite meeting of the International Symposium on Chemical Kinetics Related to Atomspheric Chemistry held on June 6–10, 1982 in Tsukuba, Japan (Chairperson: Prof. Ikuzo Tanaka *(Tokyo Inst. of Tech. & IMS)*). The symposium was devoted to the dynamics of chemical reactions and energy transfer processes, and was attended by 65 participants including 14 overseas participants. The main talks were "The Collision Dynamics of Highly Excited States of I_2" presented by Prof. R. J. Donovan *(Univ. of Edinburgh)*, "Molecular Beam Studies on Reaction Dynamics and Primary Photochemical Processes." by Prof. Y. T. Lee *(Univ. of Calif.,*

Berkeley), and "Recent Results on the Theory of F + H_2 Reaction." by Prof. R. E. Wyatt *(Univ. of Texas, Austin and IMS)*. Other overseas speakers were Dr. J. R. McDonald *(U. S. Naval Research Lab.)*, Prof. K. H. Becker *(Univ. — Wuppertal, Germany)* and Prof. W. C. Stwalley *(Univ. of Iowa)*. Lively discussions were exchanged by the participants.

3) Cooperative Research

This is one of the most important programs IMS undertakes for conducting its own research of the common interest to both outside and IMS scientists by using the facilities at IMS. During the first half of the fiscal year of 1981 ending on September 30, 83 outside scientists including 7 invited collaborated with IMS scientists; and during the second half of the fiscal year, 81 outside scientists including 6 invited worked in collaboration with IMS scientists. The names and the affiliations of these collaborators are found in the Research Activities.

4) Use of Facility

The number of projects accepted for the Use of Facility Program of the Computer Center during the fiscal year of 1981 amounted to 112(279 users), and the computer time spend for these projects is 2926 hours (49% of the total annual CPU time).

Fifty eight projects(145 users) were accepted for the Use of Facility Program of the Instrument Center during the fiscal year of 1981.

FOREIGN SCHOLARS

Visitors from abroad play an important role in research activities and are always welcomed at IMS. The following is the list of foreign scientists who visited IMS in the past year (Aug. 1981 – July 1982). The sign *1 indicates a visitor invited to attended an Okazaki Conference, *2 a visitor on the Invited Foreign Scholars Program, and *3 a councillor of IMS.

Prof. E. Lipczyńska-Kochany	Tech. Univ. of Warsaw	(Poland)	Apr. 1981 – Sept. 1982
Prof. I. Botskor	Univ. of Ulm	(W. Germany)	Aug. – Sept. 1981
Dr. C. Chin	Univ. of Southern California	(USA)	Aug. 1981
Mrs. C. Chiu	Univ. of Southern California	(USA)	Aug. 1981
Prof. W. G. Fateley	Kansas State Univ.	(USA)	Aug. – Sept. 1981
Prof. G. Gordon	Univ. of Miami	(USA)	Aug. 1981
Prof. Y. S. Kim	Seoul National Univ.	(Korea)	Aug. 1981
Dr. A. Mackor	Inst. of Appl. Chem. TNO	(Netherlands)	Aug. 1981
Prof. W. G. Wagner	Univ. of Southern California	(USA)	Aug. 1981
Prof. W. T. Borden	Univ. of Washington	(USA)	Sept. 1981 – Jan. 1982
Prof. W. Brenig*[2]	Tech. Univ. München	(W. Germany)	Sept. – Dec. 1981
Dr. P.-M. Guyon*[2]	Univ. of Paris-Sud	(France)	Sept. – Dec. 1981
Prof. L. L. Lohr	Univ. of Michigan	(USA)	Sept. – Nov. 1981
Prof. N. Karl*[2]	Univ. Stuttgart	(W. Germany)	Sept. – Oct. 1981
Prof. H. E. Zimmerman	Univ. of Wisconsin	(USA)	Sept. – Oct. 1981
Prof. G. Allen	Sci. & Eng. Research Council	(UK)	Sept. 1981
Dr. E. A. Ashby	NSF	(USA)	Sept. 1981, Apr. 1982
Prof. C. Fadley	Univ. of Hawaii	(USA)	Sept. 1981
Dr. G. Herzberg*[1]	Herzberg Inst. of Astrophys., NRC	(Canada)	Sept. 1981
Dr. L. C. W. Hobbis	Sci. & Eng. Research Council	(UK)	Sept. 1981
Dr. A. Holt	NSF	(USA)	Sept. 1981
Dr. M. M. Martin	Univ. of Paris-Sud	(France)	Sept., Oct. 1981
Miss J. Mellville	Sci. & Eng. Research Council	(UK)	Sept. 1981
Prof. M. G. Mylroi	Univ. of Bradford	(UK)	Sept. 1981
Dr. B. W. Oakley	Sci. & Eng. Research Council	(UK)	Sept. 1981
Prof. T. Oka*[1]	Univ. of Chicago	(USA)	Sept. 1981
Prof. D. Phillips	The Royal Society	(UK)	Sept. 1981
Prof. B. M. Rode	Innsbruck Univ.	(Austria)	Sept. 1981
Dr. P. T. Warren	The Royal Society	(UK)	Sept. 1981
Prof. G. Winnewisser*[1]	Univ. of Köln	(W. Germany)	Sept. 1981
Prof. K. Y. Choo*[2]	Seoul National Univ.	(Korea)	Oct. 1981, Jan. – Apr. 1982
Prof. C. S. Foote	Univ. of California, Los Angeles	(USA)	Oct. 1981
Prof. R. M. Hochstrasser*[1]	Univ. of Pennsylvania	(USA)	Oct. 1981
Prof. C. W. Jefford	Univ. de Geneve	(Switzerland)	Oct. 1981
Dr. L. J. Jiang	Inst. of Photographic Chem., Acad. Sinica	(China)	Oct. 1981
Prof. Y. S. Koh	Seoul National Univ.	(Korea)	Oct. 1981
Prof. J. A. Koningstein	Carleton Univ.	(Canada)	Oct. 1981

Dr. J. X. Lu	Academia Sinica	(Chaina)	Oct. 1981
Prof. J. Mason	Open Univ.	(UK)	Oct. 1981
Prof. S. F. Mason	King's College, Univ. of London	(UK)	Oct. 1981
Dr. A. P. Persoons	Univ. of Leuven	(Belgium)	Oct. 1981
Prof. G. Porter*[3]	Royal Institution	(UK)	Oct. 1981
Dr. L. J. Shi	Academia Sinica	(China)	Oct. 1981
Prof. J. K. Thomas*[1]	Univ. of Nortre Dame	(USA)	Oct. 1981
Prof. A. A. Vlček	Heyrovsky Inst. of Phys. Chem. & Electrochem.	(Czechoslovakia)	Oct. 1981
Prof. A. Weller*[1]	Max-Planck-Institut für Biophisik. Chem.	(W. Germany)	Oct. 1981
Prof. M. Calvin*[3]	Univ. of California, Berkeley	(USA)	Nov. 1981
Dr. A. W. Kleyn	FOM-Inst.	(Netherlands)	Nov. 1981
Dr. V. K. Lan	Paris Observatory	(France)	Nov. 1981
Dr. M. Liu	Univ. of Prince Edward Island	(Canada)	Nov. 1981
Prof. R. Y. Qian	Inst. of Chem., Acad. Sinica	(China)	Nov. 1981
Prof. K. L. Lin	Univ. of Singapore	(Singapore)	Nov. 1981
Prof. A. K. Peng	Univ. of Singapore	(Singapore)	Nov. 1981
Prof. A. N. Rao	Univ. of Singapore	(Singapore)	Nov. 1981
Prof. A. Wan	Univ. of Singapore	(Singapore)	Nov. 1981
Prof. J. R. Shapley*[2]	Univ. of Illinois	(USA)	Dec. 1981 – Mar. 1982
Dr. D. V. O'Connor	Royal Institution	(UK)	Jan. 1982 –
Prof. M. Mizushima*[2]	Univ. of Colorado	(USA)	Jan. – June 1982
Dr. E. Berman	Arco Solar Company	(USA)	Jan. 1982
Prof. B. Brocklehurst	Univ. of Sheffield	(UK)	Feb. 1982
Prof. G. Orlandi	Univ. of Bologna	(Italy)	Feb. 1982
Dr. C. T. Owens	NSF	(USA)	Feb. 1982
Prof. R. N. Jones	National Research Council	(Canada)	Mar. 1982
Dr. M. R. Das	Cent. Cell. Mol. Biol.	(India)	Mar. 1982
Prof. N. Hasan	Council of Sci. & Indust. Res.	(India)	Mar. 1982
Dr. T. R. Misra	Indian Assoc. for the Cultivation of Sci.	(India)	Mar. 1982
Dr. V. C. Vora	Cent. Drug Res. Inst.	(India)	Mar. 1982
Dr. J. T. Hougen	NBS	(USA)	Apr. – May 1982
Dr. K. Kemnitz	Univ. Erlangen-Nürnberg	(W. Germany)	Apr. 1982 –
Dr. B. O'Connell	NSF	(USA)	Apr. 1982
Dr. G. Graner	CNRS	(France)	Apr. 1982
Dr. S. Suzuki	Univ. of Salford	(UK)	Apr. 1982
Prof. K. Wiberg	Yale Univ.	(USA)	Apr. 1982
Prof. L. S. Hsu	Univ. of Singapore	(Singapore)	Apr. 1982
Prof. T. J. Lam	Univ. of Singapore	(Singapore)	Apr. 1982
Prof. A. Rajaratnam	Univ. of Singapore	(Singapore)	Apr. 1982
Prof. B. T. G. Tan	Univ. of Singapore	(Singapore)	Apr. 1982
Prof. H. H. Teh	Univ. of Singapore	(Singapore)	Apr. 1982
Prof. S. X. Chen	Inst. of Chem., Acad. Sinica	(China)	May 1982 –
Prof. P. G. Wolynes*[2]	Univ. of Illinois	(USA)	May 1982 –
Prof. R. E. Wyatt*[2]	Univ. of Texas, Austin	(USA)	May – Aug. 1982
Prof. I. G. Csizmadia	Univ. of Toronto	(Canada)	May – June 1982
Prof. J. C. Martin	Univ. of Illinois	(USA)	May – June 1982

Prof. L. Batt	Univ. of Aberdeen	(UK)	May 1982
Prof. J. R. Bolton	Univ. of West. Ontario	(Canada)	May 1982
Dr. M. Klein	NRC	(Canada)	May 1982
Prof. P. O. Löwdin	Uppsala Univ.	(Sweden)	May 1982
Prof. S. R. Morrison	Simon Frager Univ.	(Canada)	May 1982
Prof. W. H. E. Schwarz	Gesamthochschule Siegen	(W. Germany)	May 1982
Prof. H. L. Strauss	Univ. of California, Berkeley	(USA)	May 1982
Dr. T. H. Tang	Tianjin Teacher's College	(China)	May 1982
Dr. W. R. Workman	3M Company	(USA)	May 1982
Prof. F. Stuhl	Ruhr-Univ., Bochum	(W. Germany)	June – 1982
Prof. W. C. Stwalley	Univ. of Iowa	(USA)	June – July 1982
Prof. K. H. Becker	Univ. of Wuppertal	(W. Germany)	June 1982
Dr. V. M. Bierbaum	Univ. of Colorado	(USA)	June 1982
Dr. G. Black	SRI International	(USA)	June 1982
Prof. D. Curtin	Univ. of Illinois	(USA)	June 1982
Prof. J. Dunitz	ETH	(Switzerland)	June 1982
Prof. R. J. Donovan	Univ. of Edinburgh	(UK)	June 1982
Dr. C. J. Howard	NOAA	(USA)	June 1982
Prof. M. S. Jhon	KAIST	(Korea)	June 1982
Prof. K. H. Jung	KAIST	(Korea)	June 1982
Prof. H. Kagan	Univ. of Paris-Sud	(France)	June 1982
Prof. H. Kessler	Univ. of Frankfurt	(W. Germany)	June 1982
Prof. E. K. C. Lee	Univ. of California, Irvine	(USA)	June 1982
Prof. L. C. Lee	San Diego State Univ.	(USA)	June 1982
Prof. Y. T. Lee	Univ. of California, Berkeley	(USA)	June 1982
Dr. J. R. McDonald	U. S. Naval Research Lab.	(USA)	June 1982
Dr. R. P. Mariella	American Chem. Soc.	(USA)	June 1982
Prof. R. Parry	American Chem. Soc.	(USA)	June 1982
Prof. L. F. Phillips	Univ. of Canterbury	(New Zealand)	June 1982
Dr. T. G. Slanger	SRI International	(USA)	June 1982
Prof. P. S. Song	Texas Tech. Univ.	(USA)	June 1982
Dr. M. Sutoh	San Diego State Univ.	(USA)	June 1982
Dr. J. Richards	British Council	(UK)	June 1982
Prof. D. Bethell*[2]	Univ. of Liverpool	(UK)	July 1982 – Oct. 1982
Prof. J. Demuynck	Univ. of Strasbourg	(France)	July 1982 –
Prof. T. Ziegler	Univ. of Calgary	(Canada)	July – Aug. 1982
Prof. K. Mislow	Princeton Univ.	(USA)	July 1982
Prof. S. I. Choi	Univ. of North Carolina	(USA)	July 1982
Mr. B. M. Schmid	Stuttgart Univ.	(W. Germany)	July 1982

AWARD

Prof. Hideo Yamatera received the Award of the Chemical Society of Japan in 1982 for his contribution to "Establishment of Yamatera Rule for Absorption Spectra of Metal Complexes".

Prof. Yamatera's Scientific Achievement:

In 1958 Prof. Yamatera proposed a theory to interpret the visible (and near ultraviolet) spectra of cobalt(III) complexes. The theory is a molecular-orbital perturbation theory with a small number of empirical parameters. This is the first instance of the angular overlap model, although the application was limited to orthonormal chromophores. The theory explains the features of absorption spectra of the $[CoA_nB_{6-n}]$-type complexes. The theory (Yamatera Rule) can predict the positions and dichroic properties of the split absorption bands of the $[CoA_nB_{6-n}]$-series complexes, if parameter values are known for the series. The rule is also useful in distinguishing between geometrical isomers on the basis of their spectra.

He also rationalized the charge-transfer bands in the ultraviolet region of the spectra of $[CoX(NH_3)_5]^{2+}$ (X = Cl, Br, and I), considering spin-orbit interactions.

He applied the angular overlap model to explain the rates of ligand substitution in octahedral complexes. He introduced the molecular-orbital concept of ligand field activation energy. This gave a much better agreement with the observation than shown by the electrostatic concept of crystal field activation energy.

Professor Yamatera's scientific achievement also includes other theoretical and experimental studies in the fields of coordination chemistry and solution chemistry.

LIST OF PUBLICATIONS

K. MOROKUMA and K. KITAURA, "Energy Decomposition Analysis of Molecular Interactions" in "Chemical Applications of Atomic and Molecular Electrostatic Potentials", Ed. P. Politzer and D. G. Truhlar, *Plenum*, New York (1981), p.215.

K. MOROKUMA and S. KATO, "Potential Energy Characteristics for Chemical Reactions", in "Potential Energy Surface and Dynamics Calculations", Ed. D. G. Truhlar, *Plenum*, New York (1981), p.243.

Y. SUGAWARA, A. HIRAKAWA, M. TSUBOI, S. KATO, and K. MOROKUMA, "Force Constants of Trans and Cis N-Methylformamide from *Ab Initio* SCF MO Calculations", *Chem. Phys.*, **62**, 339 (1981).

S. SAKAI, S. KATO, K. MOROKUMA, and I. KUSUNOKI, "Potential Energy Surfaces of the Reaction: $C^+ + H_2 \rightarrow CH^+ + H$", *J. Chem. Phys.*, **75**, 5398 (1981).

S. OBARA, K. KITAURA, and K. MOROKUMA, "A Comparative Study of *Ab Initio* Effective Core Potential and All-Electron Calculations for Molecular Structures and Transition States", *Theo. Chem. Acta*, **60**, 227 (1981).

S. SAKAI, K. KITAURA, and K. MOROKUMA, "Structure and Coordinate Bonding Nature of Nickel(0) and Copper(I) Carbon Dioxide Complexes. An *Ab Initio* Molecular Orbital Study", *Inorg. Chem.*, **21**, 760 (1982).

K. MOROKUMA, "Molecular Structure and Reaction Mechanisms as Studied by the *Ab Initio* Energy Gradient Method", in "Frontiers of Chemistry", Ed. K. J. Laidler, *Pergamon*, Oxford (1982), p.143.

K. OHNO and K. MOROKUMA, Ed., "Quantum Chemistry Literature Data Base — Bibliography of *Ab Initio* Calculations for 1978—1980", *Elsevier*, Amsterdam (1982).

K. KITAURA, K. MOROKUMA, and I. G. CSIZMADIA, "The Electronic Structure of Nickel Carbide", *J. Mol. Str.* (THEOCHEM), **88**, 119, (1982).

K. MOROKUMA, "Potential Energy Surface of the S_N2 Reaction in Hydrated Clusters", *J. Am. Chem. Soc.*, **104**, 3732 (1982).

H. NAKAMURA and M. NAMIKI, "Semiclassical Theory of Rotationally Induced Nonadiabatic Transitions.", *Phys. Rev.*, **A24**, 2963 (1981).

M. MORINAGA, H. ADACHI, and M. TSUKADA, "Electronic Structure of Z_rO_2 by the DV-Xα Cluster Method", *Solid State Ionics*, **3**, 131 (1981).

K. SHINJO, S. OHNISHI, M. TSUKADA, and S. SUGANO, "Theoretical Studies of Underlayer Chemisorption I: Electronic Structure of Ti_6 and Ti_6 N Clusters", *J. Phys.C:*, **14**, 5575 (1981).

M. TSUKADA and T. HOSHINO, "Electronic Structure of Vacancy and Chemisorptive Bond on Si(111) Surface by the DV-Xα Cluster Calculation", *Int. Journ. Quantum Chem.*: Quantum Chem. Symp., **15**, 445 (1981).

M. KAWAI, M. TSUKADA, and K. TAMARU, "Surface Electronic Structure of Binary Metal Oxide Catalyst ZrO_2/SiO_2", *Surface Sci.*, **111**, L716 (1981).

T. HOSHINO and M. TSUKADA, "Electronic Structure of Chemisorption Systems on Si(111) Surface I. Si(111) 7×7/H,Cl", *Surface Sci.*, **115**, 104 (1982).

H. NAGAYOSHI and M. TSUKADA, "Electronic Structure of the Si(111) Reconstructed Surface in the Vacancy Model", *Surface Sci.*, **116**, 163 (1982).

M. KAKIMOTO, S. SAITO, and E. HIROTA, "Doppler-Limited Dye Laser Exitation Spectroscopy of HCF." *J. Mol. Spectrosc.*, **88**, 300 (1981).

E. HIROTA, Y. ENDO, S. SAITO, K. YOSHIDA, I. YAMAGUCHI, and K. MACHIDA, "Microwave Spectra of Deuterated Ethylenes: Dipole Moment and r_z Structure," *J. Mol. Spectrosc.*, **89**, 223 (1981).

E. HIROTA, Y. ENDO, S. SAITO, and J. L. DUNCAN, "Microwave Spectra of Deuterated Ethanes:

Internal Rotation Potential Function and r_z Structure.", *J. Mol. Spectrosc.*, **89**, 285 (1981).

K. NAGAI, Y. ENDO, and E. HIROTA, "Diode Laser Spectroscopy of the HO_2 ν_2 Band.", *J. Mol. Spectrosc.*, **89**, 520 (1981).

K. NAGAI, C. YAMADA, Y. ENDO, and E. HIROTA, "Infrared Diode Laser Spectroscopy of FCO: The ν_1 and ν_2 Bands.", *J. Mol. Spectrosc.*, **90**, 249 (1981).

Y. ENDO, S. SAITO, and E. HIROTA, "Microwave Spectra of the HSO and DSO Radicals.", *J. Chem. Phys.*, **75**, 4379 (1981).

C. YAMADA, E. HIROTA, and K. KAWAGUCHI, "Diode Laser Study of the ν_2 Band of the Methyl Radical.", *J. Chem. Phys.*, **75**, 5256 (1981).

K. KAWAGUCHI, E. HIROTA, C. YAMADA, "Diode Laser Spectroscopy of the BO_2 Radical. Vibronic Interaction between the $\widetilde{A}^2\Pi_u$ and $\widetilde{X}^2\Pi_g$ States.", *Mol. Phys.*, **44**, 509 (1981).

T. SUZUKI, S. SAITO, and E. HIROTA, "Doppler-Limited Dye Laser Excitation Spectroscopy of DCF.", *J. Mol. Spectrosc.*, **90**, 447 (1981).

E. HIROTA, "Metastable States in Some Transient Molecules by High-Resolution Laser Spectroscopy.", *Faraday Discuss. Chem. Soc.*, **71**, 87 (1981).

K. NAGAI, K. TANAKA, and E. HIROTA, "Observation of Fine-Structure Transitions of the Helium Atom by Infrared Diode Laser Spectroscopy.", *J. Phys. B: At. Mol. Phys.*, **15**, 341 (1982).

Y. ENDO, S. SAITO, and E. HIROTA, "The Microwave Spectrum of the SF Radical.", *J. Mol. Spectrosc.*, **92**, 443 (1982).

Y. ENDO and M. MIZUSHIMA, "Microwave Resonance Lines of $^{16}O_2$ in its Electronic Ground State ($X^3\Sigma_g^-$).", *Jap. J. Appl. Phys.*, **21**, L379 (1982).

K. KAWAGUCHI, Y. ENDO, and E. HIROTA, "Infrared Diode Laser and Microwave Spectroscopy of an Unstable Molecule: ClBO.", *J. Mol. Spectrosc.*, **93**, 381 (1982).

T. AMANO, P. F. BERNATH, and C. YAMADA, "The ν_3 Fundamental Band of the Methyl Radical.", *Nature*, **296**, 372 (1982).

M. KAKIMOTO and E. HIROTA, "Hyperfine Structure of the PH_2 Radical in $\widetilde{X}^2B_1$ and $\widetilde{A}^2A_1$ from Intermodulated Fluorescence Spectroscopy.", *J. Mol. Spectrosc.*, **94**, 173 (1982).

Y. ENDO, S. SAITO, and E. HIROTA, "Microwave Spectroscopy of the CCl Radical.", *J. Mol. Spectrosc.*, **94**, 199 (1982).

R. IGARASHI, F. IIDA, C. HIROSE, and T. FUJIYAMA, "The Application of Polarization Coherent Anti-Stokes Raman Spectroscopy to the Line Shape Analysis of Liquid Sample", *Bull. Chem. Soc. Jpn.*, **54**, 3691 (1981).

M. YUDASAKA, T. SUGAWARA, H. IWAMURA, and T. FUJIYAMA, "Further Comments on the Line-broadening of the Chlorine-35 NMR Spectra and the Local Structure around a Chlorine Ion in Aqueous Solutions of Non-electrolytes", *Bull. Chem. Soc. Jpn.*, **55**, 311 (1982).

K. TAMAGAKE, S. HYODO, and T. FUJIYAMA, "Effects of Mechanical and Electrical Anharmonicities on Local Mode Spectrum", *Bull. Chem. Soc. Jpn.*, **55**, 1267 (1982).

S. HYODO, K. TAMAGAKE, and T. FUJIYAMA, "High-Overtone Spectra and Dipole Moment Functions for the C-H Stretching Vibration of Chloroform", *Bull. Chem. Soc. Jpn.*, **55**, 1272 (1982).

K. TAMAGAKE, S. HYODO, and T. FUJIYAMA, "Symmetrized Local Mode Analysis of CH_2 Stretching Mode in 1,1-Dichloroethylene", *Bull. Chem. Soc. Jpn.*, **55**, 1277 (1982).

T. KATO, M. YUDASAKA, and T. FUJIYAMA, "Salting -out Phenomenon and Clathrate Hydrate Formation in Aqueous Solution of Polar Nonelectrolyte", *Bull. Chem. Soc. Jpn.*, **55**, 1284 (1982).

H. ABE, N. MIKAMI, M. ITO, and Y. UDAGAWA, "Dispersed Fluorescence Spectra of Hydrogen-Bonded Phenols in a Supersonic Free Jet", *J. Phys. Chem.*, **86**, 2567 (1982).

T. FUJIYAMA, "The Effects of Intermolecular Potentials on the Vibrational Spectra of Condensed Systems", *J. Raman Spectrosc.*, **12**, 199 (1982).

M. SUMITANI and K. YOSHIHARA, "Direct Observation of the Rate for *Cis* → *Trans* and *Trans* → *Cis*

Photoisomerization of Stilbene with Picosecond Laser Photolysis", *Bull. Chem. Soc. Jpn.*, **55**, 85 (1982).

M. SUMITANI and K. YOSHIHARA, "Photochemistry of the Lowest Excited Singlet State: Acceleration of *trans* — *cis* Isomerization by Two Consecutive Picosecond Pulses", *J. Chem. Phys.*, **76**, 738 (1982).

K. YAGI, F. TANAKA, N. NAKASHIMA, and K. YOSHIHARA, "Picosecond Fluorescence Lifetime of FAD in D-Amino Acid Oxidase-Benzoate Complex", in "Flavins and Flavoproteins", V. Massay and H. Williams, Jr. Ed., *North Holland Inc.*, New York (1982), pp.546.

N. NAKASHIMA and K. YOSHIHARA, "Laser Flash Photolysis of Benzene IV. Physicochemical Properties of Mist Produced by Laser Excitation", *Bull. Chem. Soc. Jpn.*, **55**, 2783 (1982).

H. INOUE, M. HIDA, N. NAKASHIMA, and K. YOSHIHARA, "Picosecond Fluorescence Lifetimes of Anthraquinone Derivatives; Radiationless Deactivation *via* Intra- and Intermolecular Hydrogen Bonds", *J. Phys. Chem.*, **86**, 3184 (1982).

H. NAKAMURA, J. TANAKA, N. NAKASHIMA, and K. YOSHIHARA, "Nanosecond Laser Flash Photolysis of 1-Anilinonaphthalene", *Bull. Chem. Soc. Jpn.*, **55**, 1795 (1982).

S. YAMAMOTO and K. H. GRELLMANN, "The Triplet State of Anthracene Photodimers and the Wavelength Dependence of the Photodissociation Process", *Chem. Phys. Lett.*, **85**, 73 (1982).

T. NAKAYAMA, N. ITO, T. KAWAI, K. HASHIMOTO, and T. SAKATA, "Neutral Particle Emission from Zinc Oxide Surface Induced by High-Density Excitation", *Rad. Effects Lett.*, **67**, 129 (1982).

T. KOISO, M. OKUYAMA, T. SAKATA, and T. KAWAI, "Efficient Photoreduction of Methylviologen Sensitized by Chlorophyll Derivatives and Hydrogen Evolution by Visible Light", *Bull. Chem. Soc. Jpn.*, **55**, 2659 (1982).

T. SAKATA, T. KAWAI, and K. HASHIMOTO, "Photochemical Diode Model of Pt/TiO_2 Particle and Its Photocatalytic Activity", *Chem. Phys. Lett.*, **88**, 50 (1982).

I. HANAZAKI, "Focusing Effect of Laser Beam on the Power Dependence of Multiphoton Processes", *Appl. Phys.*, **B26**, 111 (1981).

R. NAKAGAKI and I. HANAZAKI, "Splitting of Methyl CH Stretching Vibrations in Higher Overtone Spectra of Methyl-substituted Unsaturated Hydrocarbons", *Chem. Phys. Lett.*, **83**, 512 (1981).

R. NAKAGAKI and I. HANAZAKI, "Overtone Spectra of CH Stretching Vibrations in Acetone and Acetaldehyde", *J. Phys. Chem.*, **86**, 1501 (1982).

H. SHINOHARA and N. NISHI, "Laser Photofragmentation Dynamics of an Acrolein Supersonic Molecular Beam at 193 nm", *J. Chem. Phys.*, **77**, 234 (1982).

N. NISHI, H. SHINOHARA, and I. HANAZAKI, "VUV Laser Photofragmentations of an Acrylonitrile Molecular Beam: One- Two- and Three-Photon Processes", *J. Chem. Phys.*, **77**, 246 (1982).

M. KAWASAKI, K. KASATANI, H. SATO, H. SHINOHARA, and N. NISHI, "Molecular Beam Photodissociation of Trimethylamine", *J. Chem. Phys.*, **77**, 258 (1982).

H. SHINOHARA and N. NISHI, "Multiphoton Ionization Mass Spectroscopic Detection of Ammonia Clusters", *Chem. Phys. Lett.*. **87**, 561 (1982).

Y. TAKENOSHITA, H. SHINOHARA, M. UMEMOTO, and N. NISHI, "Multiphoton Ionization Mass Spectroscopy of *p*-Xylene at 193 and 248 nm", *Chem. Phys. Lett.*, **87**, 566 (1982).

N. NISHI, H. SHINOHARA, and I. HANAZAKI, "Formation of Rotationally Highly Excited $NH(A^3\Pi_i)$ Radical by VUV Laser at 193 nm and Its Reactive Quenching by Foreign Gases", *Rev. Laser Engineering*, **10**, 394 (1982).

N. TAKAHASHI and H. KATÔ, "Laser-Induced Fluorescence of the NaRb Molecule", *J. Chem. Phys.*, **75**, 4350 (1981).

C. NODA and H. KATÔ, "Fluorescence of the $C^1\Sigma^+ - X^1\Sigma^+$ Transition of NaK and the Dissociate Atoms", *Chem. Phys. Lett.*, **86**, 415 (1982).

H. KATÔ, T. MATSUI, and C. NODA, "$Na_2(A^1\Sigma_u^+ - X^1\Sigma_g^+)$ Fluorescence Accompanied by a Continuous Spectrum", *J. Chem. Phys.*, **76**, 5678 (1982).

M. MATSUOKA, H. NAKATSUKA, and M. FUJITA, "Picosecond Backward Echo in Sodium Vapor — Relaxation and Quantum Beat Modulation", in "Picosecond Phenomena", Vol. II, Eds. R. M.

Hochstrasser, W. Kaiser, and C. V. Shank, *Springer*, New York, pp.357, (1980).

M. FUJITA, S. ASAKA, H. NAKATSUKA, and M. MATSUOKA, "The Backward Photon Echoes in Na and Na_2 in the Nanosecond and Picosecond Regions", *J. Phys. Soc. Jpn.*, **51**, 2582 (1982).

S. ASAKA, H. NAKATSUKA, M. FUJITA, and M. MATSUOKA, "Amplification System for High Power Tunable Picosecond Pulse", *Rev. Laser Engineering* (in Japanese), **10**, 325 (1982).

M. SANO, N. SATO, H. INOKUCHI, and S. TAMURA, "Graphite Filaments and Their Alkali-Metal Intercalation Compounds.", *Physica*, **105B**, 296 (1981).

N. SATO, K. SEKI, and H. INOKUCHI, "Polarization Energies of Organic Solids Determind by Ultraviolet Photoelectron Spectroscopy.", *J. Chem. Soc., Faraday Trans. 2*, **77**, 1621 (1981).

N. SATO, H. INOKUCHI, and I. SHIROTANI, "Polarization Energies of Tetrathiafluvalene Derivatives.", *Chem. Phys.*, **60**, 327 (1981).

S. HASHIMOTO, K. SEKI, N. SATO, and H. INOKUCHI, "Electronic Properties of Polymers. Anisotropic Light Absorption and Photoelectron Emission of Oriented Polyethylene Films in the Vacuum Ultraviolet Region.", *J. Chem. Phys.*, **76**, 163 (1982).

N. SATO, K. SEKI, H. INOKUCHI, Y. HARADA, and T. TAKAHASHI, "Temperature Dependence of the Photoelectron Spectra of an Evaporated Violanthrene A Film.", *Solid State Commun.*, **41**, 759 (1982).

Y. TAKAI, A. KURACHI, T. MIZUTANI, M. IEDA, K. SEKI, and H. INOKUCHI, "Photoconduction and Vacuum Ultraviolet Photoelectron Spectroscopy of Poly(*p*-xylylene).", *J. Phys. D. Appl. Phys.*, **15**, 917 (1982).

Y. TAKAI, T. MIZUTANI, M. IEDA, K. SEKI, and H. INOKUCHI, "Photoelectron Spectroscopy of Poly-*p*-xylylene Polymerized from the Vapor Phase.", *Polym. Photochem.*, **2**, 33 (1982).

K. ICHIMURA, K. KIMURA, Y. NAKAHARA, and T. YAGI, "Tetrahemoprotein, Cytochrome c_3 As an Organic Conductive Material.", *Chem. Lett.*, 19 (1982).

K. SEKI and H. INOKUCHI, "Angular- and Light-Polarization-Dependent Valence UV Photoelectron Spectra of Hexatriacontane (n-$C_{36}H_{74}$) Crystal.", *Chem. Phys. Lett.*, **89**, 268 (1982).

I. SHIROTANI, R. MANIWA, H. SATO, A. FUKIZAWA, N. SATO, Y. MARUYAMA, T. KAJIWARA, H. INOKUCHI, and S. AKIMOTO, "Preparation, Growth of Large Single Crystals, and Physicochemical Properties of Black Phosphorus at High Pressures and Temperatures.", *J. Chem. Soc. Jpn.* (in Japanese), 1604 (1982).

T. KATO, K. TANAKA, and I. KOYANO, "State Selected Ion-Molecule Reactions by a TESICO Technique. IV. Relative Importance of the Two Spin-Orbit State of Ar^+ in the Charge Transfer Reactions with N_2 and CO.", *J. Chem. Phys.*, **77**, 337 (1982).

T. KATO, K. TANAKA, and I. KOYANO, "State Selected Ion-Molecule Reactions by a TESICO Technique. V. $N_2^+(v) + Ar \rightarrow N_2 + Ar^+$.", *J. Chem. Phys.*, **77**, 834 (1982).

K. TESHIMA, K. TANAKA, T. KATO, and I. KOYANO, "Crossed-Beam Apparatus for Ion-Cluster Reaction.", *Uchuken Hokoku* (in Japanese), Suppl. 3, 85 (1982).

K. TANAKA, T. KATO, P.-M. GUYON, and I. KOYANO, "State Selected Ion-Molecule Reactions by a TESICO technique. VI. Vibronic-State Dependence of the Cross Sections in the Reactions $O_2^+(X^2\Pi_g, v; a^4\Pi_u, v) + H_2 \rightarrow O_2H^+ + H, H_2^+ + O_2$.", *J. Chem. Phys.*, **77**, 4441 (1982).

I. KOYANO, Y. ACHIBA, H. INOKUCHI, E. ISHIGURO, R. KATO, K. KIMURA, K. SEKI, K. SHOBATAKE, K. TABAYASHI, Y. TAKAGI, K. TANAKA, A. UCHIDA, and M. WATANABE, The UVSOR Facility at IMS.", *Nucl. Instrum. Methods*, **195**, 273 (1982).

K. TANAKA, T. KATO, and I. KOYANO, "State Selected Ion-Molecule Reactions.", *Proceedings of the 30th* Ann. Conf. on Mass Spectrom. and Allied Topics, 18 (1982).

Y. ACHIBA, K. SATO, K. SHOBATAKE, and K. KIMURA, "Multiphoton Ionization Electron Spectroscopy of Organic Molecules.", *J. Photochem.*, **17**, 53 (1981).

K. KIMURA, Y. ACHIBA, S. KATSUMATA, T. YAMAZAKI, and S. IWATA, "Photoionic States of Organic Molecules Studied by HeI Photoelectron Spectroscopy.", *J. Photochem.*, **17**, 199 (1981).

Y. ACHIBA, K. NOMOTO, and K. KIMURA, He(I) Photoelectron Spectroscopic Study of the Electron-Donor-Acceptor Complex Formed between Dimethyl Ether and Boron Trifluoride.", *J. Phys. Chem.*, **86**, 681 (1982).

S. TOMODA, Y. ACHIBA, and K. KIMURA, "Photoelectron Spectrum of the Water Dimer.", *Chem. Phys. Lett.*, **87**, 197 (1982).

S. KATSUMATA, H. SHIROMARU, K. MITANI, S. IWATA, and K. KIMURA, "Photoelectron Angular Distribution and Assignments of Photoelectron Spectra of Nitrogen Dioxide, Nitromethane and Nitrobenzene.", *Chem. Phys.*, **69**, 423 (1982).

Y. ACHIBA, K. SATO, K. SHOBATAKE, and K. KIMURA, "The Mechanism for Photofragmentation of H_2S Revealed by Multiphoton Ionization Photoionization Spectroscopy.", *J. Chem. Phys.*, **77**, 2709 (1982).

Y. ACHIBA, K. KIMURA, N. KAKUTA, and K. MIYAHARA, "Further Improvement of Mole Fraction Determination of Gaseous Binary Mixture in Photoelectron Intensity Measurements.", *J. Electron Spectrosc.*, **28**, 139 (1982).

S. TOMODA and K. KIMURA, "Ionization Energies of the Water Dimer and Clusters, in "Ion and Molecules" — Proceedings of the 6th Intern. Symposium on Solute-Solute-Solvent Interactions, Eds. by N. Tanaka, H. Ohtaki and R. Tamamushi.", *Elsevier*, Amsterdam (1982).

J. HARRIS, A. LIEBSCH, G. COMSA, G. MECHTERSHEIMER, B. POELSEMA, and S. TOMODA, "Refraction Effects in Atom Scattering from Stepped Surfaces.", *Surf. Sci.*, **118**, 279 (1982).

G. SAITO, T. ENOKI, K. TORIUMI, and H. INOKUCHI, "Two-Dimensionality and Suppression of Metal-Semiconductor Transition in a New Organic Metal with Alkylthio Substituted TTF and Perchlorate.", *Solid State Commun.*, **42**, 557 (1982).

G. SAITO, T. ENOKI, and H. INOKUCHI, "A Novel Behavior of Electrical Resistivity in a New Two-Dimensional Organic Metal, (BEDT-TTF)$_2$ClO$_4$(1,1,2-Trichloroethane)$_{0.5}$.", *Chem. Lett.*, 1345 (1982).

H. KOBAYASHI, A. KOBAYASHI, G. SAITO, and H. INOKUCHI, "The Crystal Structure of Di(2,3,6,7-tetramethyl-1,4,5,8-tetraselenafulvalenium) Tetrafuloroborate, (TMTSF)$_2$BF$_4$.", *Chem. Lett.*, 245 (1982).

K. MURATA, H. ANZAI, G. SAITO, K. KAJIMURA, and T. ISHIGURO, "Evidence for Three Dimensional Ordering of Superconductivity in Highly Anisotropic Organic Conductor, (TMTSF)$_2$ClO$_4$.", *J. Phys. Soc., Jpn.*, **50**, 3529 (1981).

K. MURATA, T. UKACHI, H. ANZAI, K. KAJIMURA, G. SAITO, and T. ISHIGURO, "Nonlinear Effect above the Superconducting Critical Current in (TMTSF)$_2$ClO$_4$.", *J. Phys. Soc. Jpn.*, **51**, 695 (1982).

K. MURATA, H. ANZAI, K. KAJIMURA, T. ISHIGURO, and G. SAITO, "Superconducting Transition of (TMTSF)$_2$ClO$_4$ in Magnetic Field.", *Mol. Cryst. Liq. Cryst.*, **79**, 283 (1982).

K. MURATA, T. UKACHI, H. ANZAI, G. SAITO, K. KAJIMURA, and T. ISHIGURO, "Nonlinear Effects near the Superconducting Transition of Organic Synthetic Metal (TMTSF)$_2$ClO$_4$.", *J. Phys. Soc. Jpn.*, **51**, 1817 (1982).

Y. TOKURA, T. KODA, T. MITANI, and G. SAITO, "Neutral-to-Ionic Transition in Tetrathiafulvalene-*p*-Chloranil as Investigated by Optical Reflection Spectra.", *Solid State Commun.*, **43**, 757 (1982).

K. KONISHI, A. YOSHINO, M. KATOH, K. TAKAHASHI, Y. KAWADA, T. SUGAWARA, and H. IWAMURA, "NMR Studies of Picolyl-type Carbanions. V. ^{7}Li and ^{13}C Spectra of Picolyl-type Anions with Lithium as a Counter Ion", *Bull. Chem. Soc. Jpn.*, **54**, 3117 (1981).

R. D. McKELVEY, Y. KAWADA, T. SUGAWARA, and H. IWAMURA, "Anomeric Effect in 2-Alkoxytetrahydropyrans Studied by ^{13}C and ^{17}O NMR Chemical Shifts", *J. Org. Chem.*, **46**, 4948 (1981).

K. KOBAYASHI, M. KAWANISHI, S. KOZIMA, T. HITOMI, H. IWAMURA, and T. SUGAWARA, "Reaction of Trialkylstannyllithium and Hexaalkyldistannane. ^{1}H and ^{119}Sn NMR Studies", *J. Organometal. Chem.*, **217**, 315 (1981).

W. NAKANISHI, S. MURATA, Y. IKEDA, T. SUGAWARA, Y. KAWADA, and H. IWAMURA, "A Facile Formation of Cyclic Selenuranes and a Cyclic Selenurane Oxide in the Reaction of 2-Methylseleno- and 2-Phenylselenobenzoic Acids and Their Derivatives with *t*-Butyl Hydroperoxide", *Tetrahedron Lett.*, **22**, 4241 (1981).

M. IWAMURA, T. ASANO, Y. TANAKA, and H. IWAMURA, "Unusual Photochemical Reduction and Deacylation of Naphthyl Ketones Incorporated in a Triptycene Skeleton", *Chem. Lett.*, 1423 (1981).

S. ONAKA, T. SUGAWARA, Y. KAWADA, and H. IWAMURA, "Oxygen-17 Nuclear Magnetic Resonance Spectra of Mononuclear Manganese and Dinuclear Group 6 Metal Carbonyl Complexes", *J. Chem. Soc. Dalton Trans.*, 257 (1982).

Y. TEKI, T. TAKUI, M. HIRAI, K. ITOH, and H. IWAMURA, "Optically Detected Electron-Nuclear Double Resonance and Electron-Nuclear-Nuclear Triple Resonance Study of ^{17}O Hyperfine Coupling in the Lowest $n\pi^*$ Triplet State of Benzil", *Chem. Phys. Lett.*, **89**, 263 (1982).

T. SUGAWARA, M. YUDASAKA, K. TAKAHASHI, R. TAMAMUSHI, H. IWAMURA, and T. FUJIYAMA, "On the Viscosity Correction of Line Width in ^{35}Cl NMR", *Bull. Chem. Soc. Jpn.*, **55**, 1959 (1982).

H. TUKADA, M. IWAMURA, T. SUGAWARA, and H. IWAMURA, "Equilibria and Barriers to Interconversion between the *syn* and *anti* Conformers in 9-(*o*-Substituted Phenyl)fluorenes Obtained by Phtorearrangement of Triptycenes", *Org. Magn. Reson.*, **19**, 78 (1982).

W. NAKANISHI, Y. IKEDA, and H. IWAMURA, "Reaction of 2-(Methylseleno)- and 2-(Phenylseleno)-benzoic Acids and Their Derivatives with *tert*-Butyl Hydroperoxide. Neighboring Selenium Participation and Facile Formation of Cyclic Selenuranes and a Selenurane Oxide", *J. Org. Chem.*, **47**, 2275 (1982).

S. SMOLINSKI, M. BALAZY, H. IWAMURA, T. SUGAWARA, Y. KAWADA, and M. IWAMURA, "Spirans. XXII. Spiroconjugation in Heteraspirans Studied by UV and ^{13}C NMR Spectra", *Bull. Chem. Soc. Jpn.*, **55**, 1106 (1982).

E. LIPCZYŃSKA-KOCHANY and H. IWAMURA, "Charge-Transfer Complexation with a New Class of Electron Acceptors Made of Triptycenequinone Unit", *Chem. Lett.*, 1075 (1982).

T. SUGAWARA, M. YUDASAKA, Y. YOKOYAMA, T. FUJIYAMA, and H. IWAMURA, "Behavior of Chloride Ion in Crown Ether-Potassium Chloride Complexes in Solution Studied by Chlorine-35 Nuclear Magnetic Resonance Line Width", *J. Phys. Chem.*, **86**, 2705 (1982).

M. GOTO, K. OHTA, K. TORIUMI, and T. ITO, "The Crystal and Molecular Structure of *trans*-Dichlorobis((+)-*S,S-trans*-1,2-diaminocyclopentane)cobalt(III) Chloride Hydrochloride Dihydrate, *trans*-$[CoCl_2(+cptn)_2]Cl\cdot HCl\cdot 2H_2O$", *Acta Crystallogr.*, **B37**, 1189 (1981).

T. ITO, H. ITO, and K. TORIUMI, The Molecular Structure of 1*R*,2*R*,4*S*,7*S*,8*R*,9*R*,11*S*,14*S*-Octamethyl-1,4,8,11-tetraazacyclotetradecanenickel(II) Perchlorate", *Acta Crystallogr.*, **B37**, 1412 (1981).

H. ITO, J. FUJITA, K. TORIUMI, and T. ITO, "Optical Resolution of *rac*-5,5,7,12,12,14-Hexamethyl-1,4,8,11-tetraazacyclotetradecane(L), Circular Dichroism Spectra of Ni(II) Complexes with the Active Ligand, and Absolute Configuration of $(-)_{589}$-$[\{Ni(SS\text{-}L)\}_2(d\text{-tart})(H_2O)](ClO_4)_2\cdot 2H_2O$ as Determined by the X-ray Analysis". *Bull. Chem. Soc. Jpn.*, **54**, 2988 (1981).

T. ITO, M. SUGIMOTO, K. TORIUMI, and H. ITO, "The Structure of *trans*-Dichloro(1,4,8,11-tetraazacyclotetradecane)nickel(III) Perchlorate as Determined by X-ray Analysis", *Chem. Lett.*, **1981**, 1477.

Y. FUKUDA, Y. ISHIGE, T. ITO, K. KURODA, K. SONE, Y. SUZUKI, S. YANO, and S. YOSHIKAWA, "Hydroxide Addition to the Cobalt(III) Mixed Ligand Complex, (1,1,1,5,5,5-Hexafluoroacetylacetonato)-bis(ethylenediamine)cobalt(III) Perchlorate, $[Co(hfac)(en)_2](ClO_2)_2$", *Chem, Lett.*, **1981**, 1699.

K. TORIUMI, T. ITO, H. TAKAYA, T. SOUCHI, and R. NOYORI, "Molecular Structure and Absolute Configuration of (Norborna-diene){(+)-*R*-2,2′-bis(diphenylphosphino)-1,1′-binaphthyl}rhodium(I) Perchlorate, the Precursor of the Catalyst for Highly Enantioselective Hydrogenations", *Acta Crystallogr.*, **B38**, 807 (1982).

Y. YOSHIKAWA, K. TORIUMI, T. ITO, and H. YAMATERA, "Isomerism and the Metal Complexes Containing Multidentate Ligands. IX. Structure of the meso Isomer of $[Co(hexaen)]^{3+}$ (hexaen = 1,4,7,10,13,16-Hexaazacyclooctadecane)", *Bull. Chem. Soc. Jpn.*, **55**, 1422 (1982).

K. TORIUMI, K. KOYANO, N. SATO, H. TAKAYA, T. ITO, and H. INOKUCHI, "The Crystal and Molecular Structure of Flavanthrene", *Acta Crystallogr.*, **B38**, 959 (1982).

H. SAKURAI, Y. NAKADAIRA, H. TOBITA, T. ITO, K. TORIUMI, and H. ITO, "Crystal Structure of Tetrakis(trimethylsilyl)ethylene at −70°C", *J. Am. Chem. Soc.*, **104**, 300 (1982).

H. ITO, M. SUGIMOTO, and T. ITO, "Preparation and Molecular Structure of *cis*-Diaqua-(7*S*,14*S*)-5,5,7,12,12,14-Hexamethyl-1,4,8,11-tetraazacyclotetradecanenickel(II) Chloride", *Bull. Chem. Soc. Jpn.* **55**, 1971 (1982).

F. B. UENO, Y. SASAKI, T. ITO, and K. SAITO, "Pressure Effect on Photo-induced Electron Transfer Reactions between Tris(2,2′-bipyridine)ruthenium(II) and Various Metal Complex Ions", *J. Chem. Soc. Chem. Commun.*, **1982**, 328.

R. NOYORI, N. SANO, S. MURATA, Y. OKAMOTO, H. YUKI, and T. ITO, "Preparation and Structure of (*R*)-(−)-and (*S*)-(+)-2,2′-(2,2-Dimethyl-2-silapropane-1,3-diyl)-1,1′-binaphthalene", *Tetrahedron Lett.*, **23**, 2969 (1982).

M. SATO, Y. SATO, S. YANO, S. YOSHIKAWA, K. TORIUMI, H. ITO, and T. ITO, "Absolute Configuration of $(-)_{589}$-2,2′-Bipiperidine: Crystal Structure of $(-)_{546}$-*trans*-Dinitrobis{$(-)_{589}$-2,2′-bipiperidine}cobalt(III) *d*-3-Bromocamphor-9-sulphonate Tetrahydrate, $(-)_{546}$-*trans*-$[Co(NO_2)_2\{(-)_{589}$-2,2′-bpp$\}_2]$(*d*-BCS)·$4H_2O$", *Inorg. Chem.*, **21**, 2360 (1982).

N. HARADA, J. IWABUCHI, Y. YOKOTA, H. UDA, and K. NAKANISHI, "A Chiroptical Method for Determining the Absolute Configuration of Allylic Alcohols", *J. Am. Chem. Soc.*, **103**, 5590 (1981).

T. HOSHINO, U. MATSUMOTO, N. HARADA, and T. GOTO, "Chiral Exciton Coupled Stacking of Anthocyanins: Interpretation of the Origin of Anomalous CD Induced by Anthocyanin Association", *Tetrahedron Lett.*, **22**, 3621 (1981).

N. HARADA and H. UDA, "Angular Dependence of the U.V. Absorption Maximum Wavelength in Exciton Coupling Systems", *J. Chem. Soc. Chem. Commun.*, 230 (1982).

N. HARADA, T. AI, and H. UDA, "Absolute Stereochemistry of 2,2′-Spirobi-indane-1,1′-diols as determined by the C.D. Exciton Chirality Method", *J. Chem. Soc. Chem. Commun.*, 232 (1982).

T. HOSHINO, U. MATSUMOTO, T. GOTO, and N. HARADA, "Evidence for the Self-Association of Anthocyanins IV. PMR Spectroscopic Evidence for the Vertical Stacking of Anthocyanin Molecules", *Tetrahedron Lett.*, **23**, 433 (1982).

M. SANO, Y. HATANO. H. KASHIWAGI, and H. YAMATERA, "An *Ab Initio* Calculation of the Electronic Structure of the $[Co(CN)_6]^{3-}$ Ion", *Bull. Chem. Soc. Jpn.*, **54**, 1523 (1981).

M. SANO, H. ADACHI, and H. YAMATERA, "The Electronic Structures of Bis(*cis*-1,2-dicyano-1,2-ethenedithiolatonickel Complexes", *Bull. Chem. Soc. Jpn.*, **54**, 2636 (1981).

M. SANO, H. ADACHI, and H. YAMATERA, "The DV-Xα MO Study of Electronic Structures of $[M(CN)_6]^{3-}$ (M = Cr, Mn, Fe, and Co) and $[Fe(CN)_6]^{4-}$", *Bull. Chem. Soc. Jpn.*, **54**, 2898 (1981).

M. SANO, H. ADACHI, and H. YAMATERA, "The Electronic Structures of Linear Dicyano Complexes", *Bull. Chem. Soc. Jpn.*, **55**, 1022 (1982).

Y. OSAMURA, S. YAMABE, F. HIROTA, H. HOSOYA, S. IWATA, H. KASHIWAGI, K. MOROKUMA, M. TOGASHI, S. OBARA, K. TANAKA, and K. OHNO, "Quantum Chemistry Literature Data Base", *J. Chem. Inf. Compt. Science*, **21**, 86 (1981).

H. KASHIWAGI and S. OBARA, "*Ab Initio* Molecular Obital Calculation of Fe-Porphine with a Double Zeta Basis Set", *Int. J. Quant. Chem.*, **20**, 843 (1981).

M. SANO, H. KASHIWAGI, and H. YAMATERA, "An *Ab Initio* MO Calculation for the Bonding Structure of $[Ni(CN)_4]^{2-}$", *Bull. Chem. Soc. Jpn.*, **55**, 750 (1982).

H. KASHIWAGI, "Large-Scale Theoretical Calculations in Molecular Science — Design of Big Computer

System for Molecular Science and Necessary Conditions of Future Computers", *Comp. Phys. Comm.*, **26**, 411 (1982).

T. MURAO, I. YAMAZAKI, Y. SHINDO, and K. YOSHIHARA, "A Subnanosecond Time-Resolved Spectrophotometric System by Using Synchronously Pumped, Mode-Locked Dye Laser", *J. Spectrosc. Soc. Jpn.* (in Japanese), **31**, 96 (1982).

T. MURAO, I. YAMAZAKI, and K. YOSHIHARA, "Applicability of a Microchannel Plate Photomultiplier to the Time-Correlated Photon Counting Technique", *App. Opt.*, **21**, 2297 (1982).

I. YAMAZAKI, T. MURAO, and K. YOSHIHARA, "Subnanosecond Fluorescence Lifetimes of Pyrazine-h_4 and -d_4 Vapor for Photoselected Vibrational Levels in the S_1(n, π^*) State", *Chem. Phys. Lett.*, **87**, 384 (1982).

I. YAMAZAKI, T. MURAO, K. YOSHIHARA, M. FUJITA, K. SUSHIDA, and H. BABA, "Picosecond Fluorescence Decays from Vibrational Levels in the S_1(n, π^*) State of Pyridine Vapor", *Chem. Phys. Lett.*, **92**, 421 (1982).

K. KIMURA and H. INOKUCHI, "Percolative Conduction in Biological Conductor: Cytochrome c_3 Anhydrous Film of *Desulfovibrio Vulgaris*, Miyazaki Strain", *J. Phys. Soc. Jpn.*, **51**, 2218 (1982).

T. ENOKI, M. SANO, and H. INOKUCHI, "Electron Spin Resonance of Hydrogen-Absorbed Graphite-Potassium Intercalation Compounds", *Chem. Phys. Lett.*, **86**, 285 (1982).

Y. OKAMOTO, S. HONDA, I. OKAMOTO, H. YUKI, S. MURATA, R. NOYORI, and H. TAKAYA, "Novel Packing Material for Optical Resolution: (+)-Poly(triphenylmethyl metacrylate) Coated on Macroporous Silica Gel", *J. Am. Chem. Soc.*, **103**, 6971 (1981).

H. TAKAYA, M. YAMAKAWA, and R. NOYORI, "Nickel(0)-Catalyzed [2 + 2] Cross-Addition of Bicyclo-[2.2.1]heptene Derivatives with Electron-Deficient Olefins", *Bull. Chem. Soc. Jpn.*, **55**, 852 (1982).

K. TANI, T. YAMAGATA, S. OTSUKA, S. AKUTAGAWA, H. KUMOBAYASHI, T. TAKETOMI, H. TAKAYA, A MIYASHITA, and R. NOYORI, "Cationic Rhodium(I) Complex Catalyzed Asymmetric Isomerization of Allylamines to Optically Active Enamines", *J. Chem. Soc., Chem. Commun.*, 600 (1982).

Y. TAKAGI, M. SUMITANI, N. NAKASHIMA, and K. YOSHIHARA, "High-Power UV-Visible-IR Continuously Tunable Picosecond Laser Using Optical Parametric Oscillator", *Rev. Laser Engineering*, **10**, 419 (1982).

Review Articles and Textbooks

Y. TANABE and H. NAKAMURA, "Partial Differential Equations and Boundary Value Problems", *University of Tokyo Press*, (in Japanese), 1981.

E. HIROTA, "Diode Laser. Applications to Molecular Structure.", *Optronics* (in Japanese), 16 (1982).

E. HIROTA, "Molecular Science of Carbenes. Singlet and Triplet of CH_2.", *Kagaku* (in Japanese), **37**, 311 (1982).

K. YOSHIHARA, "Ichii Taisui", *Chem. Today* (in Japanese), **No. 129**, 23 (1981).

T. SAKATA, "Hydrogen Production by Solar Energy — Photocatalytic Effect of Dyes and Semiconductors", *Kagaku* (in Japanese), **51**, 744 (1981).

H. INOKUCHI and T. YAGI, "Cytochrome c_3 — Electron Transporter of Hydrogenase.", *Kagaku* (in Japanese), **51**, 369 (1982).

S. HASHIMOTO and K. SEKI, "Electronic Properties of Polyethylene — Aiming the Clarification of Electronic Structure with Light.", *Kagaku* (in Japanese), **37**, 425 (1982).

K. TANAKA, "State Selected Ion-Molecule Reactions.", *Rad. Chem.* (in Japanese), **17**, No. 34, 2 (1982).

S. TOMODA and I. KUSUNOKI, "Atomic and Molecular Beams — as Probes for Surface Study", *Butsuri* (in Japanese), **37**, 144 (1982).

K. KIMURA, "New Light — Synchrotron Orbital Radiation", *Kagaku to Kogyo* (in Japanese), **34**, 360 (1981).

H. KASHIWAGI, "Necessary Conditions of the Computer System for Molecular Science", *Johoshori* (in Japanese), **22**, 1175 (1981).

T. OSA, N. KOBAYASHI, H. OGOSHI, H. SUGIMOTO, H. KASIWAGI, Y. OOKATSU, T. IIZUKA, and Y. ISHIMURA, "Chemistry of Porphyrins" (in Japanese), *Kyoritsu Shuppan*, Tokyo 1982.

K. TANI, T. YAMAGATA, S. OTSUKA, S. AKUTAGAWA, H. KUMOBAYASHI, T. TAKETOMI, H. TAKAYA. A. MIYASHITA, and R. NOYORI, "Asymmetric Reactions and Processes in Chemistry", E. L. Eliel and S. Otsuka, Eds., *ACS Symposium Series*, **185**, 1982, pp.187—193.

A. MIYASHITA, H. TAKAYA, and R. NOYORI, "Asymmetric Reactions and Processes in Chemistry", E. L. Eliel and S. Otsuka, Eds., *ACS Symposium Series*, **185**, 1982, pp.274—277.

Institute for Molecular Science, Myodaiji, Okazaki 444, Japan